GENERAL ELECTRIC

RESEARCH AND DEVELOPMENT CENTER

SCHENECTADY, NEW YORK

N70-21688
CR-109205

INTERIM REPORT

for

VHF RANGING AND POSITION FIXING EXPERIMENT USING ATS SATELLITES

25 November 1968 - 9 October 1969

Contract No.: NAS5-11634

Prepared by

GENERAL ELECTRIC COMPANY
Research and Development Center
Schenectady, New York

for

Goddard Space Flight Center
Greenbelt, Maryland

FACILITY FORM 602

(ACCESSION NUMBER) 192

(PAGES) 1

(NASA CR OR TMX OR AD NUMBER)

(THRU) 1

(CODE)

(CATEGORY)

S-70-1003

In compliance with the requirements of contract NAS5-11634, three glossy prints and one negative are provided for the following figures used in our report S70-1003.

Figure 3-1 Radio-Optical Observatory at Schenectady, New York

Figure 3-8 Five Circuit Board Cards

Figure 3-9 Assembled Responder Unit

Figure 3-11 Tone-Code Generator and Phase Matcher-Correlator

Figure 7-1 Sister Ship of Valiant, Equipment Used in Ship Tests

Figure 9-1 Ford Econoline Van

All of the other figures may be reproduced from the unbound copy provided.

INTERIM REPORT

for

VHF RANGING AND POSITION FIXING EXPERIMENT USING ATS SATELLITES

25 November 1968 - 9 October 1969

Contract No.: NAS5-11634

Goddard Space Flight Center

Contracting Officer: C. W. Trotter
Technical Monitor: D. V. Fordyce

Prepared by

GENERAL ELECTRIC COMPANY
Research and Development Center
Schenectady, New York

Project Manager: Roy E. Anderson

for

Goddard Space Flight Center
Greenbelt, Maryland

This report is issued by the General Electric Research and Development Center in compliance with the terms of Contract NAS5-11634.

SUMMARY

The Applications Technology Satellites, ATS-1 and ATS-3, of the National Aeronautics and Space Administration were used to test the feasibility of ranging and position fixing from synchronous satellites to small mobile terminals at VHF radio frequencies. The range measurements were made with a simple "tone-code" technique that proved to be efficient in the use of satellite energy and compatible with presently-used mobile communication equipment and bandwidth allocations.

Five vehicles were used in the tests: two aircraft, a DC-6B and a KC-135 of the Federal Aviation Administration; a Coast Guard Cutter in the Gulf of Mexico; a buoy moored in deep water off Bermuda; and a panel truck in upstate New York. Each was equipped with conventional mobile communications transmitters, receivers and antennas with a 6 inch by 8 inch by 10 inch, 6 pound experimental tone-code "responder" unit attached between the receiver and transmitter.

When a vehicle was to be located, a ground station transmitted a 0.43 second tone-code signal to one of the satellites, the "interrogating satellite", usually ATS-3. The signal consisted of a 2.4414 kHz tone burst followed by the individual user address formed by suppressing an audio cycle for a digital "zero" and transmitting an audio cycle for a digital "one". The tone-code signal was frequency modulated on a 149.22 MHz carrier with a narrow deviation so that the RF bandwidth was within the 15 kHz bandwidth of the mobile receivers.

The satellite repeated the signal on 135.6 MHz. All of the activated vehicle equipments received the signal, and each matched the phase of a locally generated audio tone to the received tone phase. The one vehicle that was addressed responded with a short burst of its properly phased locally generated tone followed by its address code, introducing a very precisely known time delay between reception and retransmission of the code. The vehicle response on 149.22 MHz was through a broad beamwidth antenna. If both satellites were in range of the vehicle, they both repeated it on 135.6 MHz.

The ground station received the returns from the two satellites separately with narrow beamwidth antennas. It measured the time interval from its initial transmission of the signal to the first return from the interrogating satellite and to the two returns from the satellites as they were relayed back from the user. From these measurements the ranges from the two known positions of the satellites to the vehicle were determined. These ranges, together with vehicle altitude and corrections for ionospheric delay, were used to compute the vehicle location. When only one satellite was in range, a line of position was computed and a fix defined as the crossing of the line with latitude or longitude of the vehicle determined by other means.

The time required for the interrogation and response was less than one second except when a data transmission was included with the user response, or for the aircraft, the equipment required a longer time to switch from receive to transmit. The usual interrogation rate was once every three seconds, although a once-per-second rate was demonstrated.

The Sea Robin buoy, in a General Electric-Office of Naval Research experiment, was moored with a 7,000 foot line about 6 miles south of Bermuda where

the water depth is 4,200 feet. It was at its mooring during April and May of 1969. During that period, it was interrogated many times, at all hours of the day and night. Nearly all of the lines of position determined from the range measurements were within 1 1/2 miles of the mooring latitude. The computed results would probably have been even closer if a better description of the ionosphere had been used. The buoy operated unattended for a period as long as two weeks. No adjustment was made to the ranging equipment throughout the entire period, and there was no discernible change in its calibration.

The responses from the buoy included a data transmission of sensor readings. The digital data, usually at 305 bits per second, but occasionally at 2441.4 bits per second, was clocked from the local generator of the tone-code responder.

The Coast Guard Cutter Valiant, in the Gulf of Mexico, was interrogated while in port and at sea. The experiment was coordinated by voice communications through the satellite using the conventional mobile receiver and transmitter of the ranging experiment. Responses were through both satellites, but because of a failure of an SHF antenna on ATS-3 NASA could not provide accurate position information for the satellite. The precision of the fixes was determined, and found to be much better than ± 1 nautical mile, 1 sigma, when the antenna on the ship was in clear view of the satellites. At certain ship headings, it was obstructed by the mast or other structures. When the antenna was obstructed, the signal level received from the satellite decreased, sometimes resulting in a response that was slightly early or late, adding or subtracting equally from the two-satellite range measurements and displacing the fix along a hyperbolic line of position.

The DC-6B four-engine propeller-driven aircraft was equipped with a Dorne and Margolin Satcom antenna as well as a conventional VHF blade antenna. The Satcom antenna is circularly polarized, and has two modes of operation. The "azimuth" or "horizon" mode has a maximum gain of approximately 3 dB, with a coverage from approximately 10 degrees to 40 degrees above the horizon. The "zenith" mode, also approximately 3 dB maximum gain, provides coverage above 40 degrees elevation. Both modes are essentially non-directional in azimuth. The DC-6B was flown over the ocean off the New Jersey coast, and also over land. Two flights were made over the midwestern United States, including a flight over Lake Michigan. While over the midwest, range measurements were made from both satellites. Position fixes agreed with Vortac fixes within 3 miles over land and over water. Vortac is a line-of-sight, VHF radio navigation aid by which aircraft determine their azimuth and distance from a ground-based station. It is used routinely, and hundreds of Vortac stations provide nearly full coverage over the United States and many other land areas of the world. While Vortac was the most accurate means available during that flight, it is not to be construed as a standard of comparison for the performance of the satellite location technique. The precision of fixes, including flight over land and water at 21,000 feet, was typified by a sample of seventy-four two-satellite measurements. All but four of the fixes were within 1 nautical mile of a mean position. The largest deviation in the sample was 1.9 miles from the mean.

The KC-135 jet aircraft was interrogated while in the vicinity of Iceland, at an altitude of 39,000 feet. Standard deviation of the lines of position was approximately ± 1 nautical mile, when using a VHF quarter-wave vertical "blade" antenna. Individual measurement displacements as large as 2 miles toward the

subsatellite point, and 4 miles away from the subsatellite point were observed, probably due to multipath. This was the poorest line-of-position precision observed in the entire experiment.

A mathematical analysis was used to predict the effects of multipath. The experimental results appear to confirm the analysis. At 5,000 feet, off the New Jersey Coast, using a Satcom antenna in the zenith mode, the standard deviation of range measurements was 2.1 microseconds, or approximately 1,000 feet. At 20,000 feet, with the same antenna, the standard deviation was 3.0 microseconds or 15,000 feet. Over the North Atlantic, using a VHF blade antenna, at 39,000 feet, the standard deviation was between 8 and 11 microseconds, 4,000 to 5,500 feet. The distribution of errors was as expected from the analysis, suggesting that the average of many range measurements approaches zero error. Multipath can cause loss of signal for a surface craft, but it cannot introduce significant range errors.

The Ford Econoline van was equipped with a mobile radio, as used in police cars and taxi cabs. Separate receive and transmit dipole antennas were used. Range measurements were made to the vehicle as it was driven along roads in the vicinity of Schenectady, New York. Lines of position were computed and the measured latitudes were compared with the latitudes of the van as determined from the topographic map. Including bias error, the latitudes were correct within approximately one mile.

Range measurements were made on nearly every interrogation when the mobile craft antenna gain toward the satellite was better than approximately 0 dB, the links were not degraded by Faraday rotation, the vehicle receiver noise figure was approximately 3.0 dB, and the vehicle transmitter power was approximately 100 watts. Faraday rotation and low vehicle antenna gain frequently caused a larger percentage of unsuccessful interrogations than would be acceptable in an operational system.

The test results indicate that an accuracy better than $\pm$ 1 nautical mile, 1 sigma, for ships and approximately $\pm$ 1 nautical mile, 1 sigma, for aircraft can be achieved at VHF. To achieve that accuracy, it will be necessary to employ calibration transponders at fixed, known locations with approximately 600 mile spacing and interrogate each one a few times per hour to determine range measurement corrections. It is recommended that calibration of vehicle equipment time delay be accomplished at the ground terminal by interrogating each craft when it is at some known location. The time delay calibration is then stored in the computer with the vehicle address. It will be necessary to employ aircraft antennas that discriminate against sea reflections, so that the reflected signal is more than 10 dB below the direct signal. The use of circular polarization for the satellite and aircraft antennas is recommended.

The experiment included a test of the General Electric Low Energy Speech Transmission technique by relay through the ATS-1 satellite. It was necessary to substitute a frequency shift waveform for the desired amplitude modulation so that the energy saving was not directly demonstrated. Although the signal path was poor, with amplitude scintillation of the signals, the intelligibility score on spondaic words exceeded 90 percent for a group of untrained listeners. Spondaic words are two-syllable words with equal emphasis on the two syllables.

TABLE OF CONTENTS

LIST OF FIGURES

LIST OF TABLES

SECTION 1. INTRODUCTION

A growing population and a growing economy in the United States and throughout the world are causing greatly increased travel and shipping for commercial, pleasure and military purposes. Technological developments are increasing the already wide range of speed, size and maneuverability of the ships and airplanes that must share the surface and air space. It is evident that there would be great value in a single world-wide full-time system that combines the functions of accurate frequent position fixing with the current positions simultaneously available ashore and a capability for communication of essential information between traffic advisory and control centers and the craft that are enroute.(1)

The Applications Technology Satellites, ATS-1 and ATS-3, of the National Aeronautics and Space Administration were used in a series of tests to determine the usefulness of VHF for locating mobile vehicles by range measurements from satellites. The specific objectives of the experimental program conducted by the General Electric Company for NASA under contract NAS5-11634 were as follows:

1. Demonstrate the feasibility of ranging and position fixing from synchronous satellites to small mobile terminals at VHF radio frequencies. It was expected that the experiment would demonstrate position fixing accuracies adequate for transoceanic air traffic control.

2. Demonstrate the advantages of a tone-code (pulse train) ranging technique that offers promise of the highly efficient use of satellite energy in simple implementation that is compatible with presently used communication equipment. In operation, the system would be easily retrofitted in existing aircraft.

3. Obtain data over a large geographical region at various times of the day to indicate the variations in ranging and position fixing accuracies caused by location and time of day.

4. Demonstrate the General Electric Company's Low Energy Speech Transmission (L.E.S.T.) technique. In an operational system, this technique would be compatible with tone-code ranging in such a way that the pulsed voice transmissions could be used in the range measuring process.

NASA's Applications Technology Satellites have shown the feasibility of voice communications between aircraft and ground terminals. Airlines that fly transoceanic routes desire to replace their inadequate HF voice communication links with the far more reliable satellite links. It is generally agreed that a satellite system should also provide surveillance of aircraft positions for air traffic control over the oceans, so that lateral spacings between the transoceanic routes can be reduced and economy of operations improved. An early implementation of an aeronautical satellite system would have to be accomplished at VHF. When suitable aircraft antennas and other avionics equipment have been developed, the L-band frequencies, 1540 to 1660 MHz, will offer the possibility for improved performance.

It is widely recognized that the maritime services would benefit from improvements in communications, radio navigation and radio location that could be provided by the use of satellites. Traffic control of ships in confluence areas could reduce the number of ship collisions and improved position fixing

could reduce the number of groundings. Weather routing of ships could result in substantial savings.

Satellites may be useful for data readout and location of remote unmanned sensors such as oceanographic buoys. Buoy location and readout were tested in parallel with the NASA contract under Navy contract N00014-68-C0467. Initial results of the buoy experiment are included in this report.

There has been a lack of agreement concerning the usefulness of VHF for position determination. A major objective of the ranging and position fixing experiment was to provide definitive data for the resolution of this question. One purpose of this report is to present information that will aid in the determination of the feasibility of using satellites in radio navigation and radio location systems and provide the basis for estimating performance and cost of such systems.

The experiment did not demonstrate an operational capability for VHF satellite position fixing, nor was there any intent that it should. The intent of this report is to provide experimental results pertaining to all principal factors affecting the use of satellites for position fixing, especially as they influence performance at VHF. It is hoped that the information it contains will be useful to the numerous organizations that are studying the application of satellites to navigation and traffic control.

REFERENCE

1. Anderson, Roy E., "Study of Satellites for Navigation"; General Electric Company report for the National Aeronautics and Space Administration on contract NASw-740; February 1964.

SECTION 2. SIGNIFICANCE OF THE TEST RESULTS

The study program did not include consideration of specific applications for radio navigation and radio location systems using satellites. It is inevitable however that the principal investigator should arrive at conclusions concerning the practical value of the technique that was tested and the performance that would be achieved if it were applied in operational systems.

In the proposal for the work, it was estimated that an accuracy of 3 to 5 nautical miles, 1 sigma, could be achieved at VHF. It is now evident that accuracy far better than that can be achieved with modest user equipment and satellite design similar to that of ATS-1 and ATS-3, provided that the ionosphere is calibrated by range measurements to fixed ground terminals containing transponders like those used in the mobile craft and provided that the calibration of user equipments is included. The use of circularly polarized antennas is recommended for the satellites and user craft.

Results indicate that an operating VHF system designed with the basic parameters used in the experiment would have an accuracy of 1 nautical mile, 1 sigma for ships, and approximately the same accuracy for aircraft. The new estimate is based on the following projections from the experimental result.

Fix precision for the Coast Guard Cutter Valiant in the Gulf of Mexico shows east-west errors much smaller than 1 nautical mile. North-south errors were sometimes greater than 1 mile, but their distribution was along a hyperbolic line of position as a result of poor signal-to-noise at the ship receiver. The use of a better ship antenna and better placement of the antenna on the ship would improve the precision along the hyperbolic line. (See Figures 7-5 through 7-10.)

In one test, aircraft fix precision using the azimuth mode of a Satcom antenna with the aircraft over land and water was 70 out of 74 fixes within 1 nautical mile. (See Figure 6-3.) It is probable that the use of antennas with higher gain and better discrimination against multipath, such as those installed on the new 747 aircraft, would insure precision equal to the referenced test result under most conditions.

Fix accuracy can be almost as good as the precision if the equipment and ionosphere delays are properly calibrated, and the positions of the satellites are known, as confirmed by the Sea Robin tests (see Figures 8-2, 8-3 and 8-4) and aircraft tests (see Tables 6-2, 6-3 and 6-4).

Calibration of narrow bandwidth user equipment can be maintained without attention for usefully long periods. No significant drift in the Sea Robin transponder was observed while it operated at sea without adjustment for twenty-seven days (see Figures 8-3 and 8-4).

Calibration stations, essentially the same as user transponders, separated approximately 600 nautical miles and each interrogated a few times per hour, may provide sufficient information for ionosphere corrections (see discussion, Section 5, page 5-1).

Scintillation in the ionosphere may cause signal strength variations of large amplitude and short period signal dropouts. They have little effect on

ranging accuracy. Range measurements can be made in a fraction of a second; scintillation may reduce the probability of a response, but it does not affect accuracy significantly or impair the ability to make frequent position fixes on user craft. (See Section 5, page 5-28.)

Not all of the test results were as precise nor as accurate as the examples cited above. The ratio of user responses to interrogations was not always high enough for an operational system. These deficiencies resulted because of the experimental nature of the program. In every case, they could be improved by engineering effort that can now be defined.

The lowest precision was experienced with a jet aircraft at high altitude over the North Atlantic using a low gain VHF blade antenna susceptible to multipath. Greatest standard deviation of the range measurements was 11 microseconds, representing a cross-track error slightly greater than 1 nautical mile. The largest single cross-track error was 4 nautical miles (see Figure 6-5). An antenna with better discrimination against multipath and higher gain in the direction of the satellite would improve accuracy to compare with the results obtained over Lake Michigan. (See Figures 6-14 and 6-15.)

Responders used in the tests were experimental units, all solid state, employing integrated circuits and printed circuit board construction. No formal attempt was made to estimate the cost of units designed and built in production quantities. However, the cost of building the experimental units suggests that the cost of a unit for adding a ranging capability to a ship or aircraft that is equipped for satellite communication would be approximately $5,000.

SECTION 3. EXPERIMENT DESCRIPTION

The experiment demonstrated for the first time that it is practical to locate mobile craft by range measurements from two satellites with a single interrogation from a ground station and a single response from the mobile craft. A short "tone-code" interrogation signal containing a single frequency tone burst followed by a user's address was transmitted from a ground terminal to ATS-1 or ATS-3, usually the latter. The satellite repeated the signal. All of the activated transponders within range of the satellite received the interrogation and each one matched the phase of a locally generated tone to the received tone phase. The one unit that was addressed recognized its own code, and transmitted a response through an omnidirectional antenna. Both satellites repeated the response when both were within view of the unit. The ground terminal measured the time from the initial transmission to the return of the interrogating signal from the one satellite, and to the returns from the user as relayed by the two satellites. The time measurements were stored on punched tape and later inserted into a computer. The known equipment delays of the user transponder and the satellites were subtracted from the measurements, and the ranges from the two satellites to the user were determined. An initial fix determination was made, the local time at the initial fix was noted, and corrections for ionospheric delay were obtained from a model of the ionosphere stored in the computer. Range corrections were applied, and the position fix determined by another iteration of the computation.

When a transponder was in view of only one satellite, lines of position were determined from the single range measurements. Computer programs were used to compute the latitude at which the line of position crossed a given longitude, or the longitude at which the line of position crossed a given latitude.

Other data were also collected during the experiment, such as the standard deviations of range measurements between the ground terminal and the satellite, and between the satellite and transponders aboard mobile vehicles or at fixed locations. Ionospheric delays were measured, and observations were made of Faraday rotation, ionospheric scintillation, and sea reflection multipath. Voice and data transmissions were made with the same transmitters and receivers used for ranging.

The ground terminal used in the experiment was the Radio-Optical Observatory of the General Electric Company, located near Schenectady, New York at 42°50'53" North latitude, and 74°04'15" West longitude. A photograph of the Observatory is shown in Figure 3-1. Interrogations to the satellite were transmitted to the satellites on 149.22 MHz with a transmitter power of 300 watts. Transmissions were through a 30 foot diameter parabolic antenna having a log periodic feed with selectable horizontal or vertical polarization. The same antenna was used to receive the signals from the interrogating satellite. In the later phases of the experiment a means was provided to switch polarization independently for transmission and reception. Except for brief tests, or when only ATS-1 was in use, the 30 foot antenna was used with ATS-3. When interrogations were made through ATS-3 and responses received from both satellites, a two-bay crossed yagi antenna with 16 dB of gain was used for receiving the signals from ATS-1. A choice of vertical and horizontal polarizations was available with the yagi antenna.

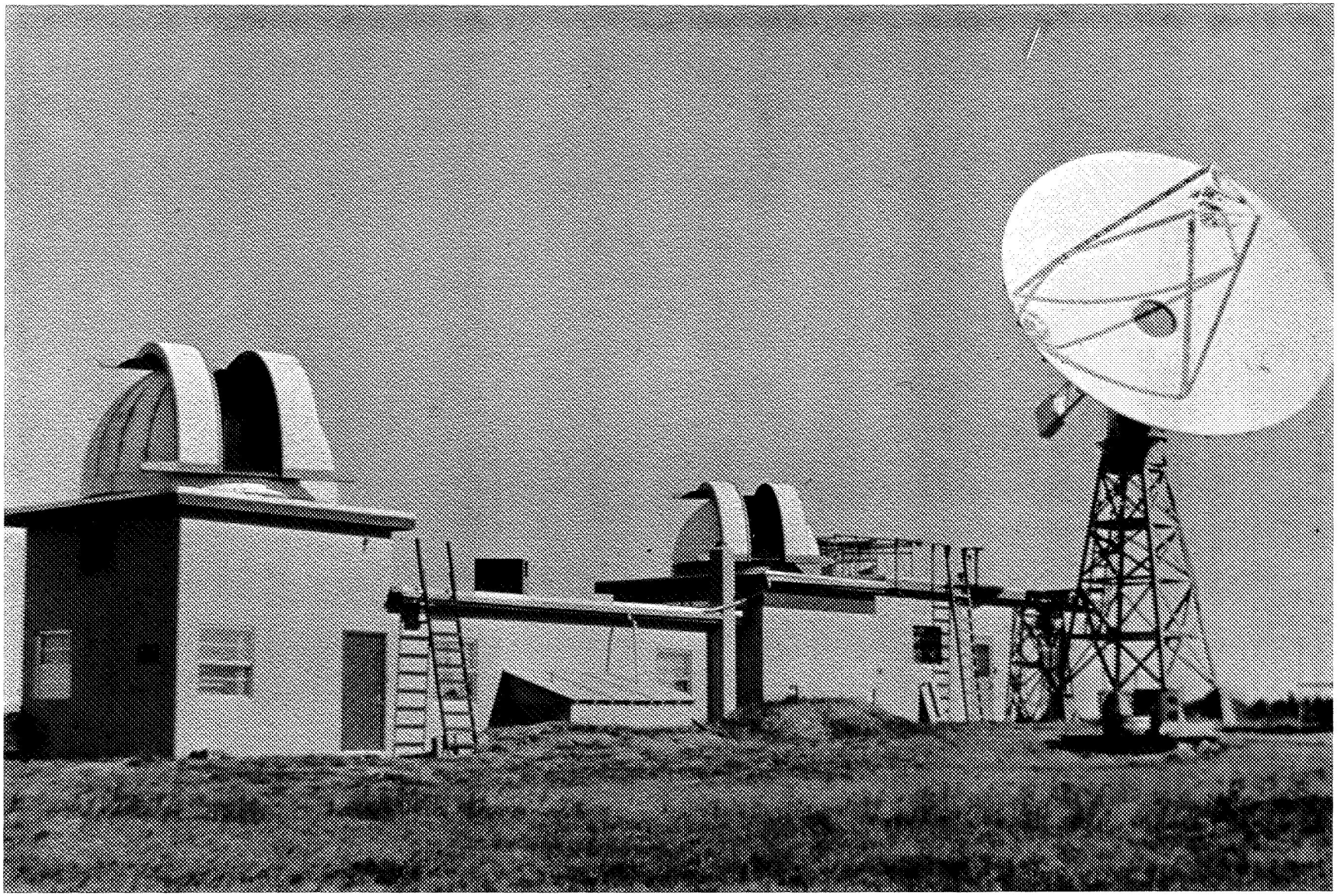

FIGURE 3-1. RADIO-OPTICAL OBSERVATORY AT SCHENECTADY, NEW YORK

Signals returned from the satellites were on 135.6 MHz. The received signals were applied to pre-amplifiers with a noise figure better than 3 dB, and then detected in FM receivers with IF bandwidths of 15 kHz.

Specially designed and constructed circuits detected the timing signals, and electronic counters measured the time intervals. They were then recorded on punched paper tape together with time of day, and information pertaining to digital bit error rates in the received user identification codes. Paper chart recordings were made of signal level and incremental time delay changes. Magnetic tape recordings of digital data returns were made when data was included with the responses.

Five vehicles were used during the experiment: an oceanographic buoy; two aircraft, a DC-6B and a KC-135; a ship; and a panel truck. The buoy, called Sea Robin, was moored in deep water off Bermuda. Range measurements were made from ATS-3 and sensor data were transmitted in digital form with the ranging response. The Sea Robin experiment was conducted jointly by General Electric and the Office of Naval Research (contract N00014-68-C0467). Lines of position were determined for hundreds of range measurements made at various times during the day and night for a three week period.

The Coast Guard Cutter Valiant, WMEC-621, located in the Gulf of Mexico, was in view of both satellites. The transponder on the ship was interrogated through one satellite. The Valiant responded through both satellites to provide dual range measurements when the ship was in port and under way. The measurements were used to determine the precision of fixes, but the failure of a mechanically despun SHF antenna on ATS-3 prevented NASA from obtaining accurate satellite position information during the period of the Valiant tests. It was therefore not possible to determine the accuracy of the fixes, although the positions of the ship when under way were accurately determined by radar measurements relative to off-shore oil rigs whose positions are known accurately.

The Federal Aviation Administration made two aircraft available: a DC-6B, a four-engine propeller-driven airplane; and a KC-135, a large jet. The DC-6B was equipped with two antennas, a blade and a Satcom. The different antenna patterns permitted observations of multipath effects. Position fixes were determined for the aircraft as it flew over the midwestern United States, including over land and over Lake Michigan. The positions were compared with Vortac fixes determined in the aircraft. The aircraft was also flown over the ocean off the coast of New Jersey where it was tracked by a precision radar of the FAA's National Aviation Facilities Experimental Center (NAFEC), but the flights were made during the period when accurate satellite information was not available.

Range measurements were made from ATS-3 to the KC-135 when the aircraft was at high altitude, flying at subsonic speed in the vicinity of Iceland. The aircraft was equipped with a VHF blade antenna. The altitude, satellite elevation angle, aircraft speed and antenna pattern combined to provide a good test of multipath effects.

The KC-135 provided an unscheduled test of the communications compatibility of the tone-code ranging technique. While the ground terminal was interrogating the Cutter Valiant, the KC-135 crew unexpectedly called the ground terminal by voice from the runway in the Azores requesting range measurements while the aircraft took off. The ground terminal switched to the address code of the KC-135 aircraft, and successfully ranged on it until it was airborne, then returned to the Valiant code.

All of the five vehicles used in the test were equipped with FM mobile radio transmitters and receivers with tone-code ranging responders attached. The transmitted powers and the antenna configurations used on the five vehicles are given in Table 3-1.

TABLE 3-1

TRANSMITTED POWERS AND ANTENNA CONFIGURATIONS OF VEHICLES USED IN TESTS

VEHICLE	POWER	ANTENNA
Buoy	120 W	Selectable linearly polarized dipole.
KC-135	500 W	VHF blade.
DC-6B	500 W	VHF blade and circularly polarized horizon and zenith mode Satcom antenna.
Ship	300 W	Circularly polarized.
Van	80 W	Separate receive and transmit linearly polarized dipoles.

The tone-code signal consisted of an audio frequency tone burst followed by a digital address code. The tone burst was 1024 cycles of 2.4414 kHz. The digital address code had 30 bits. A digital "one" was a single cycle of the audio frequency tone and a digital "zero" was a suppressed cycle. The time duration of a complete tone-code signal was approximately 0.43 second. Tone-code ranging is described in detail later in this section.

The tone-code signal modulated the transmitter with a deviation of approximately 5 kHz, resulting in an RF bandwidth for the signal of approximately 15 kHz. The transmitter was a General Electric Mastr Progress Line Desk Mate® station and 4EF5A1 power amplifier. The 300 watt, 149.22 MHz signal was transmitted to the interrogating satellite, usually ATS-3, through the 30 foot antenna.

The satellite received the interrogation signals, converted them to 135.6 MHz and retransmitted them with an effective isotropic radiated power (EIRP) of approximately 200 watts. Bandwidth of the satellite VHF transponders is approximately 100 kHz. The time delay through the transponder was given as 7.3 microseconds, the value assumed in estimates of equipment delay. Uncertainty in satellite time delay was acceptable since total time delay was calibrated for each transponder equipment with the vehicle at a known location. It is important, however, that it not change significantly during tests.

Each transponder consisted of an antenna, a mobile communications receiver, a tone-code responder unit, and a mobile radio transmitter. In the responder unit, the phase of a locally generated 2.4414 kHz audio tone is compared with and matched to the received tone phase by adding or deleting pulses in the frequency dividing chain. Each pulse added or deleted shifts the output phase by 0.4 microsecond. In this way, the locally generated tone is shifted in steps until it matches the received tone phase within the small quantized interval. The circuit design is such that the phase can be shifted 180 degrees in either direction within 400 cycles of the audio tone. Reception of only 400 cycles out of the 1024 is sufficient to insure phase match. The phase comparison is averaged over approximately 64 cycles to

reduce the effects of noise jitter. When the received address code is recognized, the phase shifting and averaging process ends and the locally generated tone remains at the phase established during the comparison with the received tone phase. The accuracy of the oscillator, better than one part in 10^6, insures that the tone phase as measured by the timing of the zero crossings of the audio tone will not shift by more than 0.25 microsecond in the following 1/2 second.

The audio frequency output of the receiver was also applied to a digital address code recognizer in the responder. When the code was centered in the register, one clock pulse from the phase matcher was gated out.

The clock pulse starts a counter that counts the next 1024 clock pulses to measure a precise time interval of 419,430.4 microseconds. During that time interval, the antenna was switched from the receiver to the transmitter and the locally generated tone was transmitted by frequency modulation with a deviation of approximately 5 kHz. At the end of the precise time interval, the address code was clocked out of the shift register and transmitted. In this way, the transponder retransmitted the tone-code signal to the satellite with the tone phase properly set for the range measurement. After the code was transmitted, the transponder returned to the receive mode.

The tone-code signal was transmitted to the satellites on 149.22 MHz and relayed by them to the ground terminal on 135.6 MHz.

At the ground terminal the first signal received back from the satellite was the interrogating signal. The propagation time to the geostationary satellite and return was approximately 0.25 second so that the ground station was still transmitting when the first part of the interrogation signal was returning. Consequently, only the last half of the interrogation was received and applied to the phase matcher-correlator, a circuit like that in the mobile responders except that address codes are selectable with a rotary switch. Because the phase matcher can bring the local tone into phase within 400 cycles, or half the tone period, the duration of the received tone was sufficiently long for the phase measurement. Correlation of the address code resolved the tone period ambiguity, and gated out a single clock pulse to mark the end of the time interval for measuring the range from the ground terminal to the satellite, and the start of the time interval for the range from the satellite to the mobile craft. The response from the craft through the interrogating satellite was received and processed by the same equipment and in the same way as the interrogation return. The full duration of the tone was received. The response relayed through the other satellite was received on a different antenna and receiver, and processed in a different phase matcher-correlator.

Three time intervals were measured and recorded. All three time interval measurements started with the transmission of the interrogation signal from the ground station. The actual start time occurred one clock period, 409 microseconds, after the transmission of the last bit in the user address code. The first time interval, approximately 0.25 second in duration, ended with the correlation of the return from the interrogating satellite. The other two intervals, each approximately 0.9 second in duration, ended with correlation of the vehicle responses through two satellites. The intervals were measured with a timing resolution of 0.1 microsecond.

The time from the start of an interrogation to the completion of the range measurements and recording of the data was less than 1 second, so that

an interrogation rate of one per second was possible and was demonstrated. The usual rate in the test was once every three seconds.

There were two exceptions to the once-per-second capability. The transponder used in the FAA aircraft could not switch quickly from receive to transmit, and therefore it was necessary to extend the responder delay from 1024 to 2048 periods of the audio frequency tone, making the total interrogation and response time approximately 1.5 seconds. The other exception was the Sea Robin buoy which transmitted a digital data readout lasting approximately 1.2 seconds as part of its response to the range interrogation. The readout followed the tone-code response and was clocked by the responder.

The time intervals were measured using Hewlett-Packard Model 5245L counters with 5262A time interval plug-ins. The time intervals were punched on paper tape along with Greenwich Mean Time, and a number representing the bits in error in the word synch and address code. The bits in error were directly related to the amplitude of the correlation pulses from the summing circuits which took on discrete values depending on the number of correct bits in the received code. Correlation could be achieved when as many as three bits were in error in the word synch or the individual address code.

The punched tape data recording format is shown in Figure 3-2. The word and address error rate symbols are separate digital voltmeter measurements of the amplitude correlation pulses of the word synch and the user address in the correlator. Numbers of approximately 66... indicate zero bits error and 58... represent one bit error in the 15 bit codes which were at a digital bit rate of 2.4414 kHz. The data sample used in the illustration was recorded during the September 5 cruise of the Coast Guard Cutter Valiant.

In addition to the punched tape recording, a four channel paper chart recording was also made. (See Figure 3-3.) The chart speed was 2.5 mm per second and each interrogation and response is resolved along the chart. The last three digits of the time interval measurements for the propagation time measurements from the Observatory to ATS-3 and return were converted from digital signals to an analog voltage and recorded in the third track. The time resolution is 1 microsecond per large division. The slope of the average value results from the changing range from the Observatory to the satellite.

When necessary, as in the data readout of Sea Robin, a magnetic tape recording was made of the received audio frequency signals.

The specific uses of the recorded data are described for each mobile vehicle in later sections of this report. The usual data processing included the determination of standard deviations for range measurements. Standard deviations for selected portions of the recorded data were computed relative to a "best fit" quadratic curve. A sample of data processed in this way is shown in Figure 3-4. In some cases, the measurements were plotted as a function of time or as histograms to observe distribution patterns influenced by noise, ionosphere propagation effects, or multipath. Lines of position and fixes were computed to determine precision and accuracy for various conditions.

FIGURE 3-2. FORMAT OF DATA RECORDED ON PUNCHED TAPE

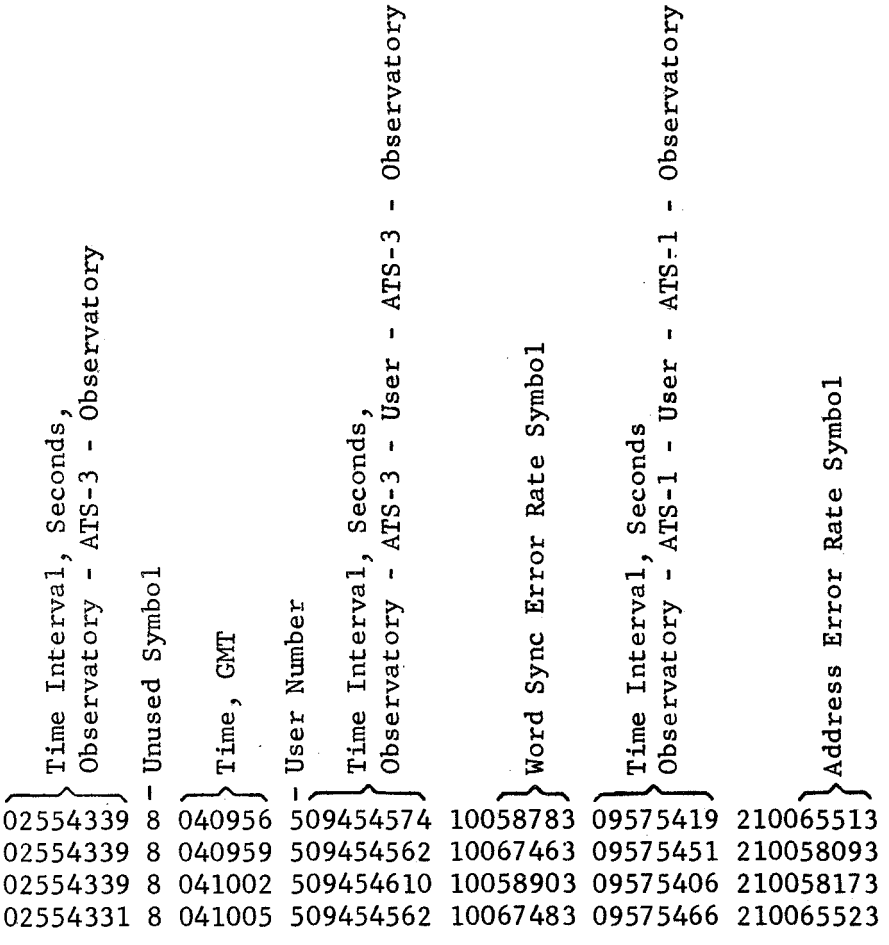

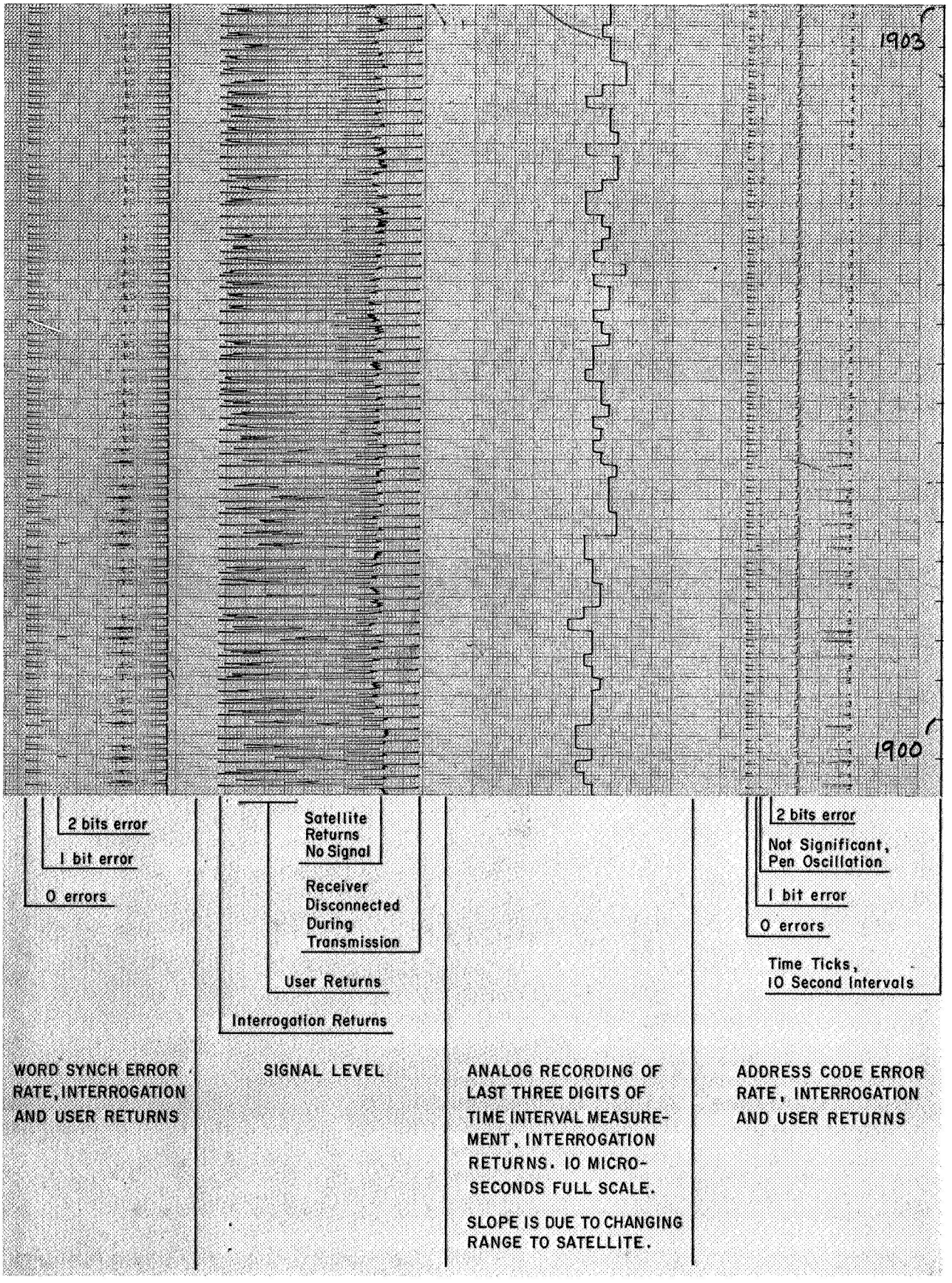

FIGURE 3-3. ACCURACY OF LINES OF POSITION

FIGURE 3-4

INITIAL PROCESSING OF RANGING DATA

```
FILE 113
DATE 6/12/69 FAA
IN FLIGHT END OF RUN
61240113
61240113
61240113
15255448 63085
NUMBER OF BAD RECORDS =                7
NUMBER OF GOOD RECORDS =             189

IN NI TNP NPU NPE GMTLOW GMTHIG  YMAX  DIFMIN DIFMAX    SD      ERRORATE
 1  1 189 120 123 142010 142958 200.0   -6.02   7.39 2.409E+00 0.
OV  1 189 120 123 142010 142958          -6.02   7.39 2.409E+00 0.

IN        A                B                C
 1 -1.52668331E-01 -1.62341159E-01  7.39304170E-06

     THATDIINT THATDIFIN DIFCHANGE
     1360511.3 1360416.3      95.0

K M GMT GMTHMS  TIMEACTUL  TIMEPREDT  DIFACTPRE  VOLTAGE ERROR

1 12787 142010  1360511.2  1360511.3       -0.1   6.7610     0
1 12790 142013  1360512.3  1360510.8        1.5   6.7600     0
1 12793 142016  1360512.2  1360510.3        1.9   6.7610     0
1 12796 142019  1360508.0  1360509.8       -1.8   6.7590     0
1 12799 142022  1360508.8  1360509.3       -0.5   6.7600     0
1 12802 142025  1360506.8  1360508.8       -2.0   6.7610     0
1 12805 142028  1360511.2  1360508.3        2.9   6.7610     0
1 12808 142031  1360507.6  1360507.8       -0.2   6.7610     0
1 12811 142034  1360507.5  1360507.3        0.2   6.7610     0
1 12814 142037  1360506.8  1360506.8       -0.0   6.7610     0
1 12817 142040  1360507.9  1360506.3        1.6   6.7610     0
1 12820 142043  1360509.2  1360505.8        3.4   6.7610     0
1 12823 142046  1360503.6  1360505.3       -1.7   6.7600     0
1 12826 142049  1360501.9  1360504.8       -2.9   6.7610     0
1 12829 142052  1360503.5  1360504.3       -0.8   6.7600     0
```

GMT LOW - START TIME OF INTERVAL FOR COMPUTATION OF BEST FIT QUADRATIC
GMT HIG - END TIME OF INTERVAL FOR COMPUTATION
YMAX - MAXIMUM DEVIATION IN MICROSECONDS OF A MEASUREMENT THAT WOULD BE ACCEPTED IN COMPUTING "BEST FIT" CURVE (± 1/2 AUDIO CYCLE PERIOD)
DIFMIN - LARGEST NEGATIVE ACTUAL RANGE MEASUREMENT DEVIATION FROM "BEST FIT" CURVE
DIFMAX - LARGEST POSITIVE ACTUAL RANGE MEASUREMENT DEVIATION FROM "BEST FIT" CURVE
DIFCHANGE - CHANGE IN RANGE, START TO END OF COMPUTED CURVE, MICROSECONDS
GMTHMS - GMT HOURS, MINUTES, SECONDS
TIMEACTUL - MEASURED TIME INTERVALS, MICROSECONDS
TIMEPREDT - VALUES OF COMPUTED CURVE FOR CORRESPONDING TIMES
DIFACTPRE - DISPLACEMENT OF ACTUAL MEASUREMENT FROM "BEST FIT" CURVE, MICROSECONDS
VOLTAGE - CORRELATOR OUTPUT AT CORRELATION
ERROR - BITS IN ERROR, ADDRESS CODE

Tone-Code Ranging Technique

The tone-code ranging technique used in the experiment has the following characteristics.

- Useful accuracy can be achieved within the modulation and radio frequency bandwidths of present-day mobile communications.
- The technique can be used with wide bandwidth for high accuracy.
- It requires only one channel for range measurement, receiving and transmitting in the simplex mode if desired without need for an antenna diplexer.
- The time required for a range measurement is a fraction of a second so that it can time-share a communication channel with little additional time usage of the channel.
- It can be implemented by the addition of an inexpensive, solid-state responder unit attached to a communication receiver-transmitter.
- It can, but need not, employ digital or digitized voice transmissions to provide synchronizing of the user responder, thereby further increasing the efficiency of channel usage.
- There are no "lane" ambiguities in the range measurements.
- User identification is simple and is confirmed in the return signal.

Range measurements from satellites are made by measuring the propagation time of a radio signal from the satellite to the user and return. The propagation time can then be converted to a range measurement by relating it to the known propagation velocity of the radio signals. The free-space propagation velocity must be corrected for ionospheric and atmospheric propagation effects. Propagation time is measured by placing a time marker in the form of a "tone-code" interrogation (Figure 3-5) on the transmitted signal and observing the time for the tone-code to go to the user and return. As used in the experiment, the interrogation signal is a short audio frequency tone transmission followed by a digital address code in which audio cycles are inhibited for zeros, transmitted for ones. Improved performance would result from the use of phase shift keying. The simpler format was chosen early in the experiment for convenience, and was not changed as its performance fulfilled the test requirements.

Each user transponder is assigned a unique digital address code. When the user's fix is to be determined, the tone burst followed by his address code is transmitted by the Observatory to one of the geostationary satellites, the "interrogating satellite", that repeats it. All of the users receive the satellite transmission, but the transponder that is addressed recognizes the address code automatically, and after a precise delay, retransmits the tone code. The satellites repeat the signal. The Observatory measures the intervals from the initial transmission to the first repetition by the interrogating satellite and to the times of the user's returns by each of the two satellites. With these measurements, it can determine the ranges from the two known positions of the satellites to the user. The range measurements determine two spheres of position centered at the satellites and having radii equal to the

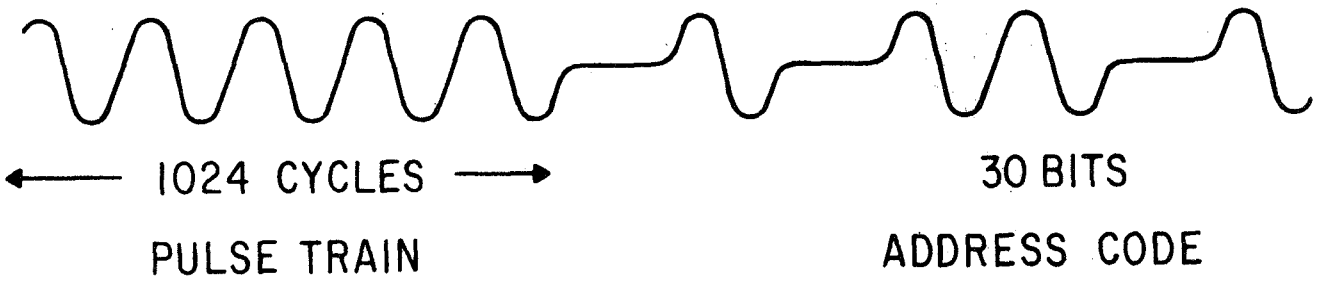

FIGURE 3-5. TONE-CODE RANGING WAVEFORM

measured ranges. A third sphere of position centered at the earth's center and having a radius equal to the earth's radius plus the user's altitude intersects the other spheres at two points — one in the northern hemisphere and one in the southern hemisphere. By a priori information, the proper point is selected at the user's location.

The tone-code frequency transmitted from the Observatory is 2.4414 kHz, derived by binary division from an accurate 10.0 MHz oscillator. The frequency is within the data bandwidth of conventional aircraft mobile communications equipment. It can be transmitted by frequency modulation, or any other modulation capable of transmitting a phase coherent audio tone. The tone duration is 1024 cycles and the code 30 bits, so that the tone-code duration is 0.43 second.

The tone-code signal is entirely compatible with voice communications and is of such short duration that it can be inserted during pauses in speech. The signals can be relayed by satellites designed for communications with aircraft without requiring any changes to the satellites and without adding a significant load to their communications capacity. The signals are also compatible with data-link digital communications. The phase of the digital clock for communications could also serve as the phase reference for ranging, and then the only signal necessary for ranging is the address code itself.

The user receives the tone cycles from the satellite on its communication receiver, as shown in Figure 3-6. All of the tone cycles received from the satellite, even though they may be interrogations from other craft, are applied to a phase matching circuit. A locally generated tone of the same frequency is also applied to the phase matcher, which adjusts the phase of the locally generated tone so that it corresponds to the phase of the received tone. The local tone is generated at the same frequency as the ground terminal tone within an accuracy of one part in 10^6 or better, an accuracy achievable from a moderately priced oscillator. The phase matcher accomplishes the phase match within 400 cycles and then averages over approximately 64 received cycles in establishing the timing of the locally generated phase. The averaging process improves the timing accuracy by the square root of the number of cycles averaged.

The locally generated tone is used to generate clock pulses that clock the received interrogation signal into an address code recognizer that consists of a shift register with summing circuits prewired to correspond to the digital address code of the user. Digital pulses timed from the received tone zero crossings are clocked into the address code recognizer. When the sequence of pulses representing the user's address code is clocked into the recognizer, it produces a single output clock pulse that opens a gate to interrupt the locally generated pulses that are clocking the shift register. The duration of the interruption is precisely controlled by a pulse counter. During the interval in which the clock pulses are interrupted, the user's transmitter is activated and the antenna is switched from the receiver to the transmitter. When the switching is completed, the locally generated 2.4414 kHz tone is transmitted until the end of the precisely measured interval. Clock pulses are then reapplied to the shift register and the address code is clocked out to key the audio tone to the transmitter and return the address code, back through the satellite to the ground station. Introduction of the delay while the antenna is switched eliminates the need for a diplexer in the user equipment. It also enables reception and retransmission to occur on the same frequency.

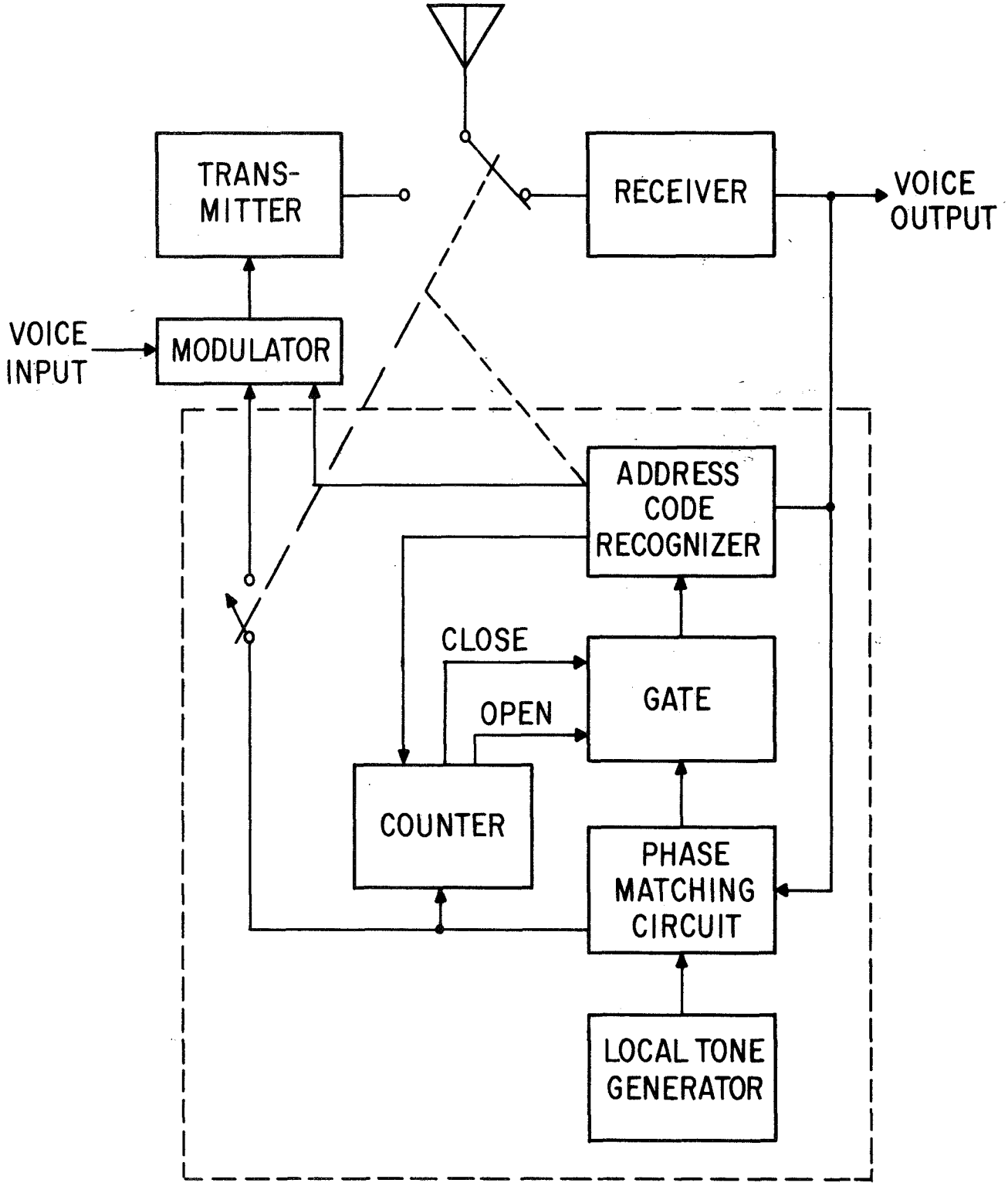

FIGURE 3-6. USER EQUIPMENTS

At the Radio-Optical Observatory, the receiver output is applied to an address code recognizer similar to that in the user equipment. Prior to the interrogation of an individual user, the taps of the summing circuit are switched to correspond to the code of the user to be addressed. When the address code is received from a satellite, a single output clock pulse occurs at the output of the summing circuit.

In the range measurement tests, time is measured from the transmission of the code to the first or "direct" return from the satellite and also to the second return, which is the user's response. The first interval, the known equipment delays, and estimated ionospheric delays are subtracted from the longer interval to yield a measure of the distance from the known position of the satellite to the user.

Equipment Description

General Electric's Radio-Optical Observatory serves as the ground terminal for the experiment. A photograph of the Observatory is shown in Figure 3-1. It is located near Schenectady, New York at 42°50'53" North latitude and 74°04'15" West longitude. The Observatory is part of the Company's Research and Development Center. Equipment used for the ranging and position fixing experiment is depicted in Figure 3-7.

A tone-code responder unit, shown in the photographs of the five circuit board cards and the assembled unit with its cover removed (Figures 3-8 and 3-9), is used with a mobile receiver and transmitter to form a transponder. The block diagram of a responder is depicted in Figure 3-10.

Each user responder performs the following sequence of functions:

1. Phase alignment of its own 2.4414 kHz clock with the received 2.4414 kHz signal prior to receiving the address code.

2. Recognition of its user address code. Each responder contains a shift register prewired for its own address.

3. Measuring a precise time delay of 1024 tone cycles duration, 419,430.4 microseconds.

4. At the start of the delay, switching transceiver from the receive mode to the transmit mode.

5. Supplying the properly phased tone modulation signal to the transmitter during the precisely known time delay.

6. Transmitting its digital address code starting precisely at the end of the delay.

7. Switching transceiver back to receive mode.

The unit employs a 10 MHz oscillator, with a long-term stability of one part per million, as its frequency reference. The oscillator is divided down by binary division to the tone frequency of 2.4414 kHz. A range measurement requires that the locally generated 2.4414 kHz signal be brought into phase with the 2.4414 kHz signal received from the satellite. At least 400 cycles of the

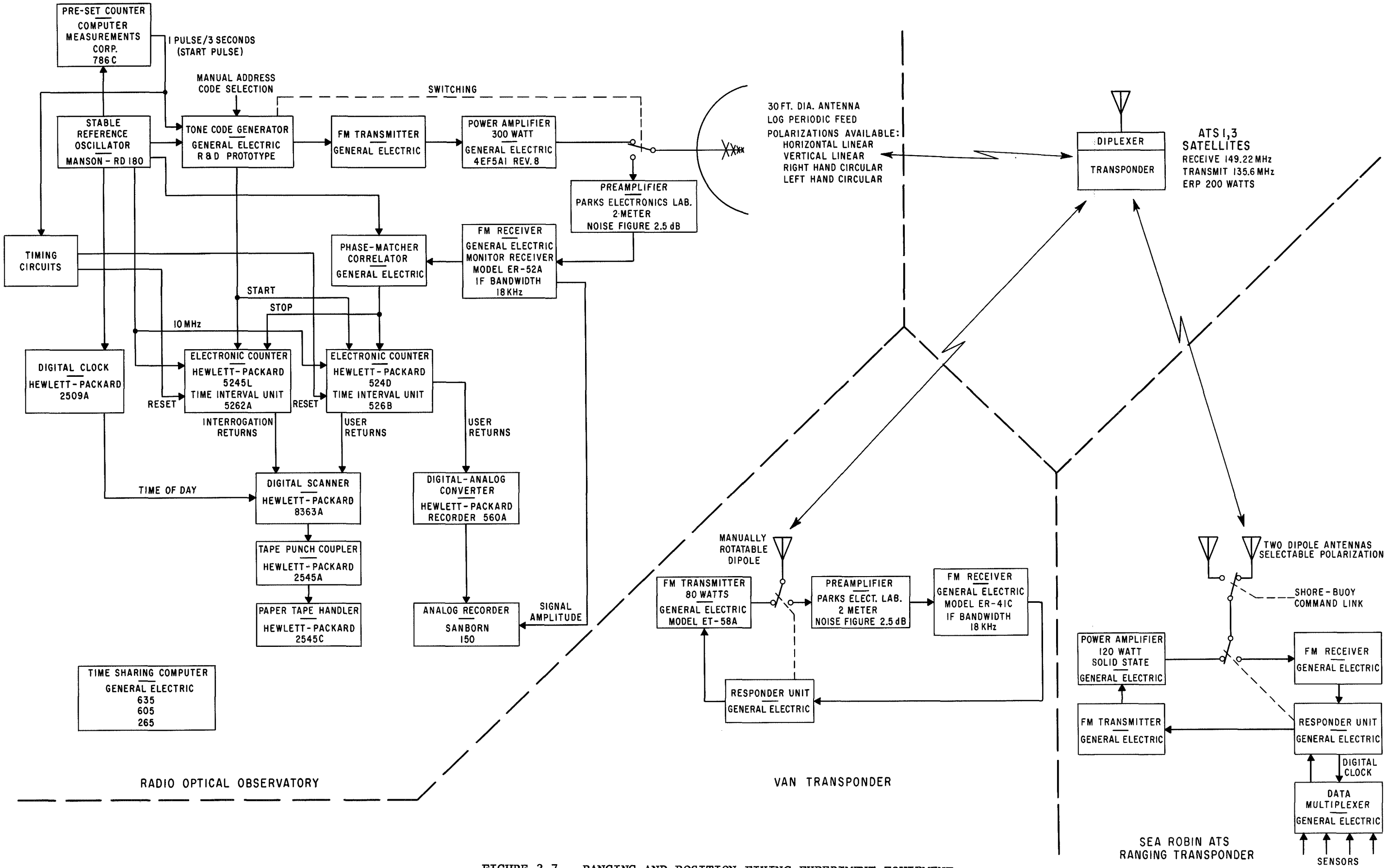

FIGURE 3-7. RANGING AND POSITION FIXING EXPERIMENT EQUIPMENT

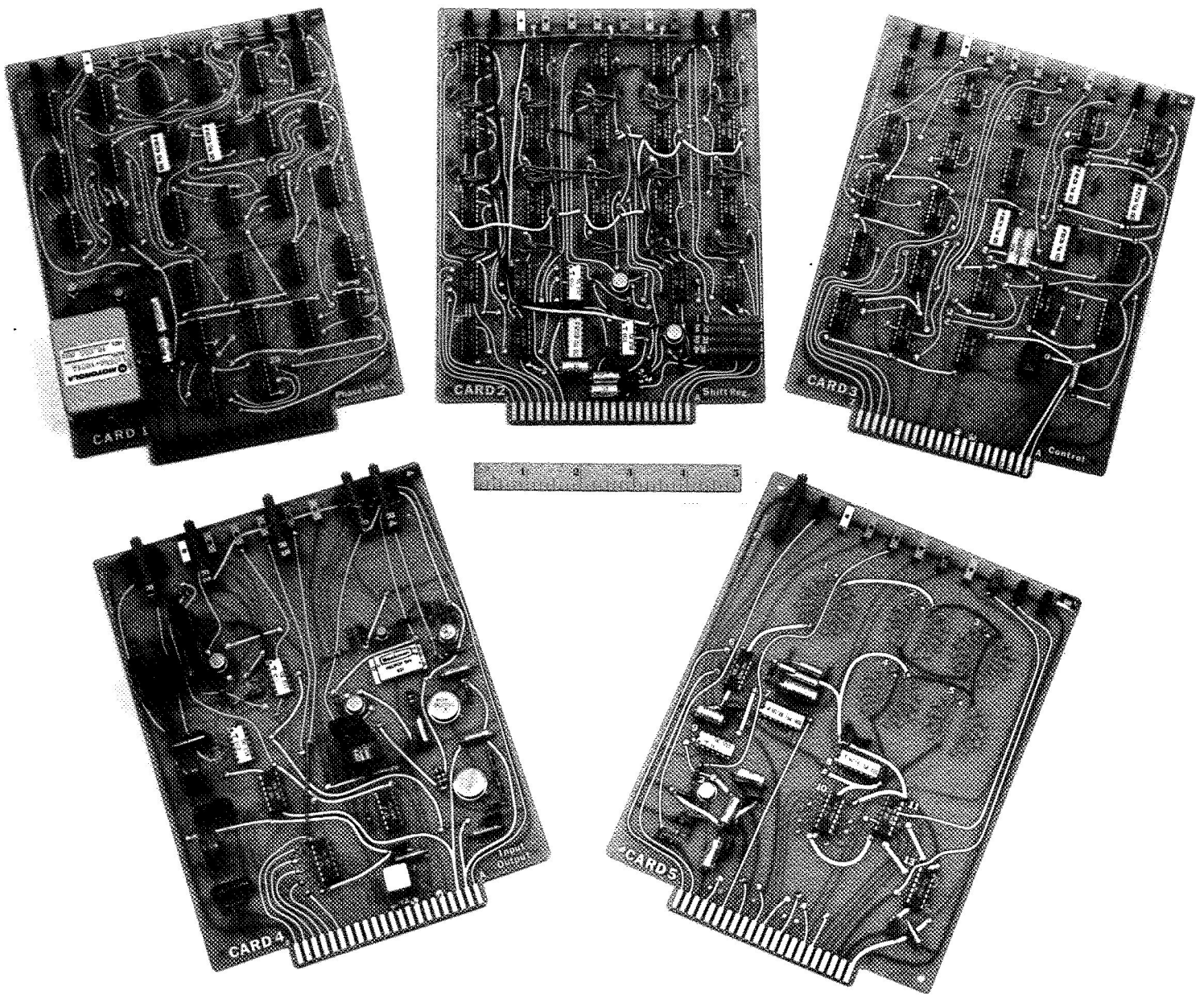

FIGURE 3-8. FIVE CIRCUIT BOARD CARDS

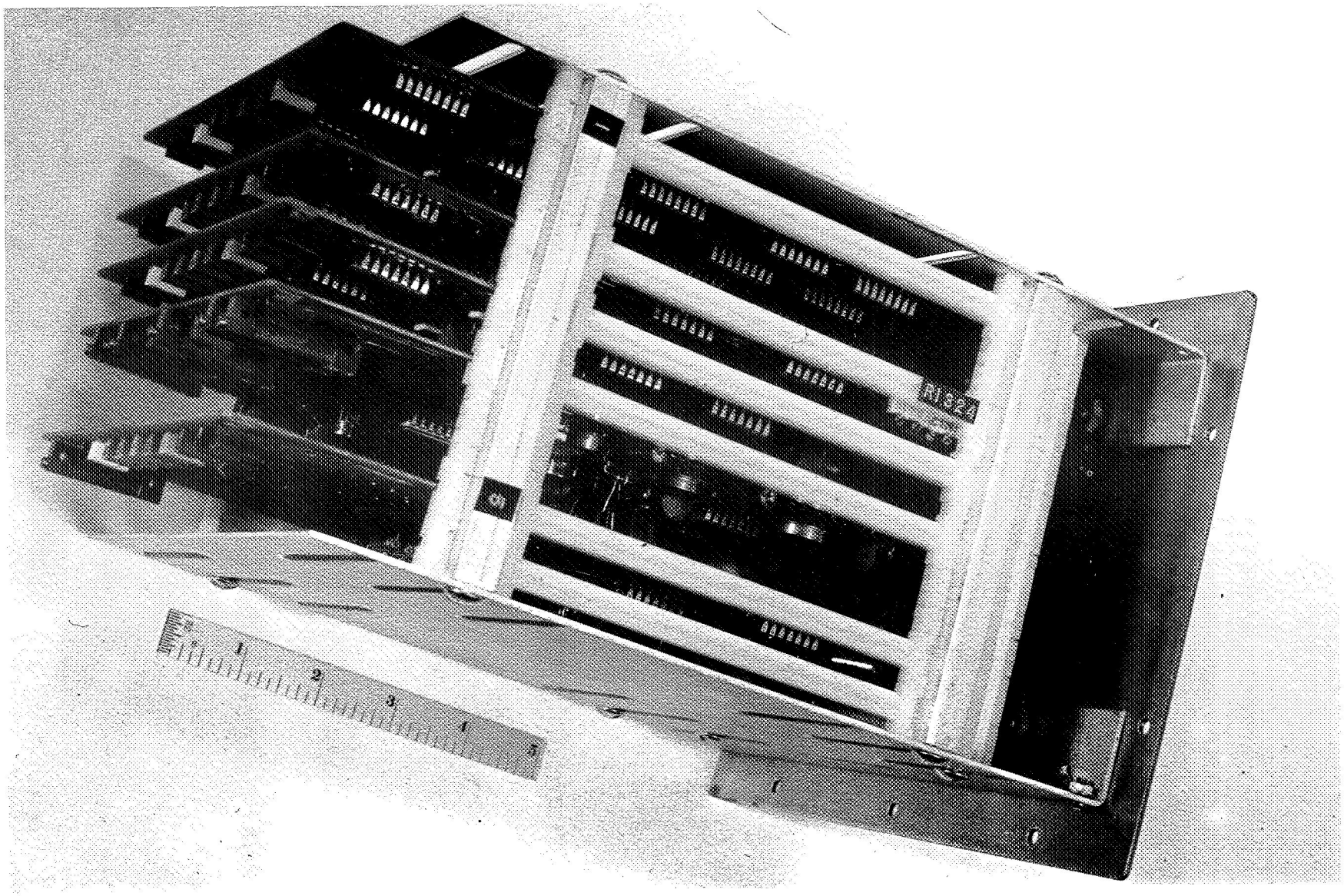

FIGURE 3-9. ASSEMBLED RESPONDER UNIT

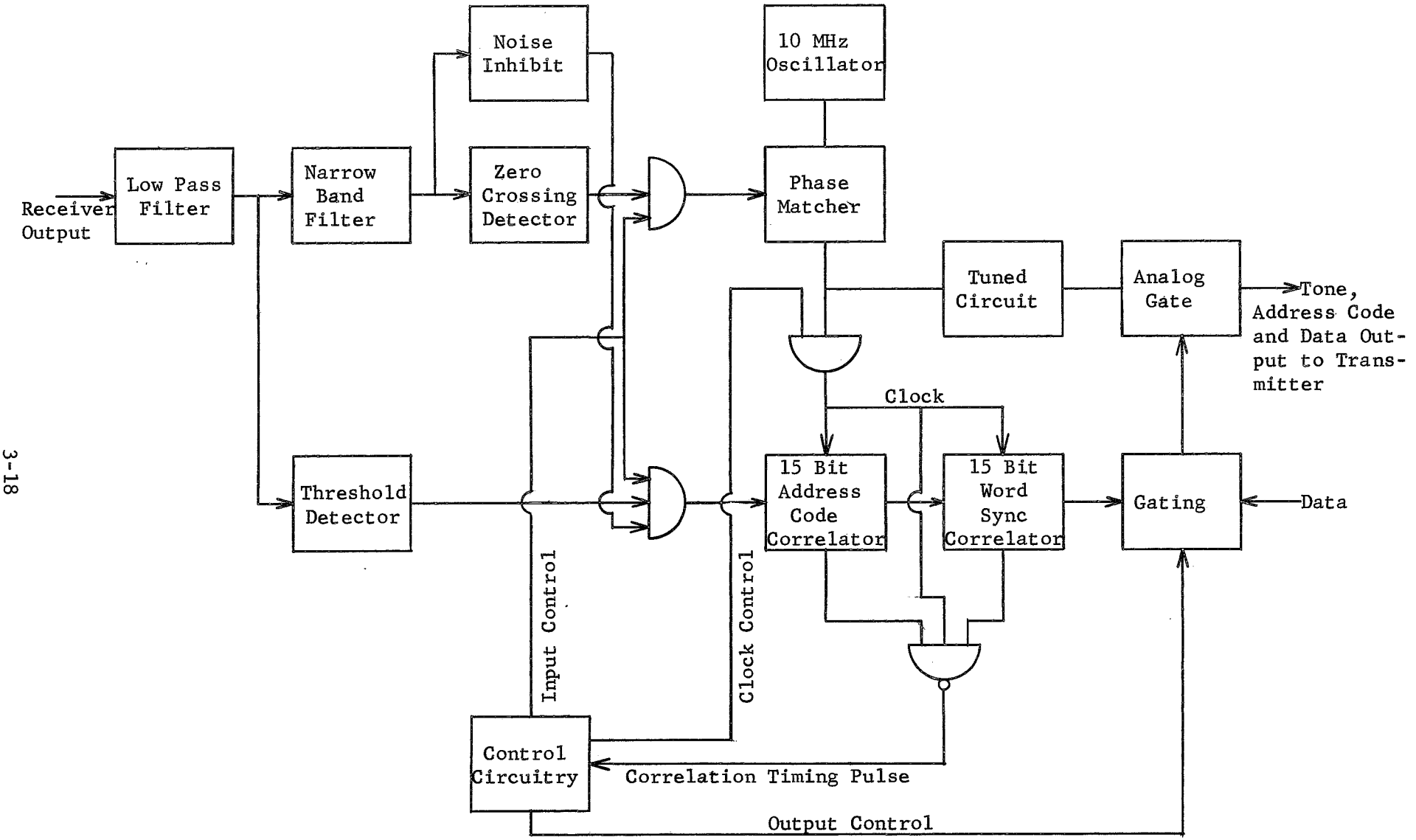

FIGURE 3-10
RESPONDER BLOCK DIAGRAM

tone must be received just before the address code to allow for phase matching and averaging. The received tone is passed through a tuned circuit of approximately 120 Hz bandwidth before its phase is compared with the locally generated 2.4414 kHz tone. Phase comparison for 400 cycles is sufficient to match the zero crossings of the received and locally generated tones to within 0.4 microsecond if the signal-to-noise ratio is high, and to average the effects of noise to an acceptable value if the ratio is low. Phase shifting the 2.4414 kHz is achieved by the addition or elimination of pulses in the divide down counter at the 2.5 MHz and 5 MHz levels.

The responder functions on a 30-bit user address code. The code consists of a 15-bit word synch and a 15-bit address. The 15-bit word synch is the same for all users. A unique 15-bit address is assigned to each user. This particular code configuration provides for 128 users with a minimum Hamming distance of 5.

The 15-bit address code shift register is wired specifically for the user's address. When the address is received following the tone, correlation occurs simultaneously in the 15-bit word synch shift register and in the 15-bit address shift register. The outputs of the shift register stages are summed in a current summing network. Centering of the word synch and address code in each of the correlators results in a peak voltage at the correlator output. The voltage peak is threshold detected and used to gate out the next clock pulse for timing purposes since the rise-time of the lead edge of the correlation waveform itself is not sufficiently accurate. The pulse starts a counter that measures a period of 1024 cycles of the locally generated tone. This timing pulse also switches the transponder into the transmit mode, and it then begins to transmit the locally generated, properly phased 2.4414 kHz tone back to the satellite. At the end of the precise time delay, the address code is transmitted. The transponder then returns to the receive mode and awaits further interrogations. During retransmission of the tone and address, the 2.4414 kHz clock has remained in phase with the previously received signal since following correlation no further input is presented to the phase matcher, thereby preventing noise from corrupting the phase alignment.

An additional feature of the responder is a noise inhibit circuit which prevents false correlations on noise during the absence of a received signal. This is achieved by half-wave rectifying, filtering and threshold detecting the output of the narrow band filter. This circuit is designed to respond only to the presence of the continuous synch tone. Once the presence of tone is detected, the received signal is then presented to the shift register.

The responder is digital. It is constructed on five printed circuit boards, 6 1/4 inches by 8 inches, and utilizes Fairchild DTL and T^2L dual in-line ceramic logic packages. The cards slide into a circuit board and connector mounting kit which is housed in an aluminum box, 6 inches by 8 inches by 10 inches. Its total weight is six pounds. A single connector on the front provides the necessary input and output functions. The power requirements are: +5 volts, 1.0 amp; +15 volts, 0.09 amp; -15 volts, 0.07 amp.

The tone-code generator and the phase matcher-correlator (Figure 3-11) in the Observatory are based on the same circuits. The printed circuit boards are designed so that they can be modified for use in a tone-code generator, a phase matcher-correlator, or a responder unit.

FIGURE 3-11
TONE-CODE GENERATOR AND PHASE MATCHER-CORRELATOR

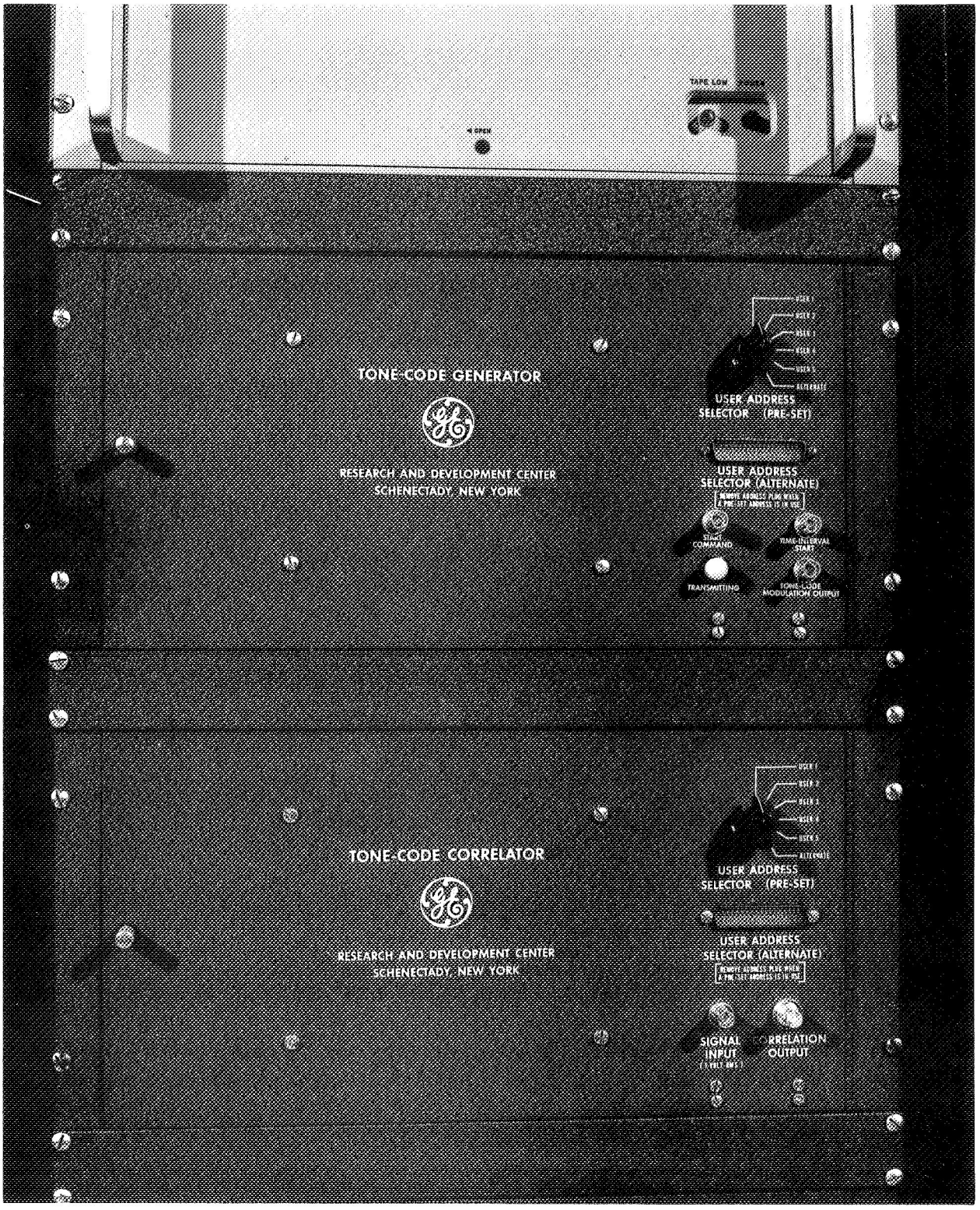

Computer Programs

The following computer programs were prepared for processing the data.

SLANTM

This GE MARK I time sharing code computes the slant range between: 1) a satellite with specified geocentric earth distance and its subsatellite longitude and geodetic latitude; and 2) a ground station whose coordinates are longitude, geodetic latitude and an altitude above the earth's surface reference ellipsoid. The flattening factor and equatorial radius presently being used are: 1/297 and 6.378166×10^6 meters.

OBSPROCi (+ files) i = 1, 2, 3, 4

These GE MARK II time sharing codes are used to process punched paper tape generated at the Observatory. The tape contains a sequence of many records each containing time (hours, minutes, seconds); two time delay measurements; and, in one version, voltage level data. These programs read the punched paper tape, check each record for completeness and correct format, and then perform least squares (second order) curve fitting versus time in a variety of options at the control of the user. The user can specify "interval markers" (N = 0, 1, 2, ... in number) which subdivide the total interval into N + 1 subintervals in each of which independent second order least squares curve fits are made. The program includes a variety of logic to exclude "wild points", such as a meaningless number printed when no response is received, from the least squares contribution. Standard output includes such quantities as the total number of observations, the number of which are taken as good points; the time at each boundary of the subintervals; the three coefficients associated with the second order model; the maximum and minimum error between the curve fit and "good" points in each subinterval; and an unbiased estimate of the standard deviation of the errors. Similar data are summarized for the whole interval. At the user's choice, various output tabulations are available showing the estimate and actual measurement and their difference along with various other time data.

The four versions are associated with that many different punched paper tape formats. Also, one version operates on the voltage level to give an indicated bit error rate in each subinterval.

LATCOM (+ files)

This code exists in two versions for both GE's MARK I and MARK II time sharing systems. One version is in a "conversational mode" for input, while the other reads files for input. The purpose of LATCOM is to compute a user's geodetic latitude, when given his longitude, altitude above the ellipsoidal first reference and slant range time delay information to one satellite whose ephemeris (geocentric earth distance, longitude and geodetic latitude) are available on a file containing date, time and the preceding quantities. The ellipsoidal earth is presently taken to have a flattening factor of 1/297 and a mean equatorial radius of 6.378166×10^6 meters. At present, the user manually inputs bias terms for equipment delays and corrections for ionosphere delays on propagation path.

POSFIX (+ files)

This GE MARK II time sharing code computes the user's longitude and geodetic latitude, when given his altitude above the ellipsoidal earth reference and slant range time delay information from two satellites whose geocentric earth distances, longitudes and geodetic latitudes are available in an ephemeris file which contains, in addition, date and time. In this code the effects of the ionosphere delays are computed on the basis of an empirical model as a function of the time of day at the intersection of the ray path with an ionosphere layer and the elevation angle associated with the slant range vector from the point on earth to the satellite. Internal to the computer program is a secant solution of two simultaneous nonlinear algebraic equations. This secant subroutine and an associated matrix inversion subroutine are called from the MARK II FSL Library programs.

SECTION 4. EQUIPMENT PERFORMANCE

Equipment design, performance, and usage influence the precision and accuracy of ranging measurements. The experiment provided an opportunity to evaluate limitations imposed by the equipment.

Bandwidth of the ranging signal influences the measurement precision. Radio range measurements can only be made by measuring propagation time, and that in turn by measuring the interval between a transmitted and received waveform. Although the modulating wave may take many forms, the highest range resolution that can be achieved is set by the ability to measure the phase of the highest frequency component in the waveform. Phase measurement precision is relatively independent of frequency. A precision of the order of one degree is usually achievable without refined techniques. The higher the frequency, the better the timing resolution.

The designer does not usually have an unrestricted choice of signal bandwidth. In the design of the ranging experiment, the radio frequency and audio frequency bandwidths of aircraft mobile communications were selected as limits. This appears to have been a proper choice, as it permits evaluation of the technique within practical limitations set by existing satellite communications equipment specifications and frequency allocations. The precision achieved within these bandwidth constraints was sufficient to resolve the VHF propagation effects.

Measurement precision is affected by noise, for noise causes a "jitter" of the signal phase. If the noise is random, the error may be reduced by averaging a number of measurements. As the signal-to-noise ratio becomes poorer, the amount of jitter increases, and the measurement precision decreases even if averaging is used. It is important in a ranging measurement that the precision be within acceptable limits at the poorest signal-to-noise ratio that is experienced. This was insured by the use of frequency modulation that yielded better signal-to-noise ratio of the detected signal than that of radio frequency signal, and by post-detection filtering. These techniques insured that an acceptable phase measurement precision was possible whenever the radio frequency signal was strong enough to be detected.

Accuracy is affected by the time delay variations of the equipment. The absolute value of the time delay is not important. If it does not change, it is subtracted from the measured interval in calculating the range. However, if the delay changes in an unknown way, it introduces an error that cannot be compensated. Electronic circuits are subject to changes in delay time, with the delay variations tending to be greater in narrow bandwidth circuits than in wide bandwidth circuits. Delay variations can occur in receivers as a function of signal level. Bandpass filters such as receiver IF stages may have time delay changes if the circuits are slightly detuned. Signals from different users operating in the same channel may experience different time delays if their carrier frequencies are not exactly the same. The effects may be minimized by the use of temperature-stable components and by careful alignment to assure a linear phase characteristic across a bandwidth that includes all significant frequency components of the signals. FM limiters may introduce time delay variations if they do not limit symmetrically about the IF zero crossings and discriminators may introduce changing time delays if they are improperly aligned.

The magnitudes of equipment time delay effects are a function of bandwidth and are independent of radio frequency. Wider bandwidth allocations at L-band than at VHF may be important if full advantage is to be realized from the better propagation characteristics.

All of the factors influencing precision and accuracy, including equipment delay characteristics and signal-to-noise ratio effects, were measured for the various equipments used in the experiment and the results of these measurements are presented in detail in this section.

Equipment Time Delay

Each electronic circuit contributes a time delay to the interval between the initiation of an interrogation and the final readout of the measurement at the ground station. The sum of these delays must be known precisely and subtracted from the total delay to yield the propagation interval. The range uncertainty introduced by uncertainty in equipment delay is the same as that for propagation time uncertainty, or approximately $\pm$ 500 feet for 1.0 microsecond. Although the equipment delays may total several hundred microseconds, they must be known to within limits appropriate to the accuracy required of the measurements.

For a statistical estimate of system performance, the delay uncertainties in ground equipment, satellite, and user equipment may be taken as the root-sum-square of their individual uncertainties since they are independent. The contribution of the ground station and satellite equipments can be maintained at a low value because they are in stable environments, and because they are available to the ground terminal for frequent measurement and compensation or calibration.

An operational system would include many user equipments subject to a wide variety of environmental conditions and maintenance skills. It may be impractical to expect that each user equipment be preset and maintained to have a predetermined time delay within the limits assigned for equipment time delay in the error budget of the system. If this is true, a better procedure may be for the ground terminal to determine each user's time delay when the user is at a known location. The delay may then be stored with the user's address in the computer memory. Computer program designers advise that automatic calibration in this manner is simple and does not tax the computer memory.

Narrow bandwidth circuits are more apt to contribute time delay uncertainty than wider bandwidth circuits, because a phase error caused by a nonlinear phase characteristic in a filter represents a larger time error at a low frequency than the same phase error at a higher frequency. Experience in designing equipment for the experiment indicates that filters employing active components are subject to larger time delay uncertainties than filters employing only passive components. Digital switching and logic circuits can be designed to keep their time delay variations to a negligible value.

Tone-code ranging has a distinct advantage because it does not require an antenna diplexer. In a separate program, a diplexer for reception of 157.86 MHz and transmission on 154.89 MHz was tested in a vehicle on a cold winter day and found to have intolerable time delay variations, depending on its temperature. A diplexer for use with a ranging technique that requires

simultaneous reception and transmission by the user equipment would have to be carefully designed to have a constant time delay over a wide temperature range. A diplexer co-located with an aircraft or ship antenna would be subject to large temperature changes.

For any active ranging technique, the user receiver must be designed for minimum time delay variations. Receivers designed for communications may have time delay variations with tuning and with signal amplitude. Tuning variations can be minimized by the use of crystal control and proper alignment for a linear phase versus frequency characteristic in the IF and other bandwidth limiting circuits. Carrier phase locking is helpful if the received signal frequency is not accurate.

During the experiment, no significant changes in time delay with tuning were observed with any of the crystal-controlled receivers. Time delay variations with signal amplitude were observed. One Bendix RTA41B aircraft receiver was measured to have approximately 1.5 microseconds total variation in delay over its dynamic range. It is understood that an objective in the design of the receiver was to minimize time delay variations. A General Electric ER-52-A receiver, designed for mobile communications without consideration to time delay variations, was found to have a total variation in time delay of approximately 7 microseconds. A different limiter was substituted for the original and the total variation reduced to less than 1 microsecond, as shown in Figure 4-1.

Figures 4-1 through 4-5 show equipment time delay as a function of signal strength and of tuning for several receivers.

Signal-to-Noise

Noise added to the demodulated tone causes jitter of the zero crossings that are used for the timing measurement. Probable phase error on one cycle may be estimated by a vector addition of the signal and noise phasors. Assuming that the noise has a gaussian distribution, which is the usual case when receiving signals from the satellite, the one sigma probability phase error is the angle in radians between the signal vector and signal-plus-noise resultant when the signal and noise vectors are at right angles, as follows:

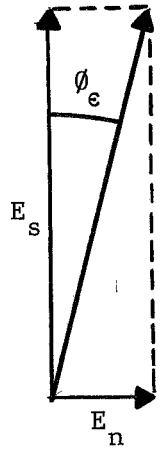

FIGURE 4-1

DELAY VERSUS SIGNAL STRENGTH AT THREE FREQUENCIES
GE TYPE ER-52-A MONITOR RECEIVER
ORIGINAL LIMITER REPLACED BY SPECIAL TUNED LIMITER

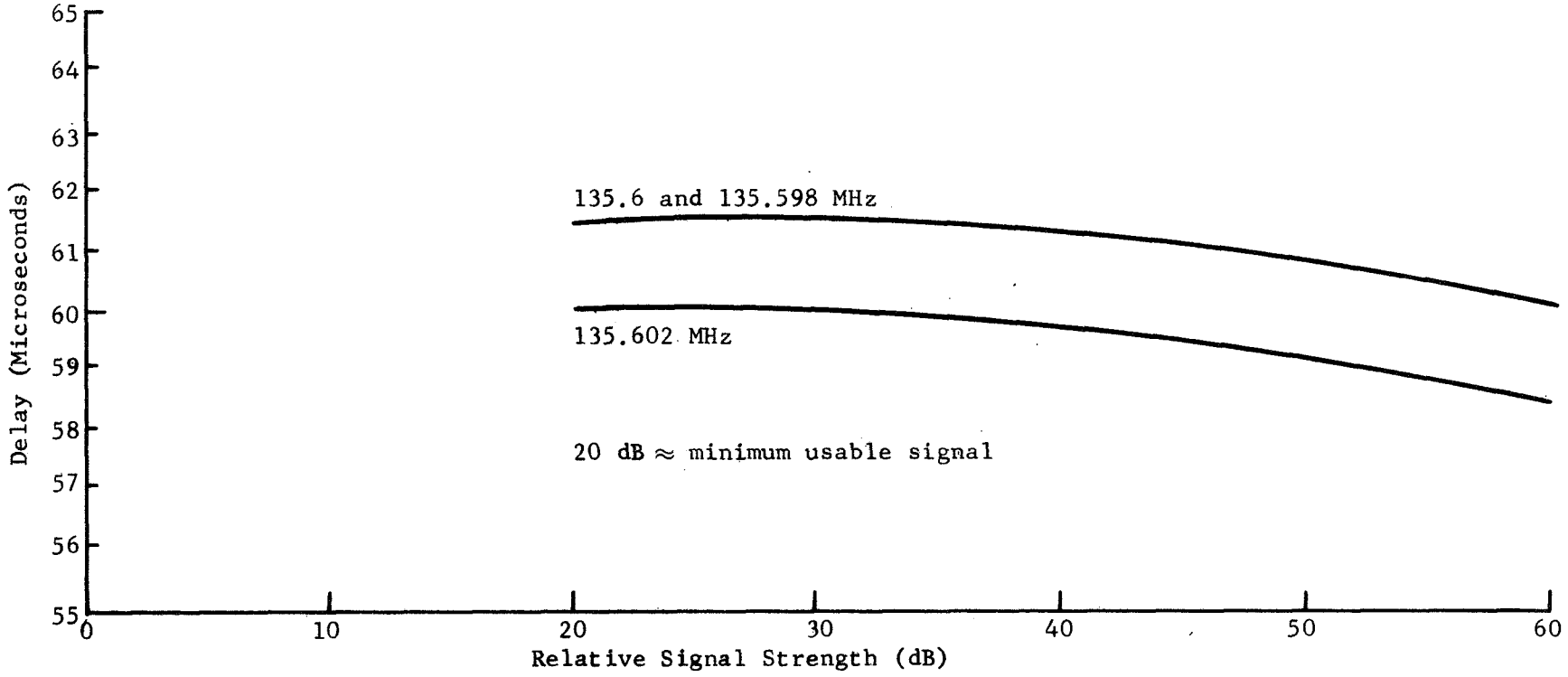

FIGURE 4-2

DELAY VERSUS SIGNAL STRENGTH
GE TYPE ER-41-C RECEIVER, MODEL 4ER41C10-21
ORIGINAL LIMITER REPLACED BY SPECIAL TUNED LIMITER

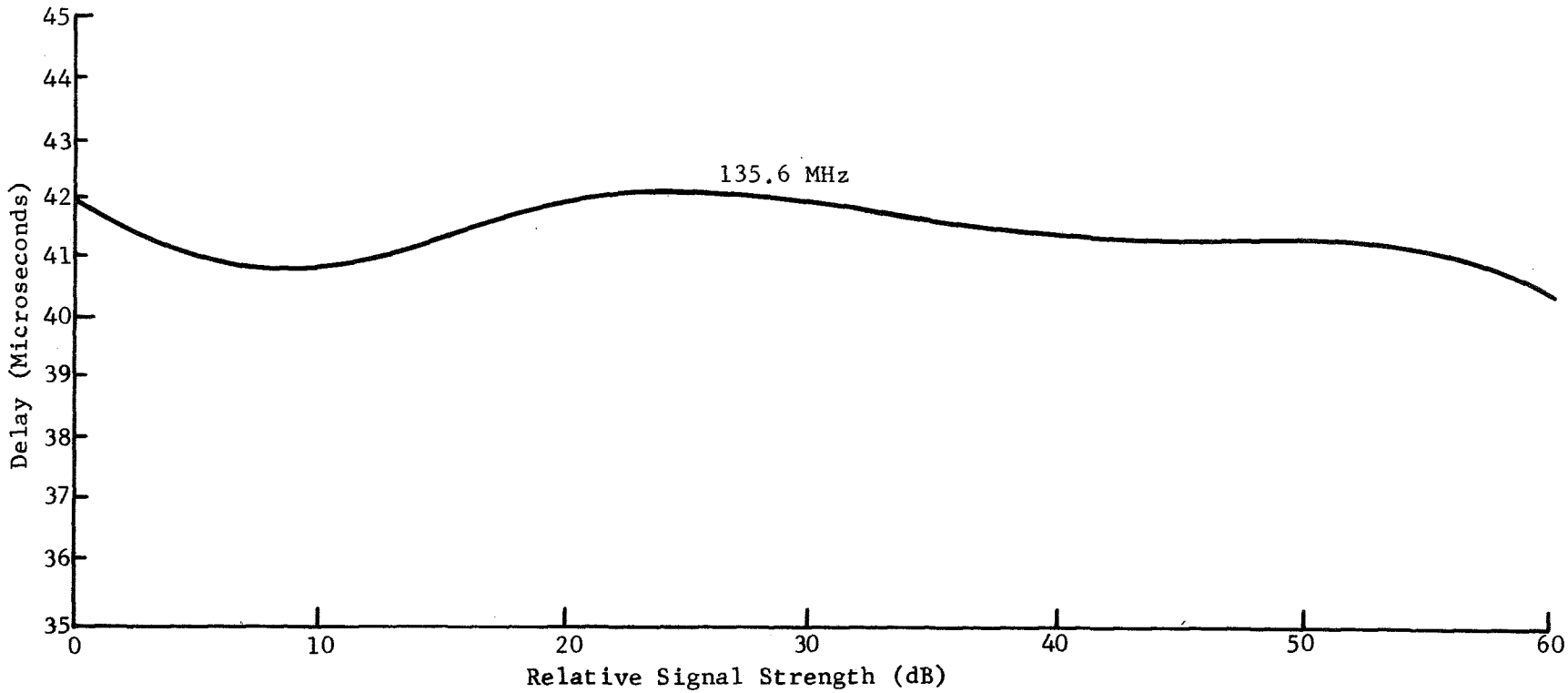

FIGURE 4-3

DELAY VERSUS SIGNAL STRENGTH
SMALL HAND TRANSCEIVER - GE PORTABLE PR36RDS66, NO. 9051072)
(VALUES APPROXIMATE DUE TO STRAY SIGNAL LEAKAGE)

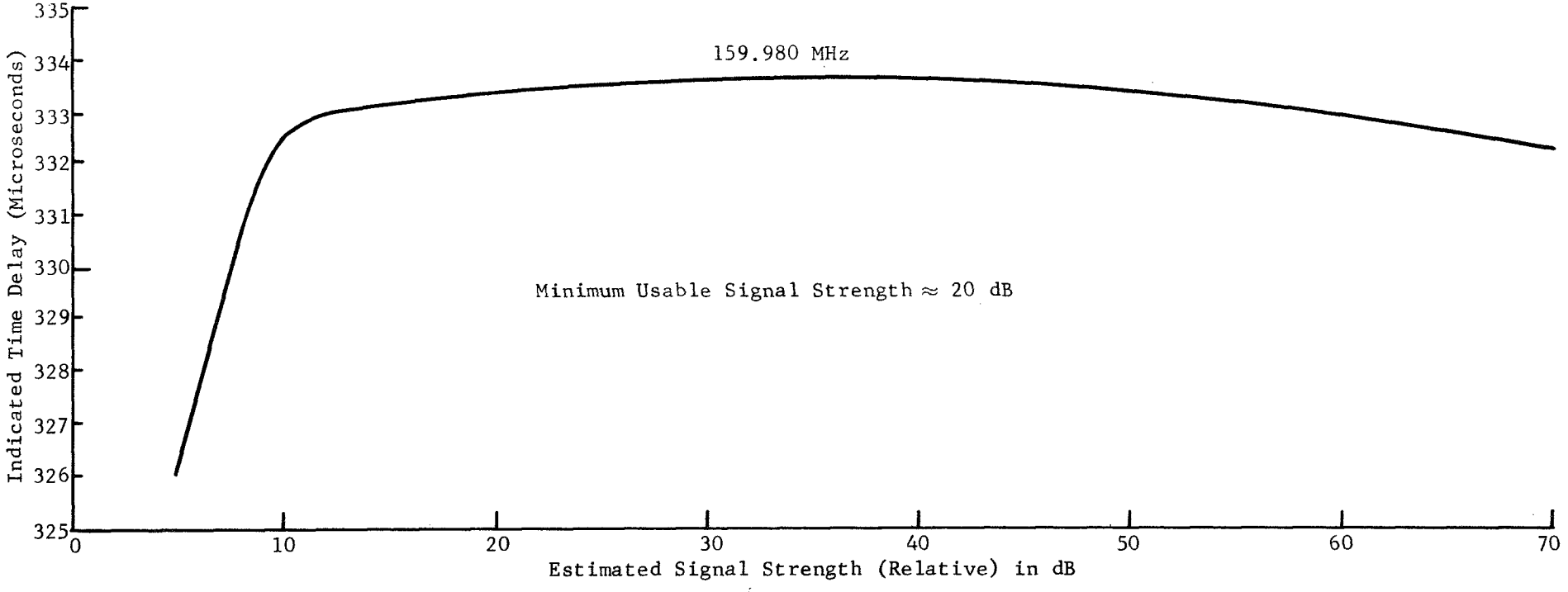

FIGURE 4-4

DELAY VERSUS FREQUENCY
GE TYPE ER-52-A MONITOR RECEIVER

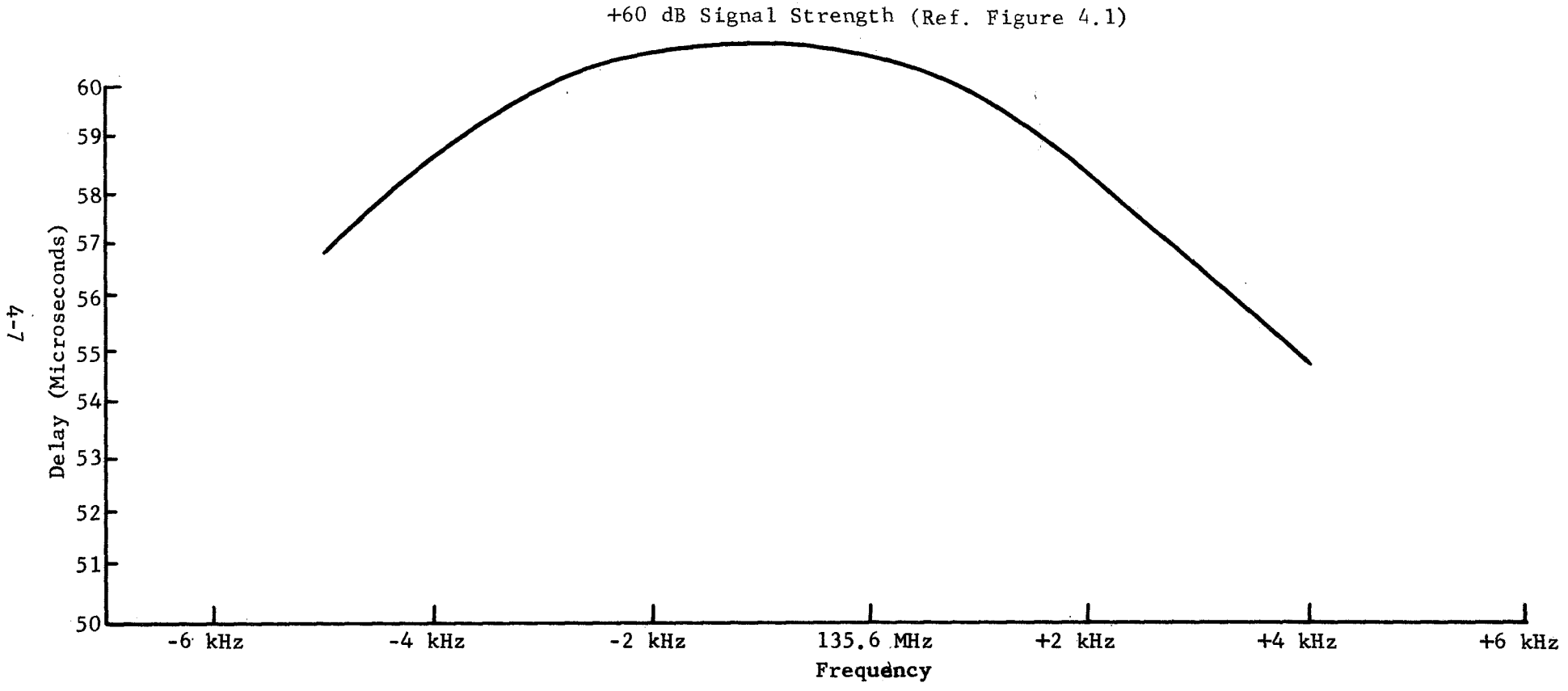

FIGURE 4-5

DELAY VERSUS FREQUENCY
GE TYPE ER-41-C RECEIVER, MODEL 4ER41C10-21
ORIGINAL LIMITER REPLACED BY SPECIAL TUNED LIMITER

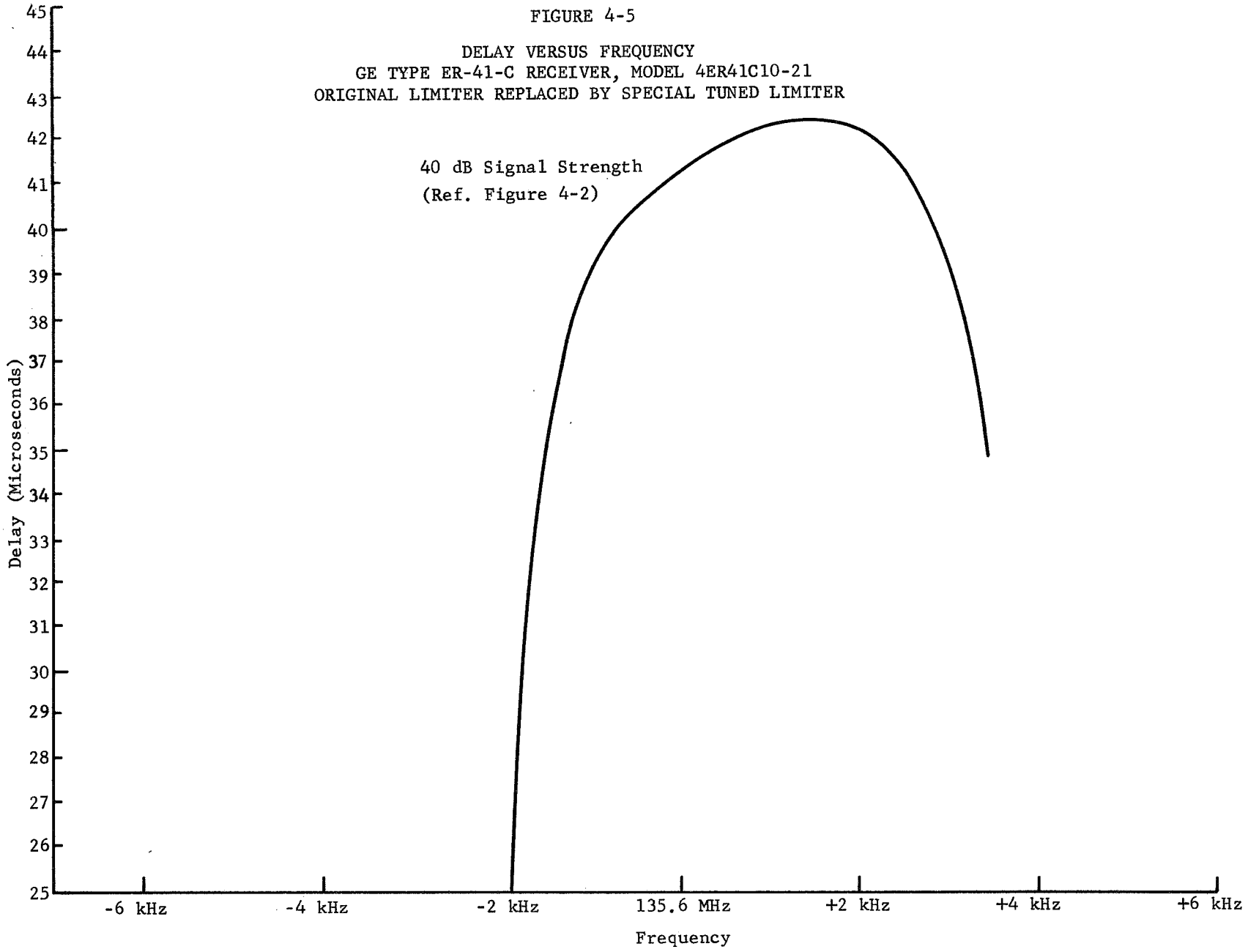

where E_n = RMS noise voltage
E_s = signal voltage
ϕ_ϵ = 1 sigma phase error in radians

$$\text{Signal-to-noise ratio, dB} = 20 \log \frac{E_s}{E_n}$$

The phase measurement precision is improved by the square root of the number of cycles averaged.

For the narrow bandwidth frequency modulation used in the experiment, the minimum signal-to-noise ratio for detection is 5 dB in the 15 kHz bandwidth of the receiver. The equivalent signal-to-noise ratio out of the 4 kHz bandwidth detector is 10 dB. The detected 2.4414 kHz tone is passed through a 120 Hz bandpass filter before it is applied to the phase detector. Considering fluctuation noise, the signal-to-noise improvement provided by the bandpass filter is 4000/120, or 15 dB. The lowest signal-to-noise ratio into the phase detector is thus $\approx$ 25 dB. The one sigma phase error on a single cycle is

$$\phi_\epsilon = \frac{1}{\sqrt{320}} \times 57.3^\circ \approx 3^\circ$$

The phase measurement is averaged over approximately 64 cycles, to provide an improvement of approximately 8. The one sigma phase error should thus be 0.4 degree.. As the period of one audio cycle is 409 microseconds, the timing precision should be

$$0.4 \times \frac{409}{360} \approx 0.45 \text{ microsecond}$$

Measurement of responder performance shows that the theoretical precision was not achieved at the detection threshold. Figure 4-6 relates RF signal-to-noise ratio and one sigma timing precision as determined in laboratory tests. Although the experimental results are worse than the theoretical by a factor of 3:1, the range measurement variation does not exceed practical limits at the lowest received signal levels; i.e. if the signal can be received at all, it is precise enough to be used.

Tests were conducted to determine the performance of the phase matching and correlation process with various signal-to-noise ratios. The tests were performed at baseband (no RF link) by summing the output of the ground terminal tone-code generator with fluctuation noise and feeding the resulting output directly into the ground terminal correlator. The ground terminal correlator uses the same phase matching process as a responder. RMS-signal-to-RMS-noise ratios were measured at the output of the 4 kHz low pass filter used in both the ground terminal correlator and a responder. The signal was held constant at 1 volt RMS while the noise was adjusted to give the desired signal-to-noise ratio. Each was measured in the absence of the other using a Hewlett-Packard 1400A RMS voltmeter. A block diagram of the test set-up is shown in Figure 4-7.

The test consisted of determining the standard deviation and number of bits in error in the 30 bit user code in the absence of additive noise and for signal-to-noise ratios between 20 dB and 0 dB.

Data were collected for ten minutes for each signal-to-noise ratio. The code generator was caused to give an output once per two seconds resulting in 300 correlations for each test condition. The time interval measurements for

FIGURE 4-6

STANDARD DEVIATION AS A FUNCTION OF
SIGNAL-TO-NOISE RATIO WITHIN A 4 kHz AUDIO BANDWIDTH

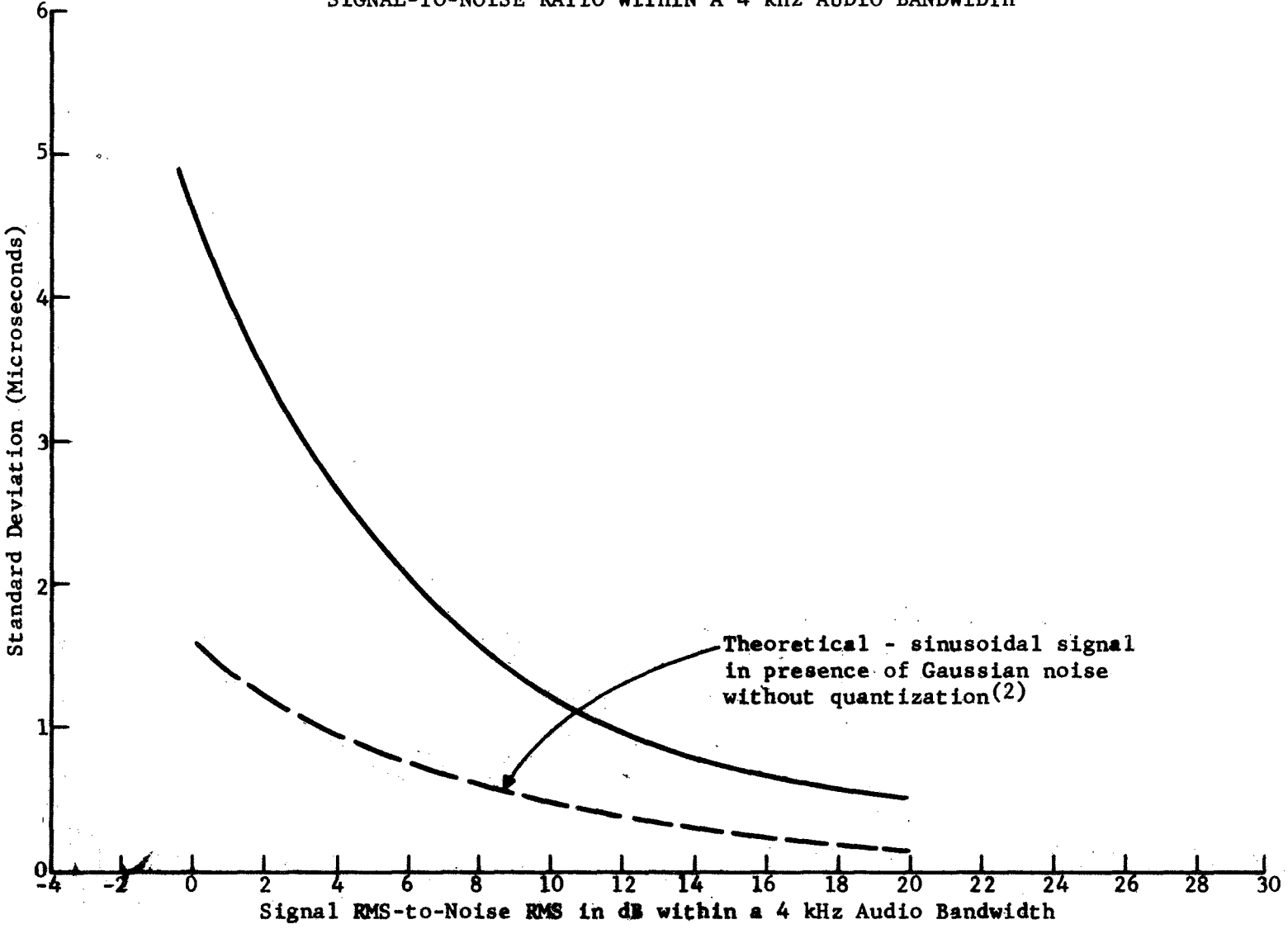

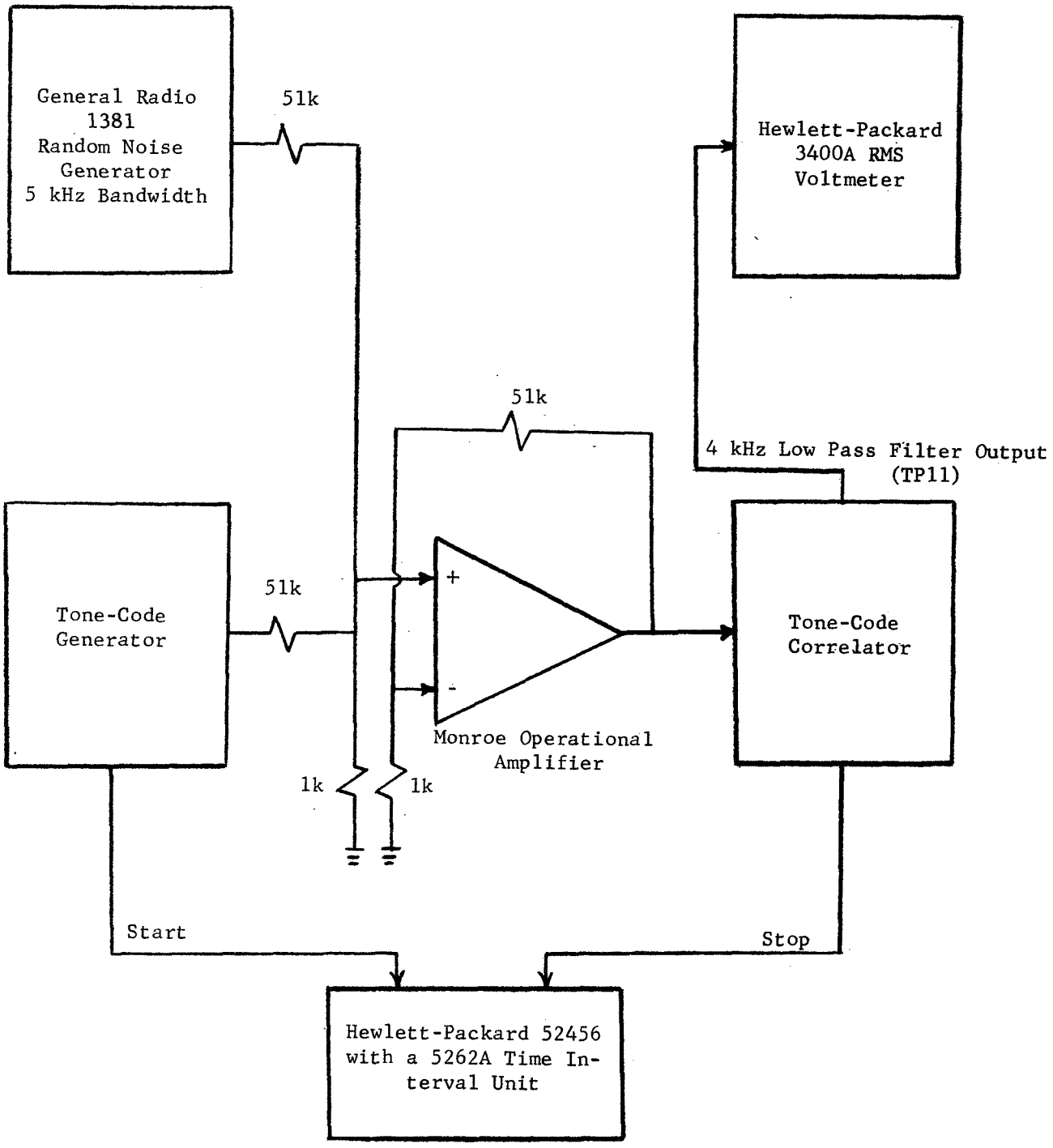

FIGURE 4-7

EQUIPMENT PERFORMANCE TEST

determining the standard deviation were the intervals from code generation to correlation.

Since each correlation involves the monitoring of a code which is 30 bits in length (15 bits word synch plus 15 bits address), the maximum number of bits monitored during the ten minutes is 9,000. For each missed correlation, the number will be reduced by 30 bits.

The results of the test are presented in Table 4-1. The bits in error are shown for both the word synch and address since they were monitored independently. The total bits in error is their sum. Also presented are the number of missed correlations and the maximum deviations from the mean in both positive and negative directions. The number of bits monitored is 9,000 minus 30 times the number of missed correlations. P_E is the bit error probability and was calculated by dividing the number of bits in error by the number of bits monitored.

During the test, as during all the experiments, the correlator threshold levels on both word synch and address were set such that correlations will not occur if there are more than 3 bits in error in either word synch or address.

Bit error probability, percent correlations and standard deviation, are each plotted as a function of signal-to-noise ratio in Figures 4-8, 4-9 and 4-6 respectively. The distributions of time interval measurements (histogram) for each signal-to-noise ratio are presented in Figures 4-10 through 4-16.

A measure of system performance in terms of accuracy and reliability is provided by comparison of the solid and dashed theoretical curves shown in figures 4-6 and 4-8 respectively.

The term reliability is used here in reference to the probability of a successful correlation. This is directly related to the bit error rate. Figure 4-8 presents bit error probability as a function of signal-to-noise ratio within a 4 kHz bandwidth. The dashed curve is theoretical[1] and is representative of that which can be achieved using an optimum filter. Both curves are for on-off modulation. Comparison of these curves indicates that the present system is operating below optimum by a maximum of 3 dB. System reliability can be improved by 3 dB if phase modulation (polar) is used.

A measurement of system accuracy is provided in Figure 4-6. The dashed curve which provides a measure of system performance was derived based on material presented by Mischa Schwartz[2]. In his material, he derives the probability density function for the phase of a sinusoidal signal in the presence of gaussian noise.

The expression for $f(\theta)$ is as follows: (Ref. 2)

$$f(\theta) = \frac{e^{-S^2}}{2\pi} + \frac{1}{2}\sqrt{\frac{S^2}{\pi}} \cos\theta\, e^{-S^2 \sin^2\theta}\,[1 + \operatorname{erf}(S\cos\theta)]$$

where S = signal-to-noise voltage ratio. For $S^2 = 0$ (no signal) the equation reduces to $f(\theta) = 1/2\pi$, as expected. For signal-to-noise ratios $\gg 1$ and $|\theta| < 5^\circ$, this expression reduces to

TABLE 4-1
EQUIPMENT PERFORMANCE TEST DATA

S/N RATIO	STANDARD DEVIATION IN μs	MAXIMUM DEVIATION FROM MEAN IN μs		NUMBER OF BITS IN ERROR		TOTAL BITS IN ERROR	NO. OF MISSED CORRELATIONS	NO. OF BITS MONITORED	P_E
		POSITIVE	NEGATIVE	WORD SYNC	ADDRESS				
>20 dB*	0.4046	1.27	1.54	0	0	0	0	9000	--
20 dB	0.5161	1.99	1.59	0	0	0	0	9000	--
18 dB	0.5663	1.66	1.96	0	0	0	0	9000	--
16 dB	0.6225	2.25	1.79	1	0	1	0	9000	0.00011
14 dB	0.8192	2.18	2.01	11	6	17	0	9000	0.0019
12 dB	0.9368	2.39	2.48	35	25	60	0	9000	0.0067
10 dB	1.283	3.33	3.29	142	116	258	0	9000	0.0287
8 dB	1.619	5.00	4.23	276	244	520	7	8790	0.059
6 dB	2.003	6.25	5.31	394	332	726	30	8100	0.090
3 dB	2.951	7.24	7.29	388	365	753	80	6600	0.114
0 dB	4.566	12.86	12.10	258	238	496	200	3000	0.165

*Noise Generator Off

FIGURE 4-8

BIT ERROR PROBABILITY AS A FUNCTION OF
SIGNAL-TO-NOISE RATIO WITHIN A 4 kHz AUDIO BANDWIDTH

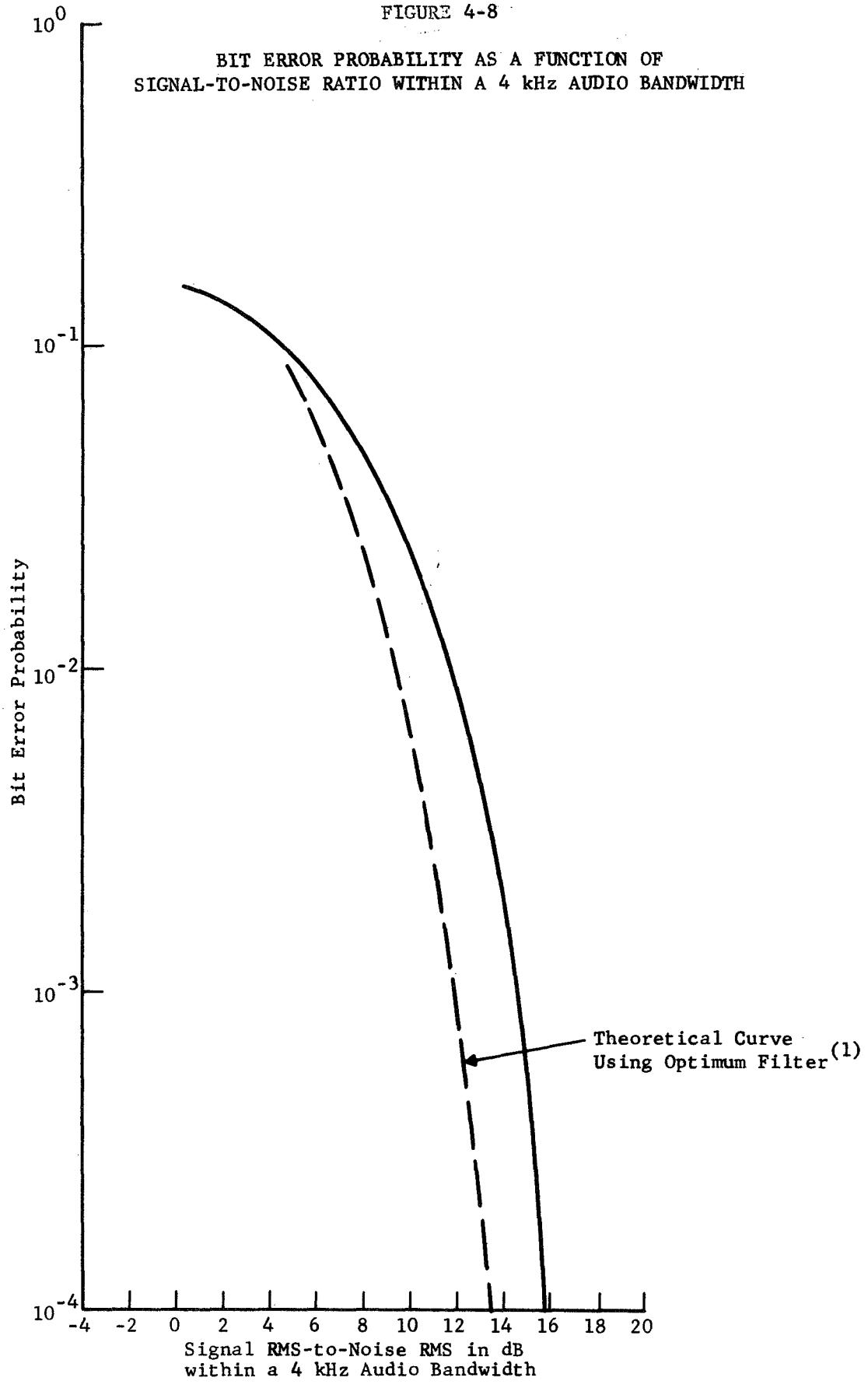

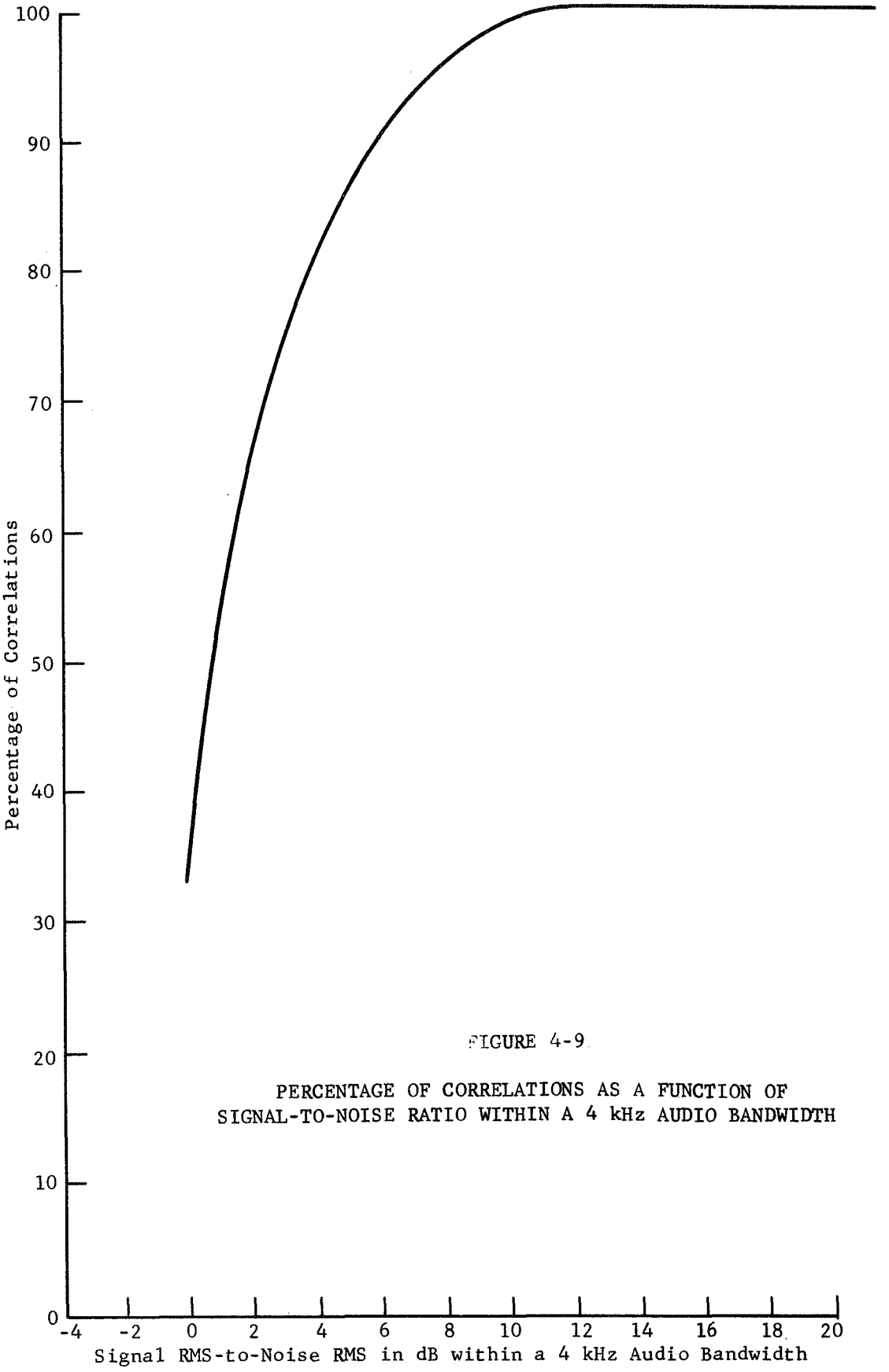

FIGURE 4-9

PERCENTAGE OF CORRELATIONS AS A FUNCTION OF
SIGNAL-TO-NOISE RATIO WITHIN A 4 kHz AUDIO BANDWIDTH

FIGURE 4-10

DISTRIBUTION OF TIME INTERVAL MEASUREMENTS FOR SIGNAL-TO-NOISE RATIO OF ≥20 dB WITHIN A 4 kHz BANDWIDTH, I.E. NOISE GENERATOR OFF

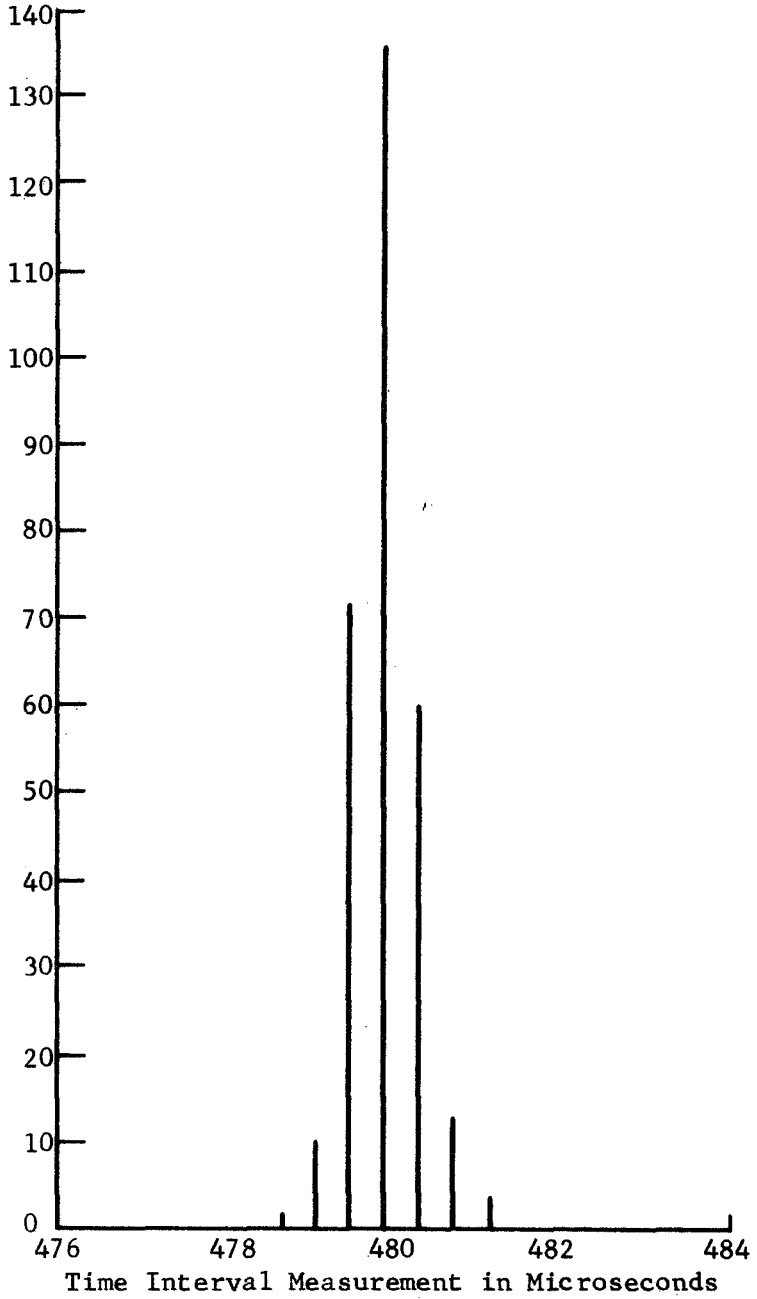

Standard Deviation 0.4046
100 Percent Correlations

FIGURE 4-11

DISTRIBUTION OF TIME INTERVAL MEASUREMENTS
FOR A SIGNAL-TO-NOISE RATIO OF 18 dB
WITHIN A 4 kHz BANDWIDTH

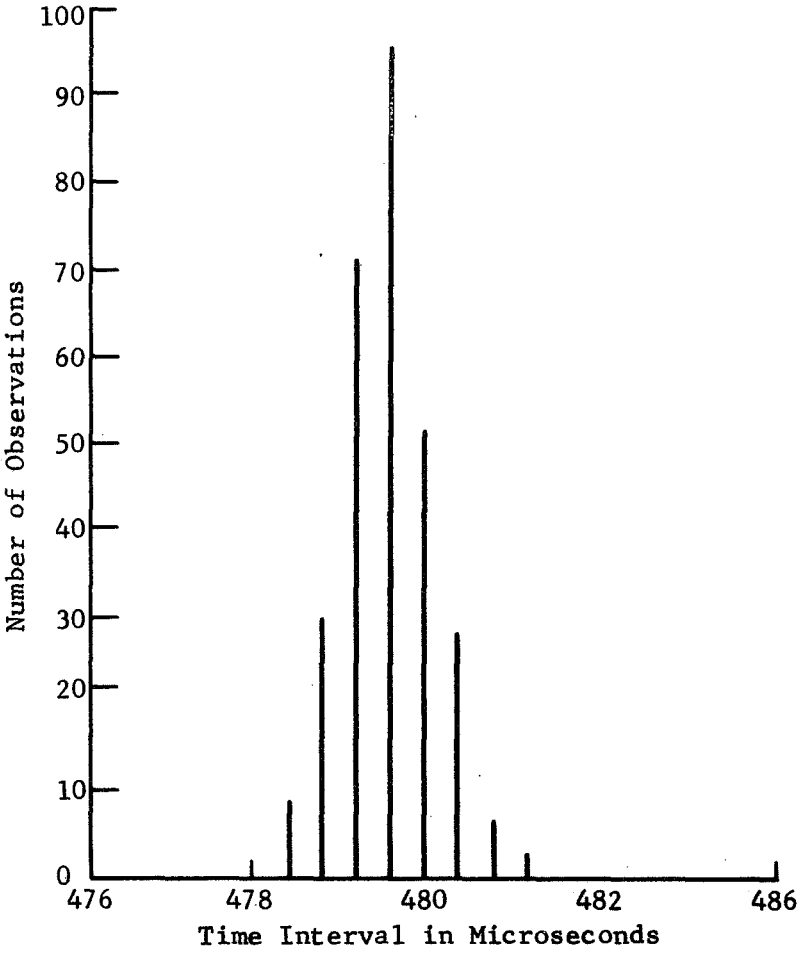

Standard Deviation 0.4046
100 Percent Correlations

FIGURE 4-12

DISTRIBUTION OF TIME INTERVAL MEASUREMENTS
FOR A SIGNAL-TO-NOISE RATIO OF 14 dB
WITHIN A 4 kHz BANDWIDTH

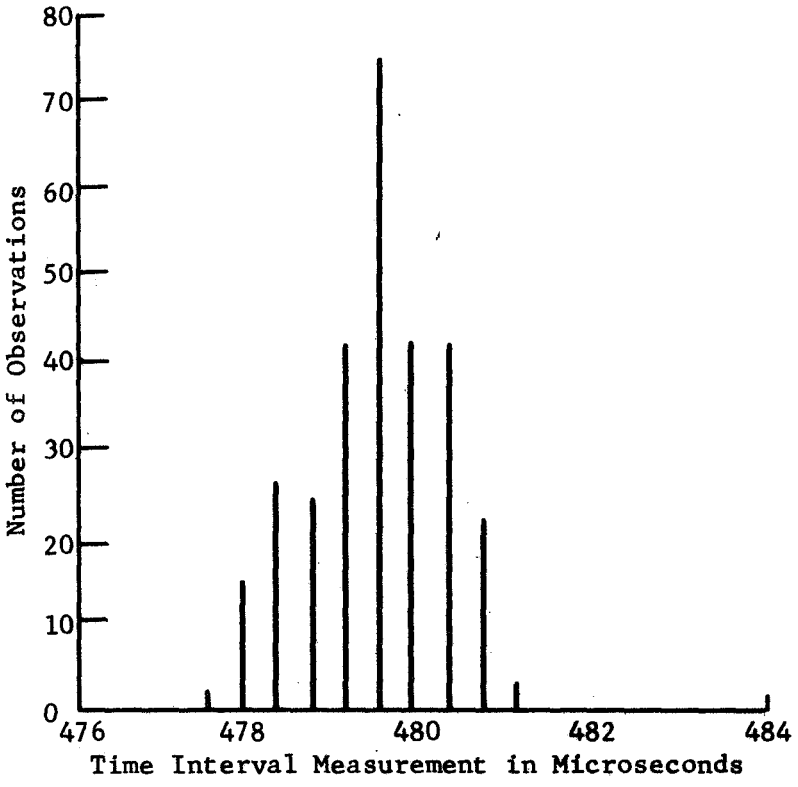

Standard Deviation 0.8192
100 Percent Correlations

FIGURE 4-13

DISTRIBUTION OF TIME INTERVAL MEASUREMENTS
FOR A SIGNAL-TO-NOISE RATIO OF 10 dB
WITHIN A 4 kHz BANDWIDTH

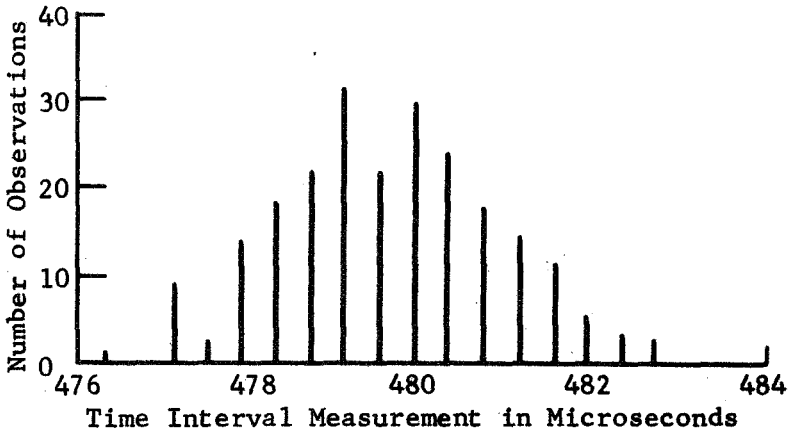

Standard Deviation 1.283
100 Percent Correlations

FIGURE 4-14

DISTRIBUTION OF TIME INTERVAL MEASUREMENT
FOR A SIGNAL-TO-NOISE RATIO OF 6 dB
WITHIN A 4 kHz BANDWIDTH

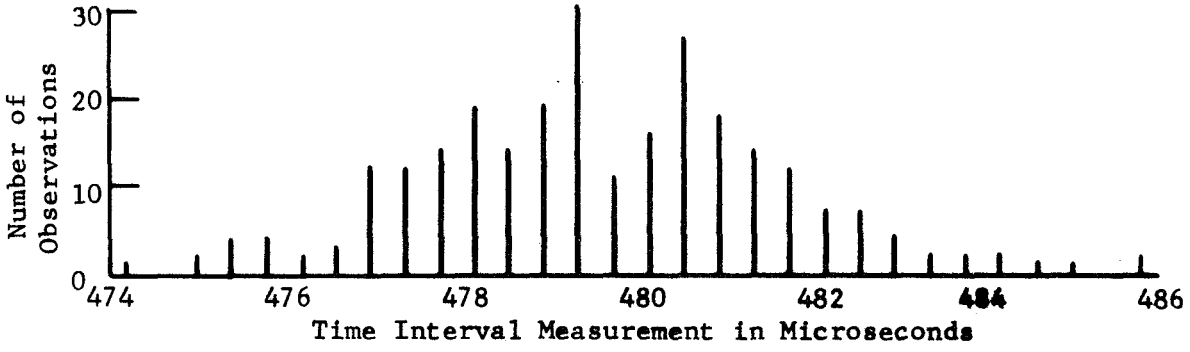

Standard Deviation 2.003
90 Percent Correlations

FIGURE 4-15

DISTRIBUTION OF TIME INTERVAL MEASUREMENTS FOR A
SIGNAL-TO-NOISE RATIO OF 3 dB WITHIN A 4 kHz BANDWIDTH

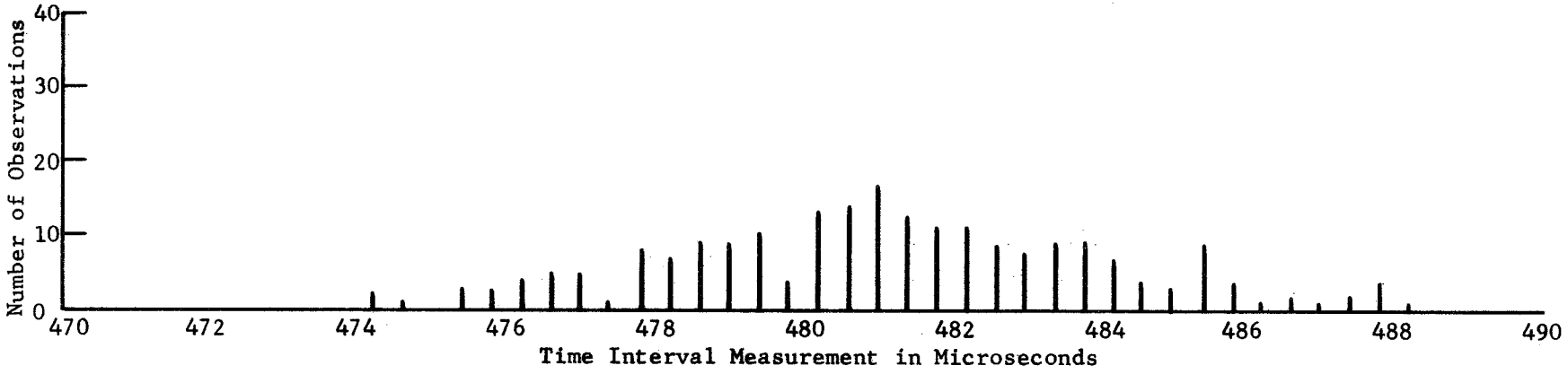

Standard Deviation 2.951
74 Percent Correlations

FIGURE 4-10

DISTRIBUTION OF TIME INTERVAL MEASUREMENTS FOR A
SIGNAL-TO-NOISE RATIO OF 0 dB WITHIN A 4 kHz BANDWIDTH

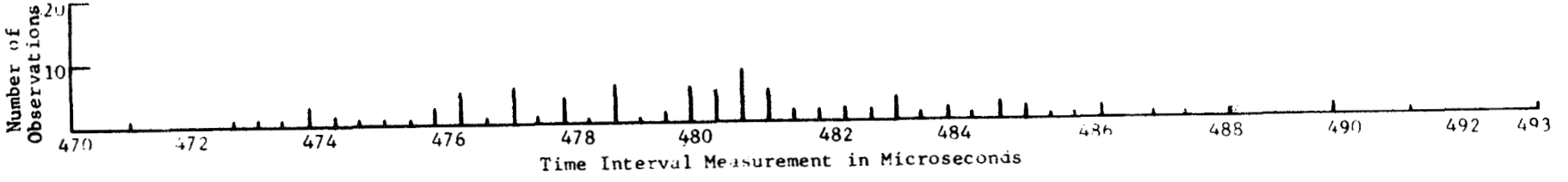

Standard Deviation 4.566
33 Percent Correlations

$$f(\theta) = \frac{e^{-S^2\theta^2}}{\sqrt{\pi/S^2}}$$

This represents a gaussian distribution with zero mean and standard deviation

$$\sigma = \frac{1}{S\sqrt{2}} \text{ radians.}$$

The digital phase lock loop has a bandwidth of approximately 5 Hz resulting in a 30:1 improvement on the signal-to-noise ratio at the output of the 4 kHz low pass filter. If signal-to-noise ratios of 0 dB and greater within a 4 kHz bandwidth are considered, then the expression

$$\sigma = \frac{1}{S\sqrt{2}}$$

is valid. This is applicable since the equivalent signal-to-noise ratio within the loop bandwidth is $\geq$ 30 dB (ratio of 30:1) which is much greater than 1. The dashed curve was generated by calculating the standard deviation as a function of signal-to-noise ratio using the expression

$$\sigma = \frac{1}{S\sqrt{2}}$$

radians and converting to microseconds via the relationship

$$1 \text{ rad} = \frac{180}{\pi} \text{ degrees}$$

and one period of a 2.4414 kHz waveform is equal to 409 microseconds. Therefore

$$\sigma = \frac{1}{S\sqrt{2}} \text{ radians} \times \frac{180 \text{ degrees}}{\pi \text{ radians}} \times \frac{409 \text{ microseconds}}{360 \text{ degrees}}$$

or

$$\sigma = \frac{46}{S} \text{ microseconds}$$

A comparison of these curves indicates a possible 3:1 improvement in accuracy.

Interrogation Response Rate

Many thousands of interrogations were made to ranging transponders during the experiment. The usual interrogation rate was once each three seconds although interrogation rates of once each two seconds and once per second were also used successfully. During some interrogation periods, the transponders relied on nearly every interrogation but during some periods the interrogation rate was lower than would be acceptable in an operational system. There were

several factors that contributed to lower response rates, some of them deliberately designed into the experiment to study propagation effects, and some factors that suggest precautions that must be taken in the design of a ranging system.

The poorest propagation link was usually the one from the satellite to the transponder. Irregularly shaped antenna patterns, Faraday rotation, and sea reflections sometimes caused the signal level into the vehicle transponder to drop below the detection threshold. Signal amplitude scintillation due to the ionosphere occurred infrequently but was observed. Scintillation causes amplitude fading over a large range at VHF and can cause the signal to fall below the detection threshold.

The Sea Robin buoy was interrogated a total of 2525 times during the periods of April 14 through 25, 1969 and May 9 and 10, 1969. One thousand seven hundred eleven responses were received at the Observatory. Of these, 860 resulted in successful range measurements. The design of the experiment caused a deliberate reduction in the response rate in order to observe the effects of Faraday rotation. Interrogation periods were three minutes long. The best receive polarization for the buoy was selected just prior to the three minute interrogation period and that receive polarization at the buoy was used throughout the entire test period. The responses from the buoy during the first minute and one-half were of the same polarization as the receiver but during the second minute and one-half they were transmitted with the orthogonal polarization. Since the up-link and down-link paths are at different frequencies and Faraday rotation varies as $1/f^2$, the preferred orientation of linearly polarized antennas can be different at the two frequencies. During that period of the experiment the ground terminal antenna had vertical or horizontal polarization but the polarization was the same for both transmission and reception. At a later time the ground terminal was arranged for independent selection on a transmission and reception. The effects of Faraday rotation were evident in these experiments because signal levels were often much better when different polarizations were used for transmission and reception. If the satellite were circularly polarized the response rate would be improved by reducing the effects of Faraday rotation.

Signals reflected from the sea combined with the direct signal from the satellite to enhance or reduce the signal level into the antenna. When the direct and reflected signals arrive in phase, the signal level can be as much as 3 dB stronger than the direct signal alone, but when they arrive out of phase they tend to cancel and the signal level may drop below the detection threshold. For a vehicle with an antenna a few wavelengths above the sea surface, as on a ship or the Sea Robin buoy, the effect is to produce an antenna pattern with lobes representing good signal reception alternating with nulls in the vertical plane. As the sea surface tilts and the antenna moves due to the action of the waves, the lobe pattern moves in elevation angle to cause an alternate enhancement and cancellation of the received signal. In the experiment the transmitted and received wavelengths were different, making the lobe patterns different for reception and transmission. A successful interrogation occurred when the lobe patterns permitted adequate signal strengths on both the up and down links. Tone-code ranging requires a signal duration shorter than the roll period of a buoy or ship and therefore a successful interrogation can be made except when a null in the pattern is directed toward the satellite. Other techniques that require longer signal transmissions for range measurement may suffer greater deterioration due to the rolling of the craft. The effect of sea reflection can be minimized by

the use of circular polarization on the satellite and the craft, if the elevation angle to the satellite is above the Brewster angle. Then the rotation sense of the reflected signal is reversed, its amplitude is reduced relative to the direct signal and the depth of the nulls is reduced.

Sea reflections affect received signal amplitude in aircraft much as they do in ships. Because of the higher altitude, the nulls are very closely spaced in elevation and aircraft can fly for several seconds in straight and level flight if the satellite is abeam, but if the aircraft is flying towards or away from the satellite or climbing or descending it passes through the interference pattern quickly and rapid fading of the signal may be experienced. An antenna pattern designed to discriminate against the reflected signal can reduce or nearly eliminate the effect. The use of circular polarization on the satellite and aircraft would be helpful.

Lower response rates were experienced in aircraft when using the VHF blade antenna than when using the Satcom antenna, due in part to sea reflections, but also to the poor azimuth and elevation pattern characteristics of the VHF blade. During some periods of flight the response rate approached 100 percent for the aircraft when the Satcom antenna was in use. In certain flight directions using the VHF blade antenna, the response rate was as low as 10 or 20 percent, especially when the aircraft was in a noisy environment as whey flying in the vicinity of thunder storms.

The mast and other structures of the Cutter Valiant had a large effect on the pattern of the omnidirectional antenna. When the low gain circularly polarized antenna had a clear view in the direction of the satellites, the interrogation response rate was nearly 100 percent. When the mast was between the satellite and the antenna, the response rate dropped to below 50 percent.

Scintillation in the reception of a VHF signal from a satellite results from focusing of the signals due to horizontal gradients of electron density in the ionosphere. The columnar electron content seldom varies more than two percent, so the gradients have very little effect on the propagation delay time and therefore do not significantly affect the accuracy of range measurements. However, the focusing of the energy causes the signal strength to be high at some points on the ground and low at other points. Because the density variations move horizontally, the signal strength observed at a fixed point may vary from a strong enhancement to almost complete cancellation. The fading periods vary from seconds to minutes. The signal level may fall below the detection threshold for periods on the order of a few seconds. The proportion of time that the signal is below the threshold is in part a function of the fading margin designed into the propagation links, but it would not be practical to allow sufficient margin to guarantee 100 percent response at VHF frequencies. The effect is smaller at higher frequencies. Scintillation is experienced at high latitudes more frequently than at mid-latitudes. The effect on a ranging system need not be serious if the ranging techniques require short interrogation periods, although it may require that a user be interrogated more than once during the times when scintillation is present in order to insure that a response is obtained.

The transmission links from ATS to the experimental transponders were considered to be marginal. However, it is concluded from the experiments that modest design changes would insure reliable performance at VHF. These design changes would include the use of circular polarization on the satellite

and more suitable design of the antennas on the mobile vehicles. While greater effective radiated power from the satellite would be desirable, it would probably not be necessary.

An occasional false correlation was experienced in the mobile craft, and at the terminal. Under noisy conditions false correlations were observed more than one percent of the time. A one percent false correlation rate would not be acceptable in a system involving a large number of user craft, for there would be frequent transmissions from craft that were not interrogated, thus tending to increase interference on the transmission links. Several simple measures are now apparent that would improve the design of the codes and insure an acceptably low rate of false interrogations. These improvements include the use of phase reversal modulation in the codes to improve the signal-to-noise ratio by 3 dB and gating to insure that the correlators search only for the code and are not activated by noise during periods when code transmissions are not being received.

Experience gained during the program has resulted in the definition of engineering design changes which could result in reliable performance within the cost, size and power constraints used in the experimental design.

REFERENCES

1. W. R. Benett, and J. R. Davey, Data Transmission, McGraw-Hill, 1965, page 114.

2. M. Schwartz, Information Transmission Modulation and Noise, McGraw-Hill, 1959, page 412.

SECTION 5. ATMOSPHERIC PROPAGATION EFFECTS

A major objective of the experiment was to obtain data on the effect of the ionosphere on the ranging and position fixing accuracy of range measurements from satellites at VHF. The up- and down-link frequencies of the ATS satellites are near the lower limit that may be considered for useful range measurements.

The largest effect of the ionosphere is propagation time delay because the index of refraction of the ionosphere is different than that of free space. In addition to the time delay the refractive effect causes bending of the ray so that the ray path length between the satellite and the earth's surface is increased.

The presence of the earth's magnetic field in the ionosphere causes a rotation of the plane of polarization of a radio signal, called Faraday rotation, that can influence the strength of a received radio signal unless circular polarization is employed.

There is a propagation delay or radio wave retardation in the troposphere as well as in the ionosphere. Tropospheric retardation is independent of frequency. At sea level, 100 percent humidity, and zero elevation, it is 116 meters(1). It decreases with increasing elevation angle from the observer to the satellite and his altitude.

A summary of atmospheric propagation effects is presented in Table 5-1.

Ionospheric Bias Error

The ionospheric retardation at VHF is usually much greater than the tropospheric retardation. During undisturbed daytime and nighttime conditions the one-way range bias due to tropospheric and ionospheric retardation is as shown in Figure 5-1. It is expected that corrections based on predictions of electron content in the ionosphere may reduce the bias errors of the ionosphere to within 20 to 40 percent of the total bias.

If calibration stations were used in conjunction with range determination measurements it is probable that corrections to less than 10 percent of the total range bias might be achieved in the region surrounding the station assuming that the distance from the satellite to the station were accurately known. The calibration stations could be equipped with repeaters like those used in mobile craft. The known range from the satellite would be subtracted for a calibration range measurement to derive an accurate range correction.

Unpredictable solar disturbances can cause changes in the ionosphere that can increase range bias by more than 50 percent over the values shown in Figure 5-1 at high latitudes and cause even larger changes in tropical regions. If range measurements from two satellites were used for fix determination without an applied correction, the effect of the disturbance would be an apparent systematic displacement of all the craft in a limited area. The relative position determinations of these craft would not be significantly affected.

More data are needed on the size of the area in which the information from a calibration station can be used, and therefore the number required in the

FIGURE 5-1. ONE-WAY RANGE BIAS DUE TO TROPOSPHERIC AND IONOSPHERIC RETARDATION

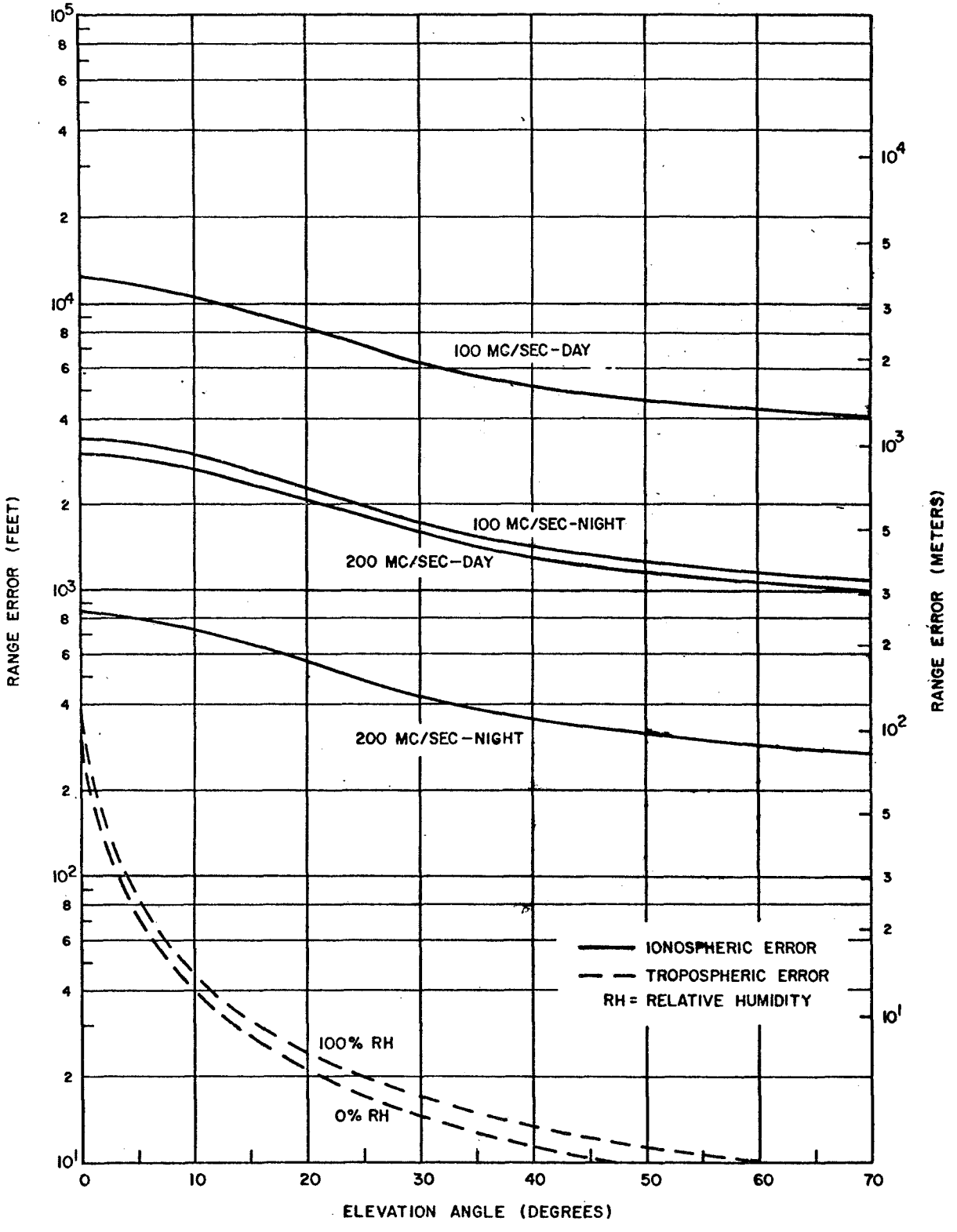

EFFECTS	MATHEMATICAL DESCRIPTIONS	DEFINITION OF TERMS & COMMENTS
Tropospheric Refraction	$(n - 1) \times 10^6 = \frac{a}{T}\left(p + \frac{b\epsilon}{T}\right)$	n = refractive index T = air temperature (°K) p = total pressure (millibars) ϵ = partial pressure of water vapor (millibars) Note: Refraction is frequency independent
Ionospheric Refraction	$n = 1 - \left[\frac{4\pi N_e e^2}{m\omega^2}\right]^{1/2}$	n = refractive index N_e = number of electrons/cm^3 e = electron charge (4.8×10^{-10} esu) m = electron mass (9.1×10^{-28} gm) ω = angular frequency of incident waves (radians/second)
Ionospheric Attenuation	$A = \frac{1.17 \times 10^{-2}}{f^2} \int_0^S N_e \nu \, ds$	f = frequency (cps) Ne = electrons/cm^3 ds = path differential (cm) ν = electron collision frequency (collisions/sec.)
Ionospheric Polarization Rotation	$\varphi = \frac{2.362 \times 10^4}{f^2} \int_0^h f(h) \, H \cos\theta \, N_e \, dh$	φ = angular rotation H = magnetic field intensity (gauss) f(h) = secant of angle between ray path and zenith dh = height differential (cm) θ = angle between magnetic lines and propagation path
Ionospheric Dispersion	$\Delta\varphi = \frac{40 \times 10^6 \, fs}{c f^2} \int_0^S N_e \, ds$	$\Delta\varphi$ = differential phase shifts (in cycles) for CW transmissions of frequency separation f_s f = average of the two transmitted frequencies (cps) The integral is the integrated electron density along the path (electrons/cm^2).
Angle of Arrival Scintillation	$\overline{\theta^2} = \frac{2 \times 10^{-12} \sqrt{\pi} \, L\overline{\Delta N^2}}{\ell_o}$ Angle of Arrival for a Turbulent Troposphere	$\overline{\theta^2}$ = mean squared angle of arrival L = path length through turbulence ℓ_o = scale length of the turbulence eddy ΔN^2 = mean square fluctuations in the refractivity, N
Tropospheric Phase Scintillation	$\overline{\Delta\varphi^2} = \frac{8 \times 10^{12} \pi^2 \ell_o L\overline{\Delta N^2}}{\lambda^2}$	$\Delta\varphi^2$ = mean square phase fluctuations Note: Typical values for 100 Kilometer path length • 1000 MHz: $(\overline{\varphi^2})^{1/2} \approx 2°$ • 100 MHz: $(\overline{\varphi^2})^{1/2} \approx 0.2°$
Ionospheric Phase Scintillation	$\overline{\Delta\varphi^2} = \frac{\ell_o L \omega_N^4}{4 c^2 \omega^2} \left(\frac{\overline{\Delta N_e}}{N_e}\right)^2$	ω_N = angular plasma frequency C = speed of light $\left(\frac{\Delta N_e}{N_e}\right)^2$ = mean square fractional deviation of electron density Note: Typical values for 100 Kilometer path length at 100 MHz is 1.9°
Amplitude Scintillation	$\left(\frac{\Delta A}{A}\right)^2 = \frac{\pi^2 z^2 L \omega_N^4}{\ell_o^3 \omega^4} \left(\frac{\Delta N_e}{N_e}\right)^2$ or $\left(\frac{\Delta A}{A}\right)^2 = \left(\frac{2\pi cz}{\ell_o^2 \omega}\right)^2 \overline{\Delta\varphi^2}$	$\left(\frac{\Delta A}{A}\right)^2$ = mean square fractional deviation of amplitude of signal from infinite distance where ΔA and A are the amplitude deviation and mean amplitude of the resultant signal. Z = distance of ionospheric scatters from the ground
Tropospheric Time Delay		Independent of frequency. Maximum range error of 380 feet at sea level. Effect negligible at jet aircraft altitude.
Ionospheric Time Delay	$\Delta R_g = \frac{40 \times 10^6}{f^2} \int_0^S N_e \, ds$	ΔR_g = one way range increase (cm)
Tropospheric Doppler Shift Error	$\Delta f_d = -\frac{f}{c} \Delta E_T \, V \sin\psi$ where $\Delta E_T = \cos^{-1}\left[\frac{r_o}{r_o + h} \cos(E - \Delta E)\right]$ $-\cos^{-1}\left[\frac{n_G r_o}{n_T(r_o + h)} \cos E\right]$	Δf_d = additional doppler shift over free-space doppler caused by troposphere V = velocity of moving object c = free-space velocity of propagation ΔE_T = angle defined by second equation (radians) n_G = refractive index at the ground n_T = refractive index at the space vehicle r_o = earth radius ΔE = refraction angle error at elevation angle, E, and height, h
Ionospheric Doppler Frequency Error	$\Delta f_d = -\frac{40 \times 10^6}{cf} \frac{d}{dt} \int_0^S N_e \, ds$	Δf_d = additional doppler shift over free-space doppler caused by the ionosphere

Table 5-1. Tropospheric and Ionospheric Propagation Effects

FIGURE 5-2

ELECTRON CONTENT DUE TO MAGNETIC STORM

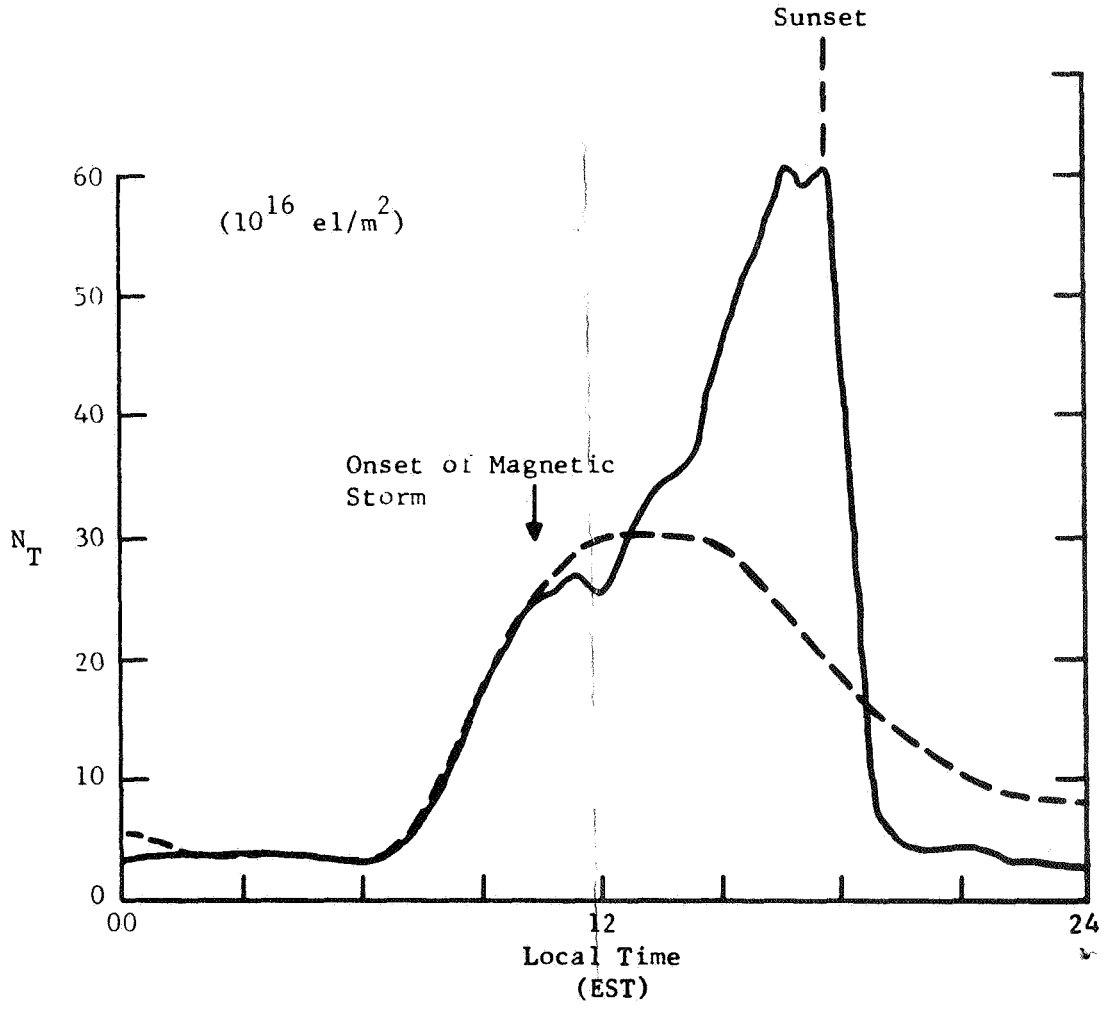

February 2, 1969

area served. However, an estimate can be made on the basis of an extreme case reported by Mendillo, et al[2], Figure 5-2. In that instance, sunset occurred at the peak of the disturbance, and the total electron content dropped by a factor of ten in one hour. It would have caused a change in total range bias from approximately 2700 to 270 meters for an elevation of 20 degrees. Assuming that the principal cause of the decay is related to sunset, the east-west gradient of electron density and hence range bias would have been over a distance approximating the distance the terminator moved over the earth in one hour, or approximately 1000 kilometers. Calibration stations at 1000 kilometer intervals would probably have been sufficient to determine the range bias correction during that event.

Ionospheric time delay is reduced as $1/f^2$ so that it would be negligible at L-band, 1540-1660 MHz. However, at that higher frequency, the design of aerodynamically acceptable antennas having the required radiation pattern presents a problem that has not been satisfactorily solved. As stated in a previous study[3], 400 to 700 MHz is the optimum frequency band for most applications of range measurements from satellites.

The time delay in the ionosphere is important at 135 to 150 MHz because the exact delay at any time or place cannot be predicted accurately. An ionospheric model adapted from Lawrence, et al[4] and Millman[1] was used in the computer program for determining fixes. (Appendix II) The procedure for including the bias in the fix determination was to compute the fix on the basis of the measurements without correction to find the approximate location of the user equipment, then to determine the time of day at the user's location. An ionospheric correction for each satellite-to-user ray path was determined from the ionospheric model. The range measurements were then corrected in accordance with the estimates derived from the model, the fix was immediately recomputed and then printed out.

Propagation delay due to the slowing of the wave velocity as it passes through the ionosphere was studied by analysis of data previously obtained during a separate, General Electric Company-funded program.

The separate investigation of propagation effects conducted at the Radio-Optical Observatory employed signals from the S-66 and the GEOS-I satellites. The passes over Schenectady included all azimuth and elevation angles at changing times of day. The passes had a maximum period of approximately 20 minutes, so that an essentially stationary ionosphere was scanned.

The satellites transmitted highly stable, phase-coherent signals at 162 and 324 MHz. They were received on highly stable phase-locked receivers at the Observatory. A 30-foot steerable antenna was used to receive the signals so that the data were not noticeably disturbed by noise. The voltage controlled oscillators of the two phase-locked receivers were on the same frequency. If there were no ionosphere, they would have a constant phase difference between them when locked to the coherent signals from the satellite. Doppler shift was channeled out by this process. At a point in the frequency multiplying chains where both signals were at 162 MHz, the signals were applied to a phase comparator and thence to a paper chart recorder. The integral of the phase difference was also recorded. Once cycle of phase difference was recorded each time the path delay difference changed by the period of one cycle at 162 MHz (6.07 feet). A portion of a recording is shown in Figure 5-3.

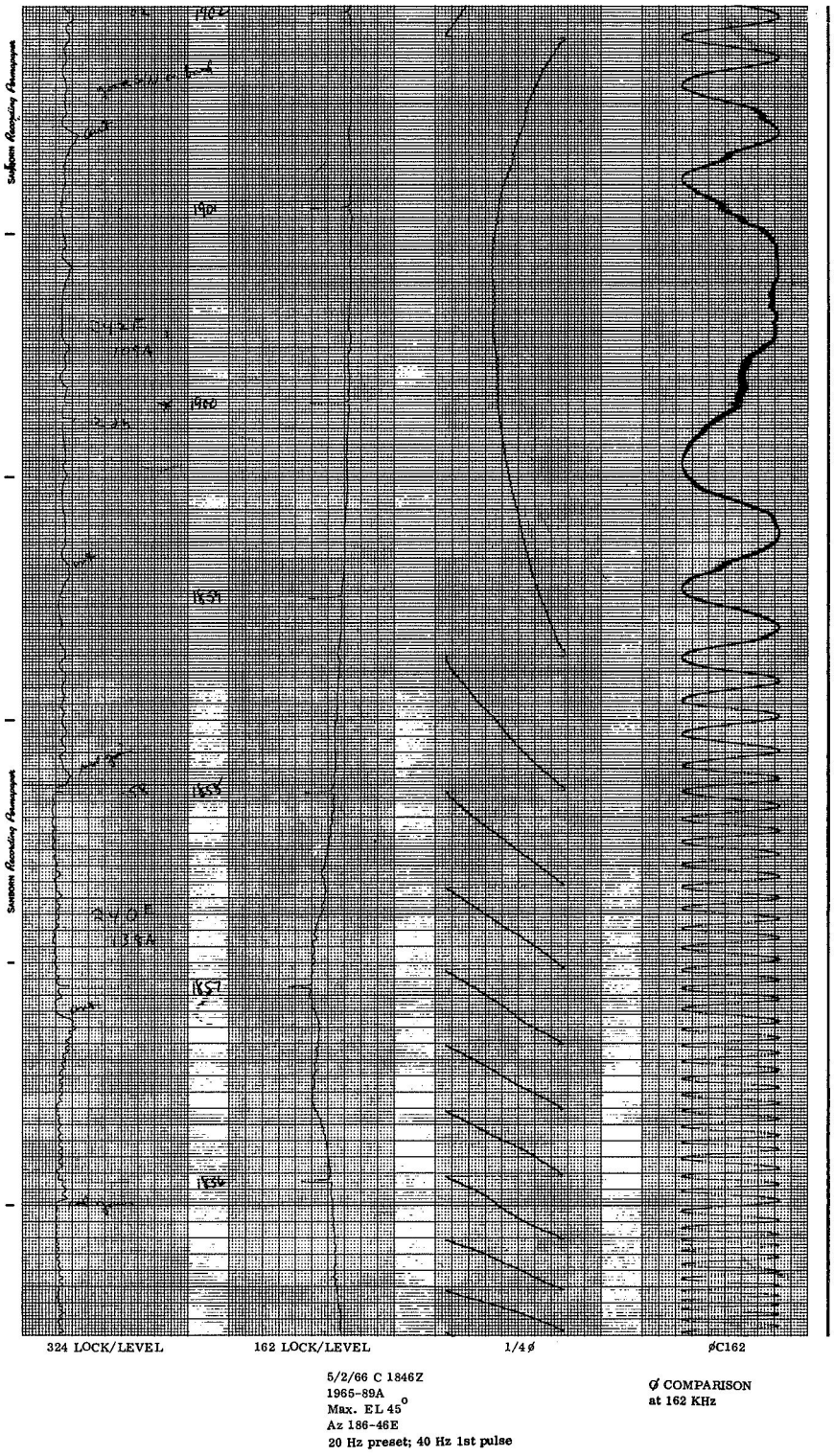

FIGURE 5-3. PORTION OF TYPICAL RECORDING FOR GEOS-I SATELLITE SIGNAL

Plots of integrated phase difference for three passes are shown in Figure 5-4. The first plot indicates that the ionosphere was uniform in its structure; the second shows an interesting phase reversal that was observed frequently but only within narrow azimuth and elevation limits; and the third indicates a very irregular structure. The reason for the phase reversals was not determined, but it has been noted that they occurred when the ray path was through or along the edge of the auroral zone.

The phase difference recordings provide a direct and precise measurement of the difference in path length change at 162 and 324 MHz. Assuming that the effects are proportional to $1/f^2$, a close estimate of the path length change can be made at 162 and, similarly, at 118 to 136 MHz.

Data from 36 passes taken at various times of day were plotted to determine the path length change caused by the ionosphere for each 5^o change in elevation angle. The results are summarized in Figures 5-5 through 5-8, which can be used to determine the mean and the 90 percentile values at any elevation angle.

The values in Figures 5-5 through 5-8 are not to be taken as total range error due to the ionosphere, because they do not include the error at the zenith.

The zenith angle range error can be estimated from the ionospheric time delay equation of Table 5-1, except that the path is considered to be vertical through the ionosphere

$$\Delta R_z = \frac{40 \times 10^6}{f^2} \int_o^h N_e dh \qquad (5\text{-}1)$$

The range of values for the integral is from 10^{12} to 10^{14}, depending on diurnal, seasonal, and solar activity changes. Conditions of the ionosphere are known at any time so that the zenith angle range uncertainty, ΔR_2 can be reduced to much less than the 50 to 5,000 foot total variation of ΔR_z at very high frequencies.

From Equation 5-1, the zenith angle range error is found to vary from 50 to 5,000 feet, depending on diurnal, seasonal, and solar activity changes. Ionospheric soundings will generally not be available in regions of interest. Thus, the value of the zenith angle range error will have to be estimated. It is conservative to estimate that the residual uncertainty in a zenith range measurement will be less than 1,500 feet when all of the known factors are applied.

Similarly, the additional error for lower elevation angles to the satellite will also have to be estimated. Figures 5-5 through 5-8 provide a basis for initial estimates, although much better estimates can be made for an operational system by ranging on transponders at fixed locations in the area of operations.

It is immediately evident from the data that the ranging error will be less than during nighttime hours and at locations where the elevation angles to the satellite are high. The data, Figures 5-5 through 5-8, were collected over a year's time and are presented for four periods of the day as expected at 125 MHz.

FIGURE 5-4. PLOT OF INTEGRATED PHASE DIFFERENCE FOR THREE PASSES

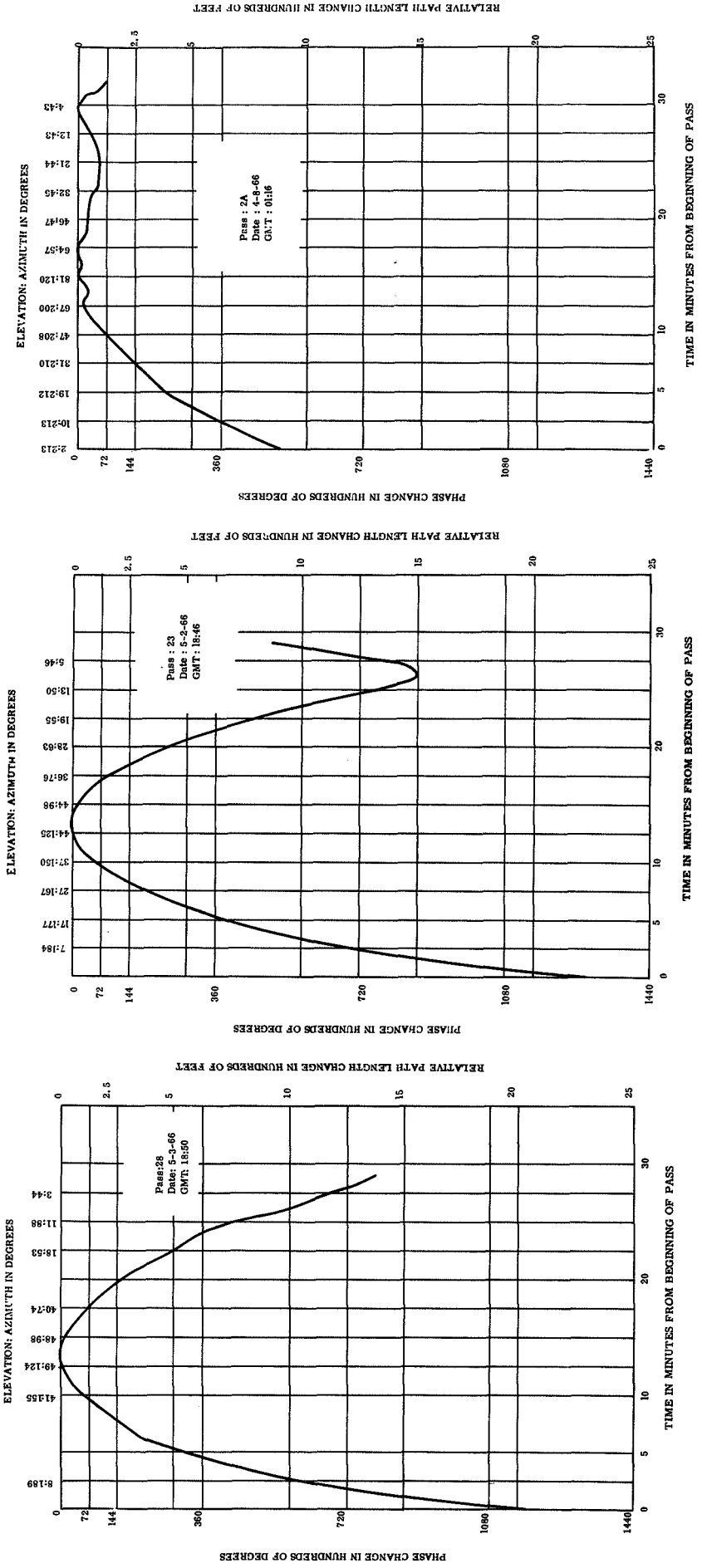

FIGURE 5-5

TOTAL PATHLENGTH CHANGE ACCUMULATED FROM 90° ELEVATION
(GMT 05:00 - 11:00)

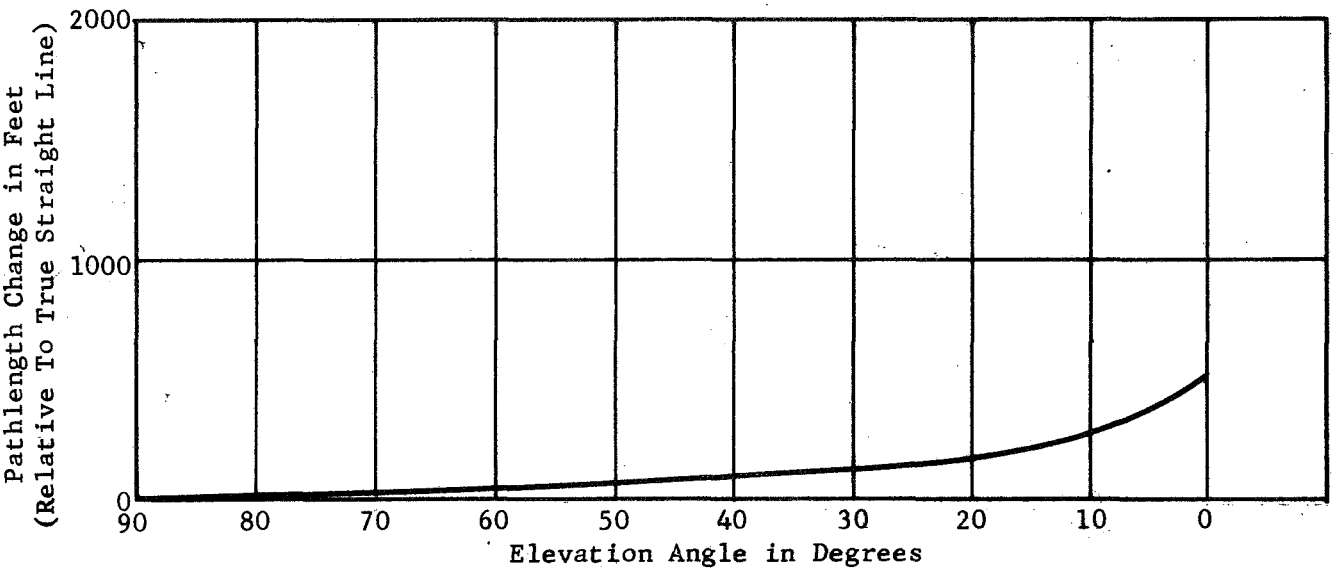

FIGURE 5-6

TOTAL PATHLENGTH CHANGE ACCUMULATED FROM 90° ELEVATION
(GMT 11:00 - 17:00)

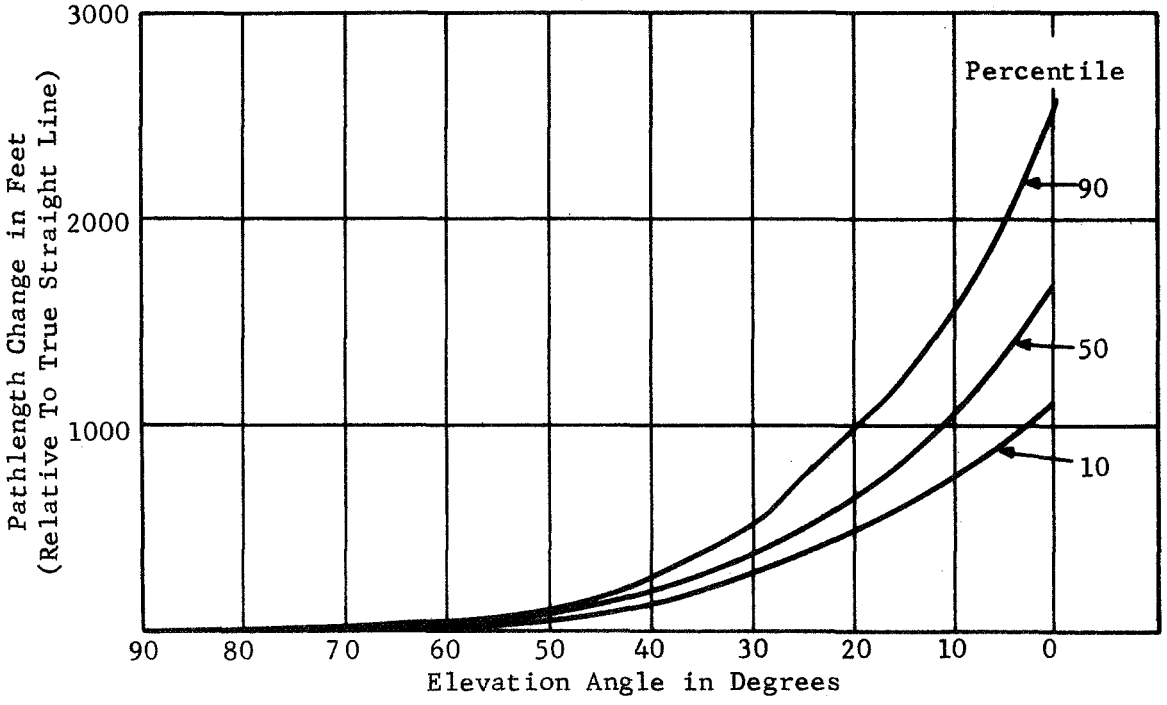

FIGURE 5-7

TOTAL PATHLENGTH CHANGE ACCUMULATED FROM 90° ELEVATION
(GMT 17:00 - 23:00)

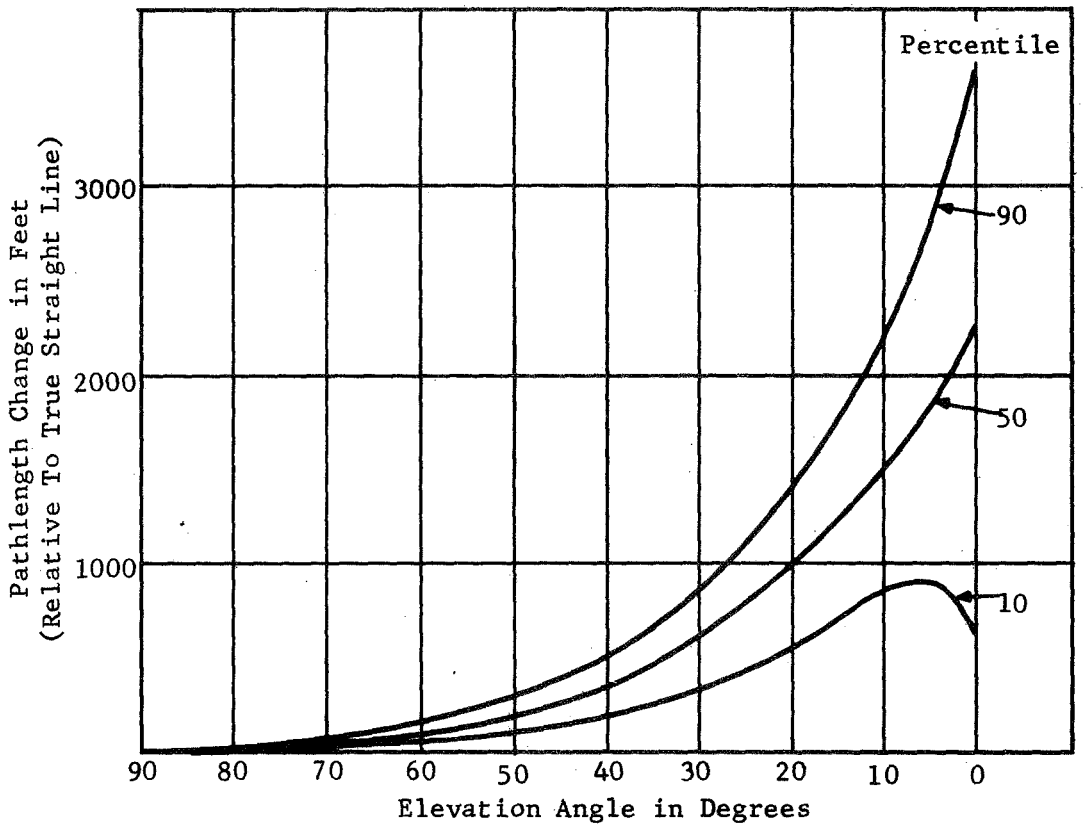

FIGURE 5-8

TOTAL PATHLENGTH CHANGE ACCUMULATED FROM 90° ELEVATION
(GMT 23:00 - 05:00)

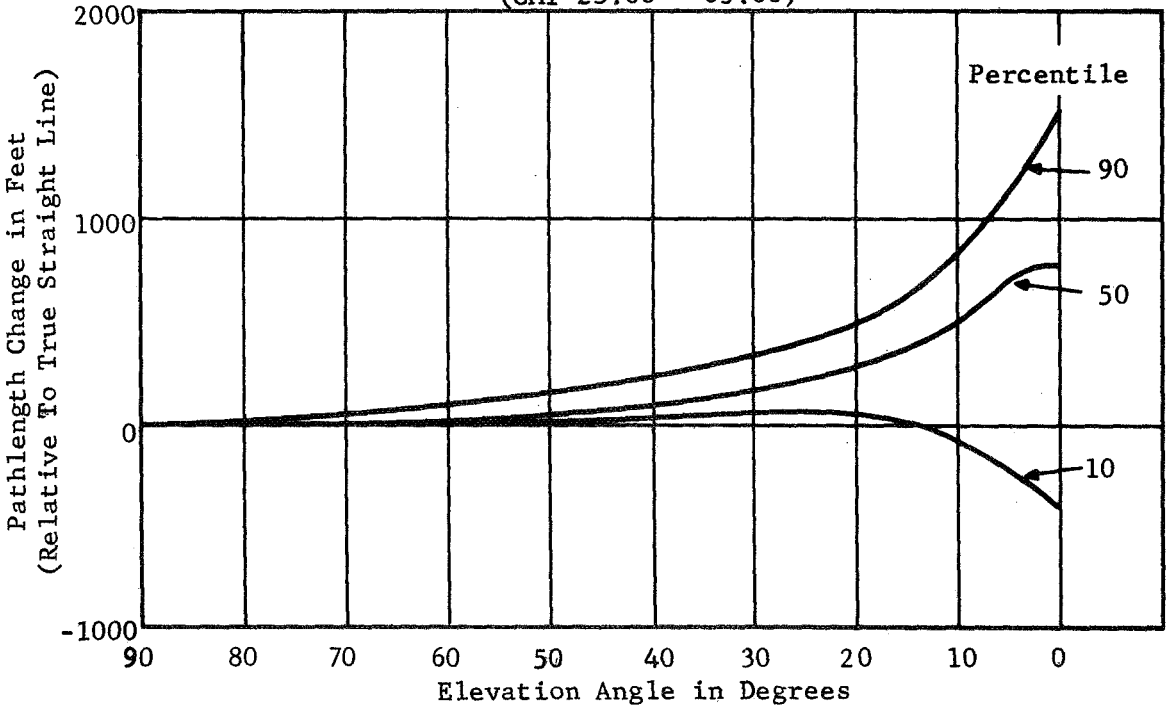

The zenith angle uncertainty cannot be derived from the experimental data analyzed to date. As noted above, it can vary from 50 to 5,000 feet with the largest contribution caused by known factors. Therefore, a bias value can be approximated for any location and time. The remaining uncertainty in the zenith angle measurement is estimated to be 25 percent of the bias value. Assuming the bias will be 5,000 feet during midday, near the peak of the sunspot cycle, and assuming the zenith value varies in proportion to the observed mean values for lower elevation angles throughout the day, the zenith angle range uncertainty is estimated to be as shown in Table 5-2.

Table 5-2

Range Uncertainty at Zenith Angle

Local Time			
0000-0600	0600-1200	1200-1800	1800-2400
250'	850'	1200'	500'

It is conservative to estimate that the uncertainty in range measurement for other than the zenith angle will be the zenith angle uncertainty plus the difference in values between the 10 and 90 percentile curves of Figures 5-5, 5-6 and 5-7 and one-half the total values of Figure 5-8. The values to be added to the zenith angle uncertainty for lower elevation angles are:

Table 5-3

Range Uncertainty as a Function of Elevation Angle

Elevation Angle	Local Time			
	0000-0600	0600-1200	1200-1800	1800-2400
5^{o}	450'	1950'	3000'	1800'
10	400	1600	2400	1400
20	350	1350	1900	900
30	325	1100	1600	700
45	300	900	1400	600
60	275	875	1300	575
90	250	850	1200	500

Total range uncertainty is twice the value, since the same uncertainty will apply to the signal path from the satellite to the user as the path from the user to the satellite. The path from the ground station to the satellite and return will not affect the measurement because the ionosphere does not change significantly during the interrogation time, and the first and second repetitions of the signal by the satellite have the same delay in propagating from the satellite to the ground. The time interval, representing the propagation time from the satellite to the user is not affected by the satellite to the ground station path. The total uncertainty caused by the electron content in the ionosphere is twice that of the values of Table 5-3. However, the range measurement uncertainty in two-way ranging is one-half the total; i.e., the one-way uncertainty.

The range measurements from a ground terminal to the satellite can be used to determine ionospheric delay by comparing the measured propagation time

with the computed free space propagation time between the satellite and the terminal. Comparisons of measured time intervals were made on some of the Observatory-to-satellite measurements. Diurnal variations were observed and resolution was adequate for calibration purposes. The data were not used in the computations as the requirements of the experiment were fulfilled with the ionosphere model.

The comparison of computed geometrical and measured ranges is of potential value for ionospheric studies and real time monitoring of ionospheric electron density on a world-wide basis. Low-cost unattended transponders could be distributed over the Earth and interrogated individually to serve as a widely dispersed network for monitoring ionospheric conditions. For ionospheric studies, the satellite position should be known to a fraction of the expected delays in the ionosphere. Accurate real-time tracking of the satellites using a frequency other than VHF would probably be necessary. A shorter time quantizing interval than the presently used 0.4 microsecond is recommended if the technique is to be used for collecting precise scientific data about the ionosphere. It is probable that the calibration stations of an operating system could provide useful scientific and ionospheric propagation data in addition to their primary function.

The various data sources examined in the experiment agree in a general way. None is based on sufficient data to provide a convincing statistical estimate of delay. The experimental results obtained using S-66 and GEOS-1 and the ATS-3 measurements agree with the model selected for the computer program sufficiently well to indicate that ionospheric delay may be estimated well enough to provide range measurement precision within 3,000 feet when conditions are such as to cause the greatest errors. Much of the time, as at night, the ionosphere will not have a significant effect for position fixing applications that can tolerate position errors of a mile or two. The validity of the results is supported by the accuracy of lines of position made during the experiment, as presented in Figure 8-4. It is expected that better estimates of ionospheric delay can be made for an operational system that includes transponders at fixed locations in the operating areas so that the ionospheric delay can be monitored in the area of interest and at the time of interest.

Data of several tests were selected and plotted to illustrate some of the important factors affecting range measurements at VHF. In all of the plots time is Greenwich Mean Time. Five hours should be subtracted to obtain local Eastern Standard Time. The time interval measurements in microseconds are represented as they were recorded. The equipment delay times and propation delays were not subtracted from the readings. Each plot is identified in the following description by date and time.

The ATS-1 satellite was located at approximately 150° west longitude, less than 2° above the western horizon at Schenectady. The ATS-3 satellite was at an elevation angle exceeding 30°.

September 27, 1968 - 1446Z (Figure 5-9)

ATS-1 was interrogated using the 30-foot dish to transmit and receive with 80 watts of transmitted power. The equipment was operated in a "round robin" mode in which the return signal interrogated the transponder and caused it to transmit another interrogation. As a result, a range measurement was made once each 3/4 second, approximately. The data plot from

FIGURE 5-9

ROUND-ROBIN TEST THROUGH ATS-1
September 27, 1968
DISH-DISH USING GE TRANSCEIVER

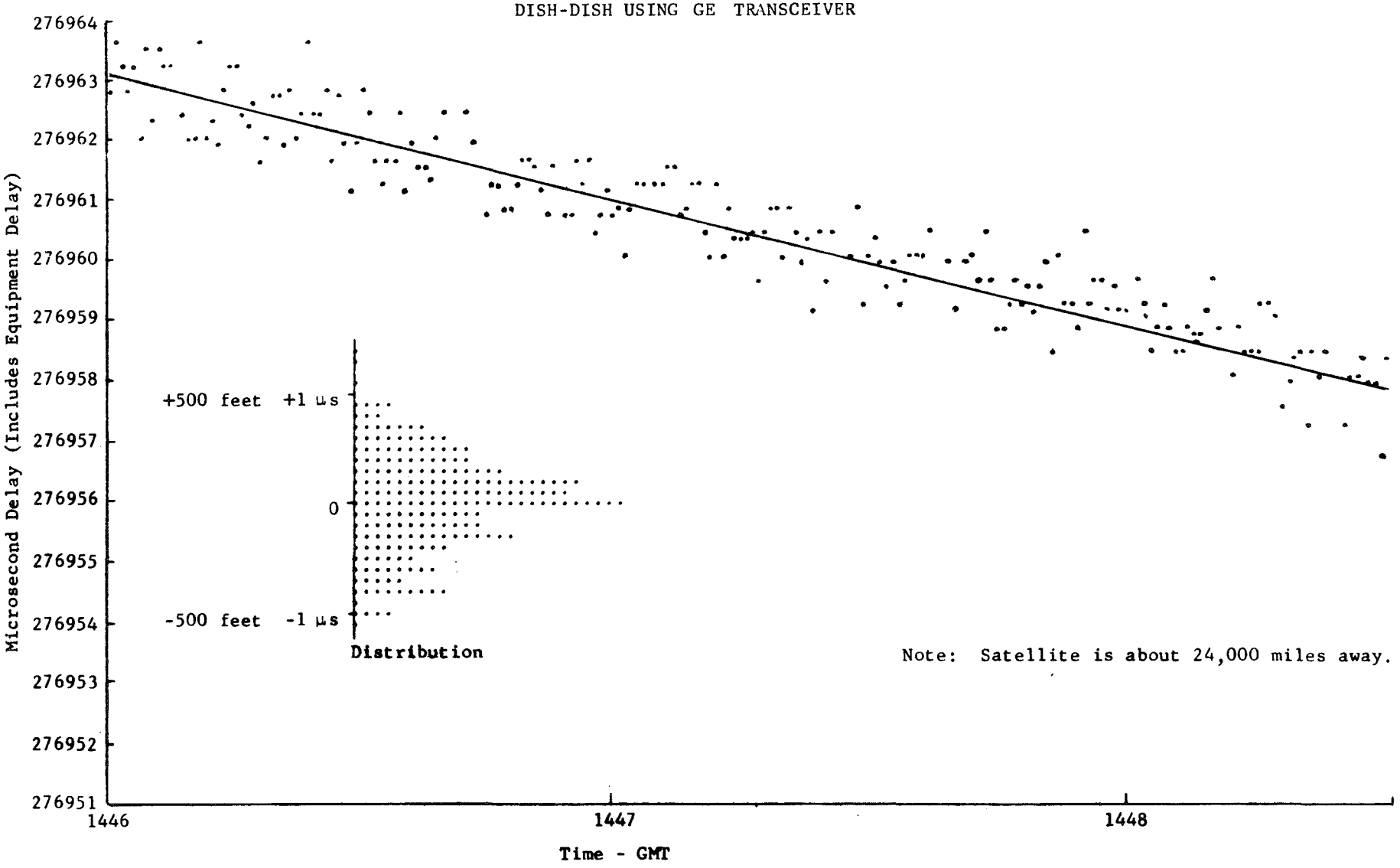

14 46 00 to 14 48 30 includes all of the range measurements made during the 2.5 minute period. A visual estimate of a straight line drawn through the data represents the range change of the satellite. Although the satellites are in geostationary orbit, their orbits are slightly inclined so that they trace a figure-eight pattern in the sky over a 24-hour period. During an interval as short as fifteen minutes, the range change may be approximated by a straight line. The distribution of the points about the line is typical of the small deviation when the signal-to-noise ratio is high and the ionosphere is quiet.

November 22, 1968 - 1146Z (Figure 5-10)

The interrogation period for ATS-1 was chosen to include sunrise along the ray path through the ionosphere. Each point on the plot represents the average of ten readings to emphasize the longer term variation of the range measurements. Because the satellite is at such a low elevation angle above the western horizon, sunrise occurred in the ionosphere shortly before it occurred on the ground at Schenectady. Within a one-minute period shortly before sunrise at Schenectady, the range measurement increased approximately 3 microseconds. It is assumed this change was due to the sudden onset of ionization in the ionosphere at sunrise.

January 26, 1969 - 2014Z (Figure 5-11)

A plot of the range measurements on ATS-3 exhibits a pattern suggesting a beating effect, even though each measurement is entirely independent. A similar effect may be observed on the Observatory returns on the February 11 plot. The pattern is due to the 0.4 microsecond time quantizing interval of the responder. In the January 26 and February 11 tests, a different oscillator was used for the tone-code generator than for the phase matcher-correlator. It was postulated that a slight relative phase shift between the two oscillators was responsible for the cyclic nature of the patterns. This was later tested by using the same oscillator as the reference for both. The plot of the February 12 Observatory returns shows the quantizing interval without the cyclic pattern previously observed. The ability to resolve the quantizing interval indicates a high signal-to-noise ratio and excellent precision for the phase matcher.

February 11, 1969 - 0157Z (Figures 5-12 and 5-13)

Plots are presented for both the Observatory returns from the satellite and the returns from the Sea Robin buoy. The data were taken during a visible aurora at Schenectady and it is reported that a severe magnetic disturbance was in progress, peaking within an hour prior to the test period. The State University of New York reported that an M-arc was present in the aurora. The Observatory returns indicate the range change of the satellite relative to the Observatory while the Sea Robin returns exhibit the sum of the range changes from the Observatory to the satellite and the satellite to the Sea Robin. Histograms of the returns relative to a straight line approximation of the data are presented. The presence of the magnetic disturbance seemed to have little effect on the scatter of the measurements.

February 12, 1969 - 0200Z (Figures 5-14, 5-15 and 5-16)

Severe scintillation, assumed to be associated with the magnetic activity, caused the amplitude of the received signals to vary widely, as noted on the

FIGURE 5-10

EFFECT OF SUNRISE IN THE IONOSPHERE

ATS-1 - November 22, 1968
10 Reading Averages

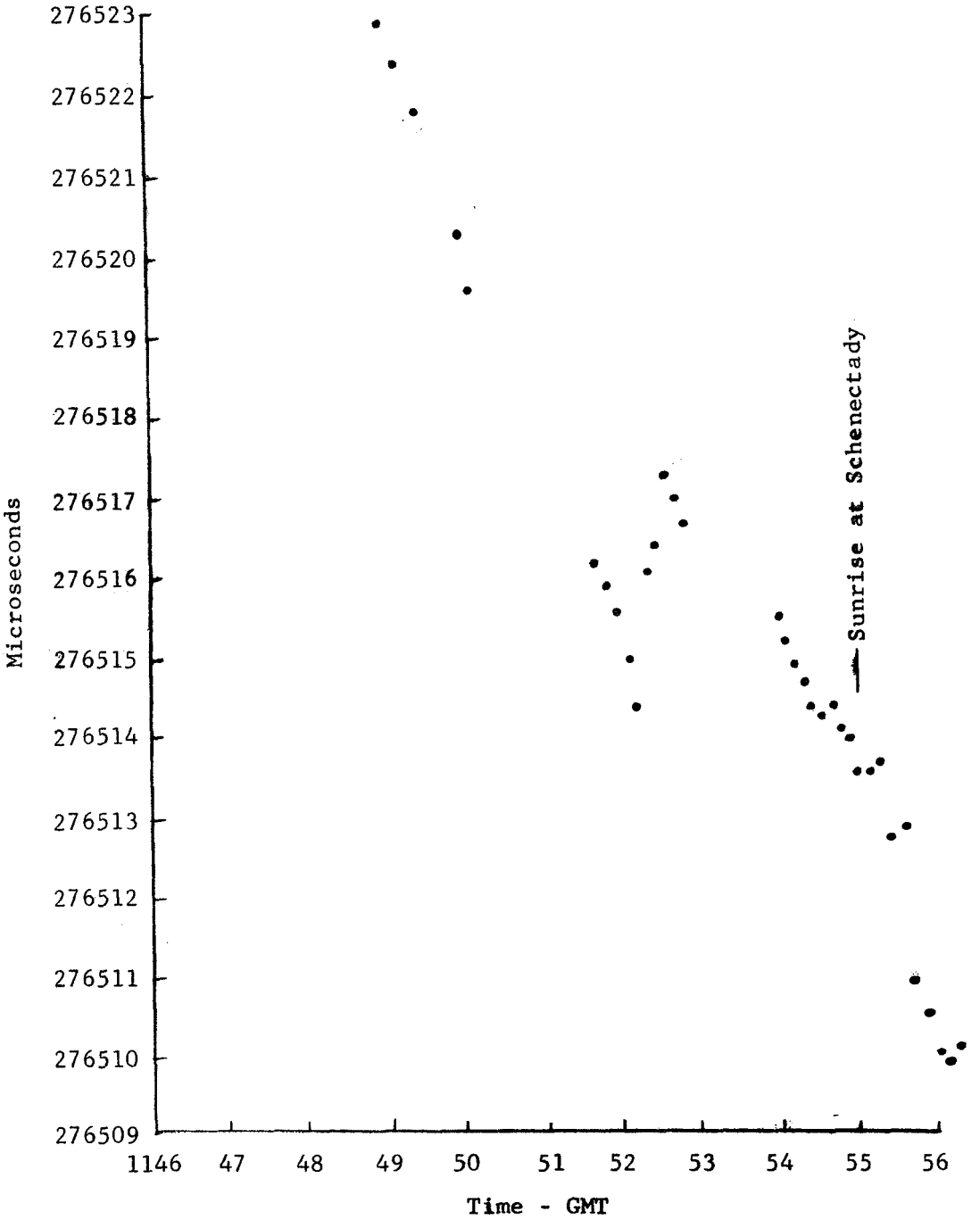

FIGURE 5-11

ATS-3 - JANUARY 26, 1969

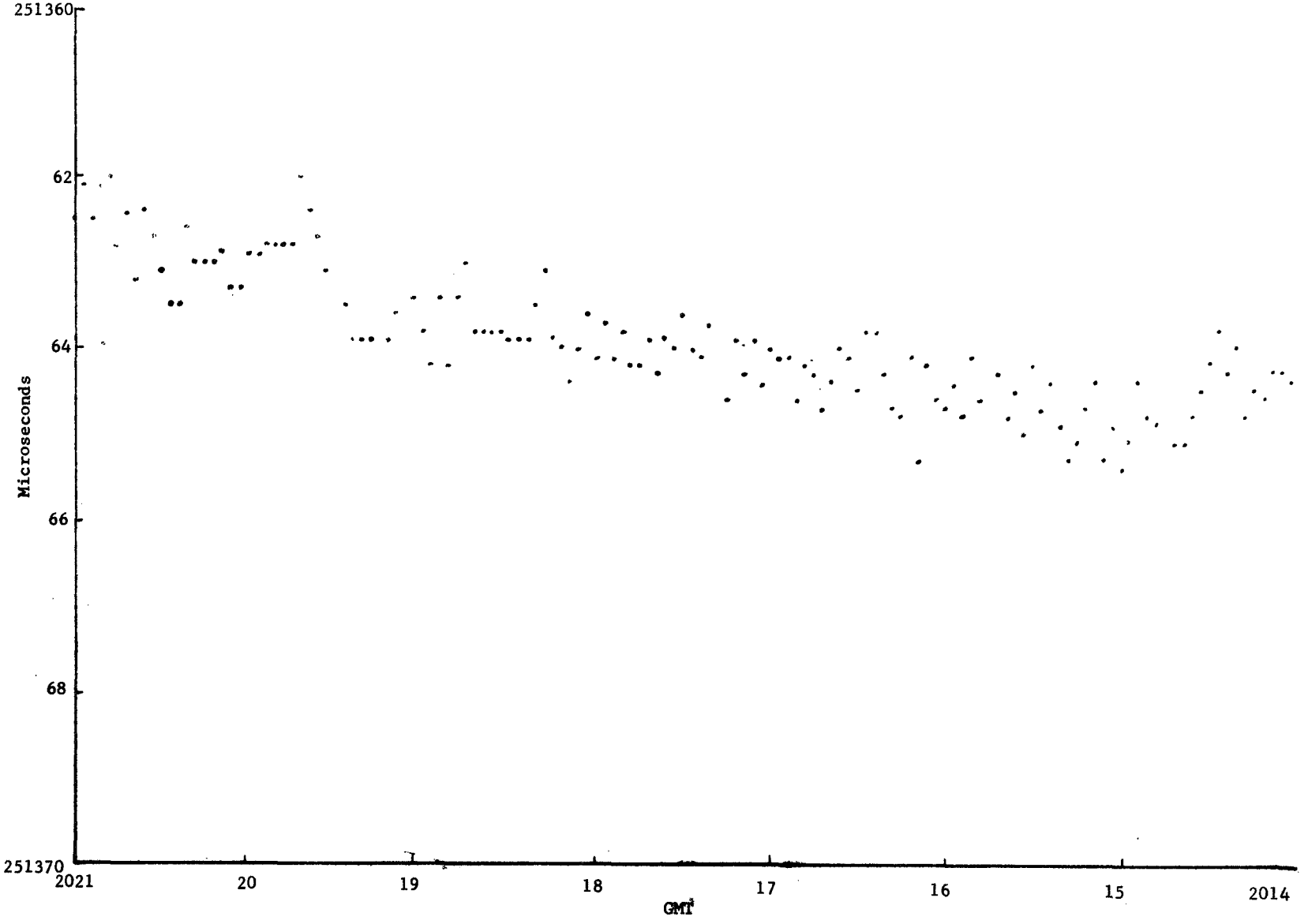

FIGURE 5-12
OBSERVATORY RETURNS - AURORAL ACTIVITY
February 11, 1969

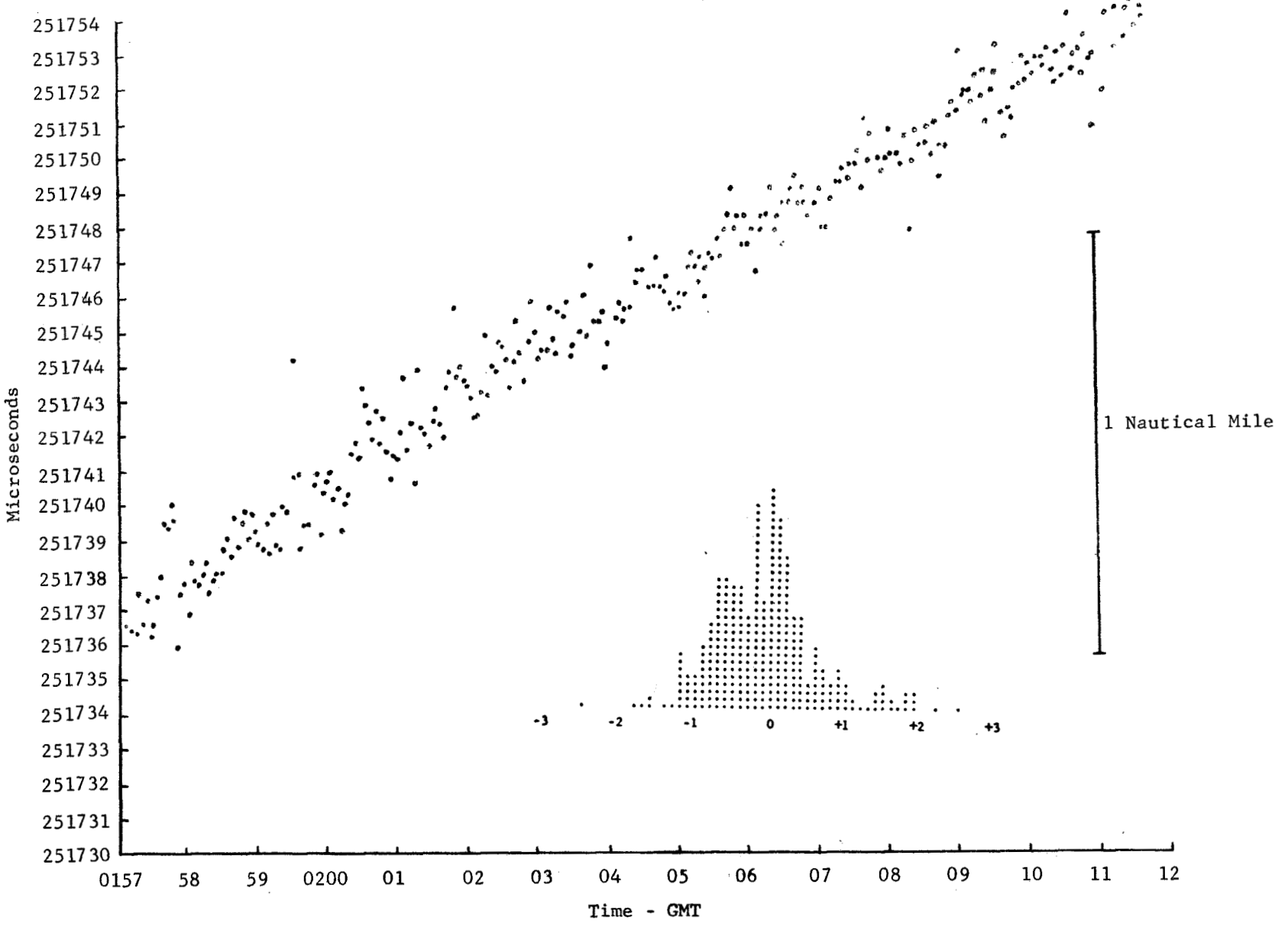

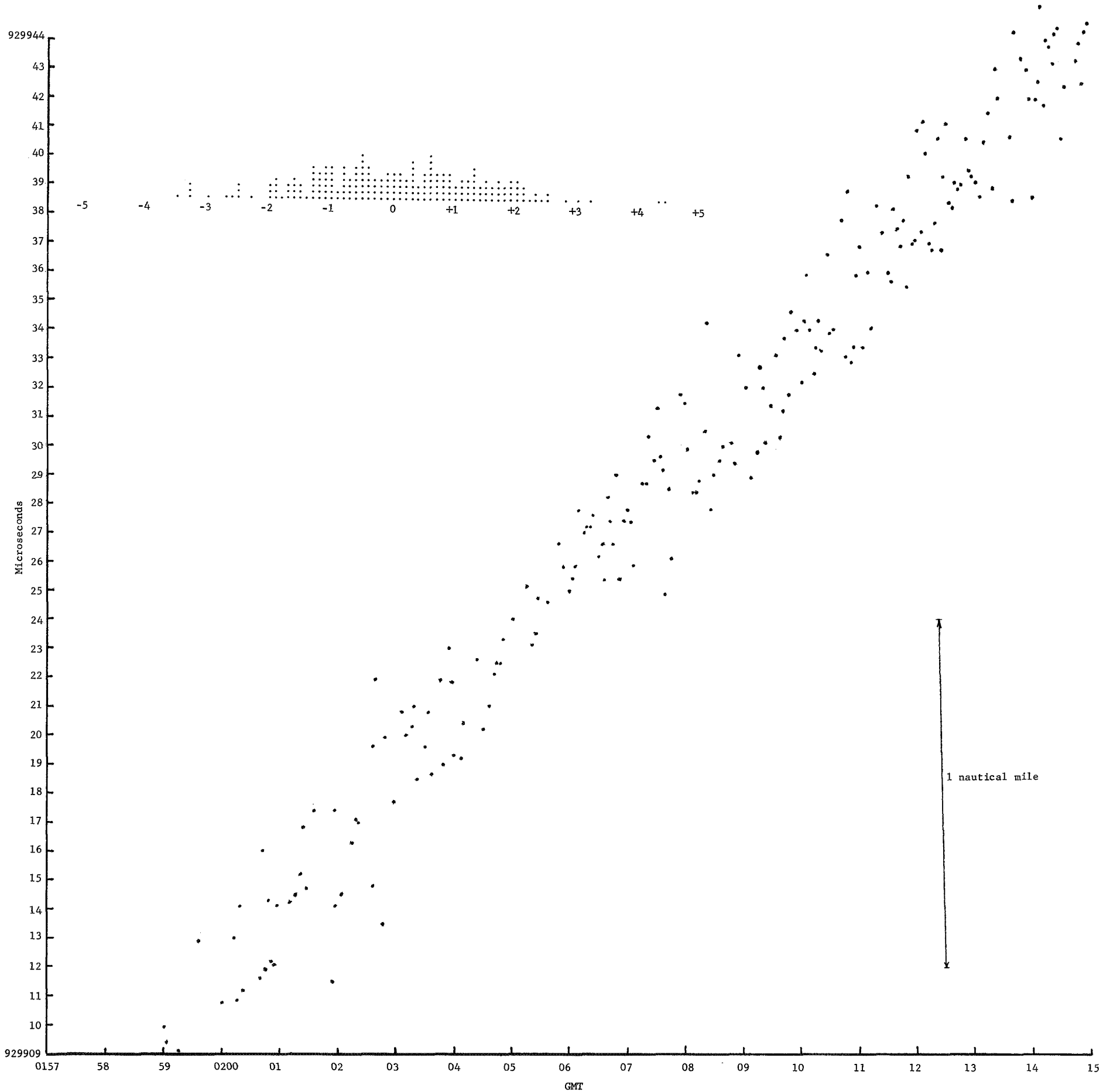

FIGURE 5-13. SEA ROBIN RETURNS (2/11/69)

FIGURE 5-14. ATS-3 SIGNAL AMPLITUDE VARIATIONS DUE TO SCINTILLATION

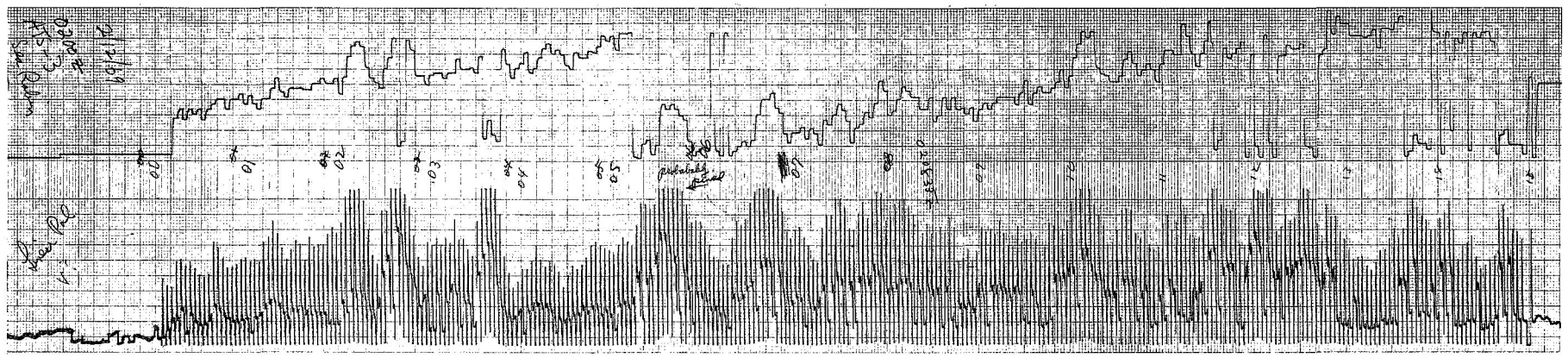

FIGURE 5-15

OBSERVATORY RETURNS
February 12, 1969

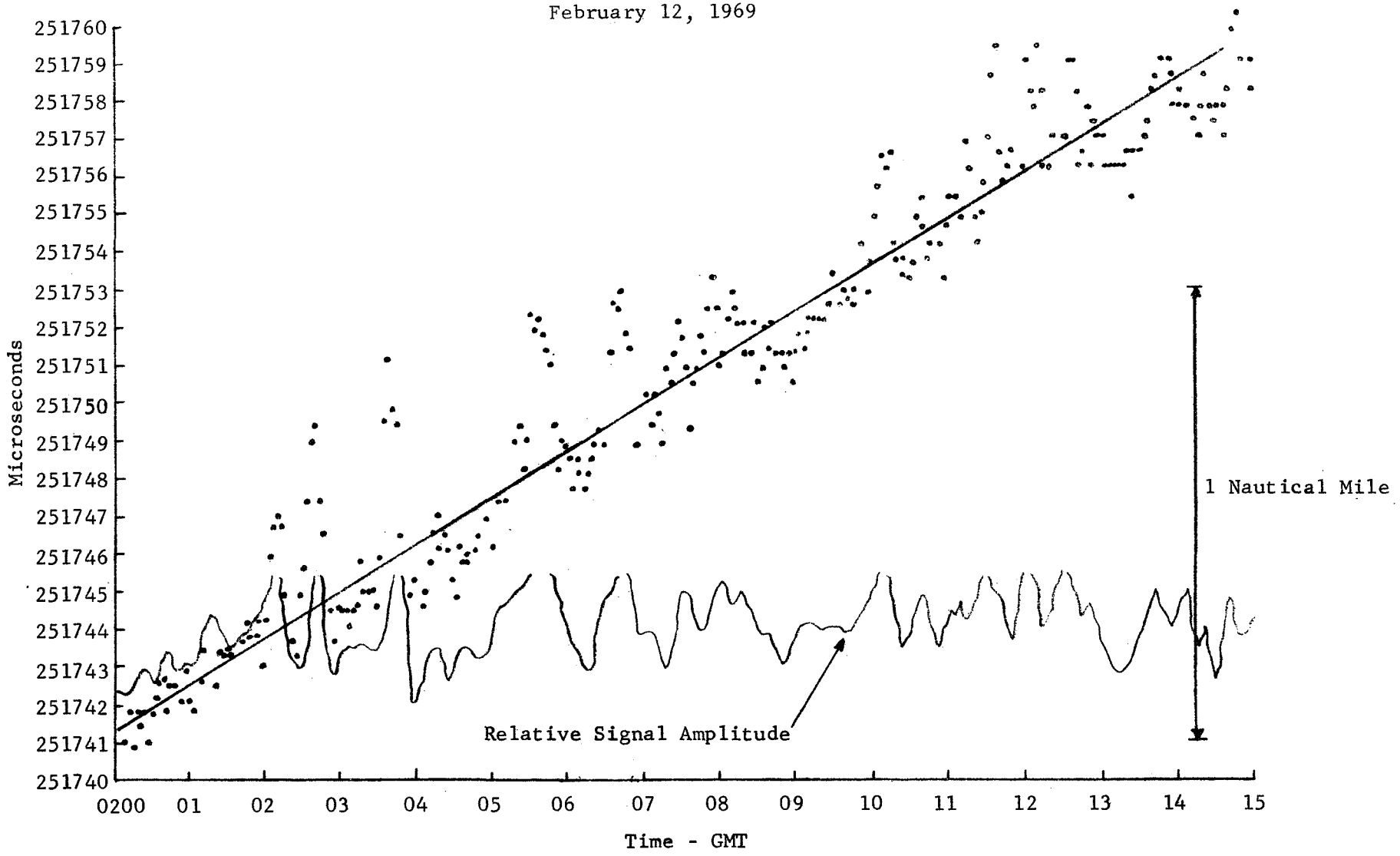

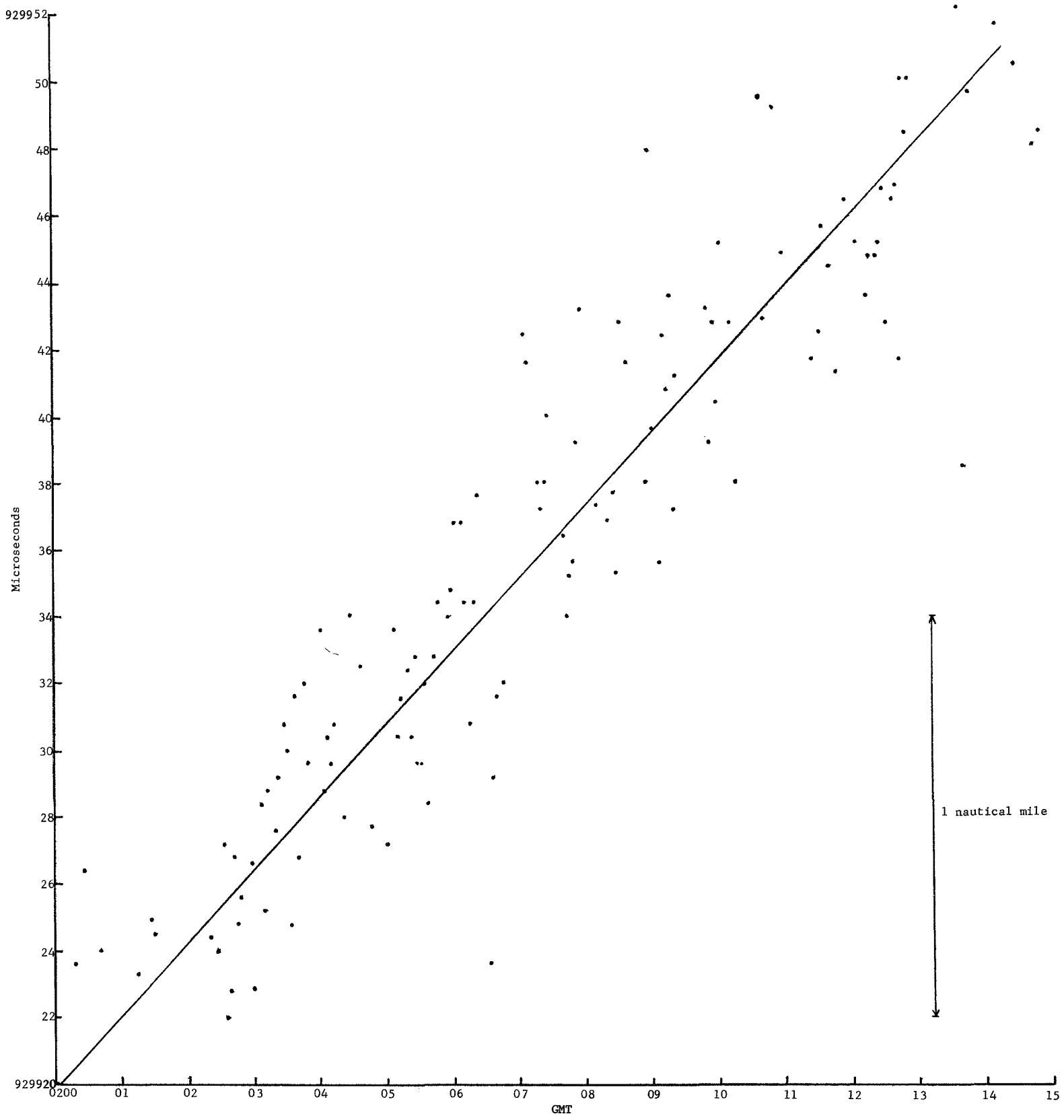

FIGURE 5-16. SEA ROBIN RETURNS
(2/12/69)

analog recording, Figure 5-14. The relative signal amplitude is plotted with the Observatory returns to show the correlation between the range measurement displacement and signal amplitude in Figure 5-15. The Sea Robin returns for February 12 exhibited larger scatter than on February 11, Figure 5-16. The analog recording (Figure 5-14) shows two plots. The upper plot is a recording of a digital-to-analog conversion of a change in propagation time with one large division representing one microsecond. The higher peaks in the lower recording are the signal amplitude of each interrogation for the direct signal return. The intermediate values are the relative amplitude of the Sea Robin returns. It is interesting to note that the Sea Robin amplitude variations are correlated with the direct returns, suggesting that the path from the Observatory to the satellite was disturbed by the magnetic activity, but that the path from the satellite to the buoy in Bermuda was not affected. The change in range measurement with signal amplitude is attributed to the Observatory receiver, which had a change delay with signal amplitude, as explained in Section 4. These data should be compared with those of September 5, 1969, when scintillation was present but had no discernible effect on the range measurements, Figures 5-22 and 5-23. An improved limiter was in use on September 5.

February 24, 1969 - 1200Z (Figures 5-17, 5-18 and 5-19)

Polarization and antenna pointing were changed during the test period to measure the effects of signal amplitude change on the direct returns, Figure 5-18, and van returns through the satellite, Figure 5-19. The signal level during the first minute of the test was low because of the polarization adjustment of the 30-foot dish. There was a marked displacement towards a shorter delay for the direct returns and for a longer delay of the van returns. Signal amplitude is shown on the analog recording, Figure 5-19, and the changes in antenna adjustment are noted on the data plots. A displacement of 5 to 7 microseconds was observed over the large range of signal level change. The analog recording exhibits a cyclic change in amplitude that suggests a beat between the satellite spin rate and the 3 second interrogation rate, although this has not been definitely assigned as the cause.

February 18, 1969 - 1405Z (Figures 5-20 and 5-21)

Further evidence of the change in time delay through the receiver with signal amplitude is suggested by the plots of the computed curves compared with the relative signal amplitudes. The data were taken before the tuned limiters were installed in the receivers. The computed curves are of second order as determined by a least squares fit to the data. The direct returns present a curve downward for decreased signal level, whereas the van returns exhibit an upward curve for signal level. The shape of the parabola for the first interval is curved sharply because the curve is based on a relatively small number of data points which, by chance, included several points which were high. All of the data points on the van return are plotted to illustrate how the computed curve fits the actual data. The encircled points are computed points for defining the curve and are not data points. The standard deviations are computed about the smooth curves to determine the short term stability of the range measurements. It will be noted that the signal level pattern for the van returns does not correspond to the signal level of the direct returns. The differences result from the polarization angle changes due to Faraday rotation. A difference in the Faraday rotation at the transmit and receive frequencies was frequently observed.

FIGURE 5-17

DIRECT RETURNS - ATS-3

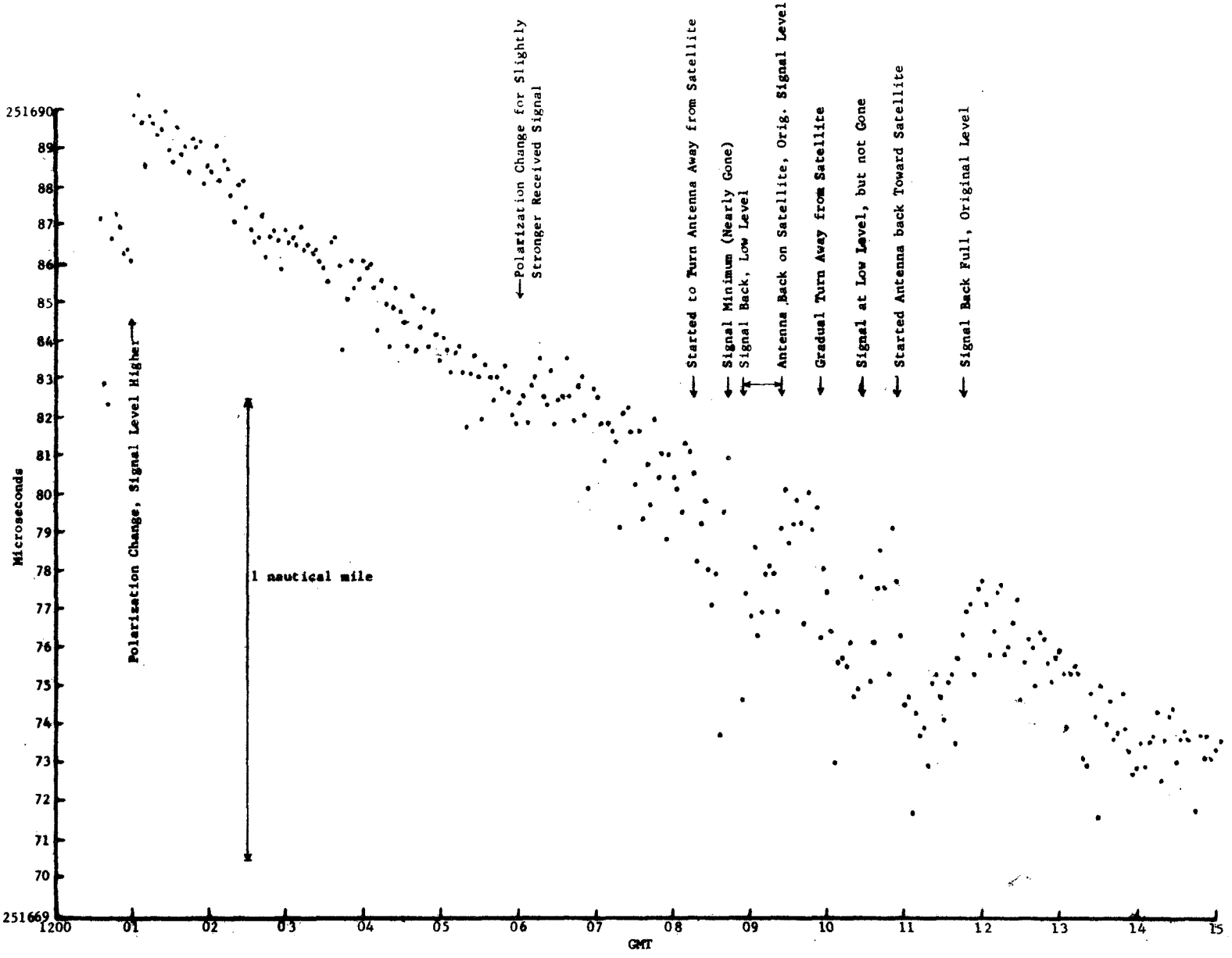

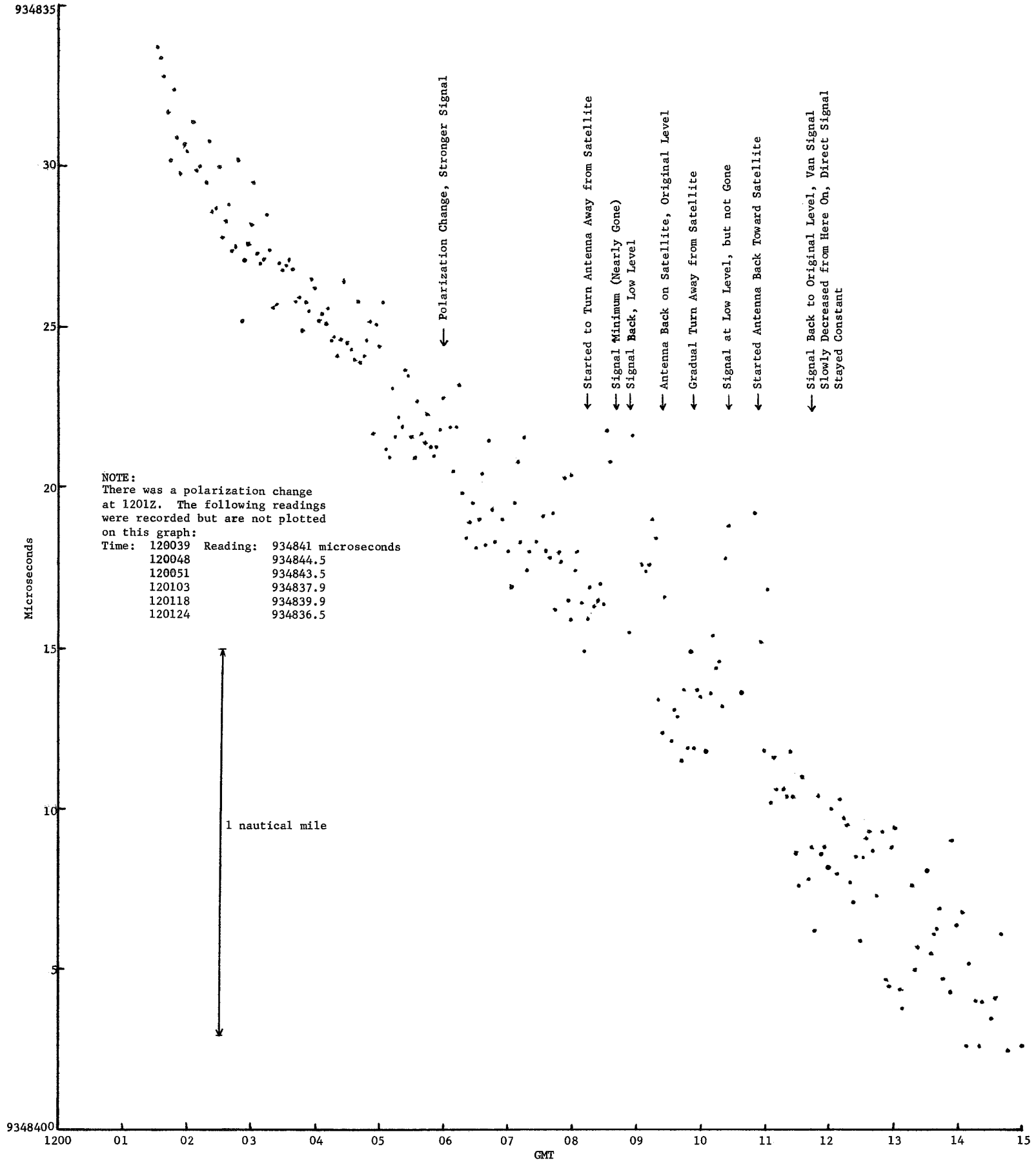

FIGURE 5-18. VAN RETURNS
(2/24/69)

FIGURE 5-19. SIGNAL AMPLITUDE - VAN RETURNS - FEBRUARY 24, 1969 TEST

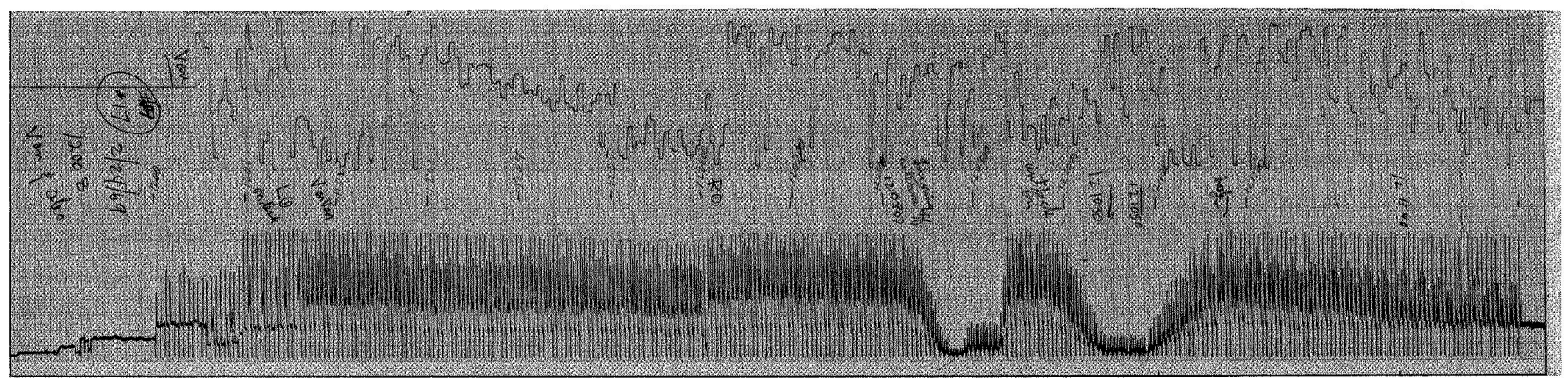

FIGURE 5-20

DIRECT RETURNS

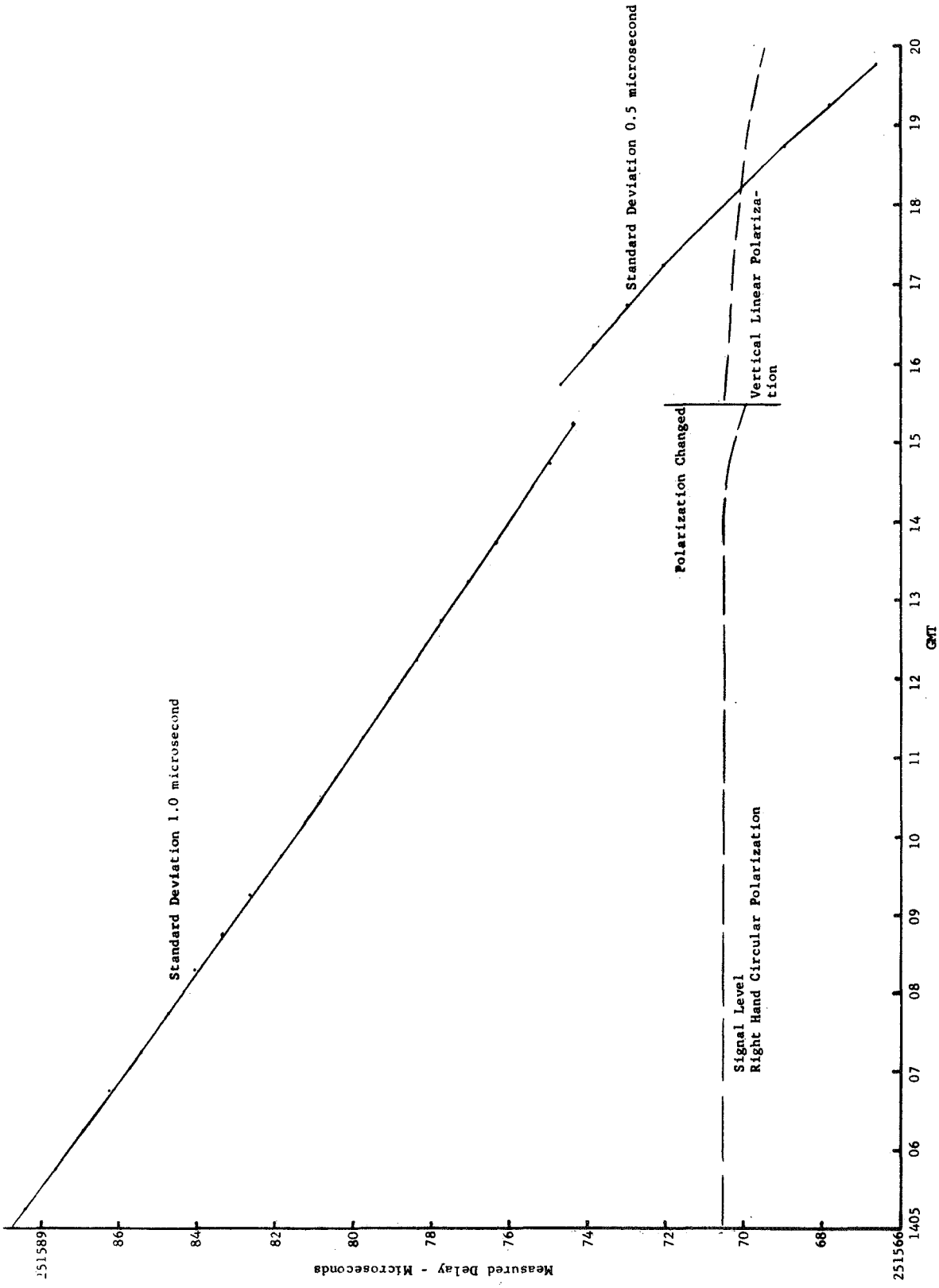

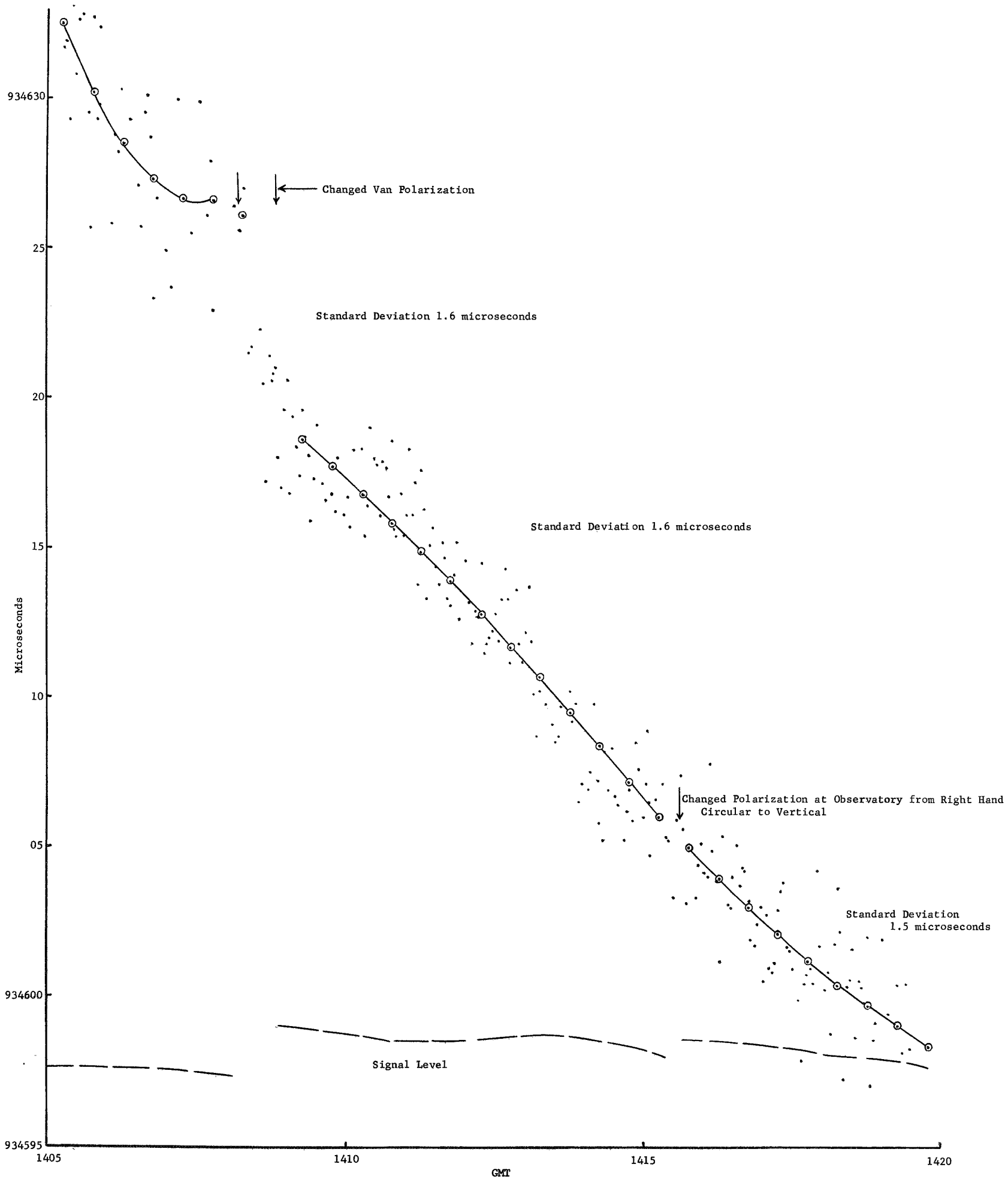

FIGURE 5-21. VAN RETURNS (2/18/69)

September 5, 1969 (Figures 5-22 and 5-23)

Two important facts are evident from the data. The improved limiter, Section 4, nearly eliminated the change in receiver delay as a function of signal amplitude; and signal amplitude scintillation due to the ionosphere had no discernible effect on the range measurements. The data were recorded while interrogating the Coast Guard Cutter Valiant in the Gulf of Mexico. Signal amplitude for each interrogation is shown by the peak deflections in the left hand chart, Figure 5-22. The Valiant returns are the second largest deflections; the background signal from the satellite with no signal into the satellite is the third, darker, response of the pen. The excursions to the right edge of the chart occurred during transmission from the Observatory when the receiver was turned off.

The lower signal level marked "pol. switch" occurred when the polarization of the Observatory antenna was switched to check the best polarization angle. The other amplitude changes with time were due to scintillation. The correlation of the Observatory, Valiant, and satellite background signals indicates that the scintillation was present on the Observatory to satellite path, but not on the satellite to Valiant path.

The right-hand chart, Figure 5-22, is an analog display of the last three digits of the time interval recording for the propagation time from the Observatory to ATS-3 and return.

Full scale is ten microseconds. A large division is one microsecond. The slope indicates the range change due to satellite motion. In spite of the signal amplitude changes, the standard deviation of the range measurements was 0.49 microsecond, and the largest deviations of any measurements from the computed "best fit" curve were -1.84 and +1.16 microseconds.

The time intervals are plotted as a function of time in Figure 5-23. There is no evidence of range measurement change with signal amplitude change. The computed "best fit" curve and a histogram showing deviations from the curve are also plotted. It is interesting to note the effect on the measured intervals of the phase matcher's 0.4 microsecond quantization increment.

REFERENCES

1. G. H. Millman, "A Survey of Tropospheric, Ionospheric, and Extraterrestrial Effects on Radio Propagation Between the Earth and Space Vehicles", General Electric Company Report TIS R66EMH1, 1966.

2. M. Mendillo, et al, "Mid-latitude Ionospheric Variations During Magnetic Storms", Paper presented at the Symposium on the Application of Atmospheric Studies to Satellite Transmissions sponsored by AFCRL, Boston, September, 1969.

3. General Electric Company Report, "Study of Satellites for Navigation", Contract NASw-740, February, 1964.

4. R. S. Lawrence, D. J. Posakony, O. Garriott, and S. C. Hall, "The Total Electron Content of the Ionosphere at Middle Latitude Near the Peak of the Solar Cycle", Jr. Geophys. Res., Vol. 68, No. 7, April 1, 1963, p. 1889.

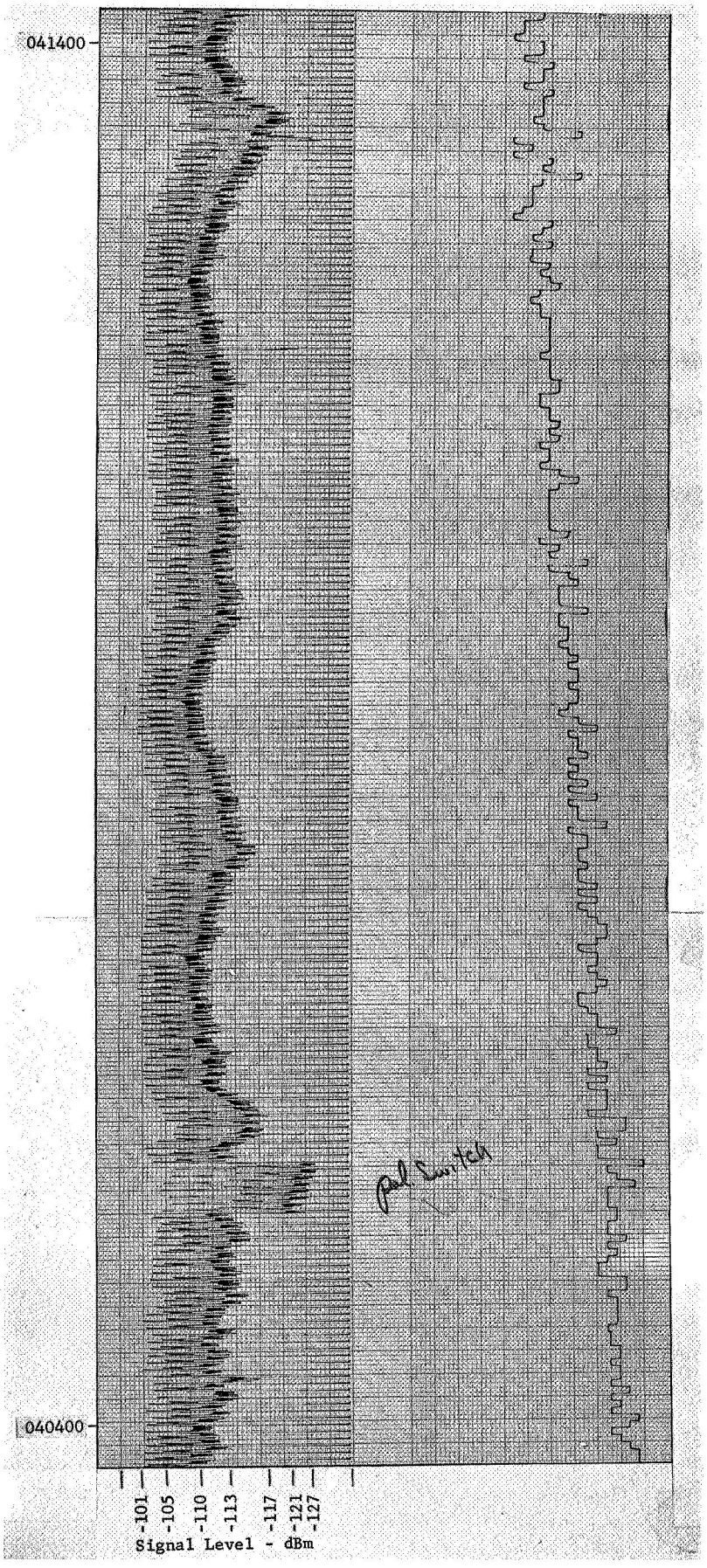

FIGURE 5-22. SIGNAL AMPLITUDE AND TIME DELAY VARIATIONS

FIGURE 5-23

OBSERVATORY RETURNS, ATS-3
SCINTILLATION
September 5, 1969

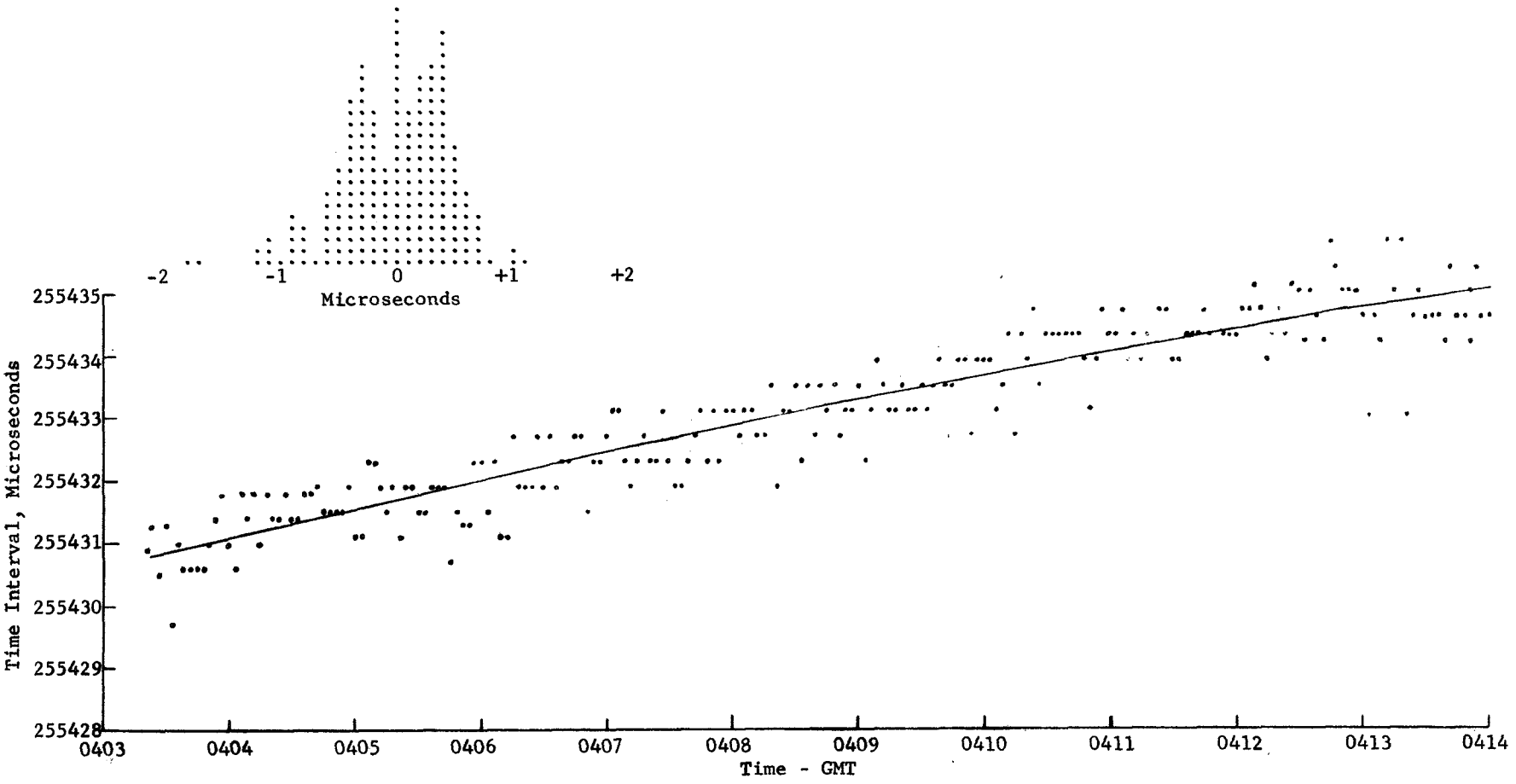

SECTION 6. AIRCRAFT TESTS

The Federal Aviation Administration furnished the use of two aircraft - a DC-6 and a KC-135 as well as the use of a receiver-transmitter used previously for voice communication tests through the ATS satellites. The transceiver is a Bendix type RTA41B with an MDA41 modem for frequency modulation and a PAA41A 500 watt power amplifier. A type LNA41 low-noise preamplifier was used.

A tone-code ranging responder was connected between the data output of the receiver and the data input of the transmitter. The "turn-around time" of the unit, the time to switch from receive to transmit, was so long that there was not sufficient time for the tone response within 1024 cycle periods. It was necessary therefore to lengthen the delay in the responder between correlation of the code and retransmission of the code from the usual period of 1024 cycles of the 2.4414 kHz tone frequency to 2048 periods. This was done by rewiring a connection in the responder's binary divider. This lengthened the time between correlation of the code in the unit and retransmission of the code to 0.86 second. It is reported that new units designed for the 747 aircraft will have a turn-around time shorter than 110 milliseconds, which is short enough to employ the 0.43 second built-in time delay in the other tone-code responders.

When a responder unit is attached to a receiver-transmitter, we refer to the complete unit as a tone-code ranging transponder.

Attachment of the responder unit did not affect the usefulness of the receiver-transmitter for voice communication.

As an example, while the Coast Guard Cutter Valiant was being interrogated through ATS-3 on June 27, the FAA KC-135 aircraft, N96, made a voice call through the satellite which was received at Schenectady while the interrogation of the Coast Guard ship was in progress. The aircraft stated that it was on the runway at Lajes Airfield in the Azores, ready for take-off, and requested that range measurements be made on the aircraft until it was airborne. The tone-code generator and correlator were switched to the aircraft code at the Observatory and successful range measurements were made to the aircraft as it proceeded down the runway and became airborne. Interrogation of the Coast Guard ship at Galveston was then resumed by switching back to its address code. The unplanned exercise demonstrated the voice and ranging compatibility of the tone-code ranging technique, as well as the ability to interrogate one user while another user's transponder was turned on and receptive to interrogations.

The transponder was installed in a DC-6 aircraft at the FAA's National Aviation Facilities Experimental Center, at Atlantic City, New Jersey. The aircraft was equipped with a VHF blade antenna of conventional design and a Dorne & Margolin Satcom antenna. The VHF blade is vertically polarized and its gain pattern is not clearly defined. It is receptive to signals coming from below the horizontal plane and is therefore receptive to satellite signals reflected from the sea and subject to sea reflection interference or multipath. The Dorne & Margolin Satcom antenna is circularly polarized and has two modes of operation. Both are approximately non-directional in azimuth. The horizon mode is designed to receive signals from 10 degrees to 40 degrees elevation angle and the zenith mode is designed to receive signals

from 40 degrees elevation angle to a maximum gain in the zenith direction. Both modes, particularly the zenith mode, of the Dorne & Margolin antenna are less receptive to signals reflected from the sea than is the VHF blade antenna.

Table 6-1 is a log of flight tests made with the DC-6B aircraft. After the completion of the tests with the DC-6B aircraft the tone-code ranging transponder was reinstalled in a KC-135 aircraft at Oklahoma City. The KC-135, a jet similar to the Boeing 707, was equipped only with a VHF blade antenna. A log of flight tests with the KC-135 aircraft is given in Table 6-1 also.

The following descriptions are organized with regard to test objectives rather than chronologically.

A major objective of the June 13 flight was a test of the two satellite position fixing performance under good signal conditions over land and water. A portion of the flight path is shown on the map, Figure 6-1. The numbered positions refer to the satellite and VORTAC position fixes, shown in Table 6-2. Interrogations were made at 3 second intervals through ATS-3 and responses were returned from the aircraft through both ATS-1 and ATS-3. The horizon mode of the Satcom antenna provided the best performance, the elevation angle to ATS-1 being 9 degrees and ATS-3 being 33 degrees. Many hundreds of two satellite ranging measurements were made during the flight. From these, ten were arbitrarily selected for comparison with VORTAC positions, choosing ranging measurements made within 3 seconds of a VORTAC fix.

The first satellite position fix was recomputed several times in order to determine the correct equipment delay biases. Once these had been determined, the same biases were used for all of the other position determinations. This step was necessary as changes had been made to the aircraft equipment and to the Observatory equipment between the time the aircraft transceiver was integrated with the responder at Schenectady and installed on the aircraft. In all cases throughout the experiment it was found easier to calibrate equipment delay biases with the user equipment at a remote location rather than by measurement in the laboratory. Once the biases were determined for the June 13 flight, the same values were used for the later processing of data from the June 12 flight. There was no significant difference in the equipment delay biases for the two days.

With the bias corrections properly inserted, the computations for the arbitrarily selected ten sample measurements of the June 13 flight were made and compared with the VORTAC position determinations as provided by the FAA. The FAA's position determination method and locations of the aircraft for the June 12 and 13 flights are presented in Appendix I. The satellite and VORTAC position determinations are in such close agreement that they could not be separately plotted to the scale of the map in Figure 6-1. They are compared in Table 6-2. The VORTAC positions were determined to the nearest minute. One minute represents one nautical mile in latitude and approximately 0.7 nautical mile in longitude. All of the arbitrarily selected satellite position fixes agree with the VORTAC positions within $\pm$ 3 minutes of latitude and $\pm$ 2 minutes of longitude.

Short term variations in satellite position fixes are indicated in Figure 6-2, a plot of another ten fixes made within 45 seconds. They are numbered in time sequence. VORTAC positions for times before and after the ten satellite position fix determinations are plotted as the larger circles on the chart. The data are also presented in Table 6-3.

TABLE 6-1

DC-6B AIRCRAFT FLIGHT TESTS

DATE	TIME	LOCATION	SATELLITES	PURPOSE
6/4/69	1810-1955	Off New Jersey Coast	ATS-3	Antenna, sea reflection effects
6/6/69	1215-1430	Off New Jersey Coast	ATS-3	Sea reflection effects, altitude change
6/9/69	1240-1430	Atlantic City to Fort Royal, West Virginia	Both	Two satellite ranging over land
6/12/69	1245-1430	Joliet, Illinois to Omaha via Minneapolis	Both	Two satellite ranging over land
6/13/69	1250-1430	Omaha to Detroit via Minneapolis	Both	Two satellite ranging over land and water

KC-135 AIRCRAFT FLIGHT TESTS

DATE	TIME	LOCATION	SATELLITES	PURPOSE
6/20/69	1825-2000	56^{o}N, 55^{o}W - 63^{o}N, 30^{o}W; enroute to Iceland	ATS-3	High altitude, high speed over water ranging
6/23/69	1420-1430	Vicinity 61^{o}N, 40^{o}W	ATS-3	High altitude, high speed over water ranging
6/27/69	1342-1346	Azores	ATS-3	Ranging during takeoff

FIGURE 6-1

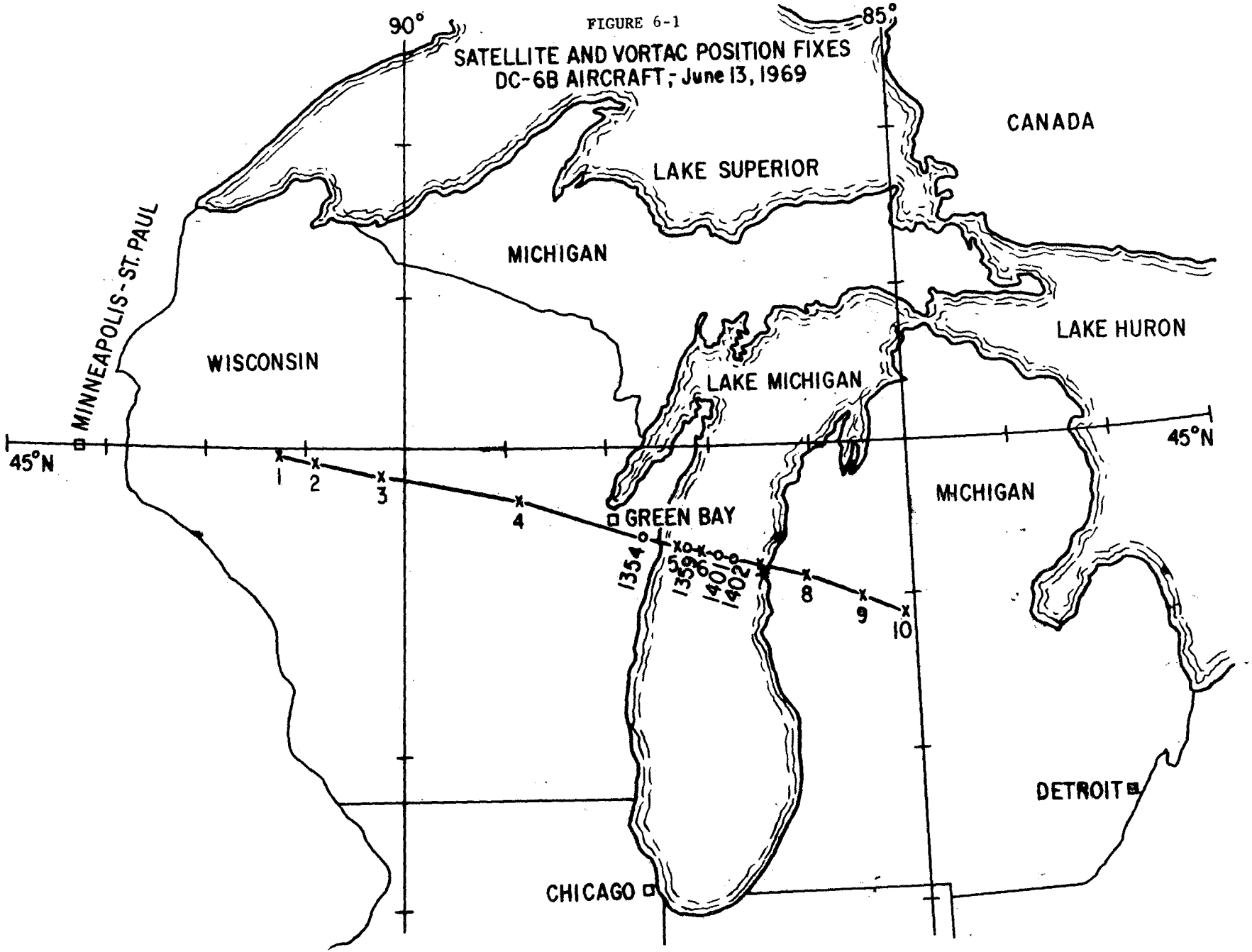
SATELLITE AND VORTAC POSITION FIXES
DC-6B AIRCRAFT; June 13, 1969
90°
85°
CANADA
LAKE SUPERIOR
MICHIGAN
MINNEAPOLIS-ST. PAUL
WISCONSIN
LAKE HURON
LAKE MICHIGAN
45°N
45°N
1
2
3
4
GREEN BAY
1354
1359
1401
1402
8
9
10
MICHIGAN
DETROIT
CHICAGO

TABLE 6-2

COMPARISON OF SATELLITE AND VORTAC POSITION FIXES
DC-6B AIRCRAFT, MINNEAPOLIS TO DETROIT
June 13, 1969

	Time-GMT	Latitude	Longitude
Satellite	13 21 54	44°59'08"	91°15'33"
VORTAC	13 21 51	44°57'	91°16'
Difference		+02'	0
Satellite	13 25 00	44°54'19"	90°56'21"
VORTAC	13 25 00	44°55'	90°55'
Difference		-01'	+01'
Satellite	13 30 45	44°48'51"	90°17'13"
VORTAC	13 30 45	44°50'	90°15'
Difference		-01'	+02'
Satellite	13 43 21	44°41'47"	88°51'29"
VORTAC	13 43 24	44°39'	88°53'
Difference		+03'	-02'
Satellite	13 57 57	44°24'28"	87°18'12"
VORTAC	13 57 57	44°22'	87°19'
Difference		+02'	-01'
Satellite	14 00 03	44°20'41"	87°06'14"
VORTAC	14 00 00	44°19'	87°04'
Difference		+02'	+02'
Satellite	14 06 00	44°12'12"	86°30'53"
VORTAC	14 06 00	44°12'	86°31'
Difference		0	0
Satellite	14 10 30	44°07'31"	86°04'15"
VORTAC	14 10 30	44°07'	86°04'
Difference		+01'	0
Satellite	14 16 06	43°58'07"	85°31'55"
VORTAC	14 16 06	43°59'	85°31'
Difference		-01'	+01'
Satellite	14 20 36	43°50'33"	85°06'42"
VORTAC	14 20 33	43°52'	85°07'
Difference		-01'	0

FIGURE 6-2

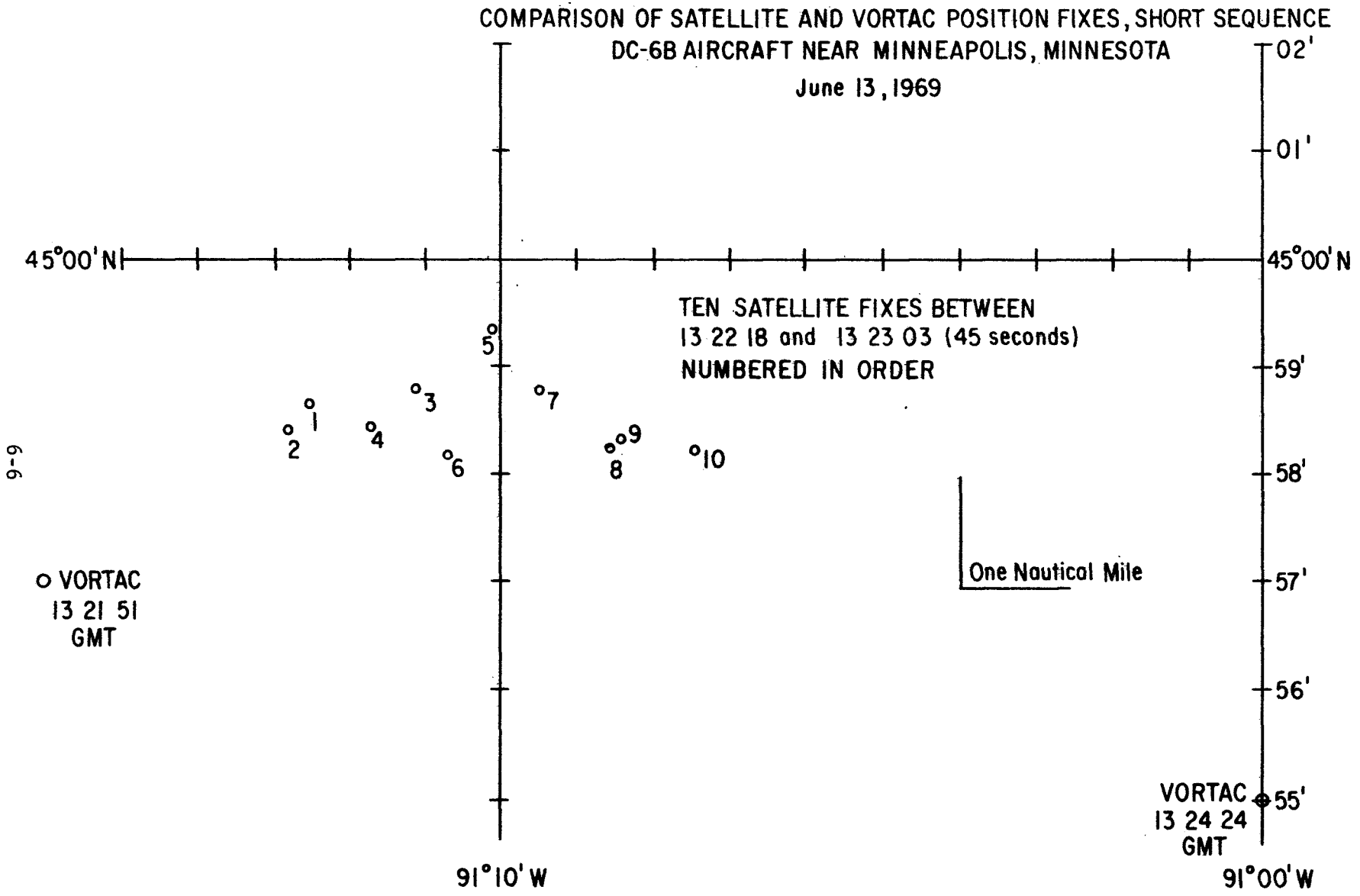
COMPARISON OF SATELLITE AND VORTAC POSITION FIXES, SHORT SEQUENCE
DC-6B AIRCRAFT NEAR MINNEAPOLIS, MINNESOTA
June 13, 1969
02'
01'
45°00'N
45°00'N
TEN SATELLITE FIXES BETWEEN
13 22 18 and 13 23 03 (45 seconds)
NUMBERED IN ORDER
59'
58'
57'
56'
55'
1
2
3
4
5
6
7
8
9
10
One Nautical Mile
VORTAC
13 21 51
GMT
VORTAC
13 24 24
GMT
91°10'W
91°00'W
6-9

TABLE 6-3

COMPARISON OF SATELLITE AND VORTAC POSITION FIXES, SHORT SEQUENCE
DC-6B AIRCRAFT NEAR MINNEAPOLIS, MINNESOTA
June 13, 1969

Satellite Position Fixes

Time-GMT	Latitude	Longitude
13 22 18	44°58'40"	91°12'35"
13 22 24	44°58'26"	91°12'48"
13 22 27	44°58'50"	91°11'06"
13 22 30	44°58'28"	91°11'43"
13 22 39	44°59'21"	91°10'03"
13 22 42	44°58'09"	91°10'41"
13 22 45	44°58'50"	91°09'31"
13 22 51	44°58'14"	91°08'36"
13 22 57	44°58'19"	91°08'25"
13 23 03	44°58'11"	91°07'24"

VORTAC Position Fixes

Time-GMT	Latitude	Longitude
13 21 51	44°57' N	91°16' W
13 24 24	44°55' N	91°00' W

Precision of the fixes was plotted relative to the mean range measurements for the period between 1354 and 1402 GMT while the aircraft was making a land-to-water transition. It shows that only four of the 74 dual responses would produce fixes in error by more than one nautical mile. (Figure 6-3)

The plot was made as follows:

1. A best-fit curve was computed for the range measurements from each satellite during the eight minute period,

2. The displacement of a range measurement from the best fit curve was determined and its projection on the earth for the elevation to the satellite was calculated.

3. A line of position was plotted at right angles to the satellite azimuth direction, and displaced from the center reference point by the distance determined in step two.

4. A second line of position for the same interrogation was plotted from the range measurement of the other satellite. The crossing of the two lines of position determines individual fix error in magnitude and direction relative to the mean of all the fixes during the time period.

Factors not included in the fix precision plots are bias errors due to ionospheric bias, satellite tracking uncertainty, aircraft altitude uncertainty and equipment time delay bias. With the possible exception of the aircraft altitude uncertainty, these bias changes have periods of hours, days or longer. The magnitudes of their effects can be controlled by monitoring the effects and calibrating the equipment and system. For example: transponders at fixed known locations along the routes traveled by the craft would enable the monitoring of ionospheric bias errors to the degree that the ionospheric bias errors are correlated over the distances between the fixed locations of the reference transponders and the craft that are enroute. Equipment delay biases can be measured by interrogating the user transponders when the craft are at known locations such as airports or docks. They may also be checked without satellite interrogation as a routine maintenance function.

All of the factors that affect the short term variations in accuracy are included in the precision plots. These include sea reflection interference (multipath), changing signal-to-noise ratio, changing signal level and its effect upon receiver time delay, as well as short-term fluctuations in ionospheric propagation delay. In an operational system signal-to-noise ratio can be high a much greater percentage of the time than was true in the test program. Equipment time delay variations can be reduced significantly for an operational system compared with the test program. A means to reduce equipment delay variations has already been implemented in some of the equipments used in the tests.

Perhaps the largest factor in fix precision in the test is sea reflection multipath. This can be minimized by improved antenna designs, although it may remain as the factor that contributes the largest errors to position fix accuracy at VHF. Its effect on overall system performance can be minimized if its characteristics are recognized and certain precautions taken in the operation of the system.

FIX ERROR DISTRIBUTION
FAA DC-6 AIRCRAFT OVER LAKE MICHIGAN
13 June 1969, 13 54 00 - 14 02 00 GMT

160 Interrogations
74 Dual Responses

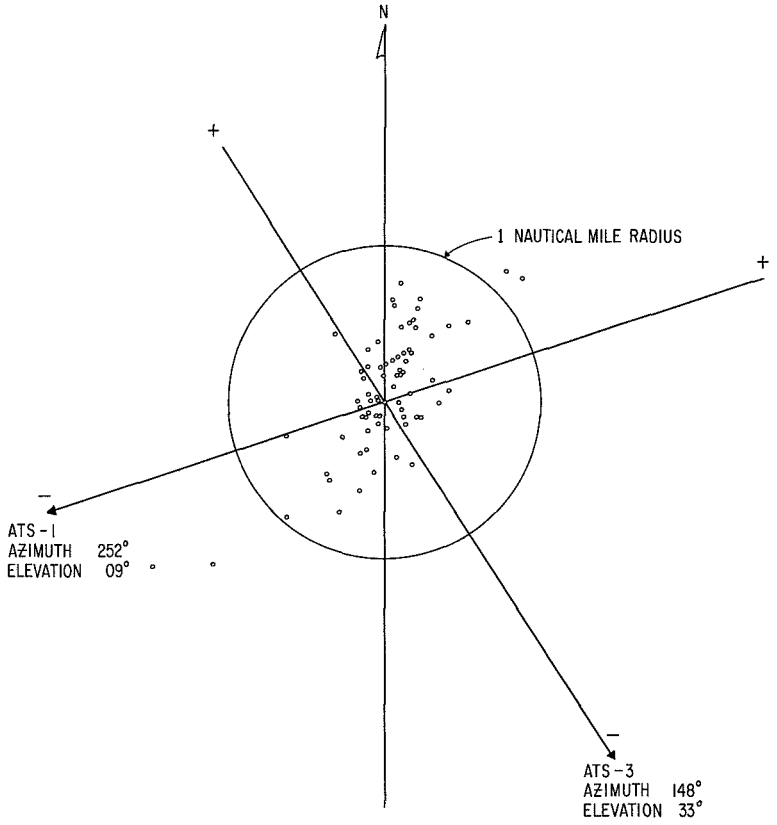

FIGURE 6-3

As shown in the multipath analysis, later in this section, the distribution of errors is centered about a value near zero error. Although an occasional single measurement may be in error by a large amount, the average error for a number of measurements tends toward zero. If the aircraft is interrogated through one satellite and the responses are returned through two satellites, the multipath error on the link from the satellite to the aircraft, that is the interrogating signal, will displace the two returns by the same amount. As a consequence a fix determination based on the measurement will have a fix error that lies along a hyperbolic line of position. Multipath on the return links from the aircraft to the satellites are independent and therefore will not tend to cause errors lying along hyperbolic lines of position. However, the overall effect of multipath is to produce fix errors that tend to lie along a hyperbolic line if interrogations are through one satellite and responses through two.

The accuracy of the VHF system can be improved by taking more than the minimum number of position fixes that are required and by relating these position fixes to each other so that the track of the craft can be monitored and those occasional fixes that show a large deviation from the expected track can be regarded with less credence than the others. If fixes are required on a craft at infrequent intervals it would be advantageous to take three or more fixes and compare them to arrive at the accepted value of the position fix. Since the largest uncontrollable factor appears to be the sea reflection multipath, surface craft will be less subject to occasional fix errors of large magnitude.

The June 12 flight from Joliet to Omaha via Minneapolis was a test of two satellite position fixing performance over land. It was the first test made with an aircraft in flight where the elevation angles from both satellites to the aircraft were high enough to correspond with the minimum elevation angles that would be used in an operational system, although the path from ATS-1 to the Observatory which influences the accuracy of the system was much below the elevation angle required for an operational system. The signal-to-noise ratio at the aircraft receiver was poor because the aircraft was flying in the vicinity of thunder storms. As a result, the link performance was worse than that of the following day when the aircraft was in the same geographical area. All three antenna modes were tested: the horizon and zenith modes of the Satcom antenna, and the VHF blade. Interrogations were made through ATS-1 as well as through ATS-3. Although the link performance was marginal throughout most of the tests, the accuracy of the position fix measurements made were not significantly different from the results obtained under good signal conditions the following day.

The same equipment delay bias values were used in computing the June 12 and 13 position fixes. A comparison of satellite and VORTAC positions is presented in Table 6-4, and plotted in Figure 6-4. The values cannot be directly compared as the times of the position fixes by the two different methods do not exactly correspond. The VORTAC and the satellite positions agree with the position fixes on the following day within expected tolerances, demonstrating that there were no observable changes in the equipment time delays.

VORTAC derived aircraft positions were the most accurate means available during the flights, but are not to be construed as a standard of comparison for the performance of the satellite location technique. At best, the VORTAC positions are accurate to ± 1 nautical mile.

FIGURE 6-4

COMPARISON OF SATELLITE AND VORTAC POSITION FIXES
DC-6B AIRCRAFT - June 12, 1969

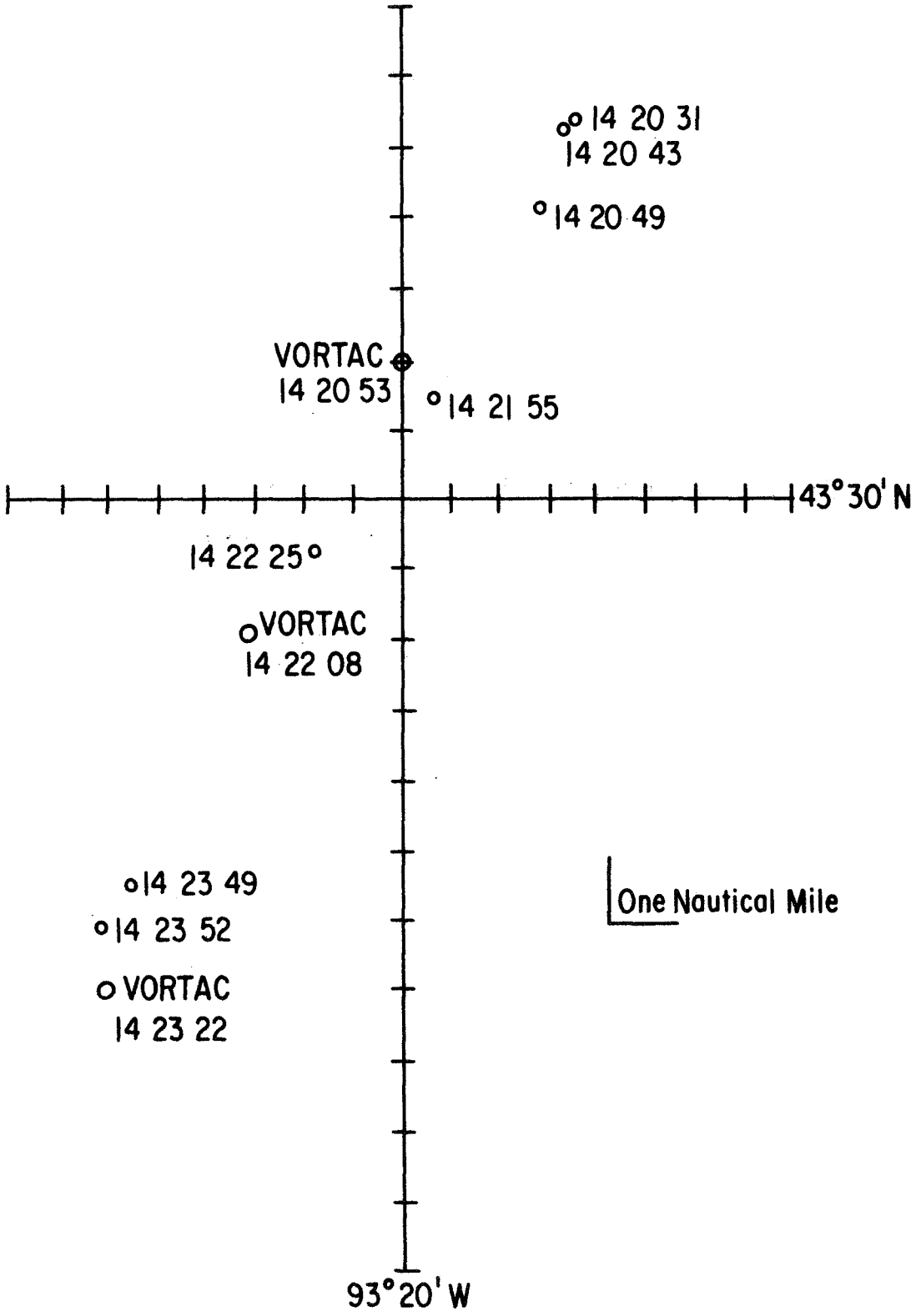

TABLE 6-4

COMPARISON OF SATELLITE AND VORTAC POSITION FIXES
DC-6B AIRCRAFT - June 12, 1969

Satellite Position Fixes

Time-GMT	Latitude	Longitude
14 17 58	43°47'24"	94°06'11"
14 20 31	43°35'23"	94°16'29"
14 20 43	43°35'19"	94°16'49"
14 20 49	43°34'12"	94°17'07"
14 21 55	43°31'30"	94°19'11"
14 22 25	43°29'18"	94°21'44"
14 23 49	43°24'32"	94°25'29"
14 23 52	43°23'57"	94°26'00"
14 24 40	43°21'07"	94°28'22"

VORTAC Position Fixes

Time-GMT	Latitude	Longitude
14 17 06	43°46'	94°12'
14 20 53	43°32'	94°20'
14 22 08	43°28'	94°23'
14 23 22	43°23'	94°26'
14 24 35	43°18'	94°28'

The June 20 flight test was made to evaluate the precision of ranging measurements through ATS-3 to a high performance jet aircraft on the North Atlantic principal routes. The KC-135 aircraft flew at 39,000 feet. The blade antenna was used throughout the test so that the effects of multipath combined with ranging fluctuations due to low signal-to-noise and receiver delay characteristics to produce scatter in the readings. Standard deviation of the measurements varied from approximately 8 microseconds to 11 microseconds. A histogram of all the range measurements is plotted in Figure 6-5. The envelope of the histogram suggests the shape of range error probability distribution that could be obtained by convolving a curve like one of the dashed line curves in Figure 6-12 of the multipath analysis that follows later in this section. The limits of the convolved curve would be double the limits of a one-way ranging curve as shown in Figure 6-6. The histogram shows a maximum deviation range measurement in the long direction which is approximately twice that of the largest deviation in the short direction. The lower scale shows the approximately cross-track error if the range measurements are projected on the earth for a satellite having an elevation angle of 25 degrees. It indicates the precision of cross-track monitoring that would be achieved for a satellite at mid-ocean longitude while monitoring cross-track positions of aircraft flying at maximum altitudes on North Atlantic routes with signal conditions like those of the experiment. It is expected that an operational system would have stronger signals, antennas with better discrimination against multipath than the VHF blade, and better ground station receiver characteristics than were used in the experiment. Nevertheless, the experimental result, as it stands, appears to have sufficient precision for useful cross-track surveillance.

Range error due to sea reflection multipath is a function of the relative amplitudes of the reflected and direct signals, the delay of the reflected signal behind the direct signal, and the radio frequency phase difference between the direct and reflected signals. As an aircraft flies through a distance such that the radio frequency path length difference of the direct and reflected signals changes by one wavelength at the radio frequency, the one-way range error due to specular sea reflection will vary in a manner typified by one of the curves in Figure 6-6. The aircraft may fly a considerable distance in straight and level flight to change the path length difference by one wavelength, but the aircraft need only move vertically a few feet to change the path length difference by one wavelength at VHF.

Figure 6-7 depicts the geometry and the time delay of the reflected signal behind the direct signal. It is assumed that the satellite is very distant and that the earth is flat in the region of the aircraft. Jet aircraft commonly fly at altitudes between 29,000 and 41,000 feet. As shown by the curve, the time delay of the reflected signal behind the direct signal can be several tens of microseconds. The long time delay can cause a considerable phase error in the detected audio frequency signal. It should be noted, however, that the maximum time delay is shorter than the period of the audio frequency used in the experiment, so that there was no ambiguity.

Figure 6-8 presents phasor relationships with sea reflection present for the carrier, the upper and lower sidebands of a narrowband frequency modulated signal, or an amplitude modulated signal. The carrier and the sidebands may each be considered as a single radio frequency which is continuous for the period of the synchronizing signal tone burst. The three signals are coherently related and separated in frequency by the modulating audio frequency.

FIGURE 6-5

RANGE MEASUREMENT DEVIATIONS

ATS-3 to KC-135 Aircraft
Blade Antenna
56°N, 55°W to 63°N, 30°W
Altitude 39,000 feet

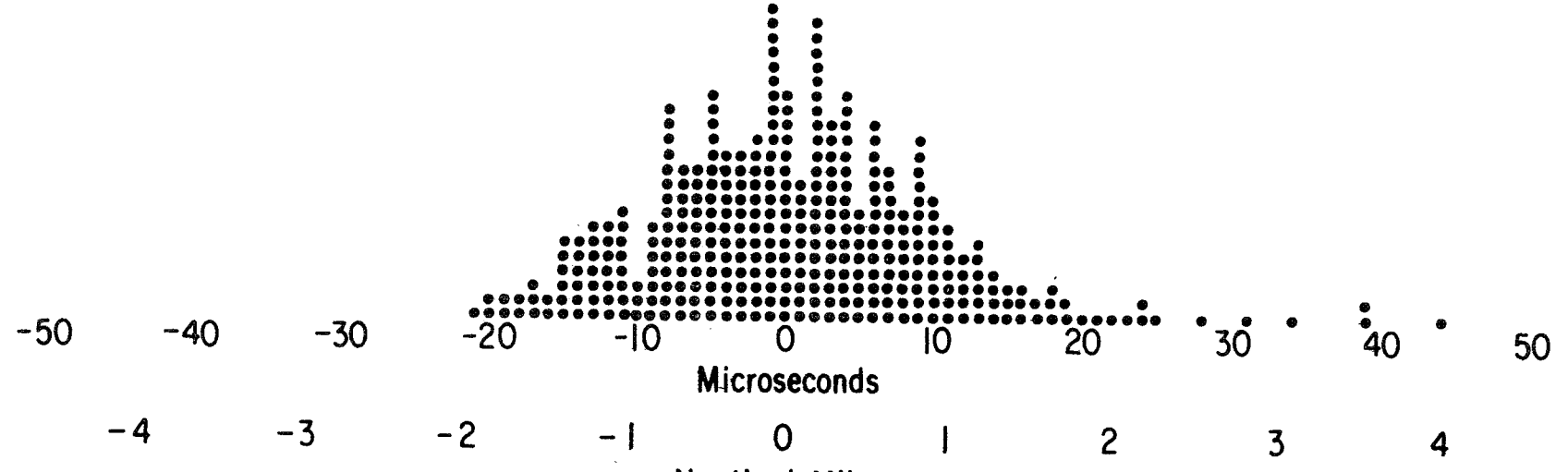

Approximate Cross-Track Error, North Atlantic Routes

FIGURE 6-6

RANGE ERROR DUE TO SPECULAR SEA REFLECTION (ONE-WAY)

Reflected Signal Delay - 25 microseconds
Radio Frequency - 135.6 MHz
Tone Frequency - 2.4414 kHz
FM Deviation - 4 kHz

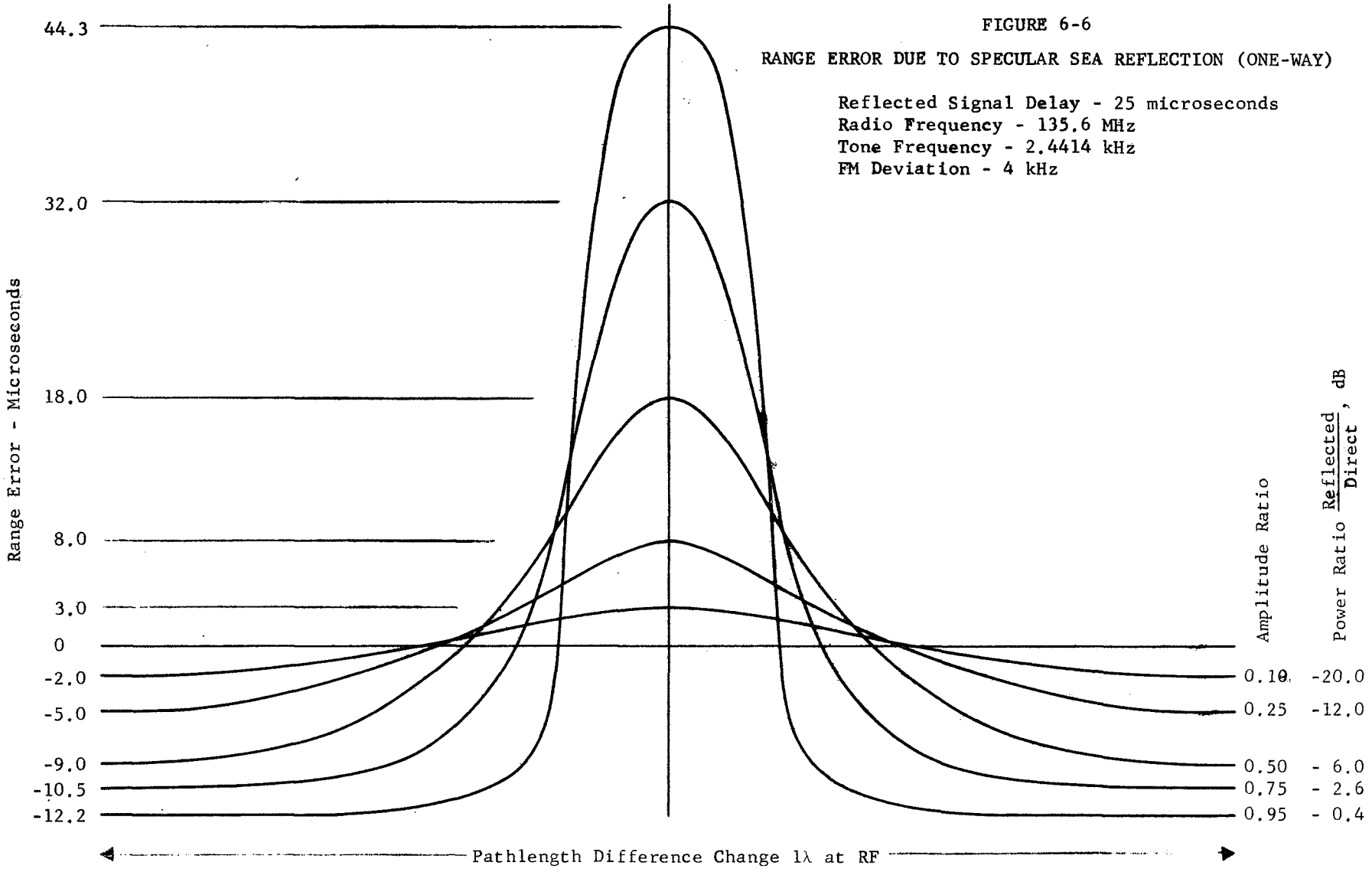

FIGURE 6-7

GEOMETRY AND TIME DELAY OF REFLECTED SIGNAL

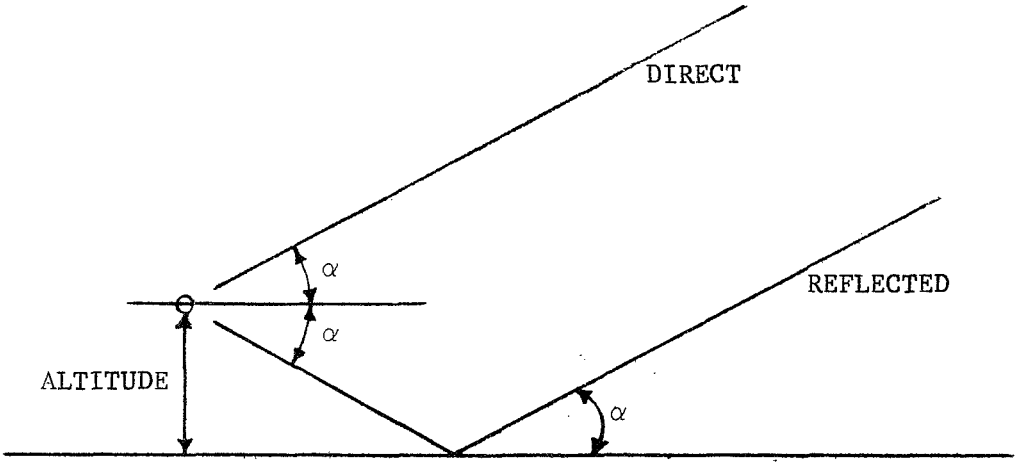

α = ELEVATION ANGLE TO SATELLITE

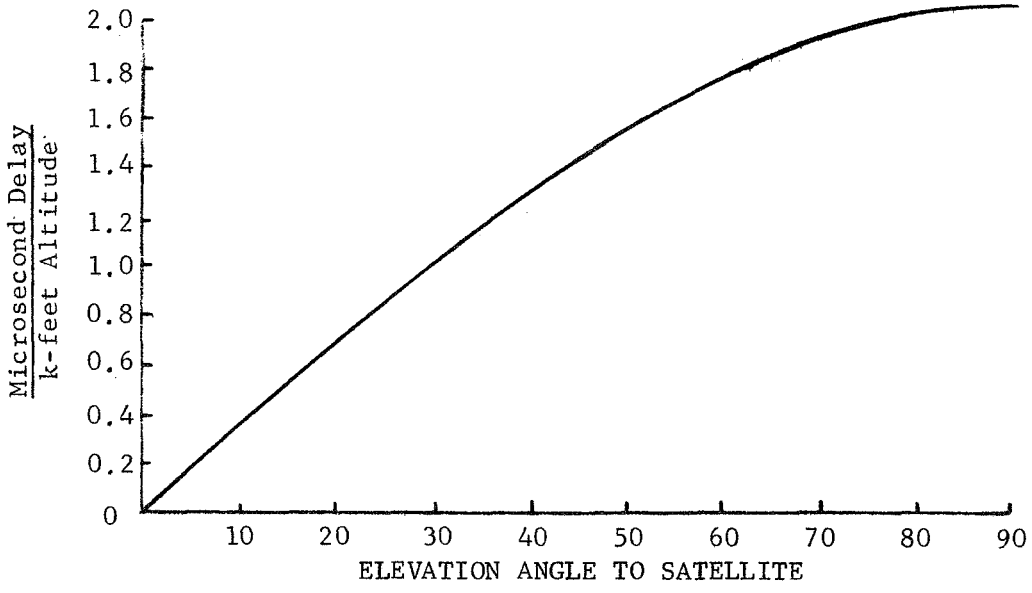

Multiply ordinate value by aircraft altitude in thousands of feet to determine reflected signal delay in microseconds.

FIGURE 6-8

PHASOR RELATIONSHIPS WITH SEA REFLECTIONS

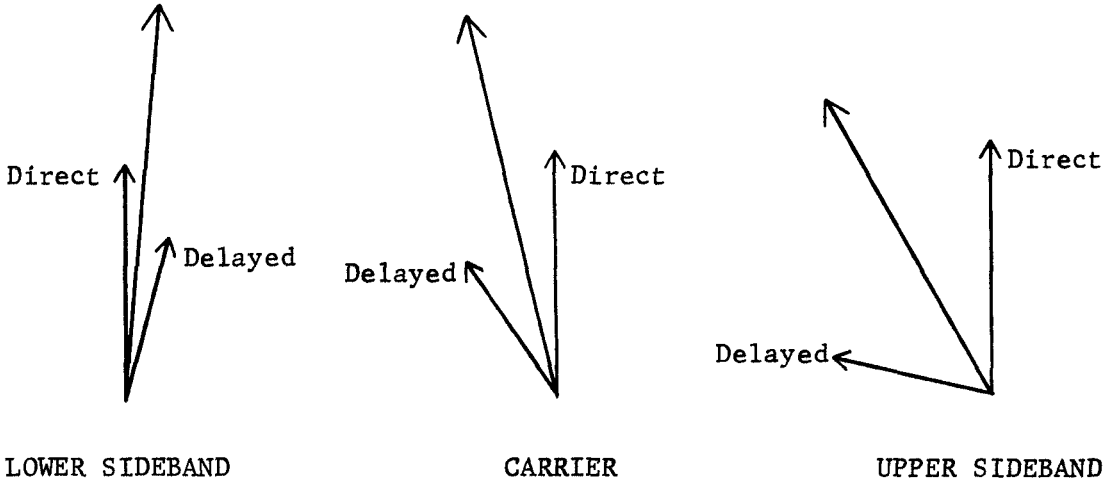

We are interested only in the phase distortion caused by the sea reflection; and therefore, we have shown the direct signals all at the same reference phase. The radio frequencies of the carrier and the sidebands are slightly different, but the time delay for the reflected signals is the same for all. The phase displacement of the delayed carrier behind the direct carrier signal becomes greater as the time delay becomes greater. Because the lower sideband is at a lower frequency, the delayed lower sideband is not displaced in phase as much as the carrier; whereas the upper sideband, because it is at a higher frequency than the carrier, is advanced farther in phase than the carrier. Their displacements from the delayed carrier phase are of the same magnitude, but in opposite directions.

The phasor resultants that are illustrated by the phasors with large arrow-heads in the figure represent the actual carrier and sideband components that are present at the input to the receiver. They are different in their relative phases and amplitudes from the signal components that would be present if there were no sea or ground reflection.

Figure 6-9 illustrates the effect on one of the signal components, the carrier or either sideband, as the aircraft moves through a distance and direction such that there is a change of one radio frequency wavelength between the direct signal and reflected signal path lengths. As this change occurs, the reflected signal component makes 360 degrees of phase change relative to the direct signal. In the figure, a circle represents the tip of the rotating reflected signal phasor relative to the direct signal phasor. The upper diagram shows the relationship for a relative signal amplitude of 0.25; that is, the amplitude of the reflected signal is one-fourth the amplitude of the direct signal. In the lower figure, the reflected signal is 0.75 times the direct signal amplitude. The dashed phasors represent the resultants for several points during the rotation of the reflected signal relative to the direct signal. It will be noted that the amplitude of the resultant phasor changes and that its phase relative to the direct signal also changes. The larger the ratio of the reflected to direct signal, the larger is the relative phase change. It is also important to note that the phase change of the resultant relative to the direct signal is not sinusoidal, but changes rather slowly when the reflected and direct signals are in phase, and changes very rapidly when they are out of phase.

Figure 6-10 presents the phase displacement of the phasor resultant relative to the direct signal phase for four different amplitude ratios as the relative path lengths change by one wavelength.

Figure 6-11 compares the phase changes of the carrier and the two sidebands as the difference in path length changes by one wavelength at the radio frequency. Referring to Figure 6-8, the Phasor Relationships with Sea Reflection, it is apparent that the pattern of phase displacement for the carrier and the sidebands is shifted by an amount proportional to the time delay of the reflected signal behind the direct signal. For one RF path length change, we may ignore the fact that the sideband delayed signal phasors as depicted in Figure 6-8 do not make exactly one rotation relative to the direct signals if the carrier does make exactly one rotation. It is, however, this very small difference that accumulates over many wavelengths difference in path length to produce the phase displacements when the delay of the reflected signal increases to significant values.

FIGURE 6-9

EFFECT OF AMPLITUDE CHANGE ON PHASOR RESULTANT

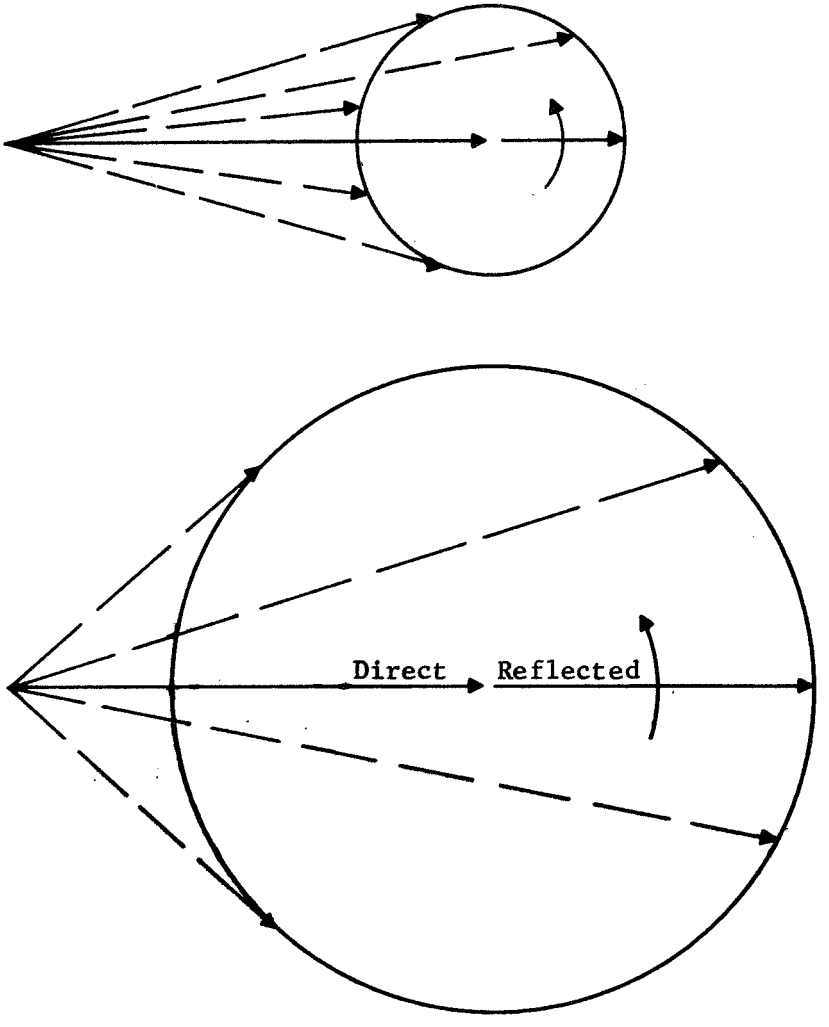

FIGURE 6-10

DISPLACEMENT OF SIGNAL PHASOR DUE TO SEA REFLECTION

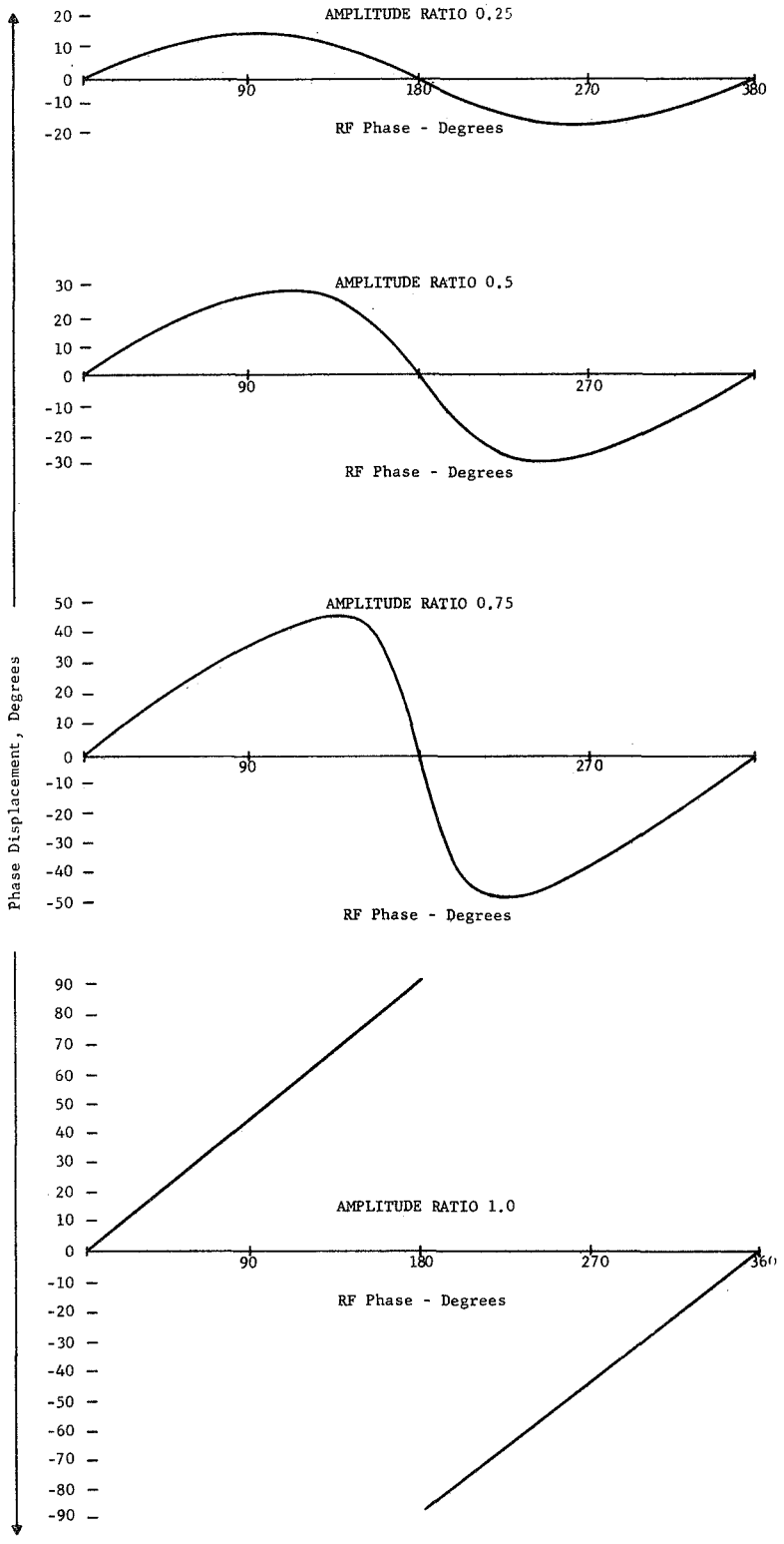

FIGURE 6-11

PHASE CHANGE FOR 360 DEGREE (RF) PATHLENGTH
CHANGE, DIRECT AND REFLECTED SIGNALS

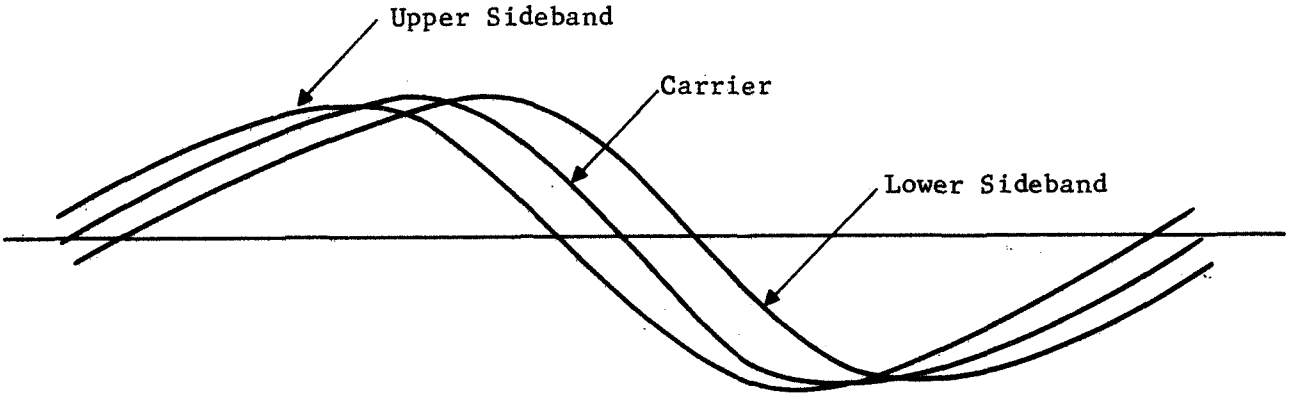

When the carrier and two sidebands of a frequency modulation signal distorted by sea reflection multipath are applied to a frequency discriminator, the detected audio frequency signal is displaced in phase from the phase it would have without multipath as shown in Figure 6-6, where phase error is plotted as a ranging time error for a specified tone frequency and reflected signal delay. The range error depends upon the ratio of the reflected signal amplitude to direct signal amplitude, the radio frequency phase difference between the direct and reflected signals, and the time delay of the reflected signal behind the direct signal. If the reflected signal amplitude is nearly equal to the direct signal amplitude, the one-way range error due to specular sea reflection varies from approximately one-half the delay time less than the true ranging time value to approximately two times greater than the delay time. The largest error tends to be eliminated because it occurs when the radio frequency signals arrive out of phase, the received signal strength tends towards zero and may not be detected.

The range error probability distribution is depicted in Figure 6-12. The solid line curve was calculated from the computed results of the 0.1 amplitude curve of Figure 6-6. The dashed line curves have limits that were computed, but their exact shape is approximated. The area under each curve represents unity probability. Although it was not proven by rigorous mathematical analysis, examination of the computed curves suggests that the probability of a range error being longer than the true value is equal to the probability that it is shorter than the true value. The magnitudes of the errors in the long direction can be larger than the magnitudes of the errors in the short direction, but their probability of occurrence is lower. The average error for a large number of range measurements tends towards zero error in the presence of specular sea reflection.

The down-link and up-link frequencies for the ATS ranging and position fixing experiment were different, being 135.6 MHz on the down-link and 149.22 MHz on the up-link. Sea reflection multipath can affect both links. Because of the very large number of RF wavelengths between the satellite and the aircraft, the radio frequency phase differences on the two paths are dependent and therefore the total effect of sea reflections on the two paths must be determined by convolving the range error probability distribution for the one-way path, shown in Figure 6-12. The result of the convolution is depicted in Figure 6-13 for the case of an amplitude ratio equal to 0.1. The convolution extends the limits to twice the limits of the one-way ranging curves with equal probabilities of errors in the long or short range directions. The maximum error expected in the short direction is less than the maximum error in the long direction. Maximum errors expected for the 0.25 amplitude ratio dashed line of Figure 6-12 would be approximately -10 and +16 microseconds, and for the 0.5 amplitude ratio, approximately -16.5 and +36 microseconds.

Experimental variations in range measurement are due to many factors, including signal-to-noise ratio, equipment time delay variations as a function of signal amplitude, and diffuse multipath effects as well as the specular multipath effects that were considered in the foregoing analysis. Some of the data obtained on over-water flights were examined to see if the effects could be observed. Time delay was plotted as a function of time for some of the over-water flights. In some cases, a cyclic pattern of range variation about the mean suggested the shape of the curve shown in Figure 6-6. An example is the plot of a portion of the June 13 DC-6B flight, shown in Figure 6-14. The DC-6B craft was at 21,000 feet over Lake Michigan using the horizon mode antenna. A portion of these data, extending over a period longer than the

FIGURE 6-12

RANGE ERROR PROBABILITY DISTRIBUTION
25 MICROSECONDS DELAY OF REFLECTED SIGNAL
ONE-WAY RANGING

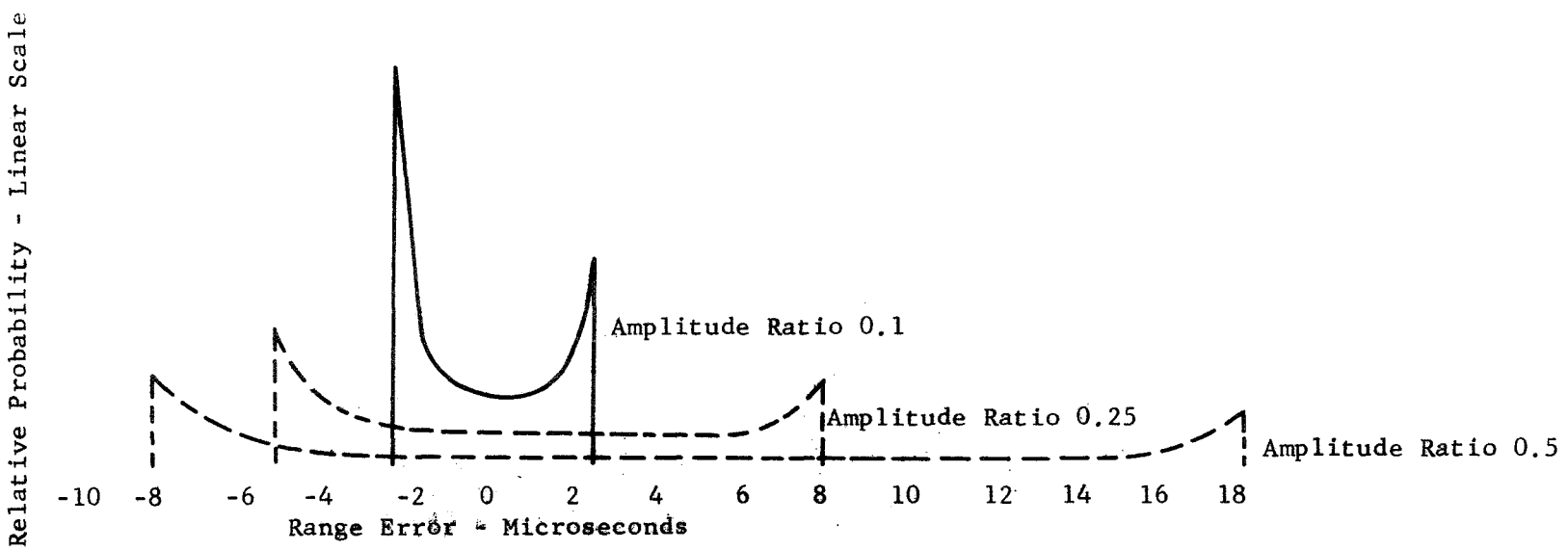

FIGURE 6-13

RANGE ERROR PROBABILITY DISTRIBUTION
25 MICROSECONDS DELAY OF REFLECTED SIGNAL
AMPLITUDE RATIO 0.1
TWO-WAY RANGING

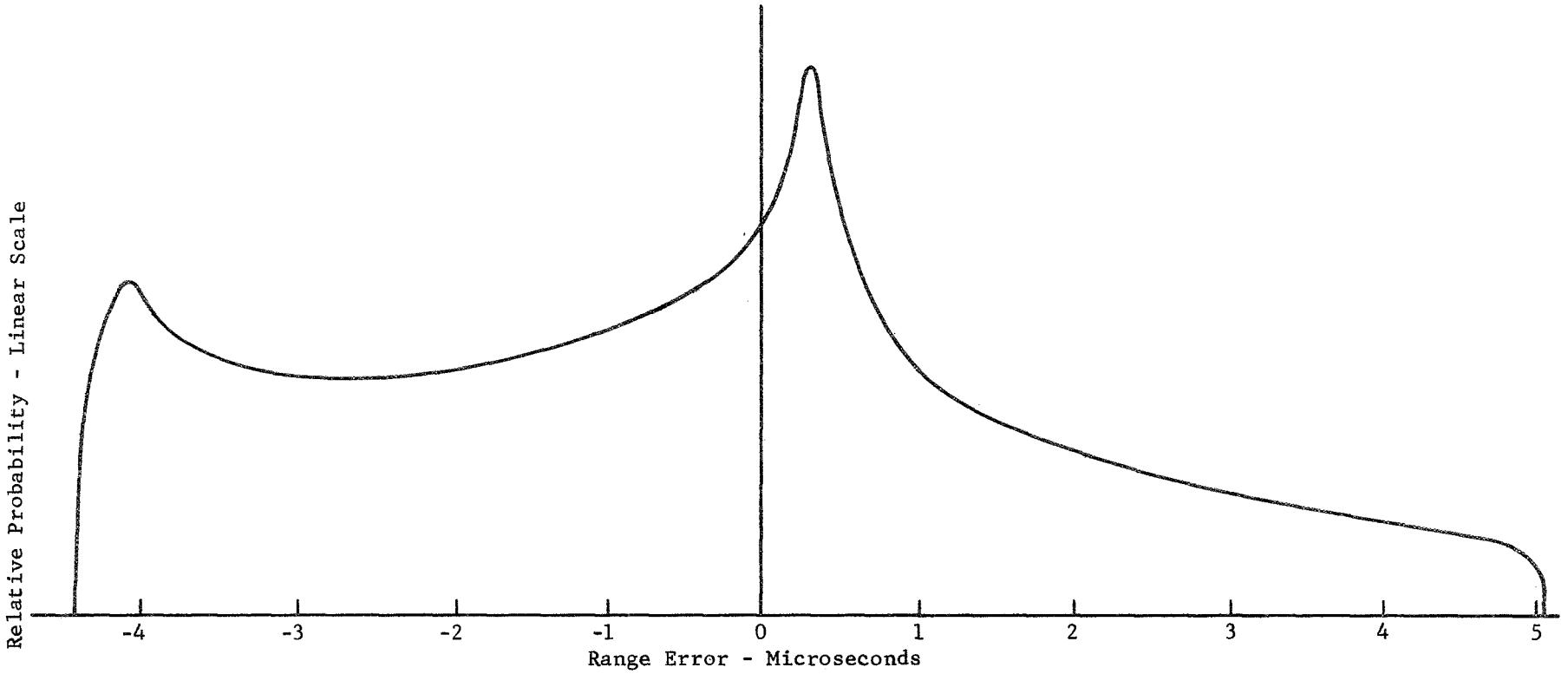

FIGURE 6-14

RANGE MEASUREMENTS FROM ATS-3
TO A DC-6 AIRCRAFT AT 21,000 FEET
OVER LAKE MICHIGAN
(6/13/69)

(Horizon Mode)

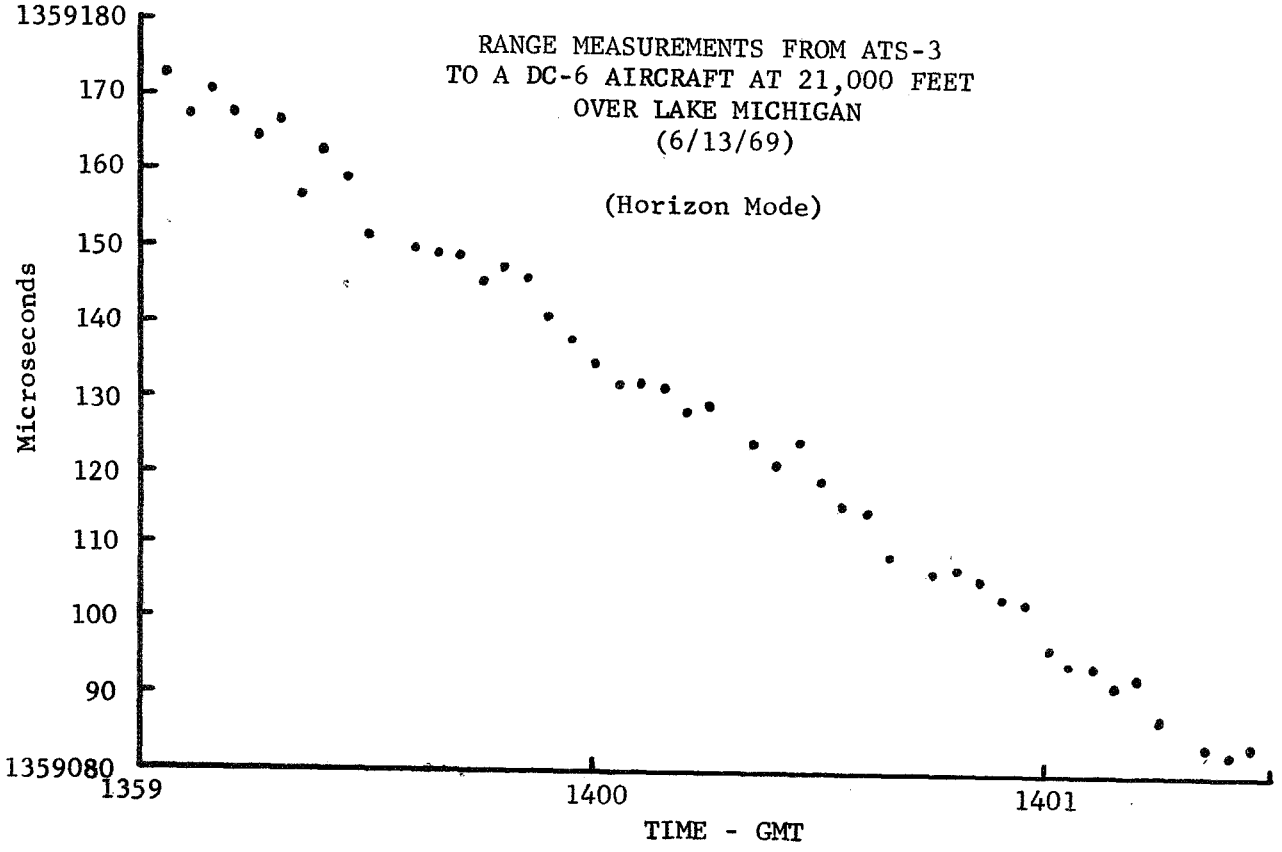

2.5 minute period of Figure 6-14, was plotted as a histogram and is presented in the lower portion of Figure 6-15. While it cannot be concluded that the envelope shape of the histogram is the result of sea reflection multipath, it is interesting to compare it with Figure 6-13. The corresponding histogram for the responses through ATS-1 is also plotted, but no significance is attached to its envelope shape.

Range measurements from ATS-3 to the KC-135 aircraft over the North Atlantic at 39,000 feet are plotted as a histogram in Figure 6-5. The envelope of the histogram suggests the shape of a distribution curve for two-way ranging that would result from convolving one of the dashed line curves of Figure 6-12. The limits of the experimental data are -21 and +44 microseconds, with comparatively few measurements near the largest, longer range values. The aircraft was using a VHF blade antenna that is sensitive to sea reflections.

Multipath errors are expected to increase with the altitude of the aircraft if the elevation angle to the satellite does not change. During the June 6 flight off the coast of New Jersey, the aircraft flew at 20,000 feet and also at 5,000 feet. Histograms of range measurements made at each altitude are presented in Figure 6-16. Standard deviation of the range measurements was 2.1 microseconds at 5,000 feet and 3.0 microseconds at 20,000 feet for the data samples plotted in the figure. The larger number of points plotted for 20,000 feet reflects the longer duration of the data sample. Both are believed to be statistically significant so that the standard deviations and histograms can be compared directly.

FIGURE 6-15. DC-6 OVER LAKE MICHIGAN

ATS-1

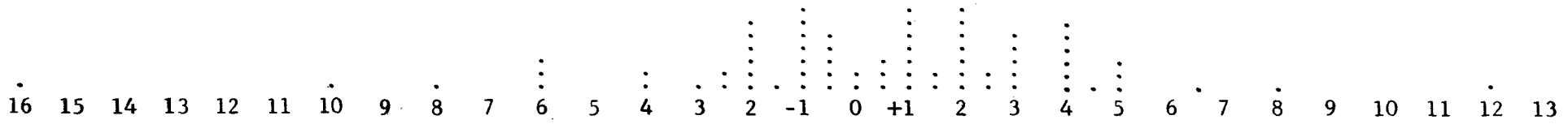

ATS-3

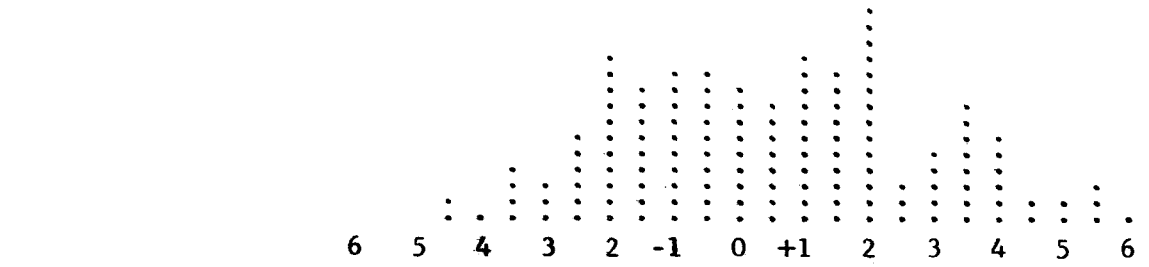

(Horizon Mode)

FIGURE 6-16

RANGE MEASUREMENT DISTRIBUTIONS
FOR TWO ALTITUDES OVER OCEAN
6 June 1969

Altitude: 20,000 feet
Heading: South
Time: 1345 - 1355 GMT
Reflected Signal Delay: 26.0 μs
Standard Deviation: 3.0 μs

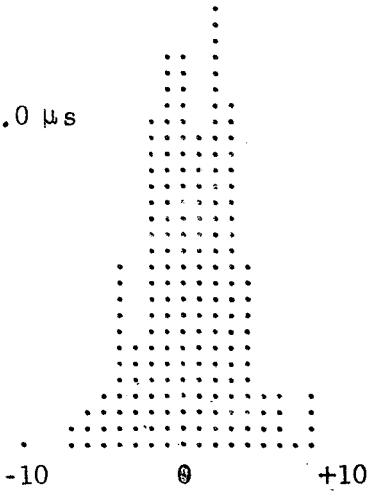

Altitude: 5,000 feet
Heading: NNE
Time: 1308 - 1313 GMT
Reflected Signal Delay: 6.5 μs
Standard Deviation: 2.1 μs

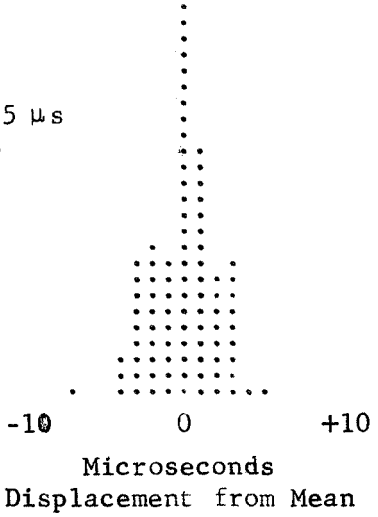

Aircraft: DC-6B
Location: Off New Jersey Coast
Antenna: Satcom, Zenith Mode

Satellite: ATS-3, Elevation ≈ 40°
Sea State:
Wind Direction:

SECTION 7. SHIP TESTS

The Coast Guard Cutter Valiant, WMEC-621, based at Galveston, Texas, is a 210 foot ship like the one shown in Figure 7-1. It was equipped with a ranging transponder, also shown in Figure 7-1. The lower unit is a General Electric type DM76LAS mobile radio base station. Within the base station unit, the tone-code responder was connected between the receiver and transmitter, together with its solid-state power supply. A Parks electronic type 144-1P preamplifier was also mounted in the unit and connected between the antenna and receiver. The 35 watt output of the mobile radio transmitter was applied to a Gonset Model 903 Mark II 300 watt power amplifier, shown above the base station unit. The oscilloscope was used for display of the signal and is not a part of the transponder. The equipment was mounted on the bridge of the ship.

The antenna shown in Figure 7-1 was mounted on the flying bridge. Originally designed for the NASA OPLE project, the antenna consists of a pair of crossed dipoles connected for circular polarization. Its gain is 3 dB toward the zenith. It has 0 dB for circular polarization at 45 degrees elevation. Variation in azimuth gain is approximately 2 dB. When used with the linearly polarized antenna on the satellite the antenna gain is effectively reduced by 3 dB so that its zenith gain is approximately 0 dB; its gain at 45 degrees is -3 dB. It is even lower at the elevation angles to the satellites, which were 29 degrees for ATS-3 and 17 degrees for ATS-1. Figure 7-1 shows the location of the antenna on the flying bridge relative to other structures of the ship. For certain headings of the ship, the mast shielded the antenna from one satellite or the other.

The equipment was shipped from Schenectady, New York to Galveston, Texas by air on June 20, 1969. It was installed on the ship and operated without adjustment.

Good voice communications were relayed through the ATS-3 satellite between the ship and the Radio-Optical Observatory at Schenectady. The equipment was tested with the ship at its berth with a southerly heading on June 27, 1969. Interrogations through ATS-3 had a standard deviation as small as 0.7 microsecond. This was the smallest deviation experienced with any user transponder in the entire experiment. While the ship was being interrogated through ATS-3 on June 27, the FAA KC-135 aircraft, N96, made a voice call through the satellite which was received at Schenectady while the interrogation of the Coast Guard ship was in progress. The aircraft stated that it was on the runway in the Azores, ready for take-off, and requested that range measurements be made on the aircraft until it was airborne. The tone-code generator and correlator were switched to the aircraft code at the Observatory and successful range measurements were made to the aircraft as it proceeded down the runway and became airborne. Interrogation of the Coast Guard ship at Galveston was then resumed by switching back to its address code. The unplanned exercise demonstrated the voice and ranging compatibility of the tone-code ranging technique, as well as the ability to interrogate one user while another user's transponder was turned on and receptive to interrogations.

On July 1, 1969, the Valiant sailed the track shown in Figure 7-2. Course changes and other aspects of the test were coordinated by voice communication through the satellite between the Observatory and the ship. While underway, the ship sailed at 15 knots. Its location was determined at one-minute intervals

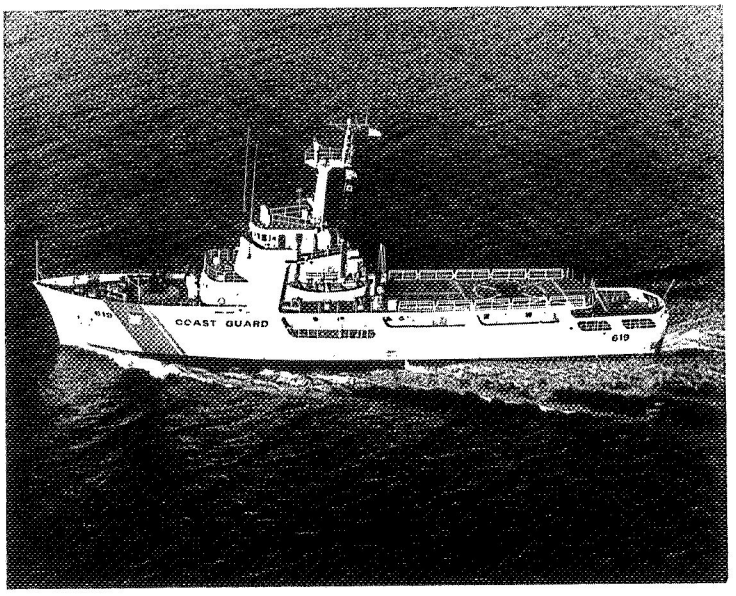

210' Coast Guard Cutter
Sister Ship of Valiant

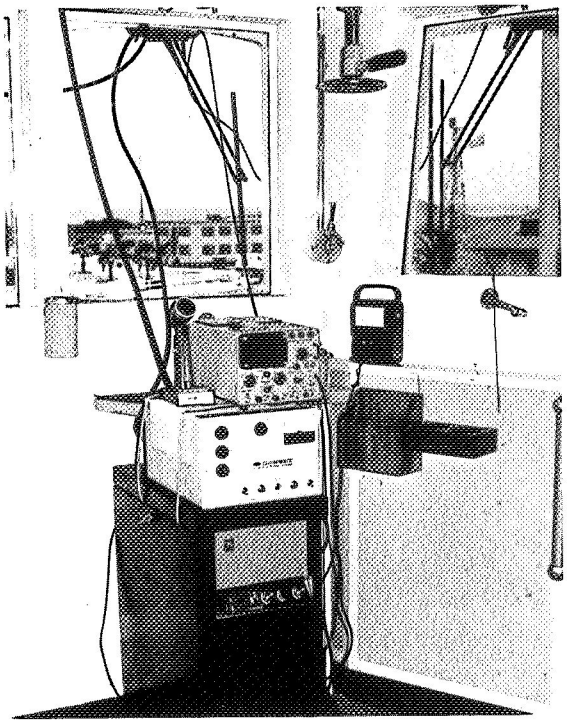

Ranging Transponder on
Bridge of Valiant

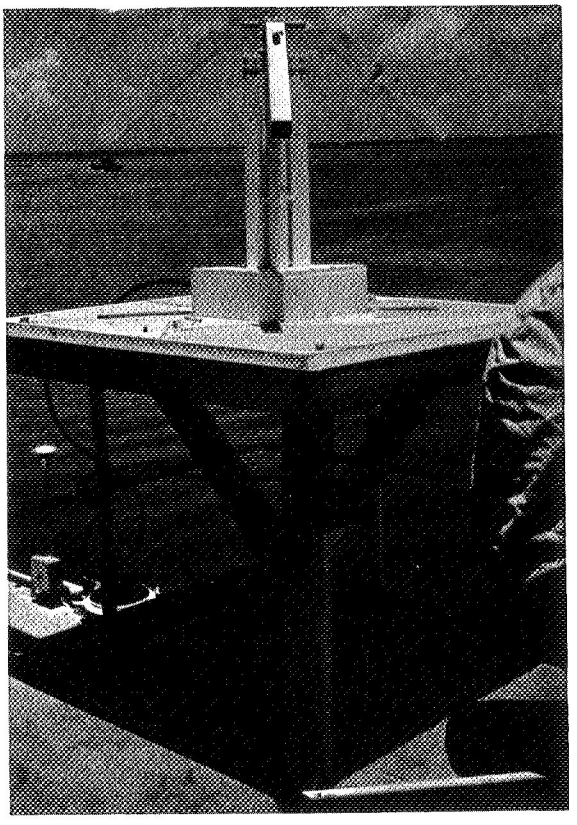

Antenna Used for Satellite
Ranging and Communications

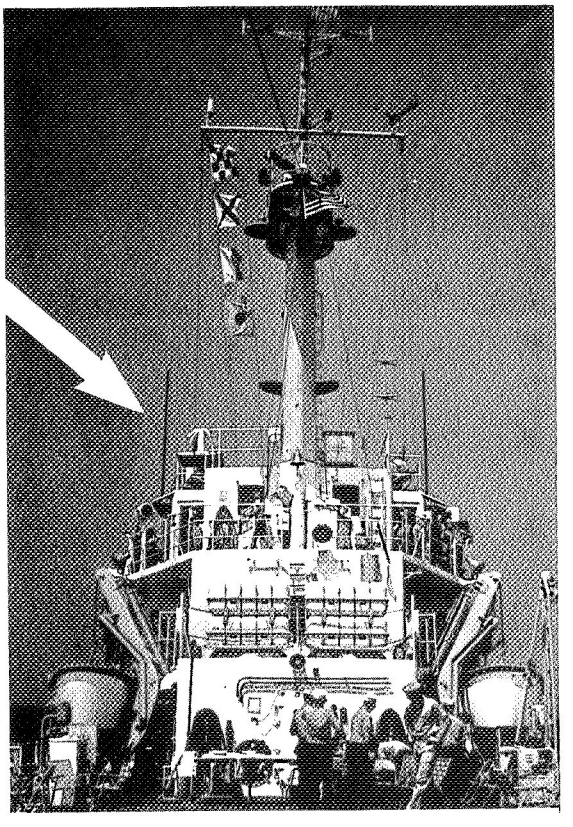

Antenna Location on
Flying Bridge of Valiant

FIGURE 7-1. SISTER SHIP OF VALIANT, EQUIPMENT USED IN SHIP TESTS

FIGURE 7-2. TRACK OF JULY 1, 1969 SHIP TEST

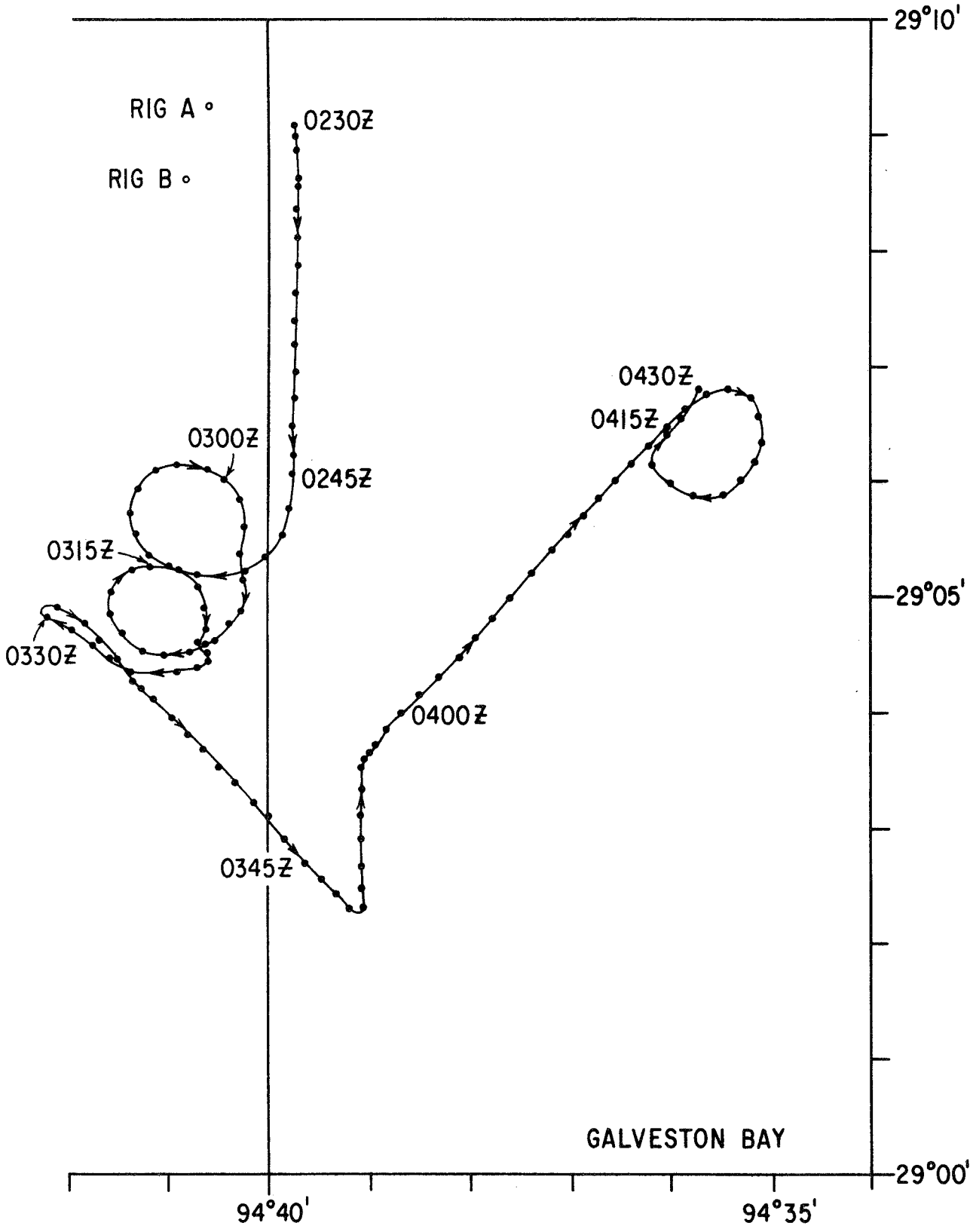

by radar measurements relative to two oil rigs at known positions A and B. In addition to straight-line courses at various headings, the ship sailed three complete circles; each circle was approximately one mile in diameter.

Except during short periods of voice communication, the ship was interrogated through one of the satellites at three-second intervals. Responses from the ship were relayed back through both satellites to the Observatory. Most of the interrogations were made through ATS-3. It was also successfully interrogated through ATS-1, although the percentage of responses was lower for ATS-1 interrogations because of the relatively poorer down-link from ATS-1 to the ship.

Figures 7-3 and 7-4 show the ranging time intervals for the satellites ATS-1 and ATS-3 as the ship sailed the circle shown in Figure 7-2 between the times 0303 and 0318 GMT. The number of returns as well as the magnitude of the variations of the time intervals clearly shows the effect of the mast and perhaps other ship structures on the antenna pattern. The performance changed with ship heading so the data was examined separately for short time intervals during the circle.

A plot of fix precision was made for each time interval. These are shown in Figures 7-5 through 7-10. The fix precision plots were constructed by first computing a best fit curve to the plots of Figures 7-3 and 7-4. Lines of position for ATS-1 and ATS-3 were then plotted for the two returns from each individual interrogation. The intersection of the two lines of position is shown as a small circle. Each line of position was constructed at right angles to the azimuth toward the satellite with the line of position advanced or retarded by an amount proportional to the displacement of the range measurement from the best fit curve. The scale factors were calculated to take into account the projection of the earth of the range measurement for the elevation angle to the satellite. Each small circle is a measure of fix precision including the effects of instrument measurement resolution, time delay variations in the instrumentation with signal amplitude or detuning, the effects of noise on the signal and geometrical dilution of position. It does not include bias errors due to the ionosphere, error in the estimates of the satellites' positions or in the estimate of equipment time delay. A more detailed discussion of the precision plots is included in the section of the report describing the aircraft experiments.

During the first period from 0303 to 031418 GMT, the signal paths were relatively good. Only one of the twenty-six fix estimates falls outside of a one nautical mile radius circle. The period from 030420 to 0307 GMT had generally good signal levels but there are several points which are displaced farther from the best fit curve than is typical of the previous or following time periods. The reason has not been definitely assigned but it is most probable that it represents a known characteristic of the receiving equipment. The receivers exhibited a change in time delay of 5 to 7 microseconds with changes in received signal level. A comparison of the range measurements for ATS-1 and ATS-3 as shown in Figures 7-3 and 7-4 reveals that the displacement of the range measurements is highly correlated in the returns from the two satellites, indicating that the variance in time delay occurred in the receiver on the ship as it received the interrogation signal from ATS-3. Because the error causes an advance or delay in the transmission of the response from the ship, it adds or subtracts an equal delay to the returns from the two satellites. The range difference of the measurements remains unchanged and therefore the fix errors tend to lie along a hyperbolic line of position. The effect is clearly evident in Figure 7-6 where the position fixes are concentrated along a generally north-south line.

COAST GUARD CUTTER VALIANT AT SEA DURING SECONL TURN - 7/.'69
ATS-! PLOT

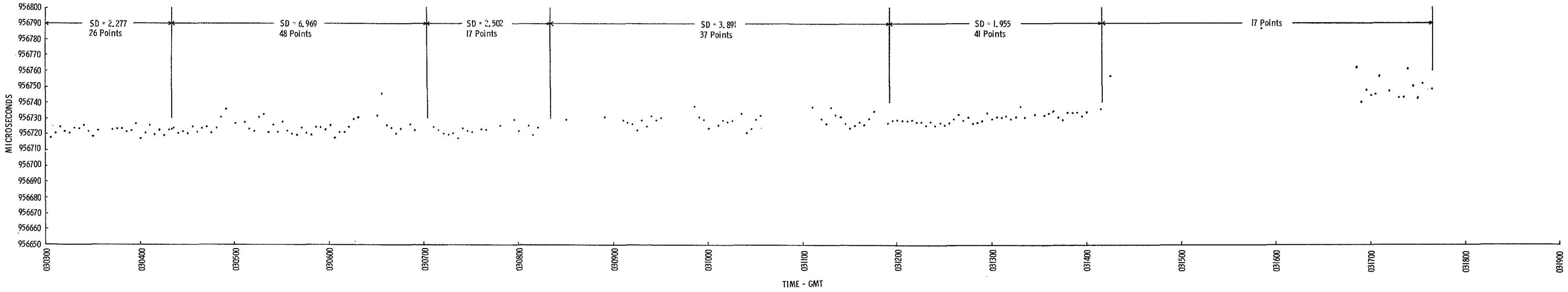

FIGURE 7-3

COAST GUARD CUTTER VALIANT AT SEA DURING SECOND TURN - 7/1/69
ATS-3 PLOT

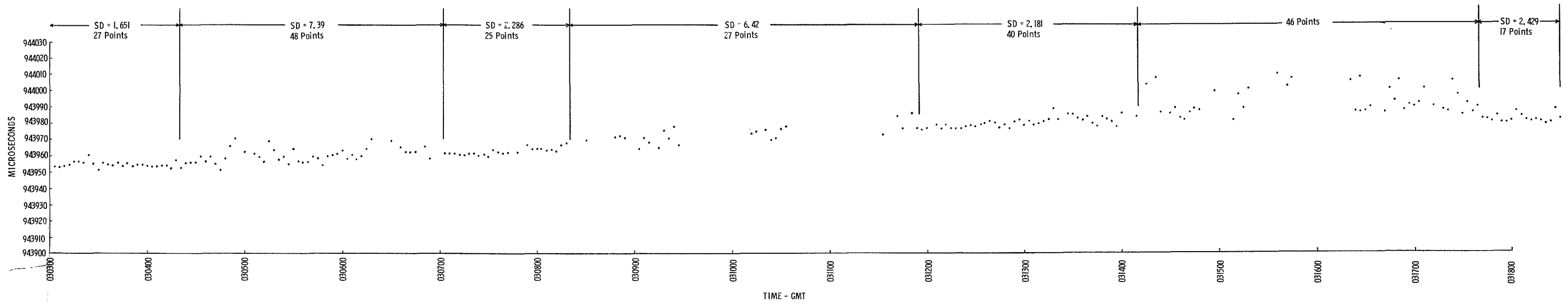

FIGURE 7-4

FIX ERROR DISTRIBUTION
USCGC VALIANT (WMEC-621)
1 July 1969, 03 03 00 - 03 04 18 GMT

Ship Heading: S
27 Interrogations
26 Dual Responses

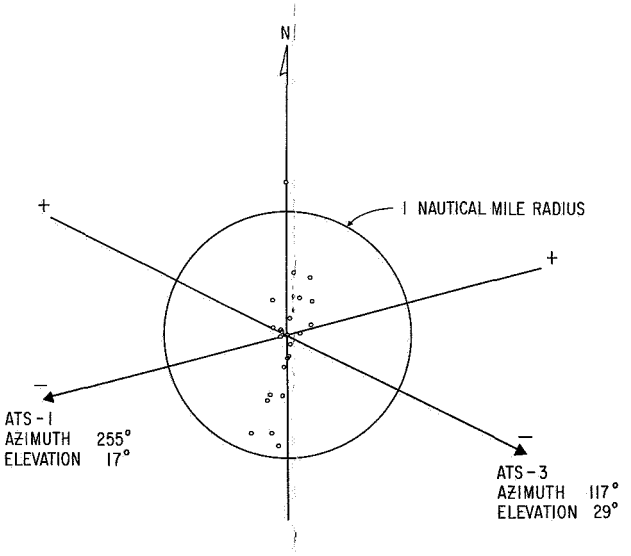

FIGURE 7-5

FIX ERROR DISTRIBUTION
USCGC VALIANT (WMEC-621)
1 July 1969, 03 04 20 - 03 07 00 GMT

Ship Heading: S to SW
54 Interrogations
48 Dual Responses

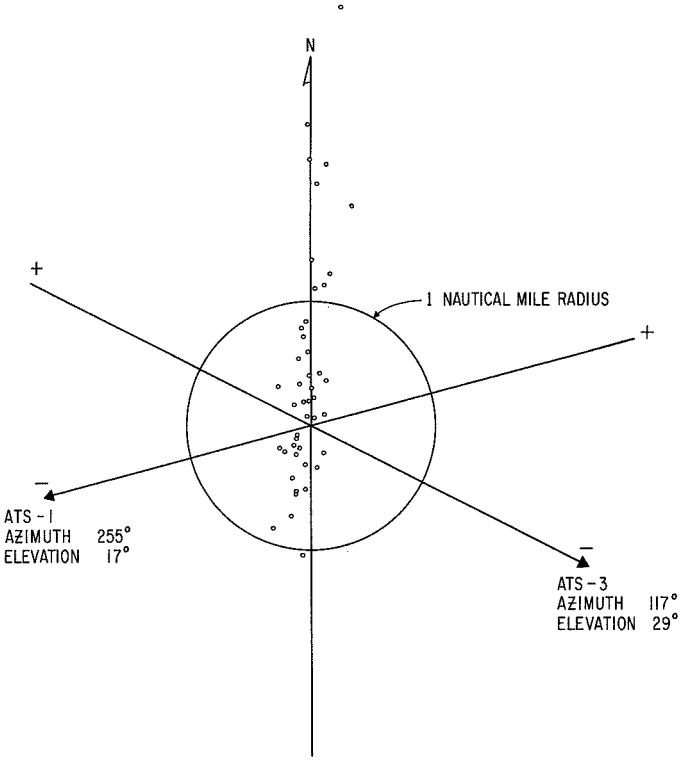

FIGURE 7-6

FIX ERROR DISTRIBUTION
USCGC VALIANT (WMEC-621)
1 July 1969, 03 07 03 - 03 08 18 GMT

Ship Heading: W
26 Interrogations
17 Dual Responses

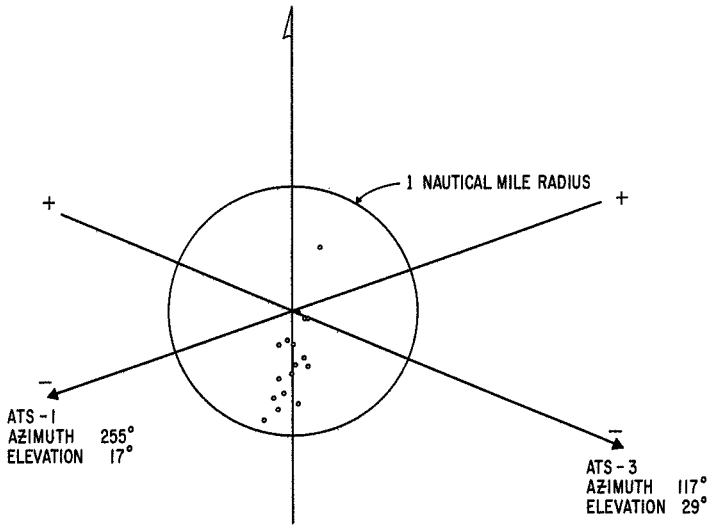

FIGURE 7-7

FIX ERROR DISTRIBUTION
USCGC VALIANT (WMEC-621)
1 July 1969, 03 08 30 - 03 11 54 GMT

Ship Heading: W to NW
Antenna Shielded From ATS-3
71 Interrogations
37 ATS-1 Responses
27 ATS-3 Responses
22 Dual Responses

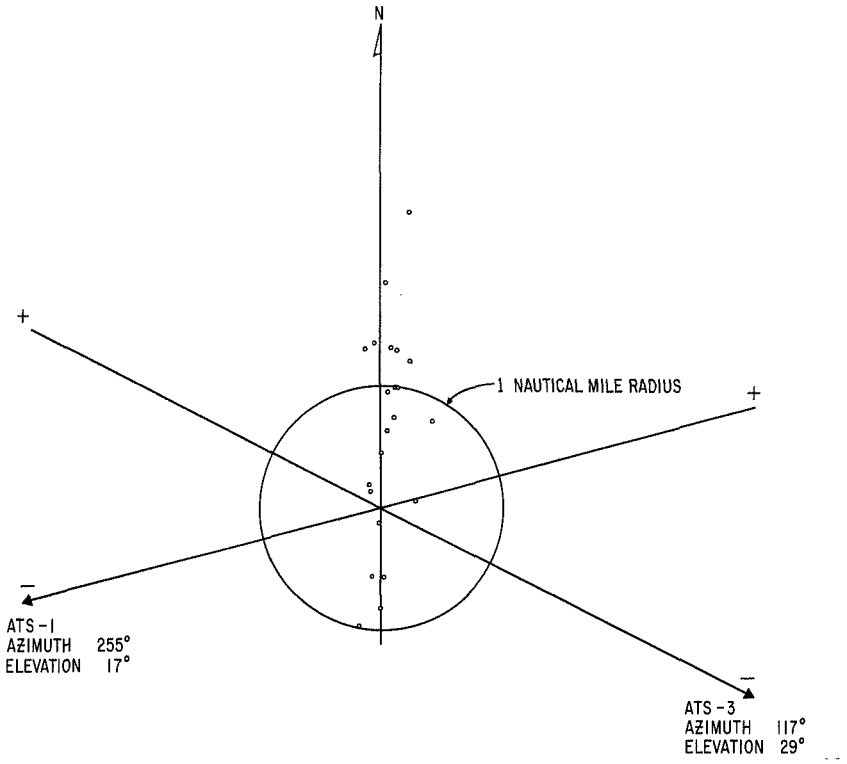

FIGURE 7-8

FIX ERROR DISTRIBUTION
USCGC VALIANT (WMEC-621)
1 July 1969, 03 11 57 - 03 14 09 GMT

Ship Heading: NNE
44 Interrogations
40 Dual Responses

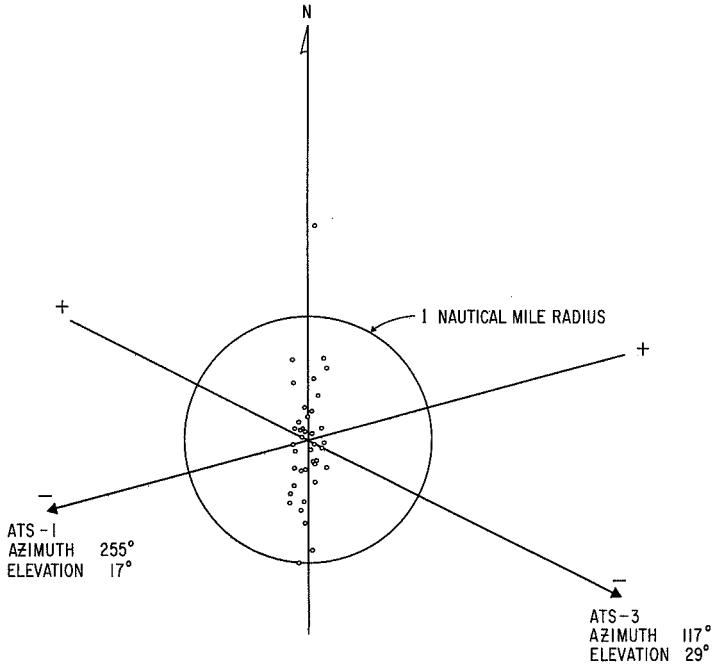

FIGURE 7-9

FIX ERROR DISTRIBUTION
USCGC VALIANT (WMEC-621)
1 July 1969, 03 14 15 - 03 17 39 GMT

Ship Heading: NE-E-SE
Antenna Shielded From ATS-1
70 Interrogations
46 Responses from ATS-3
17 Responses from ATS-1
15 Dual Responses

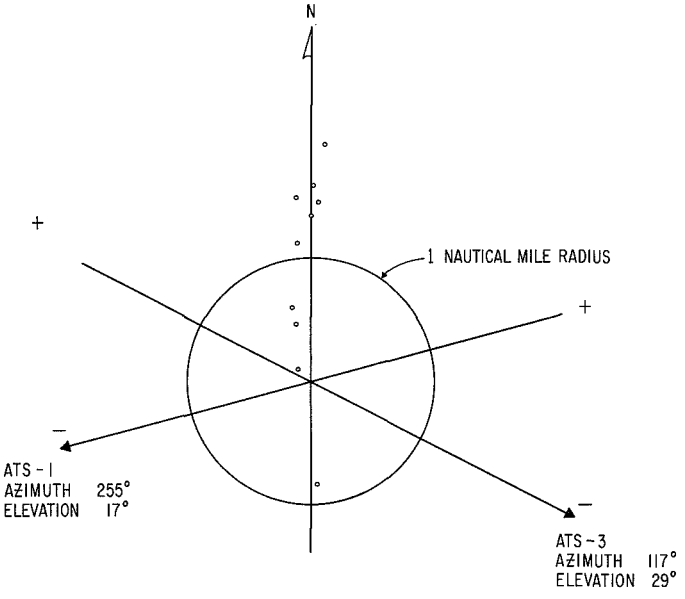

FIGURE 7-10

The period from 030703 to 030818 GMT was characterized by good signal levels, small standard deviation of the measurements, and fixes lying within a 1 nautical mile radius. Between 030830 and 031154 GMT the ship was at a heading such that the antenna was partially shielded from ATS-3 by the ship's mast. The standard deviation of the measurements was relatively high. Again, the position fixes are concentrated along the hyperbolic lines of position. The antenna was again in view of both satellites between 031157 and 031409 GMT. Standard deviations were low and the fix precision was good. From 031415 to 031739 GMT the antenna was shielded by the mast from ATS-1. The loss in signals to ATS-1 is evident in Figure 7-3. The interrogation signal from ATS-3 was not received well and the scatter of the range measurements are biased in one direction relative to the data received at good signal levels, suggesting that the signal levels as received during the period were in the part of the receiver's dynamic range to cause a change in time delay through the receiver. The cause of the changing time delay through the receiver was traced to the limiter. A new limiter design was tested and found to reduce the time delay variation to less than one microsecond over the dynamic range of receivers of the same type.

SECTION 8. BUOY TESTS

The Sea Robin buoy was developed and constructed by the General Electric Company to test key technologies applicable to remote, unattended data collection buoys for sensing and relaying oceanographic and meteorological data. Sea Robin is a modified spar buoy, approximately four feet in diameter and fifteen feet long, with stabilizing means designed for mooring in the deep ocean or for free-floating in all sea states.

During the period covered by this report, the buoy was tested ashore, in a harbor, and at a deep sea mooring near Bermuda, at 32°10'00" N, 64°54'30" W, in a joint Navy-General Electric experiment. The Navy's support was through the Office of Naval Research under Contract N00014-68-C0467. The experiment verified the sea-worthiness of the buoy when moored where the ocean depth was >4000 feet, using a 7000 foot line, under a variety of weather and sea states.

Buoy location experiments included VHF ranging from ATS-3 by the tone-code ranging technique and position fixing by OPLE. Data readout through ATS-3 employed the tone-code ranging equipment. Data readout was also accomplished at HF in a specially designed experiment.(1)

For the data transmission, the buoy sensed nineteen housekeeping, weather and oceanographic conditions. Each data transmission totaled 336 bits. Data were transmitted directly by telemetry to a van on shore which also commanded functions aboard the buoy and monitored its position by radar and telescope.

Data transmission through the satellite was accomplished by the use of the transmitter-receiver-responder unit used for the VHF ranging experiment. A data transmission followed each range interrogation, as shown in Figure 8-1. Two data rates were tested, 2.4414 bits per second and 305 bits per second. At the higher rate, a "one" bit was formed by transmitting an audio cycle, a "zero" by suppressing a cycle. At the lower rate, eight audio cycles were transmitted for a "one", and eight suppressed for a zero. A complete response from the buoy consisted of the transmission of 1024 cycles at 2.4414 kHz followed by the address code, consisting of 30 bits at the 2.4414 rate, and the address code followed by a 1.25 second data transmission to accommodate slightly more than one complete data frame at the low rate. The radio frequency energy transmitted from the buoy was approximately 50 watt seconds for the ranging signal (120 watts for 0.43 second) and 150 watt-seconds (120 watts for 1.25 seconds) for the data transmission.

The transponder aboard the Sea Robin consisted of a 35 watt, solid-state FM mobile radio transmitter-receiver with a 120 watt solid-state amplifier, and the first experimental responder unit for phase matching, address correlating, clocking for the digital data readout, and switching of the receiver and transmitter. Despite the early state of the responder development, it performed reliably throughout the test at the mooring. The tests confirmed the advantages of the tone-code ranging technique.

The satellite antenna is linearly polarized. Horizontal and vertical linear, and circular polarization were available at the Radio-Optical Observatory. Sea Robin had two linearly polarized antennas mounted at right angles with a switching arrangement to permit transmission and reception on either, or reception on one and transmission on the other. These antenna arrangements were designed so that information could be obtained about the difference in

RANGING AND DATA READ-OUT SIGNALS FROM SEA ROBIN

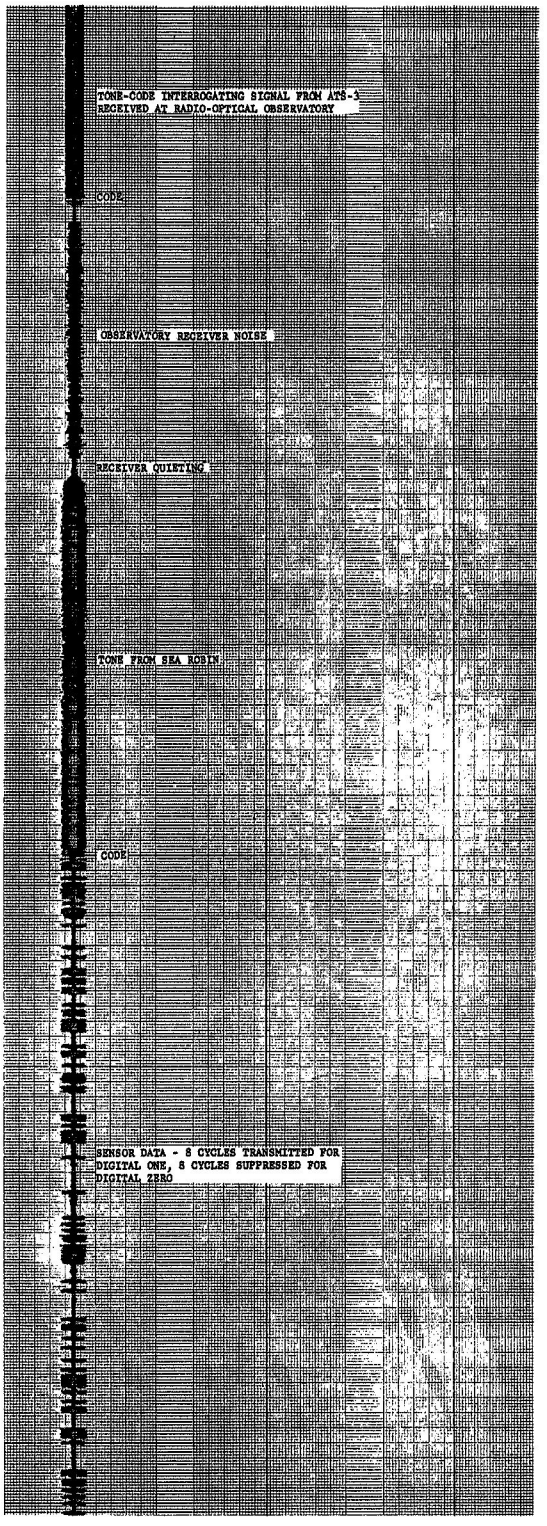

The compatibility of tone-code ranging with digital communications was demonstrated by transmitting sensor data from the buoy in digital form using the clock of the tone-code responder. A sample read-out is recorded at left.

At the top of the page is the last half of the tone-code interrogation as it was received at the Radio-Optical Observatory. During this time it was also being received by Sea Robin and the tone was used to phase the local tones in the buoy and the Observatory. The code at the end of the tone is evident in the recording as a pattern of 2.4414 kHz transmitted and suppressed cycles. Correlation of the code identifies Sea Robin and provides a timing pulse for the start of the ranging time interval. Receiver noise is evident for the time interval representing the built-in time delay in Sea Robin. The Sea Robin return signal quiets the receiver and the tone reception follows. After the tone, the address code is received and correlated. The time between correlations of the address code at the Observatory is the ranging time interval. Following the code from Sea Robin is a portion of the data read-out at

$$\frac{2.4414}{8} \approx 305 \text{ bits per second}$$

with eight transmitted cycles representing a digital one and eight suppressed cycles representing a digital zero. Sensor data were also successfully transmitted at the 2.4414 kHz rate by transmitting a single audio cycle for a one and suppressing a cycle for a zero, as in the address code transmission.

FIGURE 8-1

Faraday rotation between the up-link frequency of 149.22 MHz and the down-link frequency of 135.6 MHz. Separate receive and transmit polarization angles were not available at the Observatory during the test period. The capability was added later. A difference of approximately 90 degrees in the Faraday rotation of polarization at the two frequencies was observed frequently, making it desirable to receive on one linear polarization and transmit on the other. A switching sequence was deliberately introduced at the buoy to observe the effect, resulting in an anticipated failure to respond to some interrogations.

On one occasion, as reported in Section 5, the February 12, 1969 data, severe amplitude scintillation was observed for the path between the Observatory and ATS-3. The correlation of the fading of the Sea Robin with the Observatory return from the satellite suggests that no scintillation occurred along the path from the satellite to the Sea Robin. Range measurement variations were correlated with signal amplitude, but by an amount equal to the separately measured receiver characteristics of time delay change with signal amplitude. It was concluded that there were no significant changes in propagation time associated with the changes in signal amplitude due to scintillation. The conclusion is supported by the September 5 data, Section 5.

Ranging interrogation periods for Sea Robin totaled 222 minutes between February 13 and May 22, 1969. Full scale operational testing began on April 13, 1969 when the buoy was anchored 6.5 miles south of Bermuda in 4272 feet of water. Operation of the system continued periodically until May 30, 1969 when testing was terminated and the buoy and complete mooring were recovered. While at the deep sea mooring, an interrogation period was three minutes long, with an interrogation to the buoy each three seconds. Each interrogation period was preceded by a 30 second tone transmission from the ground station through the satellite. The signal was received in the control van at Bermuda, where the best of two linear polarization angles was determined. The Sea Robin VHF antenna was then switched by command from the van to select the best of the two polarization choices for reception. The buoy was equipped to receive on either polarization and transmit on the same or the orthogonal polarization.

Range measurements had a standard deviation of approximately 2.4 microseconds, representing a ranging precision of approximately 1200 feet and a line-of-position precision for Sea Robin of approximately 1700 feet. Distribution of the measurements appears to be Gaussian, suggesting that averaging a number of measurements would improve precision. For example, the average of ten measurements would improve the line-of-position measurement precision to approximately 550 feet.

Accuracy is affected by residual variations in biases that cannot be estimated for a particular measurement. The largest bias error contribution for Sea Robin is the ionosphere. Another significant error is equipment time delay change with signal amplitude. The ionosphere and the particular receiver type used in the experiment can each contribute several microseconds uncertainty to a range measurement. For the Sea Robin tests results as presented here, accuracy is also affected because the buoy is free to move approximately ± 1 mile from the position of its mooring. An initial evaluation of line of position accuracy was made with only an estimate of ionospheric bias, and no correction for receiver time delay variations or actual movement of the buoy. Forty-five randomly selected range measurements made during a twelve-day period were each used to make a determination of the latitude of Sea Robin. As shown in Figures 8-2 and 8-3, all of the computed positions for nighttime measurements are within approximately ± 3/4 mile of the mooring

FIGURE 8-2

SEA ROBIN

Latitude at which circle of position crosses longitude of buoy.

(Randomly Selected Measurements)

April 14-25, 1969

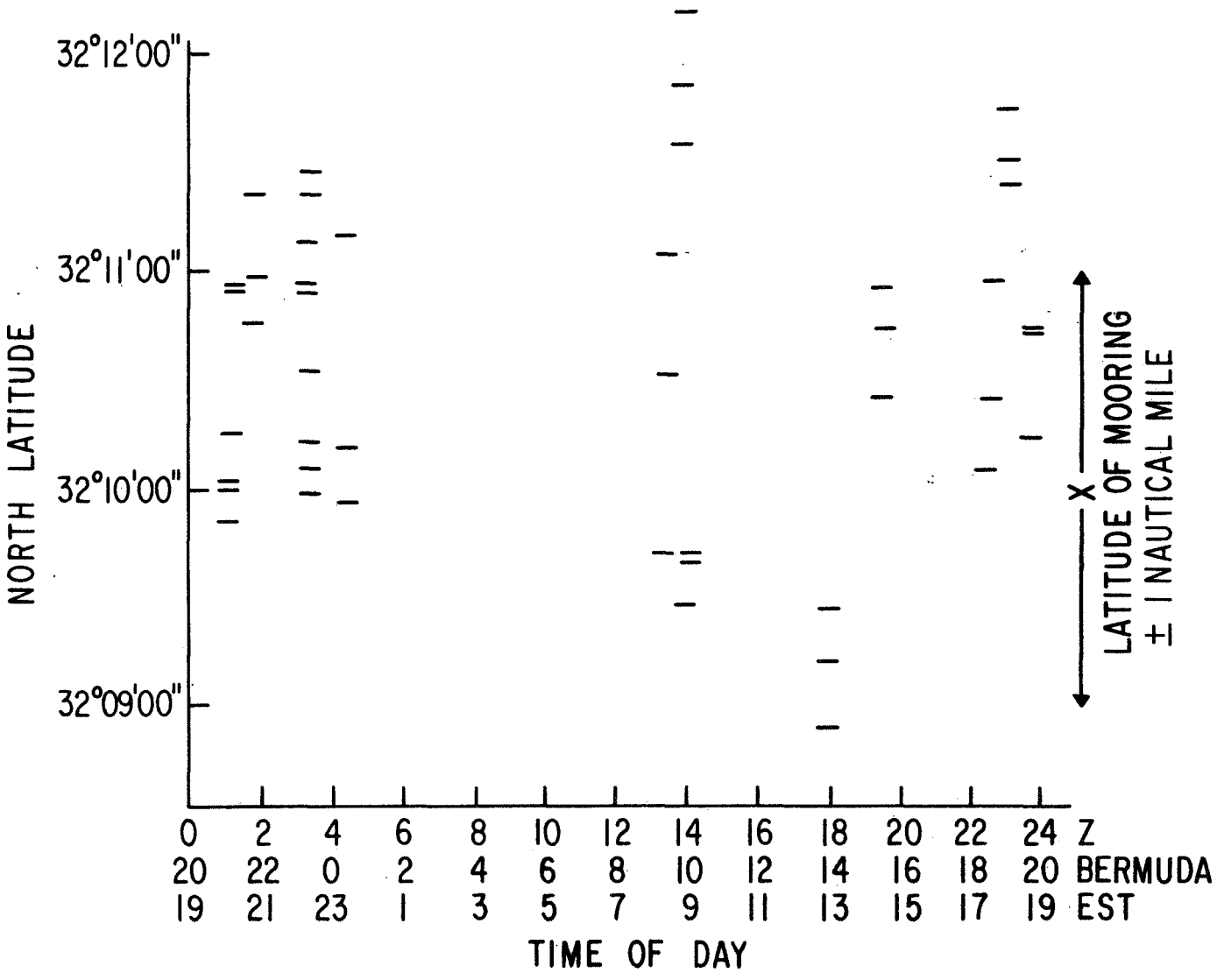

FIGURE 8-3

SEA ROBIN

Latitude at which circle of position crosses longitude of buoy.

(Randomly Selected Measurements)

April 14-25, 1969

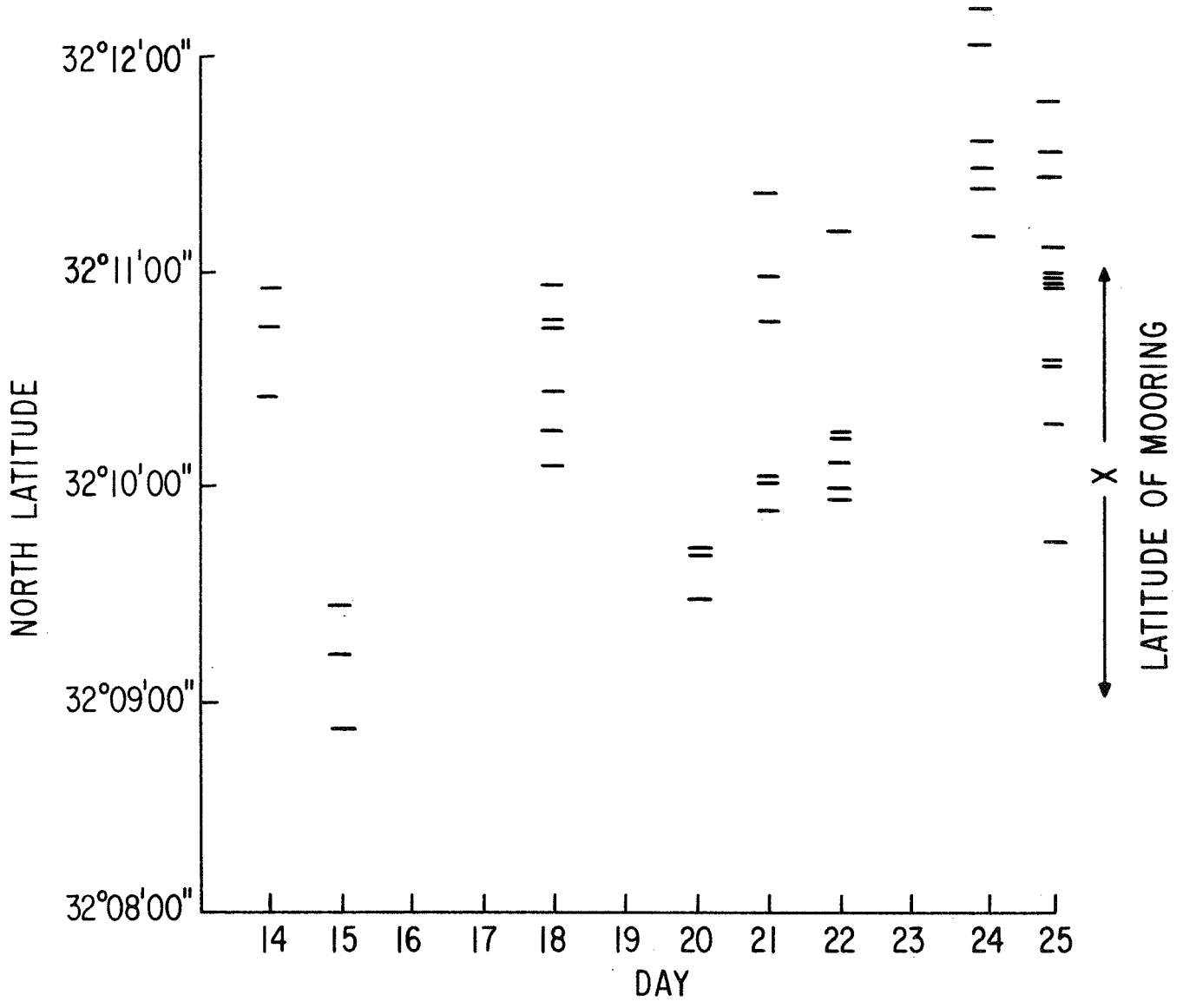

latitude, and daytime positions within approximately ± 1.5 miles. Reprocessing of the same data, taking into account actual positions of Sea Robin, corrections for receiver delay characteristics and more refined estimates of ionospheric bias would probably reveal higher accuracy than indicated by these initial results.

Another set of 93 randomly selected measurements were used to compute lines of position for the Sea Robin and are plotted as a function of time of day in Figure 8-4. The latitude determinations are shown as the short horizontal line segments. They are grouped in twos and threes by vertical lines, each group representing a measurement made near the beginning, the middle, and the end of a three minute interrogation period. The ionosphere model described in Appendix II was used rather than the crude estimates used for determinations in Figures 8-2 and 8-3. The diurnal variation in the latitude determinations suggest that the ionospheric model introduces a correction which is too large for the conditions that existed during the April 14 through 25 period.

Ranging precision was satisfactory at all received signal levels down to the FM detection threshold. However, less than one-half of the total number of interrogations resulted in correlated responses at the Observatory. This was expected because of the way the experiment was deliberately designed to reveal propagation effects, including Faraday rotation, antenna pattern lobing due to sea reflection, losses in the propagation path, and interfering signals in the satellite. Each of these effects tends to reduce signal level.

The Sea Robin data were recorded and processed as described in the Experiment Description, Section 3.

REFERENCE

1. C. E. Mortlock, Jr., "Sea Robin, An Ocean Buoy/Satellite Communications Experiment", Paper presented at the American Astronautical Society Meeting, Los Cruces, New Mexico, October 25, 1969.

FIGURE 8-4

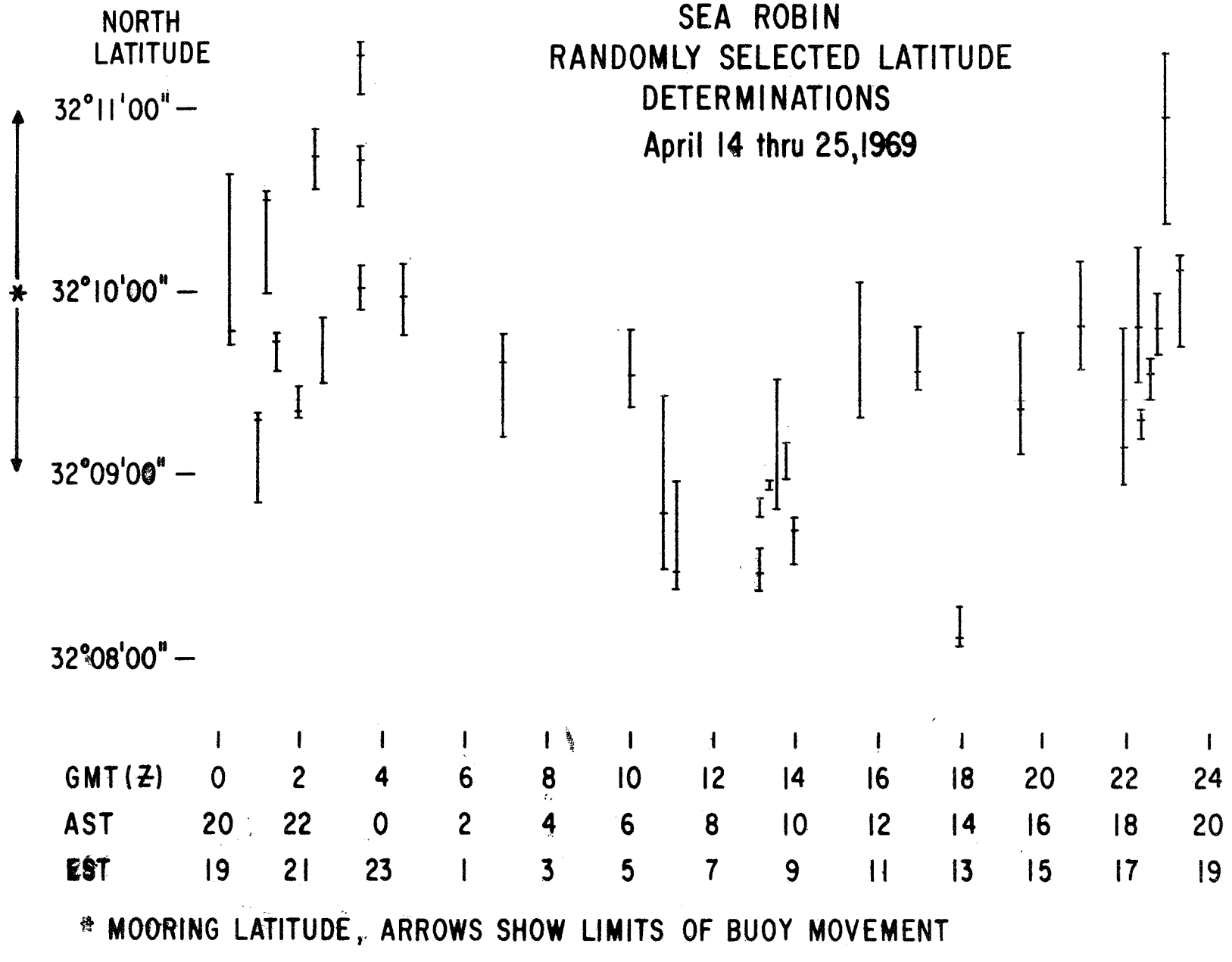
SEA ROBIN
RANDOMLY SELECTED LATITUDE DETERMINATIONS
April 14 thru 25,1969
NORTH LATITUDE
32°11'00"
32°10'00"
32°09'00"
32°08'00"
GMT (Z) 0 2 4 6 8 10 12 14 16 18 20 22 24
AST 20 22 0 2 4 6 8 10 12 14 16 18 20
EST 19 21 23 1 3 5 7 9 11 13 15 17 19
* MOORING LATITUDE, ARROWS SHOW LIMITS OF BUOY MOVEMENT

SECTION 9. VAN TESTS

A Ford Econoline van, Figure 9-1, was equipped with a GE mobile radio, as used in taxi cabs and police cars. A responder unit was connected between the receiver and the transmitter. A Parks Electronics Laboratories preamplifier model 144-1P preceded the receiver. The transmitter output power was 80 watts. Separate dipole antennas were provided for the receiver and the transmitter. They are visible as the horizontal elements near the front of the vehicle, as shown in Figure 9-1.

On March 27, the van was driven from the village of Manny Corners, New York, northward through the village of Hagaman, New York, to Route 29, then eastward on Route 29.

Range measurements were made through ATS-3 during the one-hour test period. The dipole antennas were separately oriented for best signals.

In previous mobile radio ranging tests not using satellites, it was observed that reflected signals can arrive at the receiving station antenna in any phase relative to the direct signal, and severely affect the received signal level. A vehicle position change of only a few feet can result in a large change in signal amplitude at the receiver.

During the first portion of the March 27 satellite ranging experiment, the van was moved in small increments; one foot, then two feet, then four feet, etc., to determine if a similar effect occurred between the vehicle and the satellite. The amplitude change was observed. No effects on range measurements were observed that could not be attributed to the change in receiver time delay with signal amplitude as described in Section 4. The receiver was an unmodified production unit with a time delay change of approximately 7 microseconds with signal amplitude change.

Figure 9-2 is a plot showing every range measurement made during the March 27 test. Note that the ordinate scale is marked in 10 microsecond steps rather than 1.0 microsecond steps, as on some other data plots. The shape of the data curve matches the changing range from the satellite to the vehicle. Events during the test are marked on the plot. There is a change in measured range noticeable during the first part of the test greater than the movement of the vehicle. The change in range is due to satellite motion, an effect clearly noticeable in similar plots in Section 5. Gaps in the data occurred because the range measurements were stopped when voice communications were used to coordinate the experiment. Scatter of the data points includes the variation in the time delays through the van and Observatory receivers.

Some of the range measurements were used to compute the intersection of the line of position with the road. The computation included an estimate of the equipment and ionospheric time delays. A first estimate for the delays resulted in a bias error to the south of approximately one and one-half miles. A new estimate was made to place the first location at Manny Corners, then the same equipment and ionospheric time delays were used for all the rest of the computations. Figure 9-3 shows the route which was traced from a topographic map. The actual positions of the vehicle are plotted as dots and the positions as determined from the satellite range measurements are plotted as short horizontal line segments. The satellite was nearly due south of the area at the time.

FIGURE 9-1. FORD ECONOLINE VAN

FIGURE 9-2. RANGE MEASUREMENTS THROUGH ATS-3 USING VAN

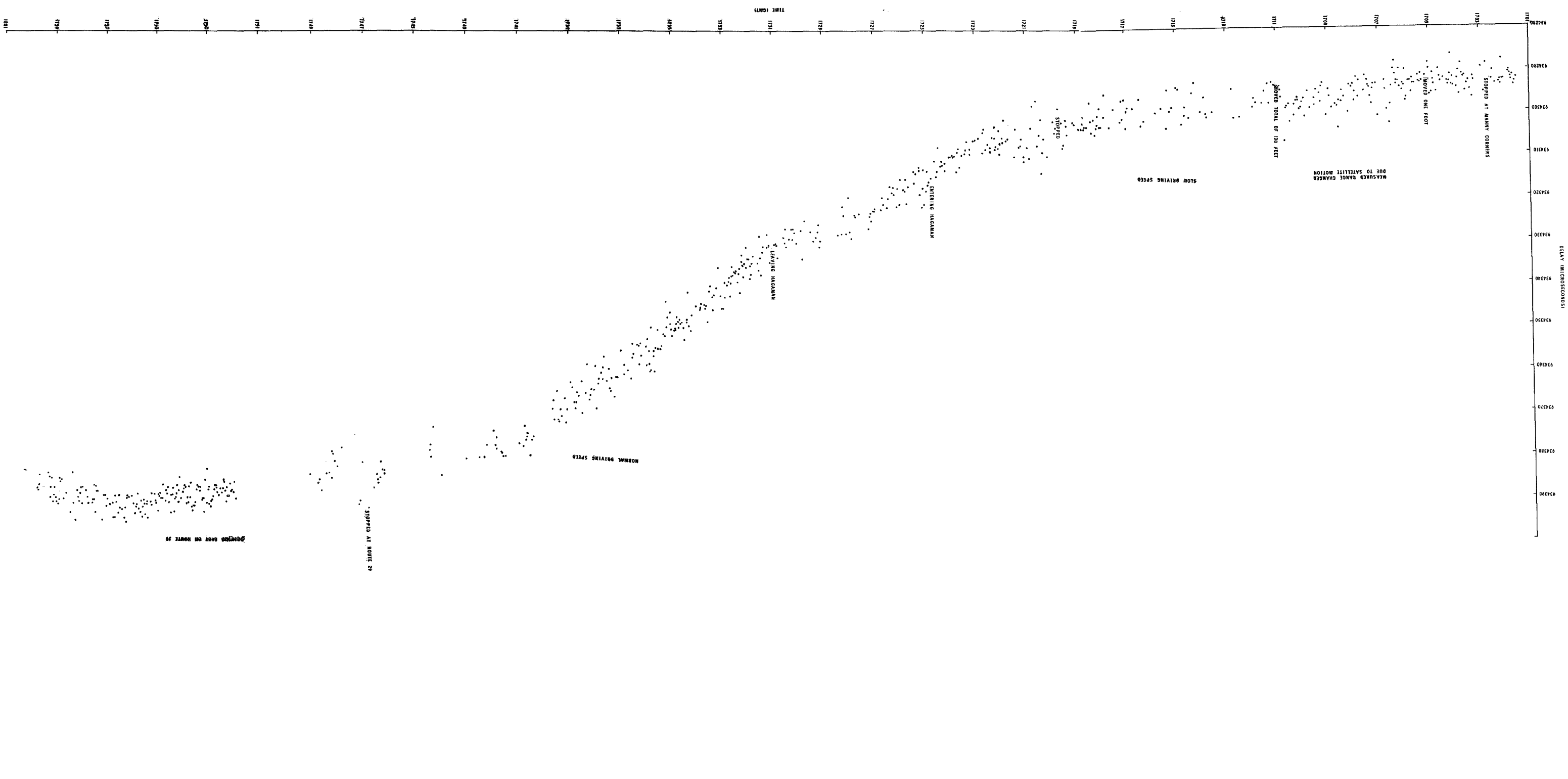

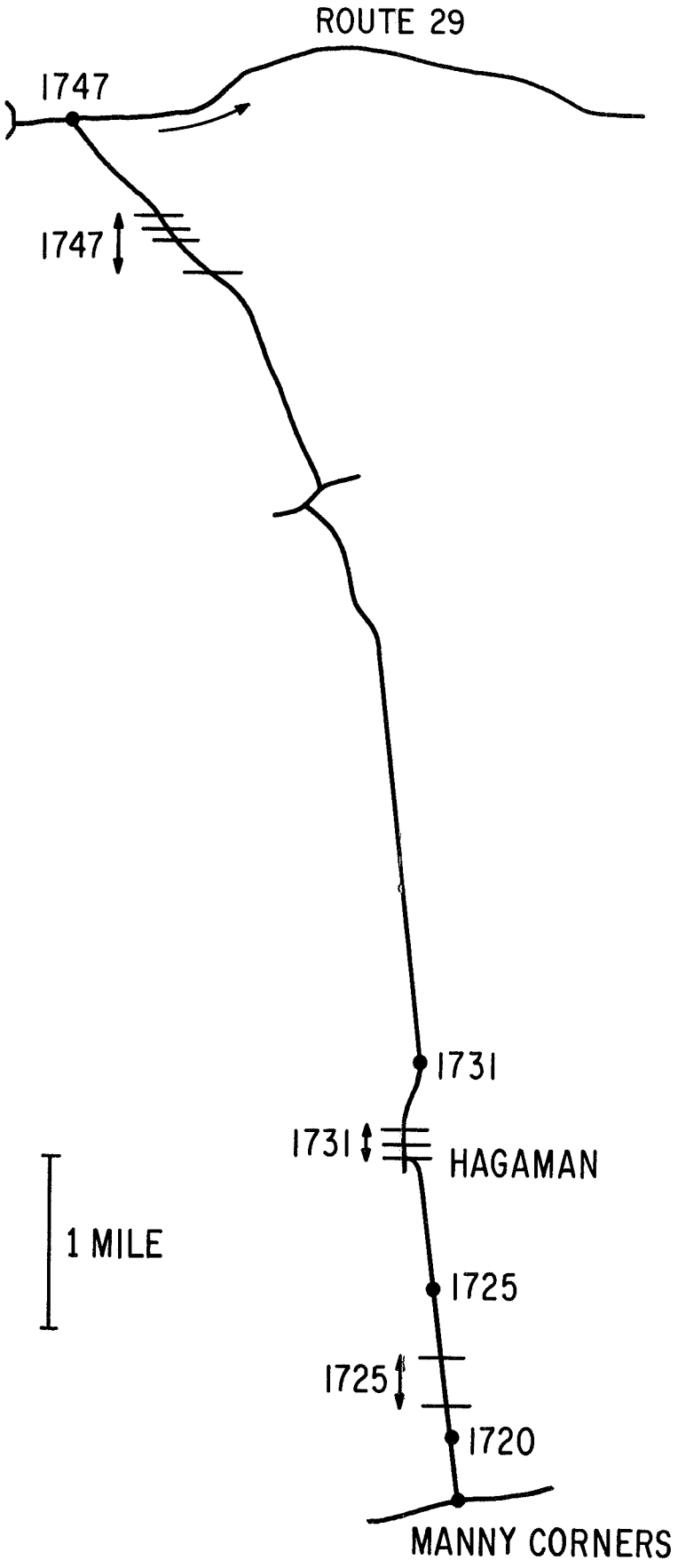

FIGURE 9-3. ROUTE OF MARCH 27, 1969 TEST

SECTION 10. L.E.S.T. TESTS

L.E.S.T. is an abbreviation for Low Energy Speech Transmission, a technique for processing and transmitting speech at a saving in power over more frequently employed techniques. The technique, developed in the General Electric Research and Development Center, is based on the work of Licklider and Pollack[1] who showed that speech, clipped nearly at the zero crossings, i.e. "infinitely" clipped speech, is highly intelligible. In L.E.S.T., the input waveform is first pre-emphasized by differentiation, then infinitely clipped and finally a short pulse is generated at each zero crossing of the infinitely clipped waveform.

The maximum rate of zero crossing pulses is limited by the audio passband, but since the average rate is far below the maximum, the duty cycle of the transmission is very low, approximately 5 percent during speech, resulting in a significant energy savings. At the receiving end, the pulses are applied to a bistable multivibrator to regain the infinitely clipped waveform of the original speech signal.

The full energy saving is accomplished by generating a pulse of RF energy at each zero crossing pulse. The transmitter is turned completely off between pulses. In the ATS-1 test, the waveform was simulated by frequency deviation rather than keying the satellite transmitter. As a result, the energy saving could not be directly demonstrated, but could be inferred from the duty cycle. Duty cycle estimates were based on laboratory measurements. The ATS-1 tests revealed that L.E.S.T. waveforms can be transmitted without distortion over satellite links.

L.E.S.T. equipment developed and constructed on a previous program was used in the experiments. Since this L.E.S.T. equipment was primarily intended for use in AM transmission systems, some modifications were necessary to adapt it to FM. Dual-polarity pulses were used to modulate the carrier frequency in an FSK (frequency shift key) mode where the carrier is on continuously but is shifted by the L.E.S.T. pulses. In the experiment, the carrier also acted to suppress noise during pauses in the L.E.S.T. speech. The low energy features of the L.E.S.T. system were simulated by considering the time during which the carrier is keyed by the L.E.S.T. pulses compared with the total time of speech transmission. Speech intelligibility was evaluated by use of spondaic word lists. These tests are described in more detail later.

Under the conditions of these experiments, one can estimate the L.E.S.T. savings in power to be between 24:1 and 48:1 compared with an FM system with continuous carrier. However, the equipment used in the experiments was not well suited for transmitting narrow L.E.S.T. pulses (low duty cycle). Therefore, the power estimates given are a limit of the experiment only and further savings should be expected in an optimum L.E.S.T. system.

Results of intelligibility tests on transmitted L.E.S.T. speech using spondaic word lists were very encouraging. Scores for two groups of listeners averaged 93.3 percent for in-house tests without the satellite link using a transponder and dummy load in the system. The scores for the fully implemented experiment using the link to ATS-1 were 96.6 percent for a word list that was familiar to the listeners and 91.5 percent for an unfamiliar list. These tests indicate that L.E.S.T. can be used for voice communications through satellites and that insignificant loss in intelligibility results from the transmission.

The L.E.S.T. equipment used in this experiment was loaned by the Company's Space Systems Operation in Philadelphia. The L.E.S.T. encoder unit is a breadboard unit while the decoder is a prototype designated #E-012. The L.E.S.T. pulses modulated the RF carrier by an amount of ± 7.5 kHz about the center frequency. Only the duty cycle of the L.E.S.T. pulses was considered when estimating the low energy properties of the system.

Figures 10-1 and 10-2 show the system block diagram and the typical waveforms respectively for the L.E.S.T. experiment. Speech input to the L.E.S.T. encoder was from a microphone or a tape player which contained recordings of spondaic word lists. The waveform at (A) shows the typical clipped speech after pre-emphasis and clipping. There is a voltage transition for each point of zero crossing in the original speech waveform.

Pulses are produced at each transition of the clipped speech waveform - a positive pulse for a positive transition and a negative pulse for a negative transition, as shown in (B). These pulses are 70 microseconds wide and are used to modulate the 149.22 MHz carrier of the transmitter. Thus, the frequency out of the transmitter would have approximately the same waveform as shown in (C) where frequency deviation would be plotted along the ordinate.

The returned transmission at 135.6 MHz is received with the typical waveform out of the FM receiver shown in (D). The discriminator output has a waveform similar to (B) and (C) because of the linear characteristics of the discriminator as shown in Figure 10-3.

Because of response limitations in the receiver and/or transmitter, the width of the pulses out of the receiver are longer than the L.E.S.T. pulses to the transmitter. The pulse width at (D) was found to be 140 microseconds, indicating some bandwidth limitation in the system. However, the highest frequency in the speech is only 2500 Hz; thus, no serious degradation in performance would be expected from these bandwidth limitations in this FM system.

Waveform (E) shows the receiver output after rectification (to make it compatible with the input requirements of the L.E.S.T. decoder). The decoder contains a flip-flop circuit which returns the waveform as shown in (F) to the same form as the clipped L.E.S.T. speech (A). Some additional high frequency filtering is done in the decoder before the output is recorded.

Figure 10-4 shows the modifications made to the L.E.S.T. equipment to make it compatible with the FM experiment. These modifications consist of a dual pulse forming circuit for the output of the encoder and an amplifier and rectifier circuit for the input to the decoder section of the L.E.S.T. equipment.

It was noted during earlier experiments that the output of the receiver could be understood by a listener even though the signal at that point had not passed through the L.E.S.T. decoder. For this reason the output of the receiver was recorded on a second channel at the same time the L.E.S.T. output was recorded to allow for separate tests of intelligibility on the two outputs. The results, to be described later, show that the level of intelligibility was significantly higher out of the L.E.S.T. decoder than out of the receiver even though the receiver output was clear enough for most speech to be understood.

The system was operated during tests in one of two modes. The first for in-house testing did not use the satellite link. During these tests the

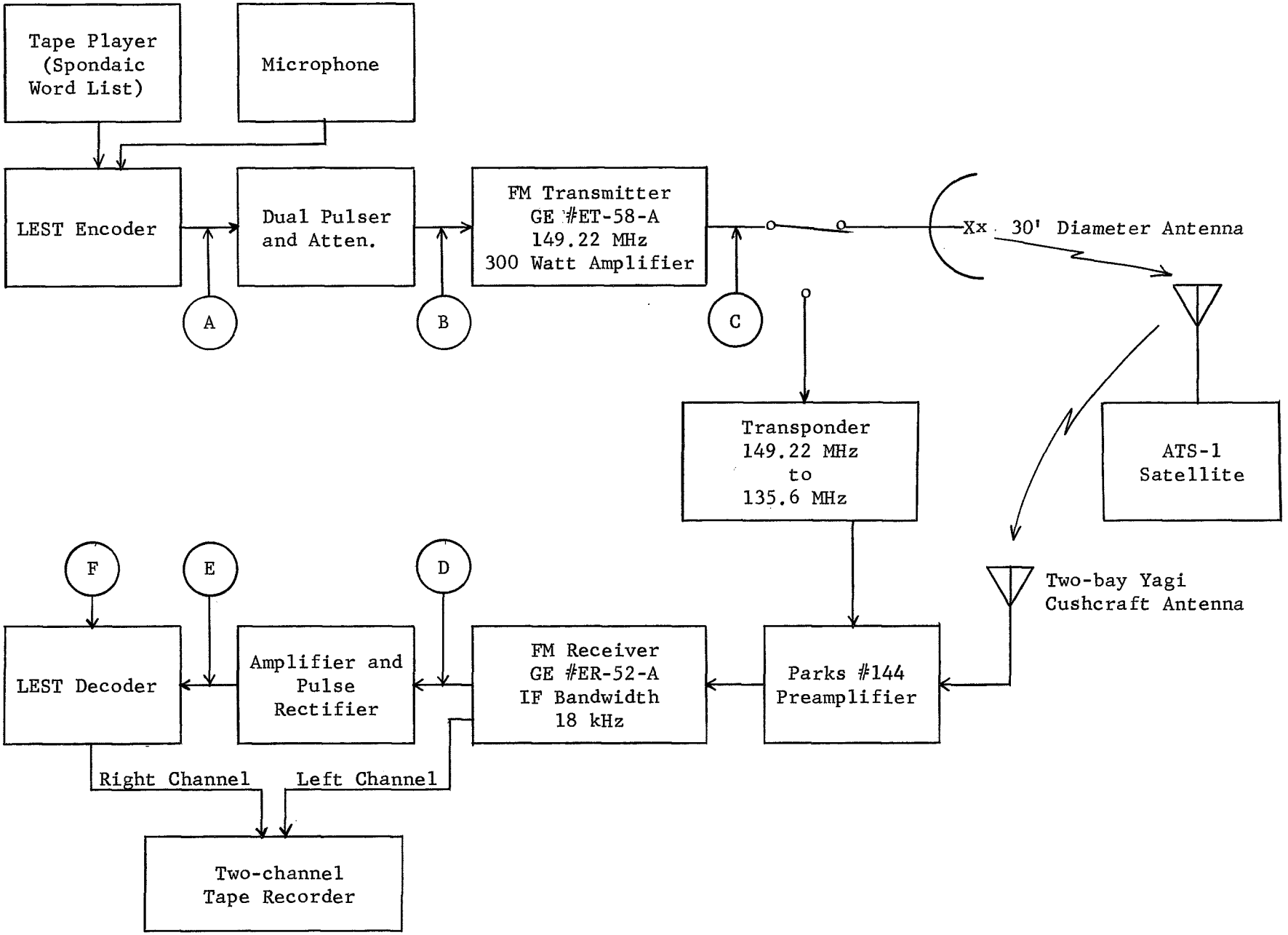

FIGURE 10-1. L.E.S.T. EXPERIMENT SYSTEM BLOCK DIAGRAM

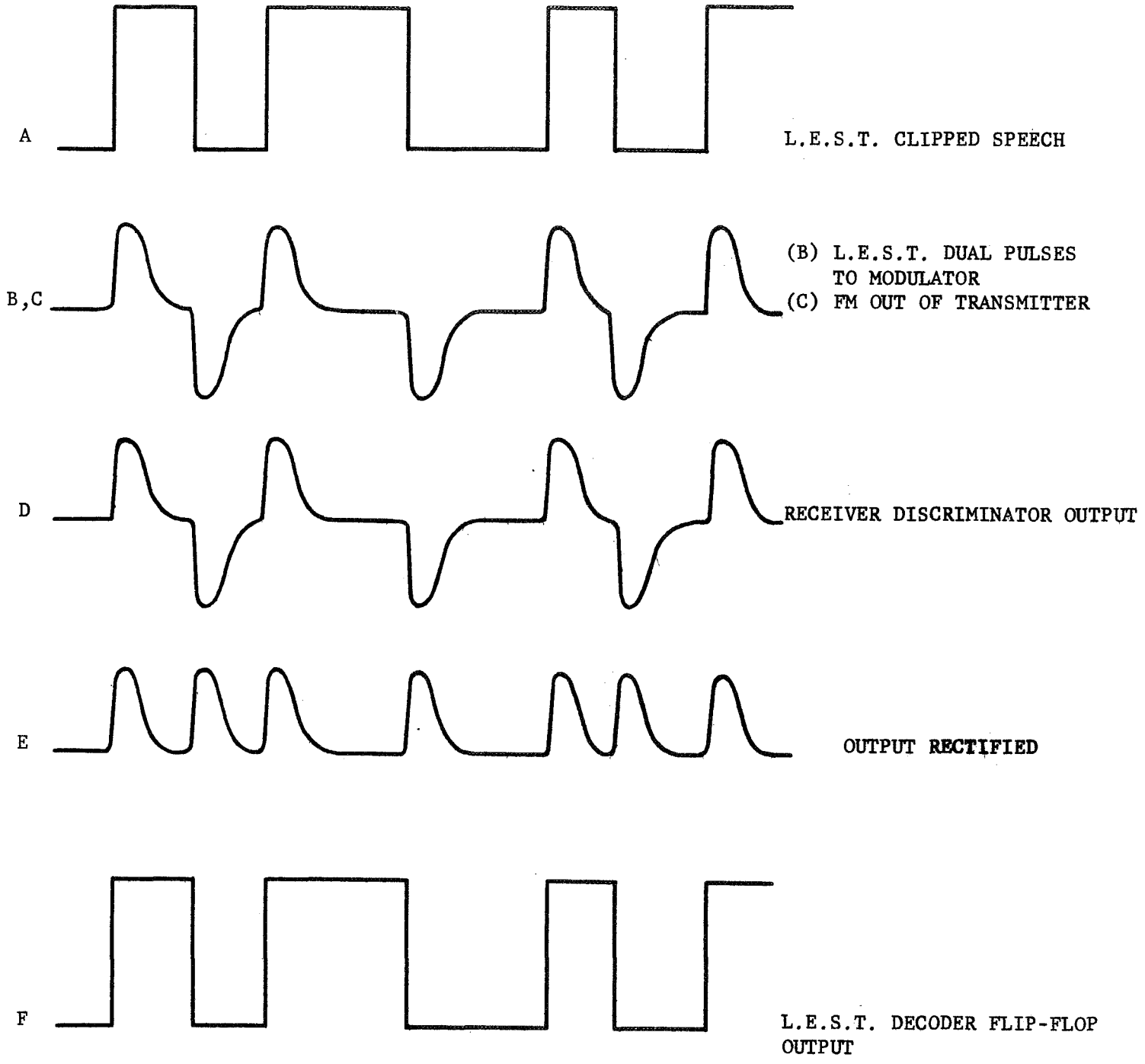

FIGURE 10-2

TYPICAL WAVEFORMS
L.E.S.T. EXPERIMENT

FIGURE 10-3

LINEAR CHARACTERISTICS OF DISCRIMINATOR

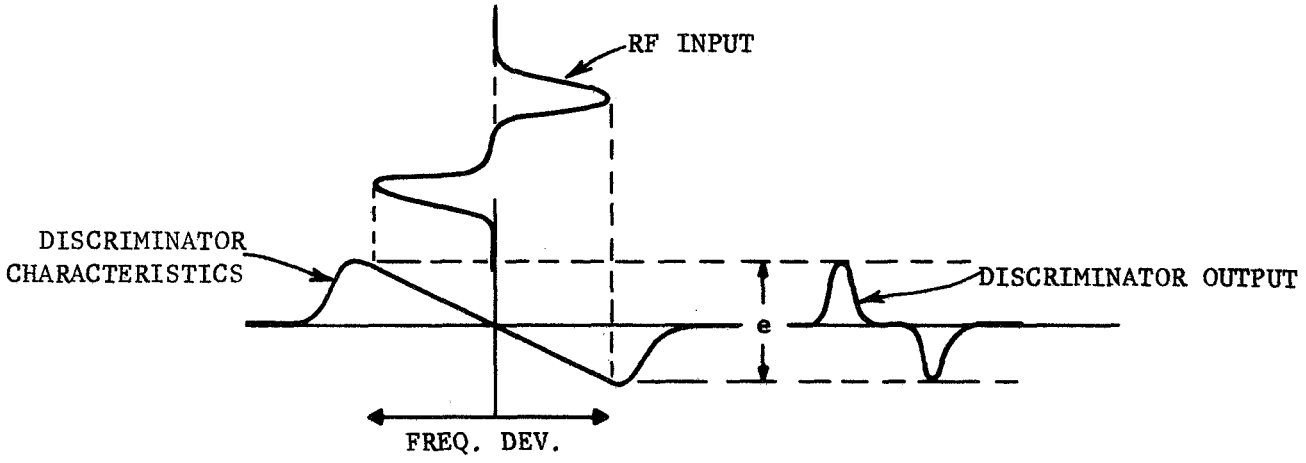

FIGURE 10-4

L.E.S.T. CIRCUIT MODIFICATIONS

Dual Pulse Former and Rectifier Circuits

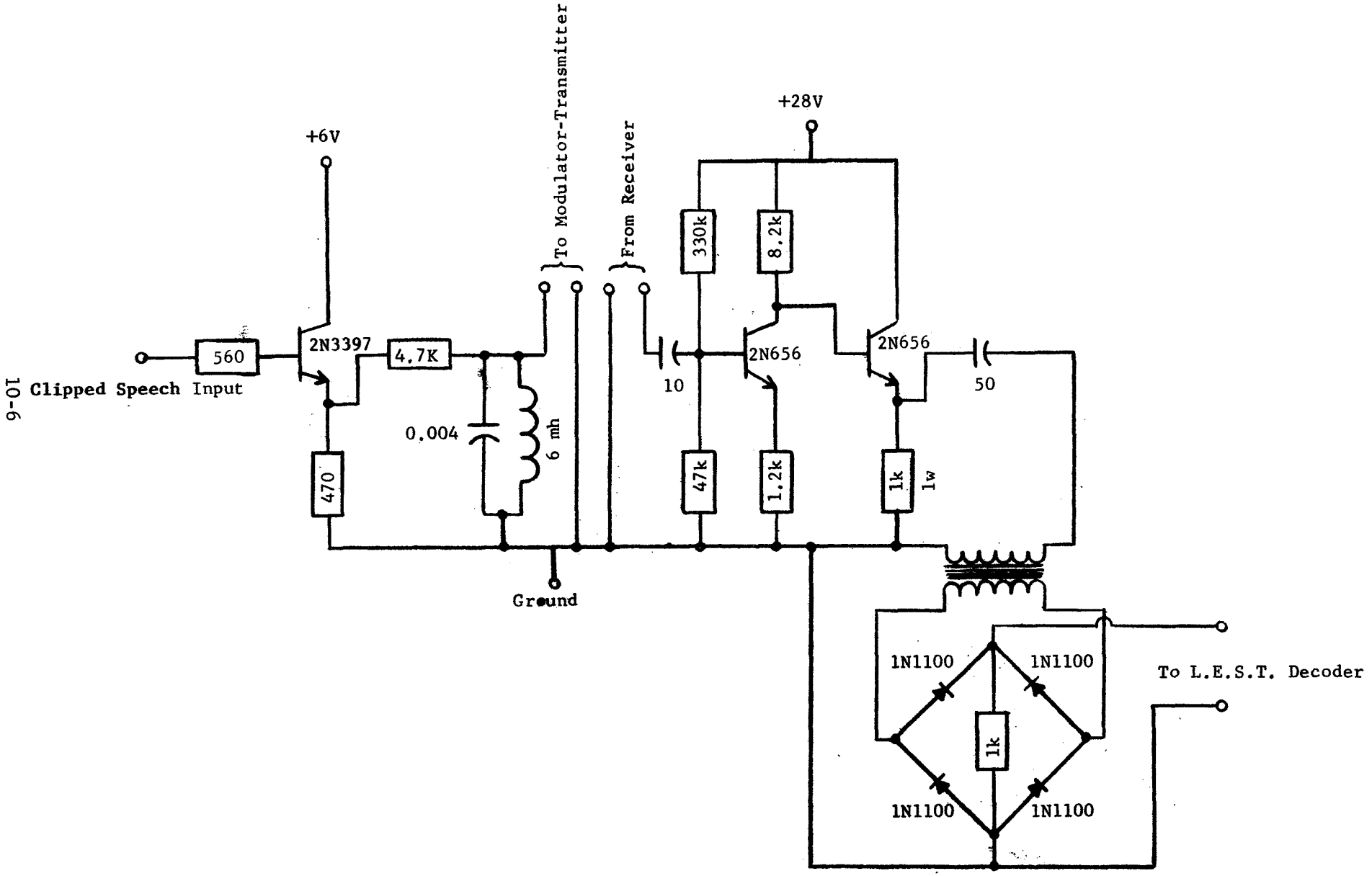

transmitter was connected to a dummy load instead of the 30 foot dish antenna and an in-house transponder was used to convert from the transmit to the receive frequency. Tests through the satellite were conducted using the 300 watt transmitter connected to the 30 foot diameter antenna to transmit to ATS-1 at 149.22 MHz. A transponder in ATS-1 converts the frequency and transmits at 135.6 MHz. This returned signal was received back at the Radio-Optical Observatory using two bays of a yagi antenna.

Lists of spondaic words were used in the experiment to aid in the determination of the intelligibility level for L.E.S.T. speech. Spondaic words have two syllables of approximately equal emphasis on each syllable. Tape recordings of the L.E.S.T. spondaic words were played before two groups of untrained listeners, five persons per group. These intelligibility tests were performed in an anachoic chamber to reduce the level of background noise, echoes, and general distractions. The test is more severe than normal speech patterns in that consecutive words are unrelated. The listener either understands the complete word or misunderstands it and both syllables must be correct. As the test was conducted, the listeners wrote the words on a prepared form.

The tests were divided into fifty-word lists. The first fifty-word test resulted from an in-house test using the local transponder and no link to the satellite. This test served to familiarize the listeners for the first time with the sound of L.E.S.T. and to calibrate the performance of the L.E.S.T. equipment against similar tests conducted on earlier programs. After a break, the listeners heard a one hundred-word list resulting from the complete test using the link to ATS-1. The first fifty words of the on hundred-word list were the same as in the first test, while the second fifty words were heard for the first time. For this reason, the two groups of fifth words were scored separately.

During the tests with ATS-1 on September 23, 1969, some difficulty was experienced in transmission due to ionospheric effects resulting in amplitude scintillation. This caused some words to be lost during transmission of the one hundred-word list. Three words in the first fifty and one word in the second fifty were completely lost and were discounted from the test. All other words including some which had amplitude fading and noise difficulties were counted in the test.

Table 10-1 shows the results of the intelligibility tests. The numbers are for the percentage of correct word answers in each test. Ten of the one hundred words used in the tests are: necktie, woodwork, greyhound, bobsled, catcall, browbeat, playmate, doormat, courtship, and hardware.

The following conclusions can be drawn from the results of these tests:

1. The scores in the calibration tests number 1 and 3 compare favorably with previous tests for L.E.S.T. speech having scores of 90 percent of better.

2. Only a slight loss in intelligibility resulted in transmission to ATS-1 compared with the laboratory test. The measured intelligibility for the ATS-1 test was 91.5 compared to 94.5 for the laboratory test.

3. Although L.E.S.T. speech is understandable directly out of the receiver, the level of intelligibility is significantly lower than the decoded speech out of the L.E.S.T. equipment. Test number 4 compared with test number 2.

TABLE 10-1

L.E.S.T. WORD TESTS

GROUP 1

Listener	Test No. 1 First 50 Words	Test No. 2 First 50 Words	Test No. 2 Second 50 Words
1	98 percent	98 percent	86 percent
2	92 percent	96 percent	90 percent
3	100 percent	98 percent	96 percent
4	98 percent	98 percent	96 percent
5	84 percent	94 percent	90 percent
	94.5 percent	96.6 percent	91.5 percent

GROUP 2

Listener	Test No. 3 First 50 Words	Test No. 4 First 50 Words	Test No. 4 Second 50 Words
6	86 percent	79 percent	82 percent
7	92 percent	94 percent	76 percent
8	98 percent	96 percent	84 percent
9	90 percent	88 percent	74 percent
10	94 percent	85 percent	71 percent
	92 percent	88.5 percent	77.5 percent

Test No. 1 and Test No. 3: In-house test recorded at L.E.S.T. decoder output.
Test No. 2: ATS-1 test recorded at L.E.S.T. decoder output.
Test No. 4: ATS-1 test recorded at receiver output (not decoded).

4. In both test number 2 and test number 4 the scores were considerably higher for the first fifty words which were by that time familiar to the listeners.

The low energy characteristics of the L.E.S.T. experiments can be evaluated by considering the time during which the FM carrier is keyed by the L.E.S.T. pulses compared with the total time of speech transmission.

Pulse width of L.E.S.T. input to transmitter (modulator)is equal to 70 microseconds. Pulse width of returned L.E.S.T. out of the receiver (discriminator) is equal to 140 microseconds.

Average frequency in normal speech is equal to 600 Hz, as measured in previous studies of L.E.S.T. speech.

There are two zero crossings per pulse, or an average of 1200 pulses per second during spoken words. Short gaps in forming words and sentences total approximately half the time while speaking, and longer pauses occupy about one-half the total time during normal speech so that the average pulse rate during conversation is typically 300 pulses per second. The pulse duration in the satellite tests was 140 microseconds. The duty cycle is thus

$$\frac{300 \times 140}{10^6} = 0.042$$

It is probable that the L.E.S.T. pulses could have been detected with approximately the same signal-to-noise ratio if they had been transmitted by AM rather than the narrow bandwidth FM. The FM noise improvement with the small deviation ratio results in a detector output signal-to-noise which is approximately the same as the input signal-to-noise, and thus the FM is approximately equivalent to AM, suggesting that the same result could have been attained with a satellite having a peak effective radiated power of 200 watts, but an average e.r.p. of only ten watts.

REFERENCE

1. J. C. R. Licklider and I. Pollack, "Effects of Differentiation, Integration and Infinite Peak Clipping Upon the Intelligibility of Speech," Journal of the Acoustical Society of America, Volume 20, Number 1, January 1948.

SECTION 11. CONCLUSIONS AND RECOMMENDATIONS

CONCLUSIONS

1. The test results indicate that an accuracy better than ± 1 nautical mile, 1 sigma for ships and approximately ± 1 nautical mile, 1 sigma for aircraft can be achieved at VHF. To achieve that accuracy, it will be necessary to employ calibration transponders at fixed, known locations with approximately 600 mile spacing, and interrogate each one a few times per hour to determine range measurement corrections. It is recommended that calibration of vehicle equipment time delay be accomplished at the ground terminal by interrogating each craft when it is at some known location. The time delay calibration is then stored in the computer with the vehicle address. It will be necessary to employ aircraft antennas that discriminate against sea reflections, so that the reflected signal is more than 10 dB below the direct signal. The use of circular polarization for the satellite and aircraft antennas is recommended.

2. Position fixing is feasible by simultaneous range measurements from two geostationary satellites operating on the same frequency. It was demonstrated by interrogating any one of several user craft through one satellite and receiving a response from the addressed user relayed through both satellites.

3. The equipment limitation on ranging resolution was approximately ± 200 feet (0.4 microsecond timing resolution) when the bandwidth limits were like those presently used for aircraft mobile communications; i.e. 4.0 kHz for data baseband, and 15 kHz for the radio frequency spectrum.

4. Ranging precision for surface craft, including VHF transmission links, was better than ± 500 feet (1.0 microsecond), one sigma for IF signal-to-noise ratios above 10 dB in a 15 kHz bandwidth; approximately 1500 feet, 1 sigma for IF signal-to-noise ratios at the 5 dB FM signal detection threshold; and better than ± 5000 feet for an aircraft at 39,000 feet over the North Atlantic using a VHF blade antenna and experiencing sea reflection multipath.

5. Position fix precision was better than 1 nautical mile, 1 sigma for a ship at sea off Galveston, Texas when the antenna was not shielded from a satellite by the mast or other structures. When the antenna was shielded, some interrogations did not result in responses. Fix precision was reduced to approximately 1 nautical mile, 1 sigma, and in that particular test the errors were along a hyperbolic line of position.

6. Position fix precision was approximately 1 nautical mile, 1 sigma for aircraft, including fixes made over water when using a Dorne and Margolin Satcom antenna in the azimuth mode.

7. Line of position accuracy for a buoy moored in deep water at middle latitudes was better than ± 1 1/2 nautical miles using an unattended transponder over approximately a two-week period, including the effects of diurnal and other ionospheric delay changes, pitch and roll of the buoy, and signal-to-noise ratio variation down to the detection threshold. Accuracy may be improved to better than ± 1 nautical mile, 1 sigma with the use of a better description of the ionosphere than was used in the test.

8. Lines of position for aircraft at jet speeds and altitudes over the North Atlantic had a standard deviation of approximately ± 1 nautical mile when using a VHF blade antenna. Individual measurement displacements larger than two miles toward the sub-satellite point and four miles away from the sub-satellite point were attributed to multipath.

9. Fixes determined by two-satellite ranging at VHF agreed with VORTAC fixes within ± 3 miles over the midwestern United States. At best, the VORTAC fixes are accurate to ± 1 nautical mile.

10. Successful range measurements were made on nearly every interrogation when the mobile craft antenna gain toward the satellite was better than approximately 0 dB, the links were not degraded by Faraday rotation or scintillation, the user receiver noise figure was approximately 3.0 dB, and the user transmitter power was approximately 100 watts. Deliberate tests for Faraday rotation and low user antenna directivity toward the satellite caused more unsuccessful interrogations than would be acceptable in an operational system. Circular polarization for the satellite and user antennas and a minimum gain of 0 dB for the user antenna may be required for an acceptable response rate. Scintillation can cause an occasional failure to respond, but the drop-outs last only a few seconds, so that repeated interrogations will insure a response within a short time period. Scintillation may reduce the response rate, but does not otherwise affect the usefulness or accuracy of tone-code ranging. Roll of a ship or buoy can cause signal drop-outs of short duration due to antenna pattern nulls caused by surface reflection. The effect is similar to that of scintillation.

11. Ranging and position fixing are compatible with mobile voice and data communications. No antenna diplexer is required for tone-code ranging, and simplex operation is feasible. No modifications are necessary to satellites designed for relaying mobile communications.

12. Ranging and position fixing measurements for locating a transponder can be made from a ground terminal through geostationary satellites within one second of time, with ranging signal transmissions shorter than one-half second.

13. Ranging and position fixing can be performed with currently available mobile radio transmitters and receivers with the addition of an inexpensive solid-state circuit, although some receiver-transmitters, as supplied commercially, may have time delay variations with signal level or tuning that introduce ranging errors as large as several thousand feet. The time delay variations can be corrected by circuit modifications such as the substitution of a different limiter.

14. Narrow bandwidth VHF user equipment in an unattended buoy moored in deep ocean retained its time delay calibration without discernible change for several weeks.

15. Voice transmissions using the Low Energy Speech Transmission (L.E.S.T.) waveforms were transmitted through satellites without significant degradation of intelligibility. Spondaic word intelligibility exceeding 90 percent was achieved and energy savings of approximately 10 dB over single sideband suppressed carrier are indicated by the test results.

RECOMMENDATIONS

1. Test the use of calibration stations to monitor propagation conditions and determine range corrections so that fix accuracy is approximately the same as the fix precision. Install ranging transponders with 10 dB gain helical antennas to serve as calibration stations at two points along a transoceanic route. Fly an aircraft equipped with a ranging transponder on the route. Use the fixed station calibration measurements to correct the aircraft measurements. Schedule flights to include day-night transitions on the route, and if possible include effects of magnetic storms.

2. Determine relative accuracy at VHF by monitoring the positions of two aircraft flying at a known separation.

3. Test long-term performance and calibration stability by the use of transponders on a ship. Suggested ships are merchant ships and weather ships that stay on station for three week periods. An excellent merchant shipping route would be from the west coast to the east coast by way of the Panama Canal.

4. Test performance at far north latitudes such as Greenland or the North slope of Alaska, to obtain statistical data on performance in the presence of scintillation and other high latitude ionospheric propagation effects.

5. Test tone-code ranging at L-band. It is suggested that ATS-5 can be used by relaying interrogations and responses through the satellite during the times when the L-band antenna is pointed toward the earth. The tone frequency should be increased to take advantage of the better propagation at L-band, and in doing so, the tone interrogating signal duration can be reduced to be within the duration of the ATS-5 antenna sweep across the earth. The interrogation rate can be synchronized with the spin rate of the satellite. With tone-code ranging, the user responses can also be delayed by a known increment to synchronize the responses with the satellite.

SECTION 12. NEW TECHNOLOGY

There has been no new technology developed on this contract.

APPENDIX I

DESCRIPTION OF POSITION DETERMINATION METHOD USED ON FLIGHT FROM ATLANTIC CITY TO OMAHA AND RETURN

This flight in a DC-6B aircraft (FAA 114) departed on 6/12/69 and returned to Atlantic City on 6/13/69 for purposes of testing the General Electric tone-code responder position determination device. The responder was interrogated regularly by the General Electric Radio-Optical Observatory at Schenectady, New York.

Since no range instrumentation position tracking system was available along the selected route, the following method of obtaining reference positions of the aircraft was devised and used.

A time display was remoted into the aircraft cockpit and driven from the digital time code generator associated with the project recording equipment, the time code generator having been previously synchronized with WWV.

Certain strategically located VORTAC navigation stations whose locations coincided with the route to be flown were selected to provide simultaneous bearing and distance information.

A qualified observer was stationed in the aircraft cockpit who manually recorded bearing and distance versus real time provided by the time code generator remote readout.

The time code generator is considered to be accurate within milliseconds while the driven remote readout, as used, has a reading resolution of 1 second.

It should be noted that the DME (distance measuring equipment) portion of the VORTAC system measures slant range only; e.g., over the station the distance being measured is the aircraft's altitude in nautical miles although the horizontal displacement from the VORTAC station is zero. Accordingly, the accuracy of positions derived from within approximately 10 miles of the VORTAC stations will suffer somewhat from this "slant range effect" alone in addition to the usual inaccuracies and biases normally encountered when taking data in this manner (humans reading dials, etc.). In the attached position data, any occurrences described as "over the station" were derived by other methods of observing station passage and one need not be concerned with slant range effects.

After the aircraft returned to Atlantic City, the flight was reconstructed on Aeronautical Sectional Charts and the bearings and associated distances from the VORTAC stations were reduced to Latitude and Longitude (to the nearest minute of arc) versus GMT time (to the nearest second of time).

A copy of these Latitude and Longitude positions and the bearing and distance information from which they were derived is attached.

Flight No. 503 - From Joliet to Omaha via Minneapolis - 6/12/69

Time (Z)	North Latitude	West Longitude		Radial	Slant Range (nmi.)	VORTAC Station
13:01:08	42° 34'	89° 36'		130°	115	Nodine, Minn.
13:02:06	42° 38'	89° 41'		"	110	"
13:03:17	42° 41'	89° 45'		"	105	"
13:04:26	42° 45'	89° 50'		"	100	"
13:05:33	42° 49'	89° 55'		"	95	"
13:06:41	42° 52'	90° 00'		"	90	"
13:11:17	43° 06'	90° 20'		"	70	"
13:12:24	43° 10'	90° 24'		"	65	"
13:13:36	43° 13'	90° 29'		"	60	"
13:14:44	43° 17'	90° 34'		"	55	"
13:15:51	43° 20'	90° 39'		"	50	"
13:17:04	43° 24'	90° 44'		"	45	"
13:18:13	43° 27'	90° 49'		"	40	"
13:19:24	43° 31'	90° 54'		"	35	"
13:20:33	43° 34'	90° 59'		"	30	"
13:21:44	43° 38'	91° 04'		"	25	"
13:23:22	43° 43'	91° 11'		"	18	"
13:24:02	43° 45'	91° 14'		"	15	"
13:25:10	43° 48'	91° 19'		"	10	"
13:26:36	43° 52'	91° 24'		"	5	"
13:27:48	43° 55'	91° 29'		---	Over Station	"
13:28:44	43° 58'	91° 34'		125°	105	Minneapolis
13:29:57	44° 02'	91° 38'		"	100	"
13:31:08	44° 05'	91° 45'		"	95	"
13:35:07	44° 17'	92° 02'		"	78	"
13:35:48	44° 18'	92° 05'		"	75	"
13:36:57	44° 22'	92° 10'		"	70	"
13:38:09	44° 25'	92° 16'		"	65	"
13:40:30	44° 32'	92° 26'		"	55	"
13:41:41	44° 35'	92° 31'		"	50	"
13:42:50	44° 39'	92° 36'		"	45	"
13:44:02	44° 42'	92° 42'	Treat with Caution - aircraft departed slightly to avoid thunderstorm.	"	40	"
13:45:42	44° 47'	92° 48'			33	"
13:46:23	44° 49'	92° 52'		"	30	"
13:47:37	44° 52'	92° 57'		"	25	"

Flight No. 503 - From Joliet to Omaha via Minneapolis - 6/12/69 (continued)

13:49:35	44° 58'	93° 05'	125°	17	Minneapolis
13:51:14	45° 02'	93° 13'	"	10	"
13:52:36	45° 06'	93° 18'	"	5	"
13:53:35	45° 09'	93° 23'	---	Over Station	"
13:56:16	45° 00'	93° 28'	198°	10	"
13:59:03	44° 51'	93° 33'	"	20	"
14:00:28	44° 46'	93° 36'	"	25	"
14:01:49	44° 41'	93° 39'	"	30	"
14:03:05	44° 37'	93° 42'	"	35	"
14:04:51	44° 31'	93° 46'	"	42	"
14:05:41	44° 27'	93° 48'	"	45	"
14:07:08	44° 22'	93° 51'	"	51	"
14:08:16	44° 18'	93° 53'	"	55	"
14:09:32	44° 14'	93° 55'	"	60	"
14:10:50	44° 10'	93° 58'	"	65	"
14:12:05	44° 05'	94° 01'	"	70	"
14:16:06	43° 48'	94° 10'	"	86	"
14:17:06	43° 46'	94° 12'	"	90	"
14:19:37	43° 37'	94° 17'	"	100	"
14:20:53	43° 32'	94° 20'	"	105	"
14:22:08	43° 28'	94° 23'	"	110	"
14:23:22	43° 23'	94° 26'	"	115	"
14:24:35	43° 18'	94° 28'	"	120	"
14:28:18					
14:29:33					

Flight No. 503 - From Omaha to Atlantic City via Minneapolis, Green Bay - 6/13/69

Time (Z)	North Latitude	West Longitude	Radial	Slant Range (nmi.)	VORTAC Station
13:04:59	45° 08'	93° 12'	091°	8	Minneapolis
13:06:30	45° 07'	93° 01'	"	15	"
13:07:32	45° 06'	92° 54'	"	20	"
13:10:03	45° 04'	92° 38'	"	32	"
13:10:38	45° 04'	92° 33'	"	35	"
13:11:54	45° 03'	92° 25'	"	41	"
13:12:41	45° 03'	92° 20	"	45	"
13:13:42	45° 02'	92° 13'	"	50	"
13:15:57	45° 01'	91° 58'	"	61	"
13:17:46	45° 00'	91° 45'	"	70	"
13:18:47	44° 59'	91° 37'	"	75	"
13:19:48	44° 58'	91° 30'	"	80	"
13:20:47	44° 57'	91° 33'	"	85	"
13:21:51	44° 57'	91° 16'	"	90	"
13:24:24	44° 55'	91° 00'	"	102	"
13:25:00	44° 55'	90° 55'	"	105	"
13:25:37	44° 54'	90° 52'	"	108	"
13:26:05	44° 54'	90° 50'	"	110	"
13:26:54	44° 53'	90° 40'	280°	110	Green Bay
13:28:05	44° 52'	90° 33	"	104	"
13:30:45	44° 50'	90° 15'	"	91	"
13:31:59	44° 49'	90° 08'	"	85	"
13:33:02	44° 48'	90° 02'	"	80	"
13:34:03	44° 47'	89° 54'	"	75	"
13:36:32	44° 45'	89° 38'	"	63	"
13:37:09	44° 44'	89° 34'	"	60	"
13:41:56	44° 40'	89° 02'	"	37	"
13:42:59	44° 39'	88° 56'	"	32	"
13:43:24	44° 39'	88° 53'	"	30	"
13:44:25	44° 38'	88° 46'	"	25	"
13:45:32	44° 37'	88° 39'	"	20	"
13:47:52	44° 35'	88° 24'	"	9	"
13:48:52	44° 34'	88° 18'	"	5	"
13:49:40	44° 34'	88° 12'	"	Over Station	"
13:54:54	44° 26'	87° 38'	105°	25	"

Flight No. 503 - From Omaha to Atlantic City via Minneapolis, Green Bay - 6/13/69 (continued)

13:57:58	44° 22'	87° 19'	105°	39	Green Bay
13:58:25	44° 22'	87° 16'	"	41	"
13:58:50	44° 21'	87° 14'	"	43	"
14:00:00	44° 19'	87° 04'	"	50	"
14:01:31	44° 18'	86° 58'	"	55	"
14:02:40	44° 17'	86° 51'	"	60	"
14:06:00	44° 12'	86° 31'	"	75	"
14:07:06	44° 11'	86° 24'	"	80	"
14:08:00	44° 10'	86° 19'	"	84	"
14:09:22	44° 08'	86° 11'	"	90	"
14:10:30	44° 07'	86° 04'	"	95	"
14:16:06	43° 59'	85° 31'	"	120	"
14:17:14	43° 58'	85° 24'	"	125	"
14:17:57	43° 56'	85° 22'	294°	122	Peck, Michigan
14:18:36	43° 55'	85° 18'	"	119	"
14:20:33	43° 52'	85° 07'	"	110	"
14:21:40	43° 50'	85° 00'	"	105	"
14:25:56	43° 45'	84° 39'	"	85	"
14:27:52	43° 42'	84° 28'	"	76	"
14:29:25	43° 40'	84° 18'	"	69	"
14:30:05	43° 39'	84° 14'	"	66	"

APPENDIX II

MODEL FOR IONOSPHERE CORRECTIONS

The following two references were used to establish a model for the effects of the ionosphere on the ranging error.

G. H. Millman, "A Survey of Tropospheric, Ionospheric, and Extra-terrestrial Effects on Radio Propagation Between the Earth and Space Vehicles", General Electric Company Report TIS R66EMH1, 1966.

R. W. Lawrence, D. J. Posakony, O. Garriott, and S. C. Hall, "The Total Electron Content of the Ionosphere at Middle Latitudes Near the Peak of the Solar Cycle", Journal of Geophysical Research, Volume 68, Number 7, April 1, 1963, page 1889.

The first reference is used to predict the effect of elevation angle and the second reference the diurnal effect on ranging error.

The following notation is used in this appendix.

E	Line-of-sight elevation angle to the satellite
R_a	Actual slant range
R_m	Measured slant range
$\Delta = R_m - R_a$	
h	Representative ionosphere altitude, say mean altitude
t	Local time (of day) on the line-of-sight at altitude h
$f(t)$	A function of t such that $0 \leq f(t) \leq 1$
$g_{max}(E)$	Maximum value of Δ as a function of E
$g_{min}(E)$	Minimum value of Δ as a function of E

The empirical model developed in this appendix should be considered a provisional "engineering prototype" since no effort has been made to account for the "thickness" of the ionosphere or the fact that two frequencies are used in the transmissions. Assuming an inverse square frequency effect, the effect of frequency can easily be accounted for.

In order to easily incorporate the data contained in the two references cited above, the following model for the range error was adopted:

$$\Delta = ba^{f(t)}$$

where $0 \leq t \leq 24$ hours

$\max f(t) = 1$

$\min f(t) = 0$

$a > 1$

Obviously over the range of f(t)

$$\Delta_{min} = b \qquad \Delta_{max} = ab$$

The first reference gives the ionosphere range errors $g_{min}(E)$ at midnight (t = 0) and $g_{max}(E)$ at noon (t = 12) as a function of the elevation angle E. Therefore

$$b = g_{min}(E) = \Delta_{min}$$

$$a = g_{max}(E)/g_{min}(E) = \Delta_{max}/\Delta_{min}$$

As noted above $g_{min}(E)$ and $g_{max}(E)$ are inversely proportional to frequency. The functions $g_{max}(E)$ and $g_{min}(E)$ are shown in Figure II-1.

The second reference (Figure II-1) contains curves showing six diurnal interval effects over various times of the season. These six curves were normalized* and suitably averaged to give the diurnal effect shown in Figure II-2.

The resulting empirical equation for the ionosphere effect is

$$\Delta = k\, g_{min}(E) \left[\frac{g_{max}(E)}{g_{min}(E)}\right]^{f(t)}$$

where the proportionality k can be adjusted to account for long-term variations in ionosphere activity/intensity. The procedure for using this equation is to first use the local ground time of day, the line-of-sight elevation angle, E, to the satellite and some mean ionosphere altitude h to compute the local time t at the intersection of the line-of-sight ray and the mean altitude h. Then the range error is computed by the above equation.

It should be noted that the ratio $g_{max}(E)/g_{min}(E)$ is frequency invariant so that the above equation could be compensated for frequency by

$$\Delta = k \left(\frac{f_{nom}}{f}\right)^2 g_{min}(E) \left[\frac{g_{max}(E)}{g_{min}(E)}\right]^{f(t)}$$

where $g_{min}(E)$ is evaluated for $f = f_{nom}$.

---

* by the equation

$$f(t) = \frac{\log\,(\Delta(t)\,) - \log\,(\Delta_{min})}{\log\,(\Delta_{max}) - \log\,(\Delta_{min})}$$

FIGURE II-1

RANGE ERROR DUE TO IONOSPHERE,
DAY AND NIGHT, VERSUS ELEVATION ANGLE

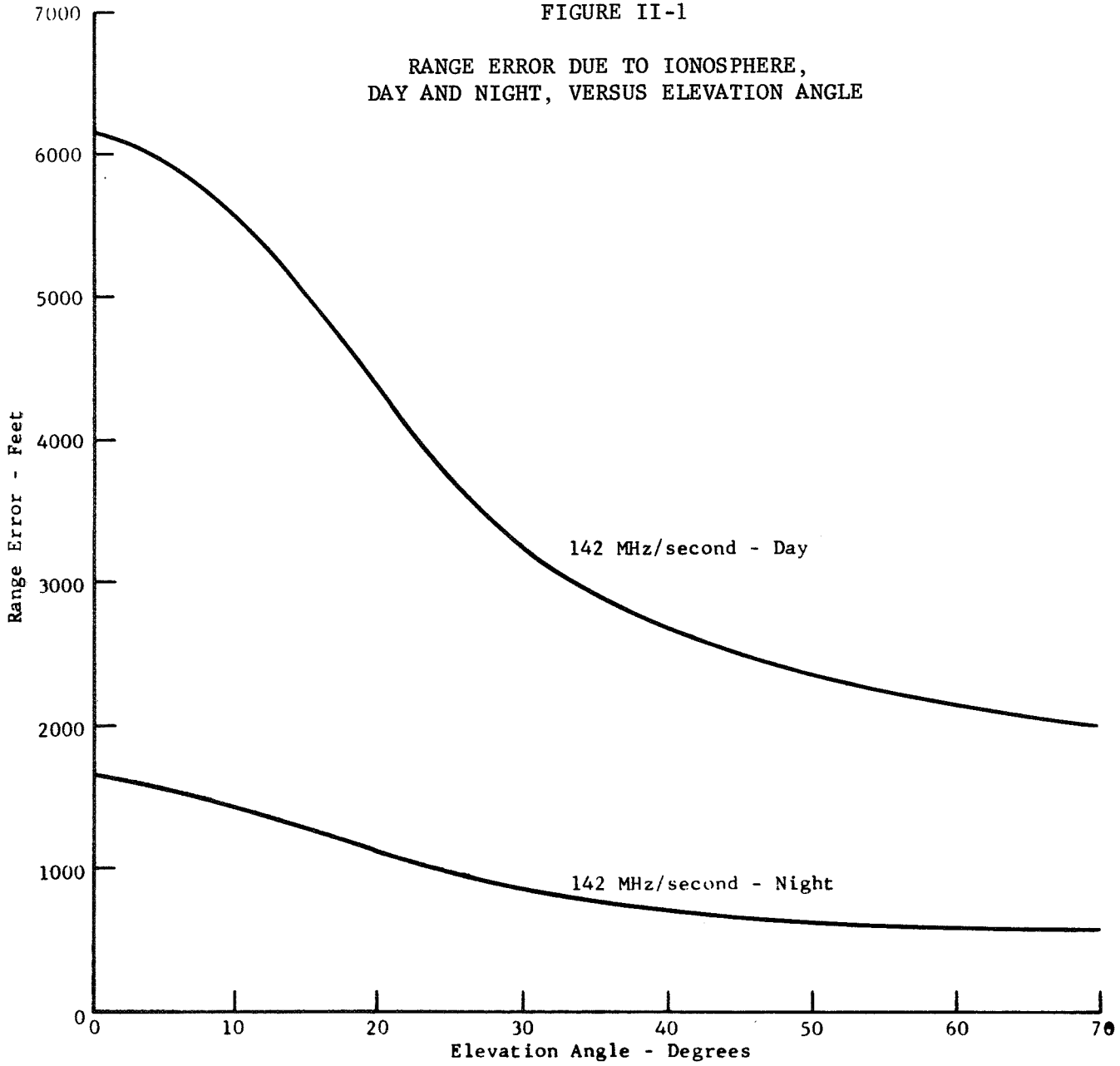

FIGURE II-2

DIURNAL VARIATION IN RANGE DUE TO IONOSPHERE (NORMALIZED)

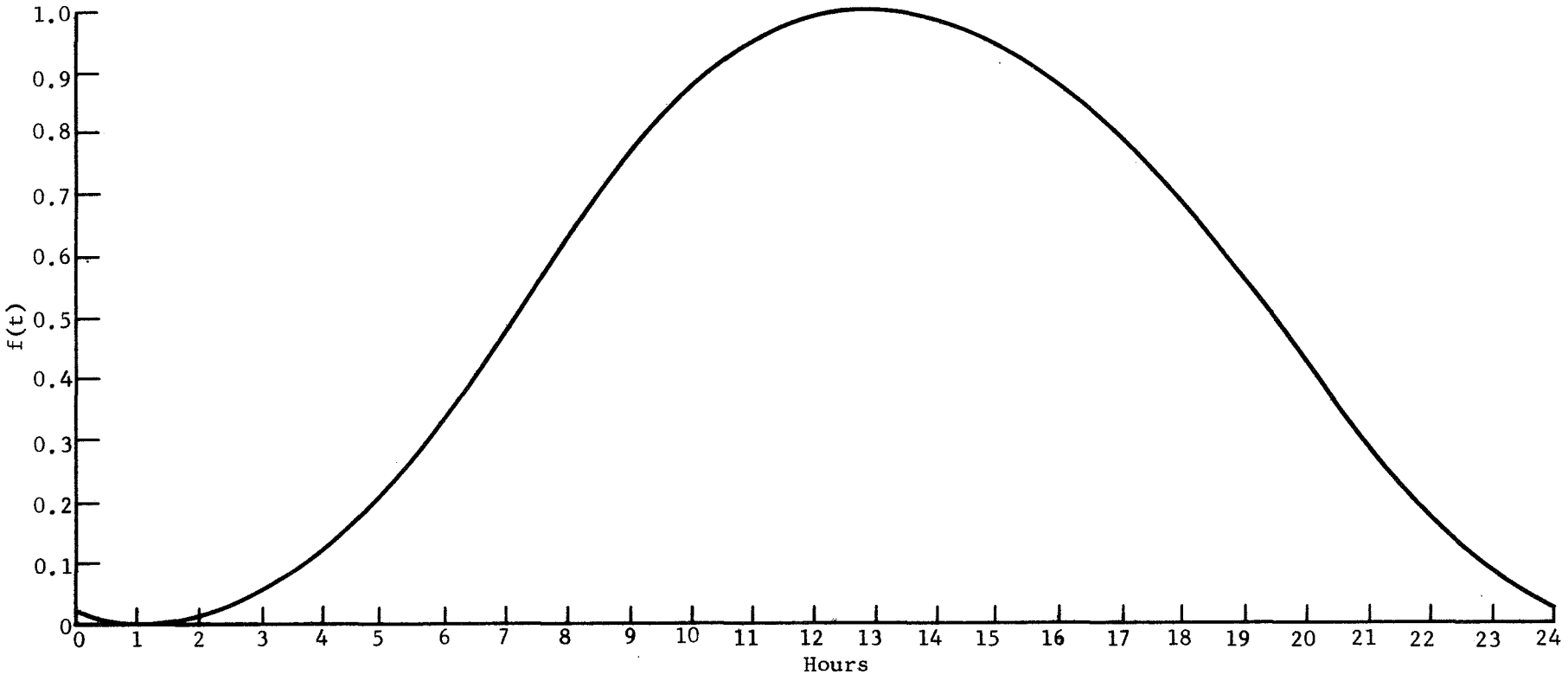

APPENDIX III

MULTIPATH ANALYSIS AND MEASUREMENT EQUIPMENT

This appendix considers the effect of a simple multipath distortion on a sinusoidally modulated FM signal. The distortion analysis is limited to the determination of the relative amplitude and phase of the fundamental component in the FM detected received signal. Range measurements to aircraft appear to show multipath effects in accordance with the analysis. In addition to the analysis, this appendix describes equipment built to measure the effect. The equipment was not flight tested.

Multipath Analysis

The simple multipath considered is shown in Figure III-1.

FIGURE III-1. MULTIPATH

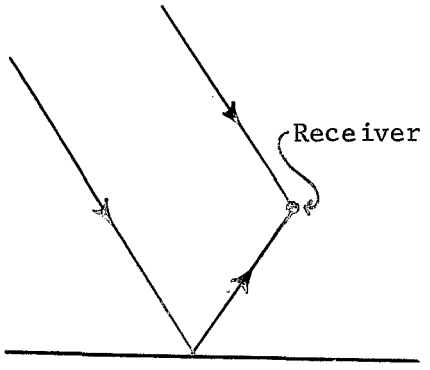

The analysis begins by letting

$$g(t) = A_m \cos(\omega_m t + \phi_m) \qquad \phi_m \text{ constant} \qquad (1)$$

define the CW modulation. Then the FM modulated transmitted signal is given by

$$e_r(t) = A_c \cos(\omega_c t + \phi_c + \Psi(t)) \qquad \phi_c \text{ constant} \qquad (2)$$

where
$$\frac{d\Psi(t)}{dt} = \dot{\Psi}(t) = k_f g(t) \qquad (3)$$

so that
$$\Psi(t) = \delta \sin(\omega_m t + \phi_m) \qquad (4)$$

where
$$\delta = \frac{k_f A_m}{\omega_m} \qquad \delta \text{ in radians} \qquad (5)$$

A perfect discriminator would detect $\dot{\Psi}(t)$; i.e., the detected signal in the absence of multipath would be $k_d\dot{\Psi}(t) = k_d k_f g(t)$. Now consider the effect of a multipath signal being received simultaneously with the direct path. Assuming the multipath can be represented by a simple reflection process with a corresponding relative amplitude and time delay, then the total received signal $e_\Sigma(t)$ before detection is

$$e_\Sigma(t) = e_T(t) + k_T e(t-T) \tag{6}$$

Substituting -2 into -6 yields after some elementary manipulation

$$e_\Sigma(t) = A_c\sqrt{1+k^2+2k\cos\left(\Psi(t)-\Psi(t-T)+\omega_c T\right)}\cos\left(\omega_c t+\phi_c+\gamma(t)\right) \tag{7}$$

where

$$\gamma(t) = \frac{\Psi(t)+\Psi(t-T)-\omega_c T}{2} + \tan^{-1}\left\{\frac{[1-k]\sin\dfrac{\Psi(t)-\Psi(t-T)+\omega_c T}{2}}{[1+k]\cos\dfrac{\Psi(t)-\Psi(t-T)+\omega_c T}{2}}\right\} \tag{8}$$

or equivalently

$$\gamma(t) = \tan^{-1}\left\{\frac{\sin(\Psi(t)) + k\sin\left(\Psi(t-T)-\omega_c T\right)}{\cos(\Psi(t)) + k\cos\left(\Psi(t-T)-\omega_c T\right)}\right\} \tag{9}$$

Then an idealized/perfect discriminator would give a detected signal

$$e_d(t) = k_d\,\dot{\gamma}(t) \tag{10}$$

Noting that

$$\frac{d\tan^{-1}X}{dt} = \frac{1}{1+X^2}\frac{dX}{dt} \tag{11}$$

and using (9) obtain

$$\dot{\gamma}(t) = \frac{\dot{\Psi}(t)[1+k\cos\left(\Psi(t)-\Psi(t-T)+\omega_c T\right)] + \dot{\Psi}(t-T)[k^2+k\cos\left(\Psi(t)-\Psi(t-T)+\omega_c T\right)]}{1+k^2+2k\cos\left(\Psi(t)-\Psi(t-T)+\omega_c T\right)} \tag{12}$$

Note from (8) or (9) or (12) that for $k = 0$ then $\dot{\gamma}(t) = \dot{\Psi}(t)$ and similarly for $k \to \infty$, $\dot{\gamma}(t) = \dot{\Psi}(t-T)$ and that for $T = 0$, $\dot{\gamma}(t) = \dot{\Psi}(t)$ which is consistent.

With $\Psi(t)$ given by (4) then

$$\dot{\Psi}(t) = \omega_m\delta\cos\left(\omega_m t + \phi_m\right) \tag{13}$$

$$\Psi(t)-\Psi(t-T) = 2\delta\sin\left(\frac{\omega_m T}{2}\right)\cos\left(\omega_m t + \phi_m - \frac{\omega_m T}{2}\right) \tag{14}$$

can be substituted into (12) which would yield a periodic function of t, with a period f_m^{-1}, that in general will not be sinusoidal. For the application of this report, it is desired to obtain the amplitude and phase of the fundamental component of $\dot{\gamma}(t)$ relative to that which would have been received in the absence of multipath.

It does not appear analytically tractable to obtain an expression for the relative phase and amplitude as a function of k and T, so that numerical integration will be used to obtain the Fourier series in-phase and quadrature fundamental components.

It is convenient to let $X = \omega_m t + \phi_m$ and normalize (12) to obtain

$$e(X) = \frac{[1+k\cos(ARG)]\cos(X) + [k^2+k\cos(ARG)]\cos(X-\omega_m T)}{1+k^2+2k\cos(ARG)} \tag{15}$$

where

$$ARG = 2\delta \sin\left(\frac{\omega_m T}{2}\right)\cos\left(X - \frac{\omega_m T}{2}\right) + \omega_c T \tag{16}$$

It is of interest to make the following observations:

1. For $k \equiv 0$

$$e(X) = \cos(X) \tag{17}$$

2. For $k \equiv 1$

$$e(X) = \frac{1}{2}[\cos(X) + \cos(X-\omega_m T)] = \cos\left(\frac{\omega_m T}{2}\right)\cos\left(X - \frac{\omega_m T}{2}\right) \tag{18}$$

3. For $1+k^2+2k\cos(ARG)$ to be zero, at some instant of time, it is necessary that $k = 1$; but then the preceeding comment (2) holds.

4. For $e(X) \equiv 0$ for all X it is necessary that $k = 1$ and $\omega_m T = 2n\pi+\pi$ and doesn't depend on $\omega_c T$. (See Comment 2.)

5. When $k = 1$ the phase error is $-\frac{\omega_m T}{2}$.

The numerical procedure for evaluating the coefficients C_1 and S_1 in the following Fourier series will now be considered.

$$e(X) = C_1 \cos(X) + S_1 \sin(X) + \text{higher frequency terms} \tag{19}$$

or equivalently

$$e(X) = \sqrt{C_1^2 + S_1^2}\cos(X - \theta) \tag{20}$$

$$\theta = \tan^{-1}\left(\frac{S_1}{C_1}\right) \tag{21}$$

and where

$$C_1 = \frac{1}{\pi}\int_0^{2\pi} e(X)\cos X\, dX \tag{22}$$

$$S_1 = \frac{1}{\pi}\int_0^{2\pi} e(X)\sin X\, dX \tag{23}$$

where e(X) is given by (15) and (16). These integrals were numerically evaluated using Simpson's rule in computed programs FMPHAS and PHAERR. These two computer programs will now be described briefly.

PHAERR (GE MARK I FORTRAN)

This program computes and plots the phase shift error, relative to the phase which would have been received without any multipath, for both FM and AM modulation. (Note AM modulation analysis has not been discussed herein.) The program specifies the frequency deviation ratio δf_m, relative multipath signal strength k, the modulating CW frequency f_m, the carrier frequency f_c and a multipath time delay TTØ. The program plots the phase shift error for values of multipath T from TTØ to TTØ + $(f_c)^{-1}$ in M intervals. As many such cases as desired can be entered on as many individual input data lines.

FMPHAS (GE MARK II FORTRAN)

This program is a variation of the preceding with the only difference being that AM modulation is not considered and the second variable is used to plot the zero phase axis.

These programs were used to compute the curves presented in the description of multipath effects in Section 6.

Multipath Measuring Equipment

The multipath measuring equipment was designed for use in an aircraft where it would process a continuous 2.4414 kHz tone signal received from a satellite when multipath conditions are expected. The equipment measures multipath effect by comparing the phase of the upper sideband with the carrier, the phase of the lower sideband with the carrier, and then summing the two resultants. The first upper and lower sidebands and the carrier are separately heterodyned to a common frequency, and the phase comparisons are made. The resulting phase of the heterodyned lower sideband is γ_-; of the upper sideband, γ_+; and of the carrier, γ_0. Phase comparison of the heterodyned lower sideband and the carrier is $\gamma_- - \gamma_0$; of the upper sideband and carrier, $\gamma_+ - \gamma_0$. The sum of the two resultants is $\gamma_+ + \gamma_- - 2\gamma_0$. The origins of γ_+, γ_-, and γ_0 are shown from expanding Equation (7) and omitting all but the first upper and first lower sidebands.

Equation (7) may be rewritten (omitting all the sidebands except the first upper and first lower):

$$e_\Sigma(t) = e_o(t) + e_2(t) =$$

$$A_c \begin{cases} \delta/2 \sqrt{1 + k^2 + 2k \cos [(\omega_c + \omega_m)\tau]} \cos \left| [\omega_c + \omega_m] t + \phi_c + \phi_m + \gamma_+ \right| \\ + \sqrt{1 + k^2 + 2k \cos (\omega_c \tau)} \cos (\omega_c t + \phi_c + \gamma_0) \\ - \delta \sqrt{2/1 + k^2 + 2k \cos [(\omega_c - \omega_m)\tau]} \cos \left| [\omega_c - \omega_m] t + \phi_c - \phi_m + \gamma_- \right| \end{cases} \quad (24)$$

where

$$\gamma_+ = \frac{-[\omega_c + \omega_m]\tau}{2} + \tan^{-1}\left[\frac{(1 - k)\sin\left\{\frac{(\omega_c + \omega_m)\tau}{2}\right\}}{(1 + k)\left\{\frac{(\omega_c + \omega_m)\tau}{2}\right\}}\right]$$

$$\gamma_0 = \frac{-\omega_c\tau}{2} + \tan^{-1}\left[\frac{(1 - k)\sin\left(\frac{\omega_c\tau}{2}\right)}{(1 + k)\cos\left(\frac{\omega_c\tau}{2}\right)}\right] \qquad (25)$$

$$\gamma_- = \frac{-[\omega_c - \omega_m]}{2} + \tan^{-1}\left[\frac{(1 - k)\sin\left(\frac{\omega_c - \omega_m}{2}\right)\tau}{(1 + k)\cos\left(\frac{\omega_c - \omega_m}{2}\right)}\right]$$

and A_c = amplitude of direct signal

ω_c = carrier frequency

ϕ_c = carrier phase

δ = sideband amplitude

ω_m = modulating frequency

ϕ_m = modulating phase

Figure III-2A compares the phase changes of the carrier and the two sidebands as the difference in path length changes by one wavelength at the radio frequency.

Figure III-2B depicts the results of translating the carrier and the sidebands all to the same frequency and then taking the phase difference of the upper sideband minus the carrier and the lower sideband minus the carrier.

The Multipath Detection Equipment designed and constructed for use in the experiment combines the sideband and carrier signal components to produce a DC output with the characteristic shown as the "Sum of B Curves". The DC signal can be recorded on a chart recorder in an aircraft. Its rates will show the rate at which the aircraft passes through direct- and reflected-signal path length changes of one wavelength. Its amplitude will show the effect of time delay and direct and reflected signal amplitude ratio. It is expected that, in horizontal flight a jet aircraft will pass through an RF path length change of one wavelength in approximately five seconds. The rate will be higher if the aircraft is climbing or descending. The amplitude and period of the multipath signal recording will be correlated with the fluctuations in range measurement made during the recording periods. The results will be useful for predicting and measuring the effects of antenna design, sea state, ground conductivity, aircraft motion and other factors that affect the magnitude of the error caused by ground reflections.

The Multipath Measurement Equipment is shown in block diagram form in Figure III-3. Several mixing and filtering circuits enable the direct measurement of $\gamma_+ - \gamma_0$ and $\gamma_- - \gamma_0$, and the sum of these phase differences $\gamma_+ + \gamma_- - 2\gamma_0$ is taken for the measure of the multipath effects.

FIGURE III-2

PHASE CHANGE FOR 360° (RF) PATHLENGTH CHANGE,
DIRECT AND REFLECTED SIGNALS

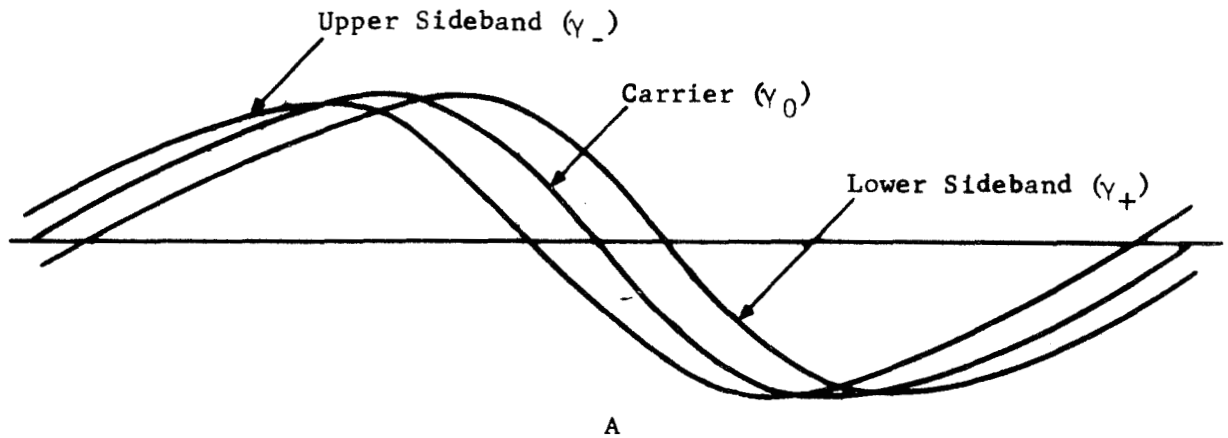

A

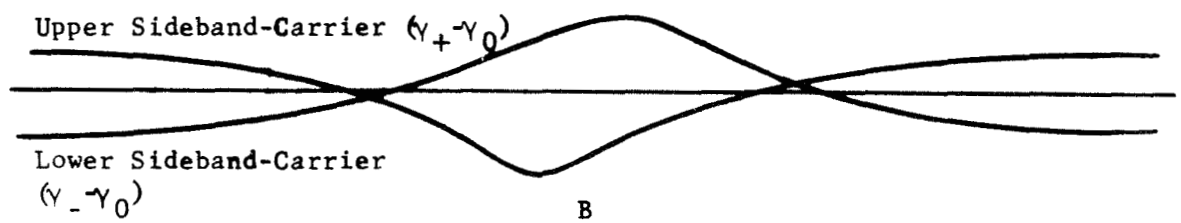

B

($\gamma_+ + \gamma_- - 2\gamma_0$)
Sum of B Curves

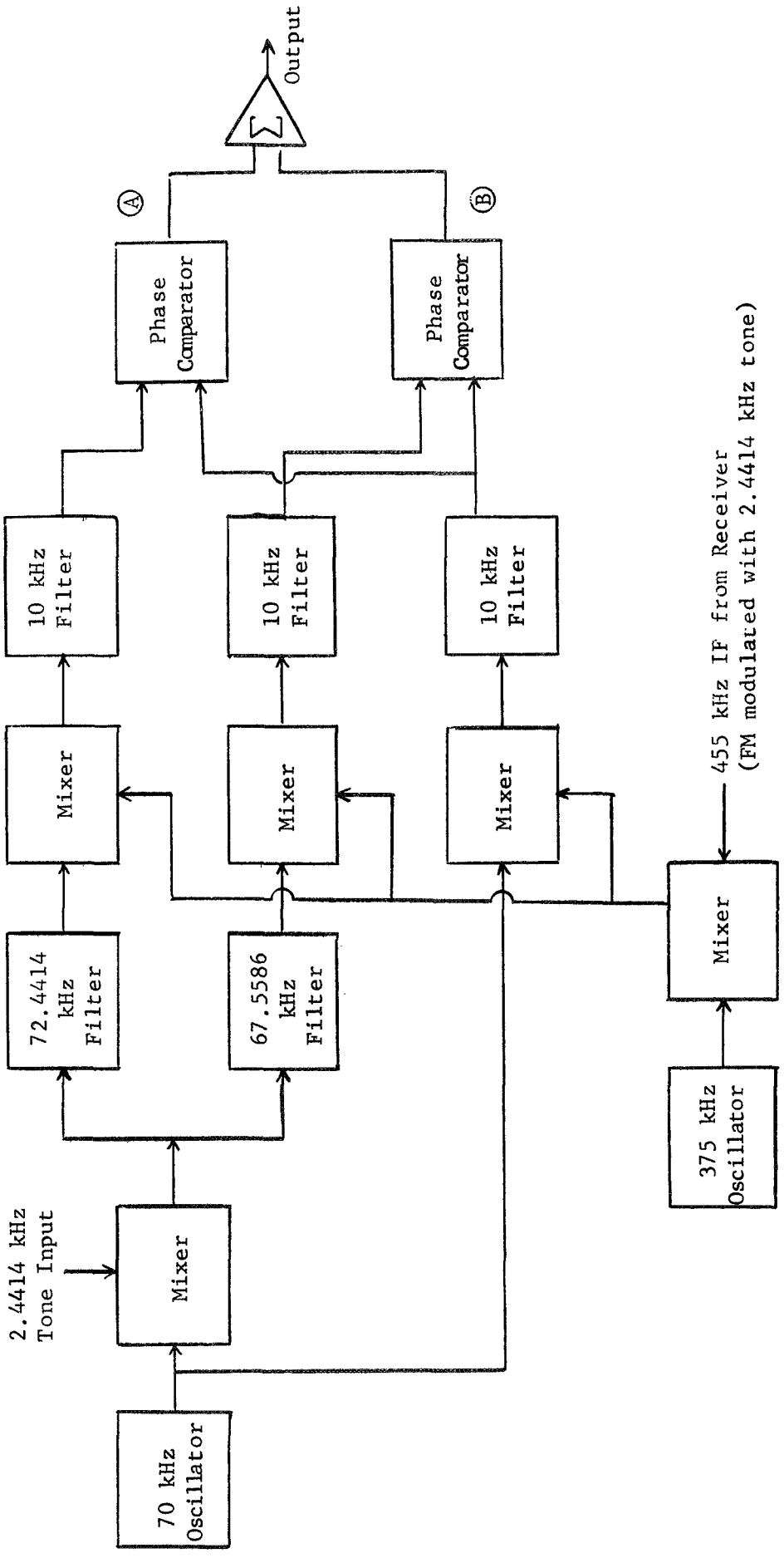

FIGURE III-3. MULTIPATH MEASUREMENT EQUIPMENT

The measurement of $\gamma_+ - \gamma_0$ will be discussed to illustrate the operation of the equipment. The received signal (at the receiver IF frequency of 455 kHz) which is FM modulated with 2.4414 kHz audio is first heterodyned down to 80 kHz by the 375 kHz oscillator and following mixer. A 10 kHz signal with the same phase as the upper sideband and another 10 kHz signal with the same phase as the carrier are generated. In the generation of the upper sideband 10 kHz signal, the 80 kHz carrier plus sidebands are heterodyned against a locally generated 72.4414 kHz signal. The 72.4414 kHz signal is obtained by mixing a local 2.4414 kHz signal with a local 70 kHz signal and filtering to obtain the upper sideband.

The result of mixing the locally generated 72.4414 signal with the 80 kHz carrier plus sidebands is an audio component at 10 kHz referenced to the phase of the signal upper sideband and two other extraneous audio signals at 12.4414 kHz and 7.5586 kHz. The 10 kHz audio signal is separated from the extraneous signals by a narrow band filter.

A 10 kHz signal with the same phase as the carrier is generated by mixing the 80 kHz carrier plus sidebands with a local 70 kHz signal. The result is the 10 kHz signal plus two extraneous signals. The 10 kHz signal is filtered out by a band pass filter.

The 10 kHz upper sideband signal is then phase compared to the 10 kHz carrier signal, and the result (at point A) is $\gamma_+ - \gamma_0$.

A similar operation is performed with the lower sideband (at 80 kHz) and the carrier to obtain $\gamma_- - \gamma_0$. The sum of these two signals is taken, and the multipath measure $\gamma_+ + \gamma_- - 2\gamma_0$ is obtained directly.

ACKNOWLEDGEMENTS

The experiment required the cooperation of several organizations and many individuals. Each participant displayed an unusually high interest in the project, and contributed to its success with enthusiasm and skill. The following is a list of organizations, other than General Electric, and their personnel who were most closely associated with the program.

NATIONAL AERONAUTICS AND SPACE ADMINISTRATION

Headquarters, Washington, D. C.

Mr. Eugene Ehrlich, Chief - Navigation and Traffic Control Program (Project Manager for NASA)

Goddard Space Flight Center

Mr. Donald Fordyce, Technical Monitor
Mr. Gene Melton, Project Coordinator
Mr. Roger Moore, Test Scheduling - Satellites

FEDERAL AVIATION ADMINISTRATION

Headquarters, Washington, D. C.

Mr. O. DeZoute, FAA-GE Liaison

National Aviation Facilities Experimental Center

Mr. F. Jefferson, Flight Test Coordinator

U.S. COAST GUARD

Headquarters, Washington, D. C.

Lt. Commander M. Johnson and Lt. Basteck - Coast Guard - GE Liaison

Valiant

Captain Meade and Captain Readi
Lt. Hornstein
ET Lawrence and ET Able - Shipboard Operation

Several organizations monitored the signals relayed through the satellites and contributed data and helpful information on a voluntary basis. COMSAT Corporation was equipped with a phase-matcher correlator. They made time interval measurements from the interrogating signal to the user return. They prepared a computer program to determine standard deviations of range measurements. COMSAT data compared closely with GE data, showing that ground stations other than the interrogating station can monitor positions of craft, and that there were no significant differences in propagation effects between the ATS-3 satellite and the Schenectady, New York and Washington, D. C. areas during the cooperative tests.

Aeronautical Radio, Incorporated of Annapolis, Maryland, and the Boeing Company of Witchita, Kansas and Seattle, Washington submitted signal strength recordings and other useful information during the tests.

General Electric Company participants were:

GENERAL ELECTRIC COMPANY RESEARCH AND DEVELOPMENT CENTER

Mr. R. E. Anderson, Principal Investigator
Mr. R. C. Sisson, Responder Circuit Design
Mr. R. W. Garrett, In charge of ground terminal operations
Mr. J. R. Lewis, Ground terminal operations, digital recording
Mr. R. C. Rustay, Performance analyses, computer program design
Mr. W. T. Warren, Multipath Measuring Equipment Design

GENERAL ELECTRIC COMPANY RE-ENTRY AND ENVIRONMENTAL SYSTEMS DEPARTMENT

Mr. R. C. McCabe, Manager-Sea Robin Project
Mr. L. Cheney, Sea Robin Project Coordinator

GENERAL ELECTRIC COMPANY HEAVY MILITARY ELECTRONIC SYSTEMS

Dr. G. H. Millman, Consultant on Ionospheric Propagation